THE UNIVERSITY OF QUEENSLAND

AUSTRALIA

A Blood Bond: Evolutionary, Pathophysiological and Biodiscovery implications of coagulotoxic snake venoms

Jordan Debono

BSc (Honours 1A, Zoology)

A thesis submitted for the degree of Doctor of Philosophy at

The University of Queensland in 2019

School of Biological Sciences

Abstract

Snakebite is a massive global burden and is a neglected area of tropical diseases. Snake venom neurotoxins have been the subject of intense research efforts, albeit significantly less is known about coagulotoxins. Venoms can deleteriously affect any physiological system reachable by the bloodstream, including being able to directly interfere with the coagulation cascade. Such coagulopathic toxins may be either anticoagulant or procoagulant and snake venoms are unique in their use of procoagulant toxins for predatory purposes. Our limited knowledge into the mechanisms of action of snake venom hinders our understanding of the clinical pathologies and also restricts our use of these powerful natural products as lead compounds in drug design and development. Two snake families which exhibit coagulant properties and lead to a range of clinical pathologies are vipers, Viperidae, and non-front-fanged snakes, Colubridae. The primary focus of this thesis was to investigate and compare the coagulotoxicity effects and mechanisms of various species of known venomous snakes that effect coagulation. Species chosen for this investigation have had limited previous research conducted, thus a knowledge gap in the literature remains. These coagulant properties were investigated through a multi-disciplinary approach, highlighting key results from both families.

Data chapters 2 and 3 explore venom from the boomslang (*Dispholidus typus*) and the twig snakes (*Thelotornis* species) - iconic African snakes belonging to the family Colubridae. Both species produce strikingly similar lethal procoagulant pathologies. Despite these similarities, antivenom is only produced for treating bites by *D. typus*, and the mechanisms of action of both venoms have been understudied. We found that *T. mossambicanus* produced a significantly stronger coagulation response compared to *D. typus*, governed by strong prothrombin activation through PIII-SVMPs. Despite similarities in symptoms and clinical manifestations, venom composition differs widely between the two species, recovered from a combined approach of venomics and transcriptomics. The neutralising capability of the available boomslang antivenom was also investigated on both species, with it being 11.3 times more effective upon *D. typus* venom than *T. mossambicanus*.

Envenomation by Crotalinae such as Asian pit vipers can induce multiple clinical complications resulting from coagulopathic and neuropathic effects. Data chapters 4 - 8 investigate the Asian Pit Viper clade. While intense research has been undertaken for some species, such as *Calloselasma rhodostoma*, functional coagulopathic effects have been neglected. As these species' venoms affect the blood coagulation cascade and are known to produce haemorrhagic shock in envenomed patients, we investigated their effects upon coagulation using venoms of 33 species from the Asian pit viper clade including *Azemiops*, *Calloselasma*, *Deinagkistrodon*, *Gloydius*, *Hypnale*, *Protobothrops*, *Trimeresurus* and *Tropidolaemus.* Fibrinogen was the main coagulation target among these species

with many varying coagulotoxic effects exhibited. Various species including *Calloselasma rhodostoma*, *Deinagkistrodon acutus*, *Hypnale hypnale*, *Protobothrops mangshanensis*, *Ovophis okinavensis* and some *Trimeresurus* species produced net anticoagulant effects through pseudo-procoagulant clotting of fibrinogen, resulting in weak, unstable, transient fibrin clots. *Protobothrops flavoviridis*, *P. tokarensis*, *Gloydius brevicaudus*, *G. saxatilis*, *G. ussuriensis* and various *Trimeresurus* species exhibited a strong anticoagulant activity through the destructive cleavage of fibrinogen (at varying rates) directly resulting in an overall anticoagulant effect. *Tropidolaemus wagleri* was only weakly pseudo-procoagulant, clotting fibrinogen with only a negligible net anticoagulant effect. *Azemiops feae* and *Tropidolaemus subannulatus* did not affect clotting and *T. subannulatus* was investigated for its alternatively derived neurotoxicity effects, sharing Waglerin's peptide propeptide region. Other clotting factors, such as FX(a), thrombin, FIX(a) and FXI(a), were only mildly affected with minimal inhibition found from varying species. Cross neutralisation of the Green Pit Viper monovalent antivenom 'Thai Red Cross Green Pit Viper antivenin' was also investigated among the *Trimeresurus* species, with *T. gumprechti*, *T. hageni* and *T. mcgregori* being unaffected. These results indicate that anticoagulation mediated by pseudo-procoagulant cleavage of fibrinogen is the basal state among Asian pit vipers, while anticoagulation produced by destructive cleavage of fibrinogen, such as that found in *Protobothrops*, is the derived state. This is the first in depth study of its kind highlighting extreme enzymatic variability, functional diversification and clotting diversification within one clade (Asian pit vipers) surrounding one target site, governed by variability in co-factor dependency. This study is also the first to examine in a phylogenetic context the coagulotoxic effects of related genera of Asiatic pit vipers.

The results of these various chapters reveal substantial variation between sister genera, providing crucial information about clinical effects and implications for antivenom cross-reactivity among venomous snake species. This study increases our understanding of not only the biodiscovery potential of these medically important species but also increases our knowledge of the pathological relationship between venom and the human coagulation cascade. These results add to the body of knowledge necessary to inform clinical management of the envenomed patient, and detail the diversity of components and characteristics which enable venom research to be such a biodiscovery treasure trove in unlimited diversity, leading to novel drug design surrounding this field.

Declaration by author

This thesis is composed of my original work, and contains no material previously published or written by another person except where due reference has been made in the text. I have clearly stated the contribution by others to jointly-authored works that I have included in my thesis.

I have clearly stated the contribution of others to my thesis as a whole, including statistical assistance, survey design, data analysis, significant technical procedures, professional editorial advice, financial support and any other original research work used or reported in my thesis. The content of my thesis is the result of work I have carried out since the commencement of my higher degree by research candidature and does not include a substantial part of work that has been submitted to qualify for the award of any other degree or diploma in any university or other tertiary institution. I have clearly stated which parts of my thesis, if any, have been submitted to qualify for another award.

I acknowledge that an electronic copy of my thesis must be lodged with the University Library and, subject to the policy and procedures of The University of Queensland, the thesis be made available for research and study in accordance with the Copyright Act 1968 unless a period of embargo has been approved by the Dean of the Graduate School.

I acknowledge that copyright of all material contained in my thesis resides with the copyright holder(s) of that material. Where appropriate I have obtained copyright permission from the copyright holder to reproduce material in this thesis and have sought permission from co-authors for any jointly authored works included in the thesis.

Publications included in this thesis

Most chapters of this thesis comprise of manuscripts recently accepted for publication or published in peer-reviewed journals. I am the lead author of these papers and am responsible for the development of ideas and analyses of data.

Incorporated as Chapter 2:

Debono, J., Casewell, N.R., Bin, L., Kwok, H.F., Fry, B.G. 2017. Coagulating colubrids: Evolutionary, pathophysiological and biodiscovery implications of variations between boomslang (*Dispholidus typus*) and twig snake (*Thelotornis mossambicanus*) venoms. Toxins, 9(5), p.171.

Contributor	**Statement of contribution**
Debono, J.	Concept and Design (80%) Performed experiments (100%) Analysis and Interpretation (100%) Drafting and Production (100%) Edited paper (10%)
Casewell, N.R.	Edited paper (15%)
Bin, L.	Edited paper (5%)
Kwok, H.F.	Edited paper (10%)
Fry, B.G.	Concept and Design (20%) Edited paper (60%)

Incorporated as Chapter 3:

Debono, J., Dashvesky, D., Nouwens, A., Fry, B.G. 2020. The sweet side of venom: glycosylated prothrombin activating metalloproteases from *Dispholidus typus* (boomslang) and *Thelotornis mossambicanus* (twig snake). Comparative Biochemistry and Physiology Part C: Toxicology & Pharmacology, 277, p. 108625.

Contributor	**Statement of contribution**
Debono, J.	Concept and Design (80%) Performed experiments (85%) Analysis and Interpretation (65%) Drafting and Production (100%) Edited paper (40%)
Dashvesky, D.	Analysis and Interpretation (25%) Performed experiments (10%) Edited paper (30%)
Nouwens, A.	Analysis and Interpretation (5%) Performed experiments (5%)
Fry, B.	Analysis and Interpretation (5%) Concept and Design (20%) Edited paper (30%)

Incorporated as Chapter 4:

Debono, J., Bos, M.H.A., Coimbra, F., Ge, L., Frank, N., Kwok, H.F., Fry, B.G. 2019. Basal but divergent: Clinical implications of differential coagulotoxicity in a clade of Asian vipers. Toxicology in Vitro, 58, p.195-206.

Contributor	**Statement of contribution**
Debono, J.	Concept and Design (80%) Performed experiments (100%) Analysis and Interpretation (90%) Drafting and Production (90%) Edited paper (40%)
Bos, M.H.A.	Edited paper (15%) Analysis and Interpretation (10%)
Coimbra, F.	Edited paper (5%) Analysis and Interpretation (10%)
Ge, L.	Edited paper (5%)
Frank, N.	Production (5%)
Kwok, H.F.	Edited paper (10%)
Fry, B.G.	Drafting and Production (5%) Concept and Design (20%) Edited paper (25%)

Incorporated as Chapter 5:

Debono, J., Bos, M.H.A, Nouwens, A., Ge, L., Frank, N., Kwok, H.F., Fry, B.G. 2018. Habu coagulotoxicity: Clinical implications of the functional diversification of *Protobothrops* snake venoms upon blood clotting factors. Toxicology in Vitro, 55, p. 62-74.

Contributor	**Statement of contribution**
Debono, J.	Concept and Design (80%) Performed experiments (95%) Analysis and Interpretation (90%) Drafting and Production (100%) Edited paper (30%)
Bos, M.H.A.	Edited paper (15%) Analysis and Interpretation (10%)
Nouwens, A.	Performed experiments (5%)
Ge, L.	Edited paper (5%)
Frank, N.	Edited paper (5%)
Kwok, H.F.	Edited paper (15%)
Fry, B.G.	Concept and Design (20%) Edited paper (30%)

Incorporated as Chapter 6:

Debono, J., Bos, M.H.A., Do, M.S., Fry, B.G. 2019. Clinical implications of coagulotoxic variations in Mamushi (Viperidae: *Gloydius*) snake venoms. Comparative Biochemistry and Physiology Part C: Toxicology & Pharmacology, 225, p.108567.

Contributor	Statement of contribution
Debono, J.	Concept and Design (65%) Performed experiments (100%) Analysis and Interpretation (100%) Drafting and Production (100%) Edited paper (40%)
Bos, M.H.A.	Edited paper (40%)
Do, M.S.	Concept and Design (5%)
Fry, B.	Concept and Design (30%) Edited paper (20%)

Incorporated as Chapter 7:

Debono, J., Bos, M.H.A, Frank, N., Fry, B.G. 2019. Clinical implications of differential antivenom efficacy in neutralising coagulotoxicity produced by venoms from species within the arboreal viperid snake genus *Trimeresurus*. Toxicology Letters, 316, p. 35-48.

Contributor	Statement of contribution
Debono, J.	Concept and Design (75%) Performed experiments (100%) Analysis and Interpretation (100%) Drafting and Production (100%) Edited paper (40%)
Bos, M.H.A.	Edited paper (40%)
Frank, N.	Concept and Design (5%)
Fry, B.G.	Concept and Design (20%) Edited paper (20%)

Incorporated as Chapter 8:

Debono, J., Xie, B., Violette, A., Fourmy, R., Jaeger, M. and Fry, B.G. 2016. Viper venom botox: the molecular origin and evolution of the Waglerin peptides used in anti-wrinkle skin cream. Journal of Molecular Evolution, 84, p. 8-11.

Contributor	Statement of contribution
Debono, J.	Concept and Design (50%) Performed experiments (100%) Analysis and Interpretation (80%) Drafting and Production (50%) Edited paper (15%)
Violette, A.	Edited paper (15%)
Fourmy, R.	Analysis and Interpretation (10%) Edited paper (15%)
Jaeger, M.	Analysis and Interpretation (10%) Edited paper (15%)
Fry, B.G.	Concept and Design (50%) Edited paper (40%) Drafting and Production (50%)

Submitted manuscripts included in this thesis

No manuscripts submitted for publication.

Other publications during candidature

Peer-reviewed papers

(*joint first authorship)

Youngman, N.J., **Debono, J**., Dobson, J.S., Zdenek, C.N., Harris, R.J., Coimbra, F.C., Naude, A., Coster, K., Sundman, E., Braun, R., Hendrikx, I., Fry, B.G. 2019. Venomous landmines: Clinical implications of extreme coagulotoxic diversification and differential neutralization by antivenom of venoms within the viperid snake genus *Bitis*. Toxins, 11(7), p.422.

Zdenek, C.N., Hay, C., Arbuckle, K., Jackson, T.N., Bos, M.H.A., Op den Brouw, B., **Debono, J**., Allen, L., Dunstan, N., Morley, T., Herrera, M., Gutiérrez, J.M., Williams, D.J., Fry, B.G. 2019. Coagulotoxic effects by brown snake (*Pseudonaja*) and taipan (*Oxyuranus*) venoms, and the efficacy of a new antivenom. Toxicology in Vitro, 58, p.97-109.

Dashevsky, D.*, **Debono, J.*,** Rokyta, D., Nouwens, A., Josh, P., Fry, B.G. 2018. Three-Finger toxin diversification in the venoms of cat-eye snakes (Colubridae: *Boiga*). Journal of Molecular Evolution, p.1-15.

Coimbra, F.C., Dobson, J., Zdenek, C.N., Op den Brouw, B., Hamilton, B., **Debono, J**., Masci, P., Frank, N., Ge, L., Kwok, H.F., Fry, B.G. 2018. Does size matter? Venom proteomic and functional comparison between night adder species (Viperidae: *Causus*) with short and long venom glands. Comparative Biochemistry and Physiology Part C: Toxicology & Pharmacology, 211, p.7-14.

Oulion, B., Dobson, J.S., Zdenek, C.N., Arbuckle, K., Lister, C., Coimbra, F.C., op den Brouw, B., **Debono, J**., Rogalski, A., Violette, A., Fourmy, R., Frank. N., Fry. B.G. 2018. Factor X activating *Atractaspis* snake venoms and the relative coagulotoxicity neutralising efficacy of African antivenoms. *Toxicology letters*, 288, p.119-128.

Goldenberg, J., Cipriani, V., Jackson, T.N., Arbuckle, K., **Debono, J**., Dashevsky, D., Panagides, N., Ikonomopoulou, M.P., Koludarov, I., Li, B., Santana, R.C., Nouwens A., Jones, A., Hay, C., Dunstan, N., Allen, L., Bush, B., Milese, J.J., Gen, L., Kwok, H.F., Fry, B.G. 2018. Proteomic and functional

variation within black snake venoms (Elapidae: *Pseudechis*). Comparative Biochemistry and Physiology Part C: Toxicology & Pharmacology, 205, p.53-61.

Koludarov, I., Jackson, T.N., Dobson, J., Dashevsky, D., Arbuckle, K., Clemente, C.J., Stockdale, E.J., Cochran, C., **Debono, J**., Stephens, C., Panagides, N., Li, B., Manchadi, M. L. R., Violette, A., Fourmy, R., Hendrikx, I., Nouwens, A., Clements, J., Martelli, P., Kwok, H. F., Fry, B.G. 2017. Enter the Dragon: The dynamic and multifunctional evolution of Anguimorpha lizard venoms. Toxins, 9(8), p.242.

Lister, C., Arbuckle, K., Jackson, T.N., **Debono, J**., Zdenek, C.N., Dashevsky, D., Dunstan, N., Allen, L., Hay, C., Bush, B. and Gillett, A., Fry, B.G. 2017. Catch a tiger snake by its tail: Differential toxicity, co-factor dependence and antivenom efficacy in a procoagulant clade of Australian venomous snakes. Comparative Biochemistry and Physiology Part C: Toxicology & Pharmacology, 202, p.39-54.

Casewell, N.R., Visser, J.C., Baumann, K., Dobson, J., Han, H., Kuruppu, S., Morgan, M., Romilio, A., Weisbecker, V., Mardon, K., Ali, S.A., **Debono, J**., Koludarov, I., Que, I., Bird, G.C., Cooke, G. M., Nouwens, A., Hodgson, W. C., Wagstaff, S. C., Cheney, K. L., Vetter, I., der Weerd, L., Richardson, M. K. and Fry, B.G. 2017. The evolution of fangs, venom, and mimicry systems in blenny fishes. Current Biology, 27(8), p.1184-1191.

Cipriani, V.*, **Debono, J**.*, Goldenberg, J., Jackson, T.N., Arbuckle, K., Dobson, J., Koludarov, I., Li, B., Hay, C., Dunstan, N., Allen, L. 2017. Correlation between ontogenetic dietary shifts and venom variation in Australian brown snakes (*Pseudonaja*). Comparative Biochemistry and Physiology Part C: Toxicology & Pharmacology, 197, p.53-60.

Han, H.*, Baumann, K.*, Casewell, N.R.*, Ali, S.A., Dobson, J., Koludarov, I., **Debono, J**., Cutmore, S.C., Rajapakse, N.W., Jackson, T.N. and Jones, R., Hodgson, W.C., Fry, B.G., Kuruppu, S. 2017. The cardiovascular and neurotoxic effects of the venoms of six bony and cartilaginous fish species. Toxins, 9(2), p.67.

Yang, D.C., Deuis, J.R., Dashevsky, D., Dobson, J., Jackson, T.N., Brust, A., Xie, B., Koludarov, I., **Debono, J**., Hendrikx, I. and Hodgson, W.C., Josh, P., Nouwens, A., Baillie, G.J., Bruxner, T.J.C., Alewood, P.F., Lim, K.K.P., Frank, N., Vetter, I., Fry, B.G. 2016. The snake with the Scorpion's

Sting: Novel Three-Finger toxin sodium channel activators from the venom of the long-glanded blue coral snake (*Calliophis bivirgatus*). Journal of Molecular Evolution, 8(10), p.303.

Debono, J.*, Cochran, C.*, Kuruppu, S., Nouwens, A., Rajapakse, N.W., Kawasaki, M., Wood, K., Dobson, J., Baumann, K., Jouiaei, M. and Jackson, T.N., Koludarov, I., Low, D., Ali, S.A., Smith, A.I., Barnes, A., Fry, B.G. 2016. Canopy venom: proteomic comparison among new world arboreal pit-viper venoms. Toxins, 8(7), p.210.

Conference Abstracts

26th World Congress of International Society of Thrombosis and Haematology, Berlin Germany (2017) - Presented project; **Debono, J.,** Fry, B.G. 'Differential coagulotoxic effects of Asian pit viper snake venoms: Evolutionary, pathophysiology and biodiscovery implications' (Poster), was presented to delegates at the World Congress of International Society of Thrombosis and Haematology, Berlin Germany.

Oxford Symposia Venoms, Oxford England (2017) - Presented project; **Debono, J.,** Casewell, N.R., Bin, L., Kwok, H.F., Fry, B.G. 'Coagulating colubrids: Evolutionary, pathophysiological and biodiscovery implications of variations between boomslang (*Dispholidus typus*) and twig snake (*Thelotornis mossambicanus*) venoms' (Oral presentation), was presented to delegates at the Oxford Symposia Venoms, Oxford UK.

19th World Congress of the International Society of Toxinology, Hainan China (2017) - Presented project; **Debono, J.,** Casewell, N.R., Bin, L., Kwok, H.F., Fry, B.G. 'Coagulating colubrids: Evolutionary, pathophysiological and biodiscovery implications of variations between boomslang (*Dispholidus typus*) and twig snake (*Thelotornis mossambicanus*) venoms' (Oral presentation), was presented to delegates at the 19th World Congress of the International Society of Toxinology, Hainan China which won 'Outstanding Student Oral Presentation Award'.

Australian Society of Herpetologists, Brisbane Australia (2018) - Presented project; **Debono, J.,** Casewell, N.R., Bin, L., Kwok, H.F., Fry, B.G. 'Coagulating colubrids: Evolutionary, pathophysiological and biodiscovery implications of variations between boomslang (*Dispholidus typus*) and twig snake (*Thelotornis mossambicanus*) venoms' (Oral presentation), was presented to delegates at the Australian Society of Herpetologists, Brisbane Australia.

27th World Congress of International Society of Thrombosis and Haematology, Melbourne Australia (2019) - Presented project; **Debono, J.,** Bos, M.H.A., Fry, B.G. 'The clinical implications of the differential coagulopathic effects of Asian pit viper snake venoms' (Poster), was presented to delegates at the World Congress of International Society of Thrombosis and Haematology, Melbourne Australia.

Contributions by others to the thesis

This thesis would not have been possible without contributions and collaborations from around the world. I would firstly like to acknowledge the contribution of the following people to this thesis: I acknowledge and thank my supervisory team Associate Professor Bryan Fry as my primary supervisor, Dr Irina Vetter and Dr Kevin Arbuckle as my co supervisors. Associate Professor Bryan Fry has significantly contributed to the body of this thesis with major contribution in concept and design as well as interpretation of data and manuscript editing. I would like to thank my committee members for their various roles in support throughout my candidature; Professor Robbie Wilson, Dr Eivind Undheim and Dr Vera Weisbecker of the University of Queensland.

The following acknowledgements of contributions are by chapter:

Chapter 2: Professor Nick Casewell for his contribution to manuscript writing and venom supply of *Dispholidus typus* and *Thelotornis mossambicanus*. Dr Amanda Nouwens and Peter Josh for their LC-MS/MS knowledge, skills and interpretation of data.

Chapter 3: Daniel Dashvesky, for his relentless troubleshooting skills and knowledge of transcriptomic analysis, contribution to manuscript writing and significant contribution to data interpretation.

Chapter 4 - 7: Dr Mettine Bos for her guidance and expertise surrounding haematology and venom effect on fibrinogen as well as significant contribution to manuscript writing.

Chapter 4, 5 & 7: Nathaniel Frank, for his consistent supply of quality venom supplies for a range of species.

Statement of parts of the thesis submitted to qualify for the award of another degree

No works submitted towards another degree have been included in this thesis.

Research Involving Human or Animal Subjects

No animal or human subjects requiring ethics were involved in this research.

Acknowledgements

I would first and foremost like to thank my supervisory team, Associate Professor Bryan Fry and Dr Irina Vetter for being outstanding supervisors, and in particular granting me a huge amount of freedom throughout my candidature to follow my passion around the world. I would also like to thank them for their constant encouragement that led to the completion of my thesis. Thank you especially to Bryan for his continued support and inspiration throughout my academic career, from the very early days when I first began in his lab, he saw something no one else did and believed I could be an amazing scientist. Thank you for the countless opportunities you have given me and the insane amount of support over the years as colleague, supervisor and friend.

I would also like to thank my rotating assemblage of committee members; Professor Robbie Wilson, Dr Eivind Undheim and Dr Vera Weisbecker for their continued support and advice going through each milestone and for stepping in when others were unable to attend. Their advice received at each milestone was invaluable, particularly advice about future prospects. I would also like to thank them for their continued following of my various additional achievements throughout my candidature.

A huge thank you to Dr Mettine H. A. Bos, for her expertise and knowledge surrounding haematology and venom, and for her continued patience and guidance throughout my candidature. A special thanks for her welcome when I spent time visiting her laboratory in Holland, struggling with certain cultural differences and for understanding when I needed help. This went above and beyond a scientific collaboration and you became a life-long friend, so I thank you for this.

A very special thanks to my mentor Dr Scott Cutmore, who may not know it but who has been instrumental in the completion of not only my PhD but also my academic career to date. He has been the shoulder to cry on and the ears and eyes I needed for the past 7 years when discussing projects, results, issues with candidature, future prospects about what direction to go in life and an all-round amazing friend and colleague – thank you.

I would also like to give special thanks to past and present members of the Venom Evolution Laboratory, particularly Dr Kate Baumann for her everlasting friendship, Dr Timothy Jackson for his undeniable wisdom and the six current PhD students – James, Dan, Christina, Bianca, Rich, Francisco - who have been the rocks throughout my journey of not only my PhD but also my undergraduate and honours degrees. Your friendship, support and singular understanding of what it is like to undertake a PhD in the V.E.L has been life-saving.

Special thanks go to my parents and brother, without whose support I would have never made it through my PhD, let alone the past 9 years at UQ. To their continued understanding of the unhealthy inability to decide what I want to do with my life and the drive that is my passion for science, for instilling in me the qualities of persistence and determination so that I could accomplish something such as a PhD. You have supported every decision I have made and been on the science journey right

beside me. My partner who deserves thanks for the countless conversations he has had to endure about my research, even when he has absolutely no clue what I am talking about, yet supports me in my decision to peruse a PhD. To all of the above, you have given me strength in believing in me when I didn’t always believe in myself. Thank you for your patience and understanding throughout this extremely rewarding journey.

Financial support

This research was supported by the Australian Research Council DP190100304, by an Australian Postgraduate Award, by the University of Queensland Candidature Development Award (2018) and by the Queensland Women in STEM Award (2017) sponsored by Advanced Queensland.

Keywords

Crotalinae, Colubridae, Asian pit viper, coagulation, venom, anticoagulant, procoagulant, evolution, fibrinogen, antivenom, transcriptome.

Australian and New Zealand Standard Research Classifications (ANZSRC)

ANZSRC code: 030406 Proteins and Peptides 30%
ANZSRC code: 110202 Haematology 50%
ANZSRC code: 060409 Molecular Evolution, 20%

Fields of Research (FoR) Classification

FoR code: 0603, Evolutionary Biology, 30%
FoR code: 1102 Cardiorespiratory Medicine and Haematology, 40%
FoR code: 0601 Biochemistry and Cell Biology, 30%

Table of Contents

Index of Figures (by chapter):

Index of Tables (by chapter):

Abbreviations

1D SDS PAGE (R/NR)	one-dimensional (1D) sodium dodecyl sulfate polyacrylamide gel electrophoresis (SDS-PAGE) - reduced/ non-reduced
2D SDS PAGE (R)	two-dimensional (2D) sodium dodecyl sulfate polyacrylamide gel electrophoresis (SDS-PAGE) - reduced
3D	Three dimensional
3FTx	Three finger toxin
ABC	ammonium bicarbonate
ACN	acetonitrile
AEBSF	4-benzenesulfonyl fluoride hydrochloride
ANOVA	Analysis of Variance
APC	activated Human Protein C
APS	ammonium sulphate
aPTT	activated Partial Thromboplastin Time
BLAST	basic local alignment search tool
$CaCl^2$	Calcium Chloride
CRiSP	cysteine rich secretory protein
DTT	dithiothreitol
fX, fVIII	eg Factor 10, Factor 13
fXa, fVIIIa	active form of eg. factor 10, factor 13
FA	formic acid
HMWK	high molecular weight kininogen
HPLC	High Pressure Liquid Chromatography
IAA	iodoacetamide
IEF	isoelectric focusing machine
IPG strip	immobilized pH gradient strip
kDA	kilodaltons
LC-MS/MS	liquid chromatography mass spectrometry/mass spectrometry
MALDI	matrix assisted laser desorption ionization mass spectrometry
MMP	matrix metalloprotease
MRI	Magnetic Resonance Imaging
mRNA	messenger ribonucleic acid
PBS	phosphate buffered saline
PCR	polymerase chain reaction

pI value	isoelectric point
PLA_2	Phospholipase A_2
PLB	Phospholipase B
RM	Repeated measures
RNA	Ribonucleic acid
HPLC	reversed phase high performance liquid chromatography
SEC	size exclusion chromatography
snaclec	snake venom C-type lectin
SVMP	snake venom metalloprotease P-I, P-II, P-III
SVSP	snake venom serine protease
TEG	Thromboelastography
TEMED	tetramethylethylenediamine
TPM	Transcripts Per Million
TOF	Time Of Flight
TFA	trifluoroacetic acid
tPA	tissue plasminogen activator
tRNA	total RNA
µg	microgram
µL	microliter
µM	micromolar

Note on style to the reader

This thesis is presented as a series of manuscripts that have been published and recently accepted for publication. As a result, there may be repetition across the introductions of each chapter and may be certain inconsistencies between chapters.

Chapter 1: Introduction – a brief overview of coagulation and snake venom

1.1 The human coagulation cascade: a brief overview

The human coagulation cascade is an extremely complex intricate highway of factor cascades which catalyse together in order to form a stable fibrin clot. The cascade is made up of three main pathways: extrinsic, intrinsic and common pathway. The extrinsic pathway begins by triggering FVII through trauma or external tissue damage. This event releases tissue factor (FIII), which combined with Ca^{2+} activates FVII into FVIIa (Jin and Gopinath, 2016; Mackman, 2009). The intrinsic pathway begins via negatively charged surface contact, such as that triggered by a disruption to the endothelium lining, by a response to the presence of pathophysiological materials and invasion pathogens such as bacteria in septic shock or prolonged severe inflammation (Vogler and Siedlecki, 2009; Wu, 2015). This surface contact activates FXII along with free platelets signalled to the area. Both the intrinsic and extrinsic pathways cross over at a mid-point, governed by Factor X (FX) (cleavage of FX into FXa is the beginning of the common pathway). The end goal is to form a stable fibrin clot to prevent further bleeding. FXa directly activates prothrombin (FII) into its active form, thrombin (FIIa). Thrombin is used to activate FVIII into FVIIIa and FV into FVa. These factors lead directly to a stable fibrin clot and help facilitate further clot formation. Fibrinogen is converted by thrombin into a fibrin monomer, adhering to fibrin polymers A and B, which aggregates with platelets to also form a stable fibrin clot, and at the same time FXIII is cleaved into FXIIIa. FXIIIa is essential for the formation of covalent bridges between fibrin units, resulting in cross-linked fibrin which is insoluble and resistant to lysis (Al-Horani et al., 2016; Heil et al., 2013; Shi and Wang, 2017). All of these catalytic reactions require the presence of Ca^{2+} (Figure 1.1).

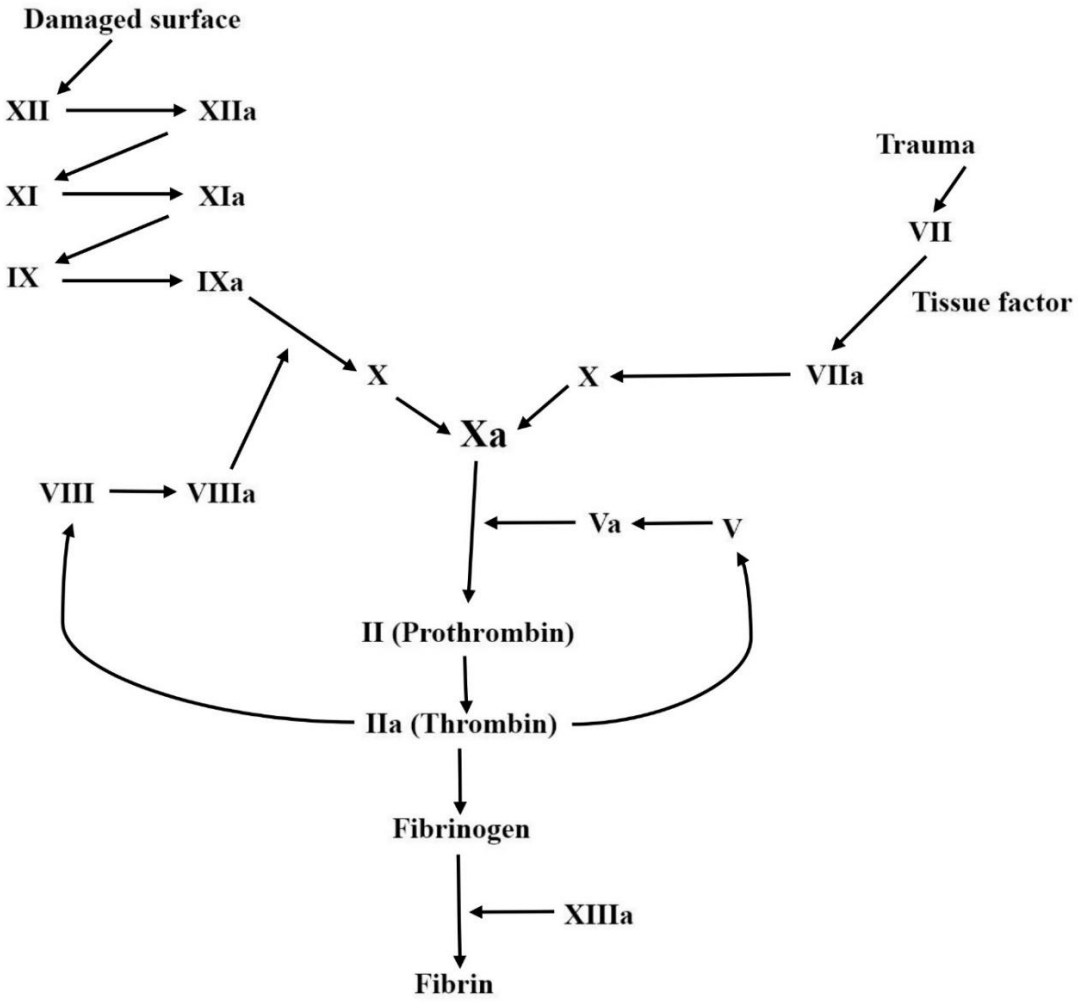

Figure 1.1 Coagulation cascade
Simplified clotting cascade outlining extrinsic, intrinsic and common pathways along with activation steps of factors to form a fibrin clot.

While the common pathway is complex on its own, it is also the place where majority of inhibition of factors takes place, regulating coagulation to prevent thrombotic diseases. Activated Protein C (APC) is a circulating zymogen which selectively inactivates FVa and FVIIIa, both essential co factors for FX activation (Esmon et al., 1987). If Protein C is inhibited, then FX will continuously activate and uncontrollable catalysing of the common pathway will continue, resulting in unmodulated fibrin being produced. Another major inhibition step taken to prevent thrombosis is plasminogen activation into plasmin which, in turn, destroys fibrin clots. This occurs once a clot has served its purpose in preventing blood loss, modulating clot formations and is known as fibrinolysis (Cesarman-Maus and Hajjar, 2005; Collet et al., 2000). Tissue plasminogen activator (tPA) is present in endothelial cells and is released in the presence of fibrin which makes up the clot. tPA is responsible for catalysing plasminogen into plasmin which degrades the fibrin network into soluble products (Cesarman-Maus and Hajjar, 2005; Rijken and Lijnen, 2009).

1.2 Snake venoms and coagulation

Venom is defined as a secretion produced in specialised cells that is delivered to a target animal through a wound which consequently disrupts normal physiological or biochemical processes (Fry et al., 2009a; Fry et al., 2009b; Nelsen et al., 2014). Venoms are complex mixtures of enzymes, toxins, peptides, organic molecules and salts (Fry et al., 2009a; Fry et al., 2009b) which are used to facilitate feeding (Fry et al., 2008; Fry et al., 2013; Fry et al., 2009b; Jackson et al., 2013), defence such as that found in spitting cobras (Cascardi et al., 1999; Hayes et al., 2008) or competition (Deufel and Cundall, 2003) for the producing organism (Fry and Wüster, 2004; Sunagar et al., 2013). Numerous studies have demonstrated that venom genes evolve at a much faster rate than housekeeping genes, facilitating a drive towards a highly specialised and complex venom composition (Casewell et al., 2013; Jackson et al., 2013; Sunagar et al., 2013; Vonk et al., 2013). This facilitated diversification allows toxins within venom to evolve rapidly, and at different rates, through a variety of different selective mechanisms. These mechanisms include but are not limited to: ecological niche occupation, which is in-turn directly related to prey ecology, and in some cases taxon-specific toxins (Jackson et al., 2013; Koludarov et al., 2014; Li et al., 2005; Pawlak et al., 2006; Pawlak et al., 2009); geographical location; and morphology (Daltry et al., 1996b; Fry et al., 2013; Sunagar et al., 2013; Sunagar et al., 2014). The toxic 'cocktail' that is venom is a mixture of proteins secreted by specialized cells, such as venom glands (Casewell et al., 2013; Fry et al., 2009a; Fry et al., 2012). These proteins have evolved from those normally expressed within the body to being recruited for secretion via the oral (venom) glands (Fry et al., 2015c; Fry et al., 2005). General characteristics of recruited proteins (despite diversification) include recruitment from secretory protein families, pre-existing biochemical roles and recruitment more frequently from body proteins which are more stable in their tertiary structures with an increase in cysteine cross-linking (Fry et al., 2015c). All proteins present within secreted venom exhibit characteristics of both plesiotypic (basal) and apotypic (derived) structural and functional forms (for further detail see (Fry, 2005; Fry et al., 2009a; Fry et al., 2012; Fry et al., 2008; Fry et al., 2013; Fry and Wüster, 2004).

Particular focus has been taken within this project to investigate the activity of two enzymes responsible for the majority of coagulant activity: snake venom metalloproteases (SVMPs) and serine proteases (SVSPs). These enzymes play an important role in coagulation activity by venoms, acting directly on platelet activity or cascade factors. Procoagulation and the varying effects of anticoagulation are the major focal points of this thesis. Procoagulant toxins can be simplified into four groups: prothrombin activators (Bos and Camire, 2010; Joseph and Kini, 2002; Kini, 2005a; Kornalik and Blombäck, 1975; Pirkle et al., 1972; Rogalski et al., 2017; Rosing and Tans, 1992; Yamada et al., 1996), Factor X activators (Chen et al., 2008; Joseph and Kini, 2002; Oulion et al., 2018; Tans and Rosing, 2002; Yamada et al., 1997), Factor V activators (Bos and Camire, 2010; Bos

et al., 2016; Rosing et al., 2001; Williams et al., 1994; Zdenek et al., 2019), and thrombin-like enzymes (Cho et al., 2001; Esnouf and Tunnah, 1967; Huang et al., 2011; Lin et al., 2009; Nielsen, 2016b; Ouyang and Teng, 1976, 1978; Pradniwat and Rojnuckarin, 2015; Tan, 2010; Tan et al., 2012; Zhang et al., 2007), while anticoagulants can affect any number of factors singularly or synergistically, such as blocking clotting enzymes while activating Protein C (Bakker et al., 1993; Esmon et al., 1987; Jin and Gopinath, 2016; Kisiel et al., 1987; Kogan et al., 1993; Nakagaki et al., 1990). These types of activators or inhibitors have been found and isolated from a number of varying families and species of venomous snakes.

This PhD focuses on members from two of these families: Colubridae and Viperidae. The Colubridae has a global distribution, and are often referred to as 'non-front-fanged snakes'. The Viperidae is a family of snakes known as the vipers (or viperid snakes), with a geographical distribution on every continent excluding Australia and Antarctica. The Viperidae is divided in to two main subfamilies; Viperinae (true or pit-less vipers) and Crotalinae (Pit Vipers). Chapters included in this thesis focus specifically on two infamous procoagulant species from the Colubridae subfamily Colubrinae, and the entire Asian Pit viper clade from the Viperidae subfamily, Crotalinae. By screening such a large group of predatory venoms (those subjected to evolutionary selection pressures for prey immobilisation (Jackson and Fry, 2016; Yang et al., 2016)) for novel coagulant properties from these snakes, this will hopefully lead to new biodiscoveries of toxins used for possible medications in blood clotting disorders.

Evolutionary selection pressures acting upon predatory venoms select for actions that facilitate prey capture via target sites reachable by the blood. Toxins that target the blood coagulation cascade do so via one of two mutually exclusive functional mechanisms: anticoagulation or procoagulation. Procoagulation, unlike anticoagulation, is a novel characteristic of snake venoms, while anticoagulant properties are more widespread across venomous lineages. Anticoagulant venoms, such as those found in most pit vipers, participate in the induction of haemorrhagic shock through a combined chemical assault on targets. These anticoagulant targets range from cleavage of fibrinogen (whether outright destruction or the production of weak clots which are readily broken down by the abundant plasmin produced by synergistic toxins which activate plasminogen) (Kini, 2006), through to platelets (aggregation inhibition or unnatural clumping effects which disrupt the normal role platelets serve in clotting) (Andrews et al., 2001; Gan et al., 1988; Kini and Koh, 2016; Navdaev et al., 2011; Peng et al., 1991; Shin and Morita, 1998; Tai et al., 2004; Wang et al., 1999); these toxic effects accompanied by other toxins that increase the permeability of the vascular bed (Assafim et al., 2016; Calvete et al., 1991; Fry et al., 2009a; Fry et al., 2015c; Gan et al., 1988; Gould et al., 1990; Samel et al., 2006). These venoms are often employed by ambush feeding vipers, which specialise upon warm-blooded prey items, and are able to efficiently track post-bite using chemoreception and heat detection sensory

arrays (Gracheva et al., 2010; Panzano et al., 2010). Procoagulant venoms however, are selected for in lineages which feed upon prey with fast-moving blood circulation rates. Such prey lineages are vulnerable to toxins which produce blood clots that rapidly subjugate through stroke induction, such as taipans (*Oxyuranus* species) feeding upon rodents (Herrera et al., 2012; Zdenek et al., 2019).

The boomslang and twig snakes: The Colubrinae

The boomslang (*Dispholidus typus*) and the twig snakes (*Thelotornis* spp.) are iconic African snakes belonging to the subfamily Colubrinae (Colubridae). Both genera produce strikingly similar lethal procoagulant pathologies (Debono et al., 2017a). Both genera cause mortality to humans and are of medical importance (Grasset and Schaafsma, 1940; Hiestand and Hiestand, 1979). Prior to the first documented deaths, they were thought to be of little harm and were commonly kept in many private collections around the world. This was until each killed two eminent herpetologists (Chapman, 1968; FitzSimons, 1909b, 1919; FitzSimons, 1962; Pla et al., 2017; Pope, 1958; Weinstein et al., 2011; Weinstein et al., 2013). Both genera are now known to cause massive haemorrhaging within 12-24 hours' post-bite (Isbister, 2010; Weinstein et al., 2011), causing a slow death. Despite these similarities, antivenom is only produced for treating bites by *D. typus* and the mechanism of action of both venoms have been understudied. For further details please see Chapters 2 and 3.

The Asian Pit viper clade: The Crotalinae

In the course of over 40 million years of evolution, Asian pit vipers have undergone a rapid radiation accompanied by extensive venom diversification. There are 10 main genera (Alencar et al., 2016) which inhabit every niche across the Asian continent, both arboreal and terrestrial, including tropical rainforests, swamp lands, mangroves, coastal hinterland, rocky offshore islands and rocky outcrops at high mountainous altitudes. They are subject to high evolutionary pressures, reflective of their prey ecology in their diverse venom compositions. Pit vipers are known for their anticoagulant effects on prey. Examples of toxins isolated for their anticoagulant properties include Ancrod, a Toxicofera Venom (TV)-Kallirkein isolated from *Calloselasma rhodostoma* (Samsa et al., 2002; Vaiyapuri et al., 2015), and Jararhagin from *Bothrops* species which affects haemostasis through fibrinogen degradation and inhibition of platelets (Kamiguti et al., 1994; Kamiguti et al., 1996; Paine et al., 1992). In contrast, there have also been procoagulant components isolated from individual pit vipers, including Alborhagin, a snaclec (snake venom C-type like-lectin proteins) isolated from *Trimeresurus albolabris* which aggregates platelets by binding to the GbIP receptor (Andrews et al., 2001; Arlinghaus et al., 2015; Peng et al., 1991) and Ecarin isolated from *Echis carinatus* which activates prothrombin directly (Casewell et al., 2015; Kornalik and Blombäck, 1975; Nishida et al., 1995). Through my research it is evident there is no one defining characteristic among the Asian pit vipers

(for further details please see Chapters 4, 5, 6, 7 and 8). There is a large diversification of haemotoxins and neurotoxins within such venoms which have been recruited on multiple occasions. This is reflective of the sporadic and random nature of evolution (Fry et al., 2009b).

1.3 Aims and directions

The main aim of this thesis was to investigate and understand the coagulant properties of members from the Colubrinae and Crotalinae families. Snake bite across the world still remains a neglected tropical disease, and with increased urbanisation and human population expanse, this number will only increase in future years to come (Fry, 2018; Gutiérrez et al., 2017; Gutiérrez et al., 2006; Kasturiratne et al., 2008; Williams et al., 2010; Williams et al., 2011). The combination of findings from the following chapters will increase our understanding of not only the biodiscovery potential of these medically important species but also increase our knowledge of the pathological relationship between venom and the human coagulation cascade. By applying this information, we can improve treatments, methodologies and diagnostics for clinical patients, especially for species which may not have antivenom currently available for treatment or in the case where medical help is not easily accessible. In doing so we can increase our overall understanding of coagulant venom which in turn can lead onto novel drug design surrounding this field.

Chapter 2: Coagulating Colubrids: Evolutionary, Pathophysiological and Biodiscovery Implications of Venom Variations between Boomslang (*Dispholidus typus*) and Twig Snake (*Thelotornis mossambicanus*)

2.1 Abstract

Venoms can deleteriously affect any physiological system reachable by the bloodstream, including directly interfering with the coagulation cascade. Such coagulopathic toxins may be anticoagulants or procoagulants. Snake venoms are unique in their use of procoagulant toxins for predatory purposes. The boomslang (*Dispholidus typus*) and the twig snakes (*Thelotornis* species) are iconic African snakes belonging to the family Colubridae. Both species produce strikingly similar lethal procoagulant pathologies. Despite these similarities, antivenom is only produced for treating bites by *D. typus*, and the mechanisms of action of both venoms have been understudied. In this study, we investigated the venom of *D. typus* and *T. mossambicanus* utilising a range of proteomic and bioactivity approaches, including determining the procoagulant properties of both venoms in relation to the human coagulation pathways. In doing so, we developed a novel procoagulant assay, utilising a Stago STA-R Max analyser, to accurately detect real time clotting in plasma at varying concentrations of venom. This approach was used to assess the clotting capabilities of the two venoms both with and without calcium and phospholipid co-factors. We found that *T. mossambicanus* produced a significantly stronger coagulation response compared to *D. typus*. Functional enzyme assays showed that *T. mossambicanus* also exhibited a higher metalloprotease and phospholipase activity but had a much lower serine protease activity relative to *D. typus* venom. The neutralising capability of the available boomslang antivenom was also investigated on both species, with it being 11.3 times more effective upon *D. typus* venom than *T. mossambicanus*. In addition to being a faster clotting venom, *T. mossambicanus* was revealed to be a much more complex venom composition than *D. typus*. This is consistent with patterns seen for other snakes with venom complexity linked to dietary complexity. Consistent with the external morphological differences in head shape between the two species, CT and MRI analyses revealed significant internal structural differences in skull architecture and venom gland anatomy. This study increases our understanding of not only the biodiscovery potential of these medically important species but also increases our knowledge of the pathological relationship between venom and the human coagulation cascade.

2.2 Introduction

Venoms are used for competitor deterrence, defence, and prey capture. These chemical cocktails use a myriad of protein types as starting substrates for the evolution of their toxic arsenals. Many of these

protein families have been convergently recruited into the secretions of various venomous animal classes (Fry et al., 2009a). Novel expression of a normal body protein in the venom gland is followed by fixation and diversification of the proteins, with duplication and diversification leading to neofunctionalisation. In reptiles, such compounds have been recruited for use at different times in the diverse history of venom in this lineage with relative expression levels rising and falling for a particular toxin type along the evolutionary continuum (Fry et al., 2015c). As venoms evolve through the birth-and-death model of protein evolution (Fry et al., 2003b), there are many instances of toxins also being lost from within a lineage (Dowell et al., 2016).

Rather than prey death, prey immobilization is the driving selection pressure upon the venom, as there is no functional difference between a prey item that is physically unable to flee or defend itself and one that is dead (Jackson et al., 2013; Yang et al., 2016). Prey capture involving chemicals will produce a different form of injury than one involving mechanical subjugation techniques such as claws or cutting teeth. Interactions among toxins are selected for a combined function, which facilitates prey subjugation in a time dependent manner. Evolutionary pressures from other variables such as post-envenomation prey detectability and prey escape potential also shape venoms. The evolutionary pressures acting upon predatory venoms select specific actions that facilitate prey capture via target sites reachable by the blood. Actions upon nerve action potentials and the blood clotting cascade are two particularly important areas. Venoms that act on the nerves are typically used by species that include reptiles as the major prey items in their diet. The specific function selected for the case of elapid snakes, which feed on sleeping lizards, is caused by alpha-neurotoxins, which antagonistically bind to the post-synaptic nicotinic acetylcholine receptor to produce flaccid paralysis (Jackson et al., 2016). Conversely, the long-glanded blue coral snake (*Calliophis bivirgatus*) and mambas (*Dendroaspis* spp.), which feed on active prey items with a high escape potential, have presynaptic-acting venoms that produce excitatory neurotoxicity, resulting in uncontrollable, uncoordinated spastic paralysis (Yang et al., 2016). In the case of *C. bivirgatus,* there is an additional selection pressure for rapid acting venom due to specialisation upon other venomous snakes, which in turn have a high chance of prey retaliation.

Toxins that target the blood coagulation cascade do so in one of two mutually exclusive functional mechanisms; overall net anticoagulation or procoagulation. Anticoagulant venoms, such as those found in most pit-vipers, participate in the formation of haemorrhagic shock through a combined chemical assault, which may include the use of procoagulant pathways as part of the net anticoagulant function. Targets ranging from the cleavage of fibrinogen (whether outright destruction or the use of procoagulant pathways to produce weak, unnatural clots that are readily broken down by the abundant plasmin produced by synergistic toxins, which activate plasminogen) through to platelets (aggregation inhibition or unnatural clumping effects, which disrupt the normal role platelets serve

in clotting), with these toxic effects accompanied by other toxins that increase the permeability of the vascular bed (Assafim et al., 2016; Calvete et al., 1991; Fry, 2015; Fry et al., 2009a; Gan et al., 1988; Gould et al., 1990; Samel et al., 2006). These venoms are often employed by ambush feeding vipers, which specialise upon warm-blooded prey items, and are able to be efficiently tracked post-bite using chemoreception and heat detection sensory arrays (Gracheva et al., 2010; Panzano et al., 2010). In contrast, strong clot forming procoagulant venoms are selected for lineages that feed upon prey with fast moving blood circulation rates. Such prey lineages are vulnerable to toxins that produce blood clots that rapidly subjugate through stroke induction, such as taipans (*Oxyuranus* species) feeding upon rodents (Herrera et al., 2012).

The African boomslang (*Dispholidus typus*) and the twig snakes (*Thelotornis* species) are closely related iconic African snakes belonging to the family Colubridae, and both inhabit arboreal, predatory niches that include prey items with a high potential for escape (Visser and Chapman, 1978; Weinstein et al., 2011). The limited work that has been undertaken upon them has revealed that both have clot-forming, procoagulant venoms (Chapman, 1968; Grasset and Schaafsma, 1940; Kamiguti et al., 2000; Smith and FitzSimons, 1958; Weinstein et al., 2011; Weinstein et al., 2013). While the venoms appear to be functionally similar in their potent action upon blood chemistry, the relative complexity of the venoms is unknown. While *Dispholidus* has been shown to have a venom dominated by P-III snake venom metalloprotease (SVMP) (Fry et al., 2008; Kamiguti et al., 2000; Pla et al., 2017), other toxin types are present in the venom in lower amounts (Fry et al., 2008; Fry et al., 2003b). In vipers, certain procoagulant P-III SVMPs have been shown to activate prothrombin (Bernardoni et al., 2014; Isbister, 2009; Joseph and Kini, 2002; Rosing and Tans, 1992) or Factor X (Bernardoni et al., 2014; Isbister, 2009; Tans and Rosing, 2002). Strong clot forming procoagulant function has been convergently evolved in the venom of *D. typus.* Similar activities are suggested for *T. capensis* (Atkinson et al., 1980). The venom composition for any *Thelotornis* species is unknown so the toxin type responsible for procoagulation can only be inferred as likely being a P-III SVMP like its related genera *Dispholidus.* From a functional perspective, these two related but very divergent snakes share a coagulotoxic action with their last common ancestor (Fry et al., 2008; Fry et al., 2003b). These snakes have evolved procoagulant venoms convergently in relation to vipers in the *Daboia* genus (Mukherjee, 2008, 2014) or elapids in the *Oxyuranus* or *Pseudonaja* genera (Isbister et al., 2010a; Marshall and Herrmann, 1983). *Daboia* use serine proteases to activate factor X, while *Oxyuranus* and *Pseudonaja* use a mutated factor Xa:factor Va complex to escape hemostatic control (Bos and Camire, 2010).

Dispholidus is genetically close to the genus *Thrasops*. *Dispholidus* and *Thrasops* are in turn sister to *Thelotornis.* The two genera differ in their occupied niches and morphology. *Dispholidus* is a monotypic genus consisting of the boomslang (*D. typus*), which is an active foraging snake with very

large eyes with circular pupils and acute vision, large round heads, and variable colour, ranging from uniform brown to green with darkened scale edges (Chapman, 1968; Weinstein et al., 2011). The large head is quite similar to the tree cobras (e.g. *Naja goldii*), including enlarged eyes. In contrast, *Thelotornis* is a genus of ambush feeding, highly cryptically and intricately patterned snakes with large eyes, horizontal pupils, and near binocular vision (Chapman, 1968; Shine et al., 1996; Weinstein et al., 2011). The elongate heads are convergently similar to other Colubridae, particularly the *Ahaetulla* genus from Asia and the *Oxybelis* genus of the southern U.S. and Central America.

Birds account for the majority of *Dispholidus* prey items as it hunts in the canopy. The fast-moving, endothermic blood circulatory system of avians is similar to mammals in being vulnerable to rapid prey subjugation by stroke formation, thus neutralising the high escape potential posed by prey items with flight ability. While lizards such as chameleons form a percentage of the *Dispholidus* diet (Visser and Chapman, 1978; Weinstein et al., 2011), they are non-dangerous and slow moving and are also taken during their diurnal activity period when blood circulation is at its maximum. *Thelotornis* may have a more complex diet than *D. typus* as it occupies a niche located near or on the forest floor and snakes of this genus are perhaps also more likely to be sensitive to prey escape potentials due to their slower movements relative to the fast moving *Dispholidus* (Shine et al., 1996; Visser and Chapman, 1978; Weinstein et al., 2011).

Neither genus of snakes was thought to be of significant medical consequence until each killed an eminent herpetologist (Robert Mertens and Karl Patterson Schmidt, respectively) (Pla et al., 2017). However, the ability for *D. typus* to cause serious harm to humans, and even death, had previously been reported by F.W. Fitzsimons as early as 1909 (Chapman, 1968; FitzSimons, 1909a, 1919; FitzSimons, 1962; Pope, 1958; Weinstein et al., 2011; Weinstein et al., 2013). Strikingly, *T. capensis* has been shown to produce nearly identical human clinical symptoms as reported for *D. typus*, with death the result of internal bleeding such as cerebral haemorrhage (Atkinson et al., 1980; Smith and FitzSimons, 1958; White, 2005). However, the existing antivenom manufactured to treat bites caused by *D. typus* is said to be ineffective in cases of *T. capensis* envenomation (Atkinson et al., 1980; Weinstein et al., 2011; Weinstein et al., 2013). While prey injected with significant concentrations of procoagulant venoms succumb to stroke (Martin, 1893), human deaths from these venoms are due to internal haemorrhage, due to the dilution of the procoagulant venom into a volume of blood much larger than the concentrated effects in prey animals, resulting in defibrinogenation due to venom induced consumptive coagulopathy (Fry, 2015; Herrera et al., 2012; Isbister, 2009; Isbister et al., 2010b; White, 2005).

Despite a monovalent antivenom existing and routinely administered to bite victims (Kamiguti et al., 2000; Weinstein et al., 2011), limited research has been conducted on the function of *D. typus* venom, with the literature being dominated by bite case reports or proteomics in the absence of bioactivity

testing. Even less is known about *Thelotornis* venoms, with limited previous publications having mainly dealt only with *T. capensis*, while the rest of the genus is unknown in its venom composition. We aimed to investigate the key similarities and differences between the two genera utilising a range of proteomic and bioactivity approaches to reconstruct their functional evolution in response to prey preference and ecological niche occupied. It is hypothesised that *T. mossambicanus* has a greater diversity of venom toxin components, reflective of its diverse diet and their associated heighted potential for prey escape, than the more specialised feeder *D. typus.*

2.3 Results

2.3.1 Skull and Venom Gland Anatomical Comparisons

Both species displayed enlarged rear-fangs, consistent with their demonstrated efficient venom delivery in predation and also defensive bites. Reflective of their difference in head shape, the *T. mossambicanus* venom gland was more elongate than that of *D. typus* (Figure 2.1).

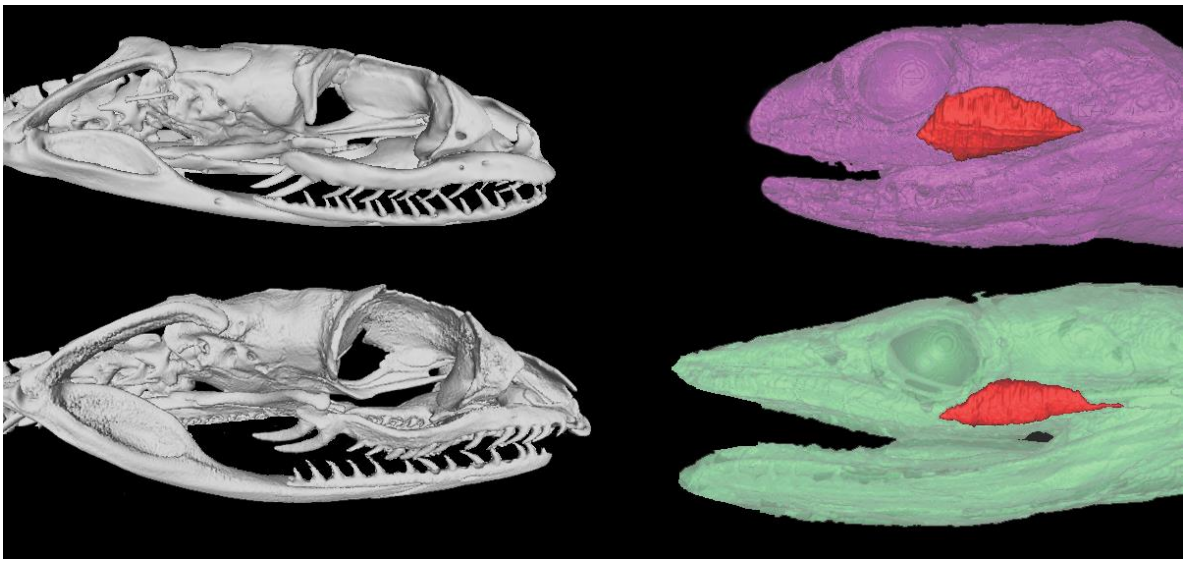

Figure 2.1 CT and MRI scan
Contrast tomography (left column) and magnetic resonance imaging (right column) comparison of *D. typus* (top row) and *T. mossambicanus* (bottom row).

2.3.2 Proteomics

Shotgun mass spectrometry analysis recovered the same five toxin types from each venom; CRiSP, PLA_2 Type IIE, 3FTx, and SVMP. However, 1D and 2D gels showed significantly different relative expression and complexity levels. While both 1D and 2D SDS gels indicate that both species are dominated by P-III SVMP (Figure 2.2 and Figure 2.3), *T. mossambicanus* also contained phospholipase A_2 (PLA_2 Type IIE) in high amounts. The presence of PLA_2 Type IIE is a significant discovery as it is the third type of PLA_2 to be characterised in snake venoms (Fry et al., 2012). The

molecular weights of identified P-III SVMP correspond to previous transcriptome and proteome data for *D. typus* (Pla et al., 2017).

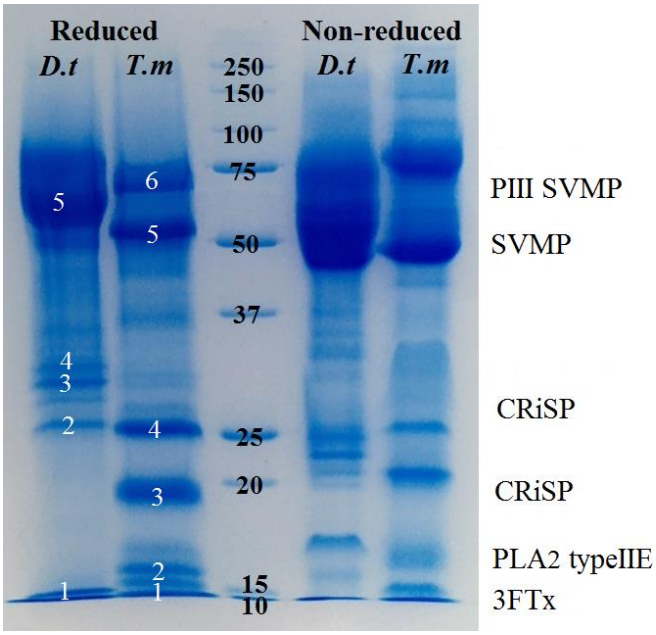

Figure 2.2 1D SDS Page
1D SDS page with identified groups of proteins. *D.t = Dispholidus typus*, *T.m = Thelotornis mossambicanus*. Reduced conditions on the left, Non-reduced conditions on the right. Molecular weight marker indicated by centered numbers (kDa). Annotations (right) refer to bands identified (white numbers) within the reduced column.

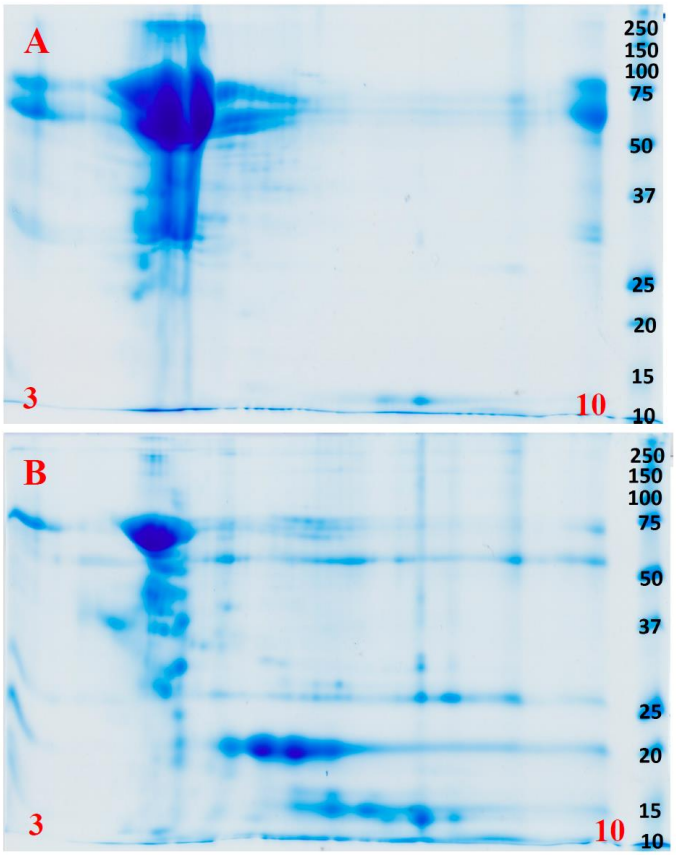

Figure 2.3 2D SDS Page
(A) 2D SDS page of *Dispholidus typus* under reducing conditions; (B) 2D SDS page of *Thelotornis mossambicanus* under reducing conditions. Molecular weight markers (kDa) are as for Figure 2. pI range is 3–10 (left to right) in red.

2.3.3 Enzymatic Assays

Fluorescent Determination of Matrix Metalloprotease and Kallikrein Activity

Despite *T. mossambicanus* having a more complex venom profile than *D. typus*, and thus lower relative amounts of P-III SVMP, it actually displayed a higher rate of cleavage of a matrix metalloprotease specific substrate (Figure 2.4). A two-way (RM) ANOVA ($\alpha = 0.05$) indicates that there is a significant difference in Column Factor (species and concentration), accounting for 78.6% of the total variance (after adjusting for matching); $F(3, 8) = 45.2$, $p < 0.001$. Tukey's post-hoc test indicated that there is a significant difference in activity between *D. typus* and *T. mossambicanus* at a concentration of 0.5 µg/100 µL ($p \leq 0.04$). The levels of *T. mossambicanus* were of a high level, similar to that of the viperid snake *Gloydius saxitilis* included for comparison.

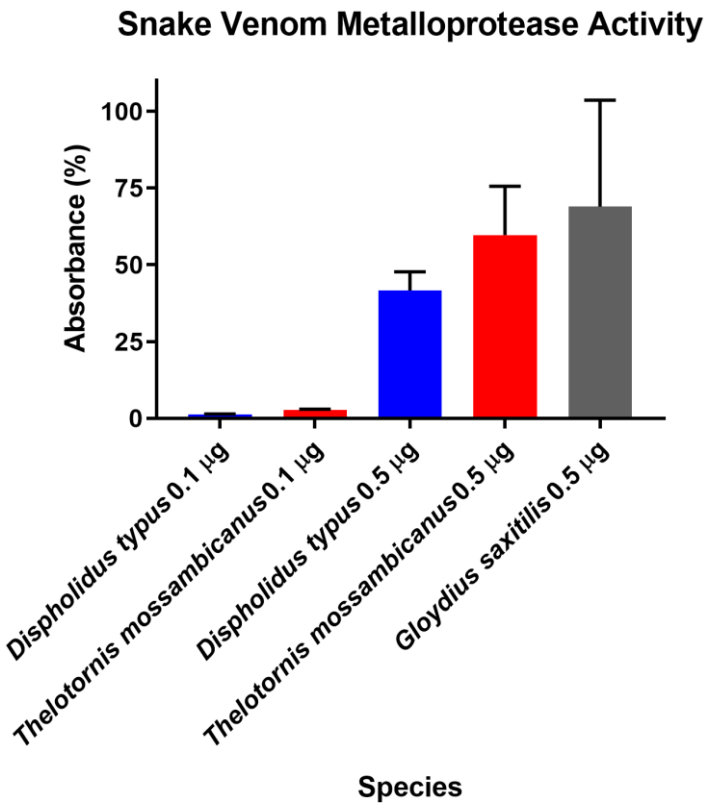

Figure 2.4 Snake Venom Metalloprotease Activity of venom
Snake Venom Metalloprotease Activity of venom (10 ng/µL and 50 ng/µL) was measured based on its ability to cleave a fluorogenic peptide substrate (Mca-PLGL-Dpa-AR-NH2 Fluorogenic MMP Substrate, Cat#ES001). Column graph of Matrix Metalloprotease activity assay of *D. typus* and *T. mossambicanus* obtained from normalisation of slope values. X axis: species name and concentration; Y axis: absorbance percentage. Analysis of triplicates was conducted on GraphPad PRISM 7.0 and error bars indicate standard deviation.

Contrastingly, *D. typus* venom demonstrated a much higher kallikrein activity compared to that of *T. mossambicanus*. *D. typus* had an active concentration of 0.1 µg/100 µL and 0.5 µg/100 µL, compared to *T. mossambicanus*, which was only slightly active at 0.5 µg/100 µL (Figure 2.5). A two-way (RM) ANOVA ($\alpha = 0.05$) indicates that there is a significant difference within the test, with Column Factor (species and concentration) accounting for 80.1% of the total variance (after adjusting for matching); $F(3, 7) = 136.6$, $p \leq 0.001$. Tukey's post-hoc test indicated that there is a highly significant difference in activity between *D. typus* and *T. mossambicanus* at both concentrations ($p \leq 0.001$). This is indicated by the increased presence of kallikrein-like serine proteases in *D. typus*' venom profile (Figure 2.2). However, even the proportionally higher *D. typus* activity levels were insignificant in relation to the representative viperid *Trimeresurus vogeli* included for comparison, thus indicating that this function is a trivial aspect of the venom, consistent with the non-detection in our proteomics and low-levels in the published *D. typus* transcriptome (Pla et al., 2017).

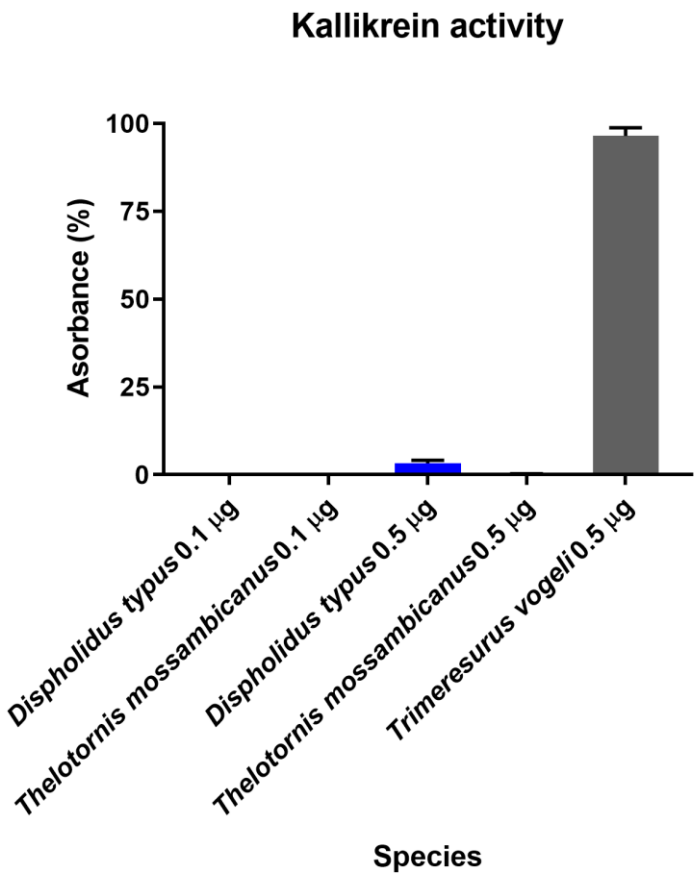

Figure 2.5 Kallikrein activity of venom
The kallikrein activity of venom (10 ng/µL and 50 ng/µL) was measured based on its ability to cleave a fluorogenic peptide substrate (Boc-VPR-AMC Fluorogenic Peptide Substrate, Cat#ES011). Column graph of Kallikerin activity assay of *D. typus* and *T. mossambicanus* obtained from normalisation of slope values. There is a highly significant difference in activity between *D. typus* and *T. mossambicanus* at both concentrations ($p \leq 0.001$). X axis: species name and concentration; Y axis: absorbance as a percentage. Analysis of triplicates was conducted on GraphPad PRISM 7.0 and error bars indicate standard deviation.

2.3.4 Fluorescent Determination of sPLA$_2$ Activity

We tested for continuous secretory phospholipase A_2 (sPLA$_2$) enzymatic activity over 100 measurement cycles using and following the EnzChek® Phospholipase A_2 Assay Kit (Cat#E10217). *T. mossambicanus* showed increased levels of sPLA$_2$ activity compared to *D. typus* at a concentration of 50 ng/µL (Figure 2.6). This increase in activity by *T. mossambicanus* is also mimicked in the venom profiling of both venoms via 1D SDS PAGE (Figure 2.2). A two-way RM ANOVA ($\alpha = 0.05$) indicates that there is a significant difference within the assay, with Column Factor (species and concentration) accounting for 63.41% of total variance (after adjusting for matching); $F(2, 6) = 78.75$, $p \leq 0.001$. Tukey's post-hoc test indicated there is a highly significant difference in activity between *D. typus* from the positive control and between *D. typus* and *T. mossambicanus* ($p \leq 0.001$). Tukey's post-hoc test also indicates a significant difference of *T.*

mossambicanus from the positive control ($p \leq 0.01$). The *T. mossambicanus* levels were similar to that of the representative viperid snake *Azemiops feae* included for comparison.

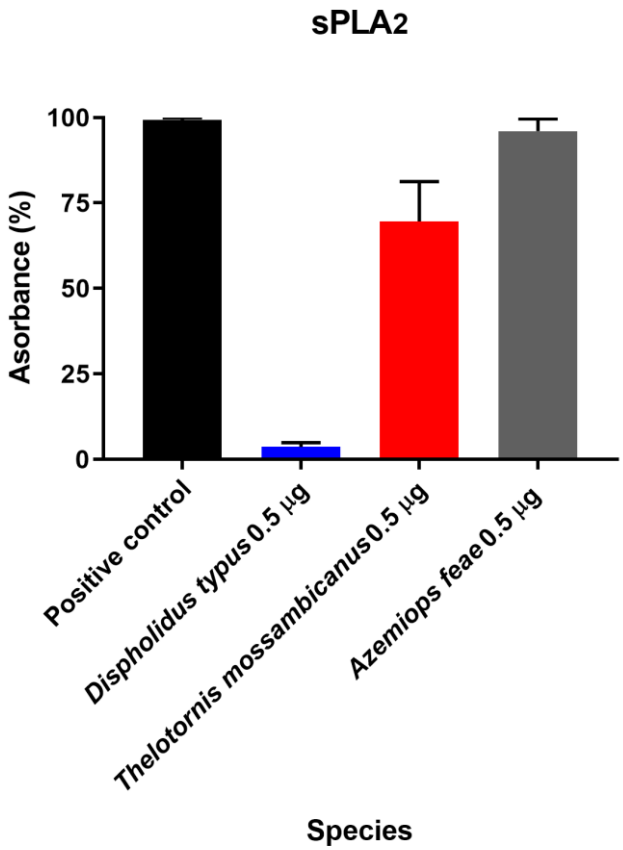

Figure 2.6 Phospholipase A_2 activity
Secretory Phospholipase A_2 was measured by its ability to cleave a fluorogenic peptide substrate EnzChek® (Cat# E10217). Column graph of $sPLA_2$ activity assay of *D. typus* and *T. mossambicanus* obtained from normalisation of slope values. There is a highly significant difference in activity between *D. typus* from the positive control and between *D. typus* and *T. mossambicanus* ($p \leq 0.001$). There is also a significant difference of *T. mossambicanus* from the positive control ($p \leq 0.01$). X axis: species name and concentration; Y axis: slope as a relative percentage. Analysis of triplicates was conducted on GraphPad PRISM 7.0 and error bars indicate standard deviation.

2.3.5 Procoagulation Analysis

While both venoms were potently procoagulant, we find that the venom of *T. mossambicanus* is much faster compared to that of *D. typus* (Figure 2.7 and Figure 2.8). At a 20 µg/mL concentration, *T. mossambicanus* venom clots the plasma on average in 7.5 sec (SD 0.15 sec), compared to *D. typus*, which clots the plasma on average in 11.2 sec (SD 0.06 sec) (Table 2.1). The *T. mossambicanus* venom is amongst the most potently coagulotoxic of any we have tested, being on par with *Oxyuranus* and *Pseudonaja* venoms tested under identical conditions (unpublished results). At a 0.05 µg/mL concentration, *T. mossambicanus* venom clots the plasma on average in 80.4 sec (SD 0.52 sec), compared to *D. typus*, which clots the plasma on average in 146.6 sec (SD 5.23 sec) (Table 2.1). Figure 2.6 demonstrates the relative potency of *T. mossambicanus* venom against human plasma, compared to *D. typus*, in the reduced variation in clotting times between dilutions. The distance

between the first vertical line and the second vertical line is longer in *T. mossambicanus* than in *D. typus*, illustrating that there is a longer rise in clotting times, depicting that *T. mossambicanus* venom holds its potency between dilutions more so than *D. typus* (Figure 2.7, Table 2.2). This is also demonstrated by the point where the curve crosses the X axis, which is higher in *D. typus* than in *T. mossambicanus* (R0 ϕ_2 = 37.83 and 23.17 sec respectively) (Table 2.2). The additional investigation with and without cofactors $CaCl_2$ and phospholipid had no impact on the clotting times of either species, with clotting times remaining the same at all dilutions (*data not shown*). This is indicative of both venoms being calcium and phospholipid independent in exerting their procoagulant coagulotoxic actions.

Table 2.1 Average clotting times
Average clotting times with standard deviations (SD) (in seconds) of *D. typus* and *T. mossambicanus* at varying dilutions with and without the addition of boomslang antivenom.

Concentration	**Without Antivenom**				**With Antivenom**			
	D. typus		***T. mossambicanus***		***D. typus***		***T. mossambicanus***	
	Mean	SD	Mean	SD	Mean	SD	Mean	SD
20 µg/mL	11.27	0.06	7.57	0.15	20.73	1.07	9.6	0.17
10 µg/mL	15.95	1.88	9.55	0.17	155	5.2	16	0.17
6.66 µg/mL	19.34	0.21	11.20	0.34	214.56	21.28	21.16	0.23
5 µg/mL	21.22	0.22	12.43	0.08	255	10.56	35.13	1.32
3.33 µg/mL	24.72	0.22	14.95	0.65	343.2	8.97	43.33	1.86
2.5 µg/mL	27.63	0.14	16.45	0.18	432.3	35.32	53.43	0.11
2 µg/mL	30.91	0.47	18.27	0.13	444.93	23.43	58.46	1.29
1.33 µg/mL	36.32	1.61	20.50	0.58	525.86	51.19	75.43	2.15
1 µg/mL	39.60	0.54	24.30	0.74	594.86	61.15	83.33	3.86
0.66 µg/mL	43.91	0.56	27.44	1.03	735.3	6.94	100.8	1.97
0.4 µg/mL	53.77	6.21	31.67	0.19	790.36	9.41	128.4	0.52
0.25 µg/mL	61.95	7.95	35.91	0.64	966.76	35.88	163.23	2.6
0.125 µg/mL	83.31	6.51	54.89	0.14	999	0	226.33	2.6
0.05 µg/mL	146.65	5.23	80.44	0.52	999	0	381.23	4.71

Table 2.2 Asymptotic regression model coefficient estimates
Asymptotic regression model coefficient estimates for *D. typus* and *T. mossambicanus* normal plasma clotting times. In this example, ϕ_1 is the asymptote as x (concentration) approaches ∞, ϕ_2 is the response at $x = 0$, and $t_{0.5}$ is the half-life. Parameter ϕ_3 is the logarithm of the rate constant which is used to enforce positivity so that an asymptote is reached in the model. The corresponding half-life is written $t_{0.5} = \log 2/\exp(\phi_3)$. Analysis and output performed in R Studio (refer to methodology *3.4.3 Coagulation Statistical analysis*).

Species	**Coefficient Estimates**		
	Aym ϕ_1	**R0 ϕ_2**	**lrc ϕ_3**
D. typus	9.095161 (s)	37.83835 (s)	−0.6711807
T. mossambicanus	2.068652 (s)	23.17609 (s)	−0.8289048

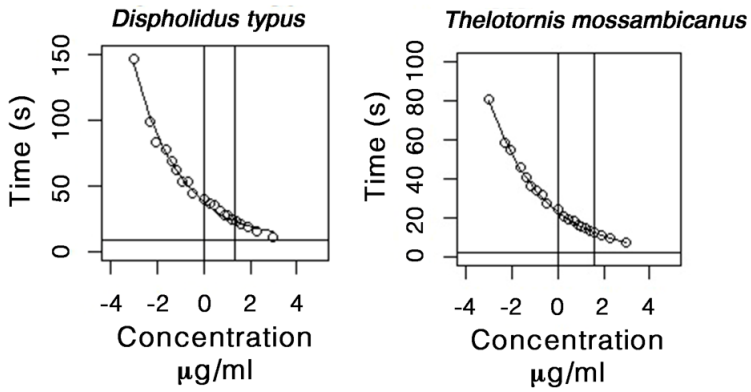

Figure 2.7 Asymptotic plot
Asymptotic plots of *D. typus* and *T. mossambicanus* procoagulation clotting against human plasma. Asymptotic time depicted by horizontal line, *D. typus* asymptote 9.09 (sec), *T. mossambicanus* asymptote 2.06 (sec). X axis: log concentration (µg/mL). Y axis: Time in seconds. Analysis and plots created in R Studio.

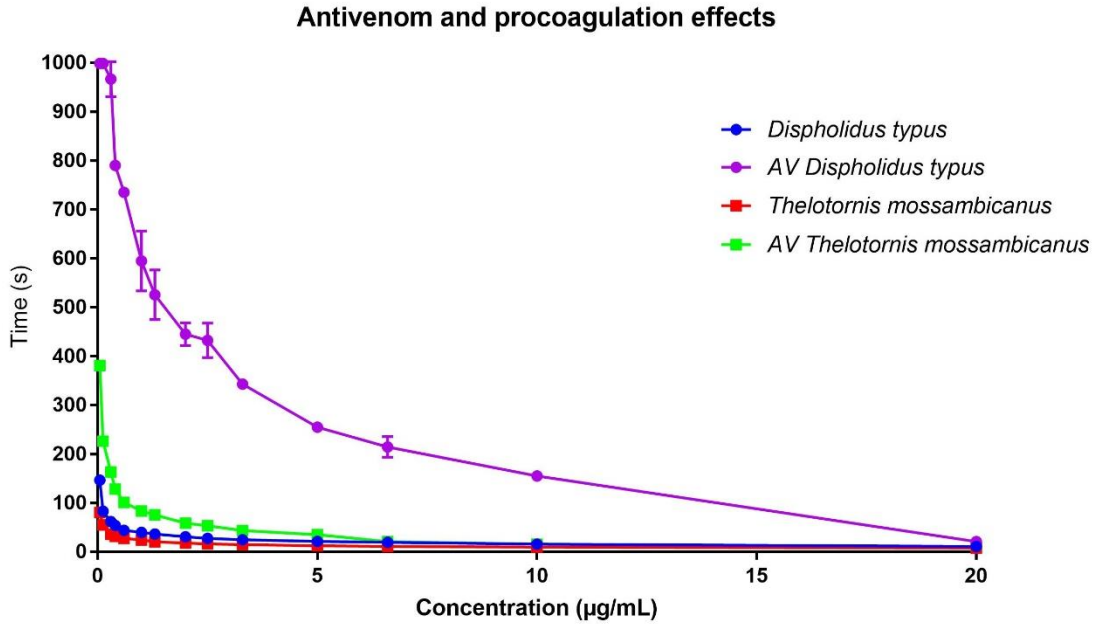

Figure 2.8 Coagulation and antivenom clotting curves
Comparison of procoagulation clotting curves of *D. typus* and *T. mossambicanus*, with and without the addition of antivenom. *D. typus* clotting curve given in blue circles, AV *D. typus* = antivenom response curve given in purple circles, *T. mossambicanus* clotting curve given in red squares, AV *T. mossambicanus* = antivenom response curve given in green squares. X axis: final venom concentration (µg/mL), Y axis: clotting time in seconds. Values are averages of triplicates (single dilution measured three times) and standard deviation error bars are shown for each, although for most the error range is smaller than the line icon.

With the addition of diluted boomslang monovalent antivenom to the dilution series, it is evident that the antivenom neutralises *D. typus* remarkably well, in contrast to having little neutralising effect on *T. mossambicanus* (Figure 2.8). At 20 µg/mL venom concentration with the antivenom at a final concentration in the 250 µL cuvette volume of 1% of that of the original vial concentration, *T.*

mossambicanus clotted the plasma in 9.6 sec (SD 0.17 sec) instead of the 7.5 sec without antivenom, compared to *D. typus*, which clotted the plasma at 20.7 sec (SD 1.07 sec) instead of the 11.2 sec without antivenom (Table 2.1). At a 0.05 µg/mL venom concentration, the added antivenom had some effect on *T. mossambicanus*, which clotted in 381.2 sec (SD 4.71 sec) instead of 80.4 sec without antivenom (Table 2.1). *D. typus* however reached maximum clotting time of 999.9 sec (Table 2.1) at a venom concentration of 0.05 µg/mL with the addition of antivenom, demonstrating a significantly greater effective neutralising ability against this species.

Comparing EC_{50} outputs, it is evident that, despite the variation in clotting times between the species (Figure 2.8), half-maximal concentration is reached at a similar point by both species. This is due to the dilution series following the same trajectory regardless of time (Figure 2.8). When transformed, this trajectory becomes more evident, as there is little x-axis difference between *T. mossambicanus* with and without antivenom (0.24 µg/mL: 95% CI 0.22–0.26 µg/mL, and 0.23 µg/mL: 95% CI 0.20–0.26 µg/mL respectively) and *T. mossambicanus* and *D. typus* without antivenom (0.24 µg/mL and 0.20 µg/mL: 95% CI 0.18–0.23 µg/mL respectively) (Figure 2.9). However, when antivenom is introduced with *D. typus*, the EC_{50} x-axis shifts significantly to the right (1.62 µg/mL: 95% CI 1.49–1.76 µg/mL) (Figure 2.9). Due to each sub data set being transformed, first by log concentration and then the normalisation of clotting time, each final data point reaches 100% (Figure 2.9). Taking into account the y-axis shift in addition to the x-axis shift (Figure 2.8), the *T. mossambicanus* venom has an antivenom induced relative shift in the clotting curve of 4.69, while the *D. typus* venom has an antivenom induced relative shift in the clotting curve of 53.12. Thus, the antivenom is 11.3 times more effective at neutralizing *D. typus* venom than *T. mossambicanus* venom. Thus, if the antivenom had no significant effect upon *T. mossambicanus* under such ideal circumstances as conducted in this study, then there is little chance of it having a therapeutic effect in a clinical scenario without the use of extreme amounts of antivenom.

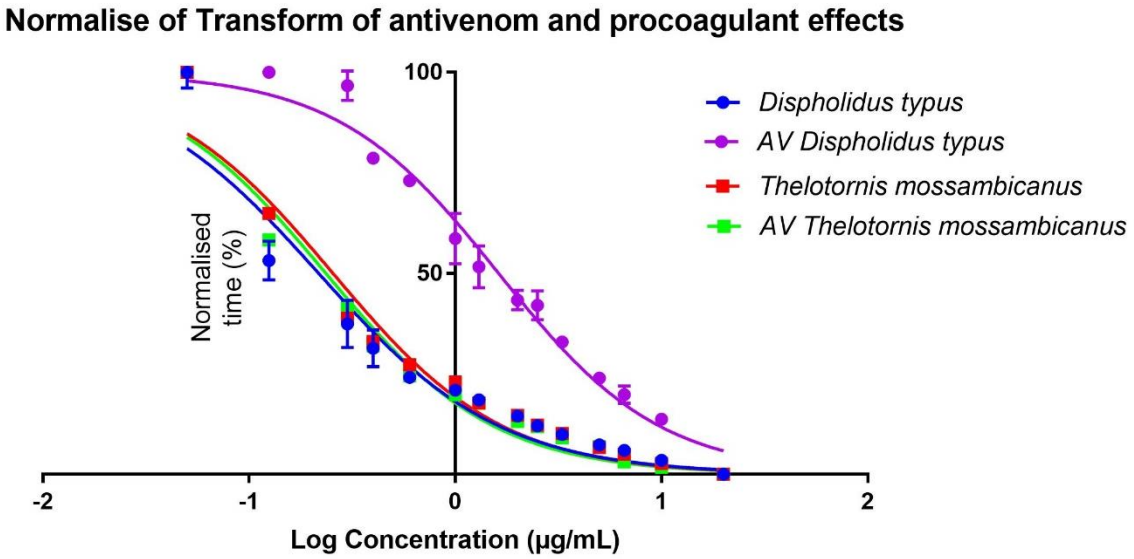

Figure 2.9 Normalisation of transformed data
Normalisation of transformed data; antivenom and procoagulant effects of *D. typus* and *T. mossambicanus*. *D. typus* clotting curve given in blue circles, AV *D. typus* = antivenom response curve given in purple circles, *T. mossambicanus* clotting curve given in red squares, AV *T. mossambicanus* = antivenom response curve given in green squares. X axis: log concentration, Y axis: Normalised time (%) (for sub data sets). Analysis performed in GraphPad PRISM 7.0. Values are averages of triplicates (single dilution measured three times), and standard deviation error bars are shown for each, although for most the error range is smaller than the line icon.

2.4 Discussion

Both venoms tested here were found to be highly procoagulant without requiring calcium or phospholipid as co-factors. However, *T. mossambicanus* is notably more potent than *D. typus*, as well as being extremely poorly neutralised by SAIMR boomslang antivenom (Table 2.1 and Table 2.2, Figure 2.7, Figure 2.8 and Figure 2.9). The decoupling from co-factors is a notable discovery as this lack of shift between tests with or without co-factors had only been well-documented for *Echis carinatus.* This is the first extensive antivenom comparison of both species marking the relative effectiveness of the available boomslang monovalent antivenom.

Previous reports have described these two species as exhibiting strikingly similar lethal envenomations (Atkinson et al., 1980; Chapman, 1968; FitzSimons, 1909a, 1919; FitzSimons, 1962; Pope, 1958; Smith and FitzSimons, 1958; Weinstein et al., 2011; Weinstein et al., 2013) that can be attributed to their venoms being dominated by P-III SVMPs (Figure 2.2 and Figure 2.3). It is notable that, despite *T. mossambicanus* having a lower concentration of SVMP due to its greater venom complexity, it displayed a higher relative rate of metalloprotease activity in addition to being more potently coagulotoxic (Figure 2.4, Figure 2.7 and Figure 2.8). Further, *T. mossambicanus* possesses two distinct molecular weight classes of SVMP as opposed to the single band present in *D. typus* venom (Figure 2.2). Thus, the differential proteomics profile is mirrored by differential coagulotoxic activity. This key difference between the species' venom profiles may also shed light as to why the

available antivenom for *D. typus* has only a small neutralising effect on *T. mossambicanus* venom (Figure 2.8 and Figure 2.9, Table 2.1).

Calcium-independent prothrombin activation is a rare feature in snake venoms, with most venoms typically requiring calcium for such a coagulotoxic activity. A previously documented notable exception is the ecarin-type P-III SVMP from *Echis carinatus*, which does not have a marked shift between tests with or without co-factors (Kornalik and Blombäck, 1975; Rosing and Tans, 1992). Thus, the presence of such an activity in the venoms of these two colubrid snakes' points towards a remarkable case of functional convergence within the same toxin class.

Procoagulation accompanied by plasmin inhibition is an effective way to potentiate the coagulotoxic effects as the blood clots formed would have a longer half-life since the role of plasmin is to break blood clots down. This synergistic activity has been documented in viper venoms (e.g. *Daboia*) and elapid venoms (e.g. *Pseudonaja*), where the procoagulation is accomplished by very different toxin types (SVMP and fXa:fVa, respectively), but the plasmin inhibition is exerted by the same toxin type (kunitz peptide) (Cheng and Tsai, 2014; Masci et al., 2000). However, neither *D. typus* or *T. mossambicanus* venoms displayed this synergistic action.

Despite having the same procoagulant mechanism, it appears evident that additional external evolutionary pressures are driving the variation between these two species. In addition to differential complexity, the venoms were functionally variable relative to each other in non-procoagulant activities, with *D. typus* having serine protease activity (Figure 2.5), while conversely *T. mossambicanus* had strong PLA_2 activity (Figure 2.6). It is known that evolution among arboreal specialists further influences venom composition of toxins' families (Debono et al., 2016). This is usually in the form of prey ecology, dependent on niche occupation. Even though both species occupy an arboreal habitat, their differential morphology and behaviour allow for varying prey interactions, thus potentially further contributing to venom variation and punctuated evolution. As *D. typus* is an agile and fast-moving snake, it is able to pursue prey, thus minimising escape potential. *T. mossambicanus* however is a slower moving cryptic snake that ambush feeds, and thus the prey escape potential may be significantly higher. Thus, there may be a stronger selection pressure operating upon *T. mossambicanus* for a venom which rapidly immobilises prey. This is consistent with what has been observed in other lineages of venomous animals in which prey escape potential is a significant shaping factor and thus the venom is under extreme selection pressure for rapid immobilising action (Aman et al., 2015; Dutertre et al., 2014; Eng et al., 2015; Fry, 2015; Fry et al., 2015a; Fry et al., 2015c; Harvey and Anderson, 1985; Harvey and Karlsson, 1980; Herrera et al., 2012; Jackson et al., 2013; Jin et al., 2015; Karlsson et al., 1983; Osman et al., 1973; Utkin et al., 2015; Yang et al., 2016).

Thus, this investigation not only has revealed the differential evolution of *D. typus* and *T. mossambicanus* venoms and the poor performance of boomslang antivenom against *T. mossambicanus* venom, but it has also reinforced that there are commonalities to venom evolution such that there may be levels of predictability in regards to niche occupation and prey escape potential shaping venom relative rates of action. The differences in ecological niches occupied was also reflected in differential skull morphology (Figure 2.1). This reinforces that, in addition to the applied application of venom research in regards to biodiscovery and clinical effects, research such as this contributes to the growing body of venom evolutionary theory.

2.5 Materials and Methods

2.5.1 Venom Supplies

Pooled venoms from *Dispholidus typus* (South African origin) and *Thelotornis mossambicanus* (Mozambique) were supplied by Latoxan (Portes-lès-Valence, France).

2.5.2 Micro-Computed Tomography (CT)

We scanned representative boomslang (*Dispholidus typus*) and the twig snakes (*Thelotornis mossambicanus*) with a Siemens Inveon micro-CT scanner. The scanner was operated at 80 KV energy, 250 µA intensity with 360 projections per 360°, and 2300 ms exposure time. The samples were scanned at a nominal isotropic resolution of 27.8 µm. The data were reconstructed using a Feldkamp conebeam back-projection algorithm provided by an Inveon Acquisition Workstation from Siemens. The images in 3D were visualized and processed with ImageJ v1.51f (Schneider et al., 2012), Materialise Mimics v19.0 (Materialise, Leuven, Belgium), and MeshLab v1.3.3 (Institute of the National Research Council of Italy, Pisa, Italy).

2.5.3 Magnetic Resonance Imaging

MRI was used to obtain a three-dimensional (3D) shape of the venom glands without intrusive dissection or sectioning techniques. For fixation, neutral buffered formalin (NBF) preserved specimens had the formalin removed by four individual hours of washing steps in phosphate buffered saline (PBS) and incubated overnight in 0.1% Magnevist® (Bayer, Leverkusen, Germany) in PBS. After the removal of NBF, the sample was submersed in perfluoro-ether Fomblin (Solvay Solexis, Alessandria, Italy) and placed under vacuum to prevent air artifacts. Imaging was performed on a 16.4 T (700 MHz) vertical 89-mm-bore system (Bruker BioSpin, Rheinstetten, Germany) using a Bruker Micro 2.5 gradient system (2.5 G/cm A), transmit/receive radiofrequency coils with diameters of 10 mm, and a quadrature birdcage resonator (M2M Imaging, Brisbane, Australia). Bruker ParaVision 6.0.1 software was used for image acquisition and anatomical images were acquired using

a 3D FLASH (Fast Low Angle Shot) gradient echo sequence. The imaging parameters were: TR/TE = 50/8 ms, flip angle 30 °C, two excitations. The field-of-view and matrix sized to fit the sample with the resulting voxels having 50–62.5 μm isotropic resolution. Total scan time was approximately 1 h per sample. MRI data was processed using Medical Imaging Processing, Analysis, and Visualization v6.0.0 (MIPAV, Centre for Information Technology, National Institutes of Health, Bethesda, MD, USA), and 3D image segmentation, surface rendering, and volumetric measurements of the glands were performed manually using ITK-SNAP (Yushkevich et al., 2006).

2.5.4 Proteomics

Our proteomic investigations including using 1D and 2D SDS-PAGE, protein band purification and crude venom Shotgun analysis. They were performed as previously described by us (Debono et al., 2016) with the exception of additional LC-MS/MS analysis, following protein extraction from isolated 1D gel bands. Shotgun samples were analyzed using the methods described below.

2.5.5 Nano HPLC-ESI-Triple Time of Flight (TOF) Mass Spectral Analysis

Protein extracts from gel bands were analysed by LC-MS/MS using a Q Exactive™ Hybrid Quadrupole-Orbitrap Mass Spectrometer (Thermo Fisher Scientific, Waltham, MA, USA) equipped with a nano electrospray ion source. An aliquot (8 μL) of each extract was injected onto a C18 trap column (75 μm × 2 cm, Thermo Scientific, Waltham, MA, USA) at 6 μL/min. Samples were de-salted on the trap column for 5 min using 0.1% formic acid at 6 μL/min. The trap column was then placed in-line with the analytical nano HPLC column (15 cm × 75 μm C18, 3.5 μm, Thermo Fisher Scientific, Waltham, MA, USA) for mass spectrometry analysis. Solvent A consisted of 2% ACN/0.1% formic acid, and solvent B contained 100%ACN, 2% LC-MS water, and 0.1% formic acid. Peptide elution was made possible via linear gradients of 1 to 40% solvent B over 32 min at 300 nl/min flow rate, followed by a steeper gradient from 40% to 95% solvent B over 3 min. Solvent B was held at 95% for 2.5 min to allow for washing of the column and returned to 1% solvent B for equilibration prior to the next sample injection. The ion spray voltage was set to 1.8 kV, and the temperature of capillary was 300 °C. The mass spectrometer acquired 3×10^6 ion count with the max injection time of 20 ms for a full scan TOF-MS data followed by 10^6 ions count with the max injection time of 110ms for a full scan product ion data in an Information Dependant Acquisition (IDA) mode. Full scan TOF-MS data was acquired over the mass range of 300–1800 m/z, while the product ion ms/ms was 100–1800 m/z. Ions observed in the TOF-MS scan exceeding a threshold of 1.8×10^5 for the precursor selection with a charge state of $^+1$ to $^+8$ were set to trigger the acquisition of the product ion, with ms/ms spectra of the resultant 20 most intense ions. The data was acquired and processed using Xcalibur™ software (Thermo Fisher Scientific, Waltham, MA, USA).

2.5.6 Protein Identification

Protein database searches were conducted against Uniprot for broad protein identification. A composite target decoy database was built with the forward and reverse sequences for calculating the FDR. Proteins were identified by database searching using PEAKS v7.5 (Bioinformatics Solutions Inc., Waterloo, ON, Canada) against the protein database. The search parameters were as follows: precursor ion mass tolerance, 10 ppm; fragment ion mass tolerance, 0.05 Da; fully tryptic enzyme specificity; one missed cleavage; monoisotopic precursor mass a fixed modification of cysteine carbamidomethylation; and variable modifications, including methionine oxidation, conversion of glutamine and glutamic acid to pyroglutamic acid, deamidation of asparagine, phosphorylation, acetylation, and sulfation. For PEAKS, *de novo* sequencing, database search, and characterising unspecific post-translational modifications (PTMs) were used to maximise the identifications; false discovery rate (FDR) was set to ≤1%; and the individual peptide ion score [−10·Log(p)] was calculated accordingly, where p is the probability that the observed match is a random event.

2.5.7 Orbitap Elite Mass Spectrometer for SHOTGUNS

For LC-MS/MS analysis, the parameters are as follows; the samples were separated using RP-chromatography on a Dionex Ultimate 3000 RSLC nano-system (Lifetech, Carlsbad, CA, USA). The samples were desalted on a Thermo PepMap 100 C18 trap (Lifetech, Carlsbad, CA, USA) (0.3 × 5 mm, 5 µm) for 5 min with a flow rate of 30 µL/min. This was followed by separation on an Acclaim PepMap RSLC C18 (Lifetech, Carlsbad, CA, USA) (150 mm × 75 µm) column at a flow rate of 300 nL/min. A gradient of 10%–70% was applied buffer B over 7 min, where buffer A (1% ACN/0.1% FA) and buffer B (80% ACN/0.1% FA) were used to separate peptides. The eluted peptides were directly analysed on an Orbitap Elite mass spectrometer (Thermo Scientific, Carlsbad, CA, USA) using an NSI electrospray interface. The source parameters included a capillary temperature of 275°C; S-Lens RF level at 60%, source voltage of 2 kV, and maximum injection times of 200 ms for MS and 150 ms for MS2. The instrument parameters included an FTMS scan across m/z range 350–1800 at 60,000 resolution followed by information dependent acquisition of the top 10 peptides across m/z 40–1800. Dynamic ion exclusion was employed using a 15 sec interval. Charge state screening was enabled with the rejection of +1 charged ions, and monoisotopic was precursor selection enabled. Data was converted to mascot generic format (mgf) using the msConvert software (ProteoWizard v3.0.9576, SCIEX, Concord, ON, Canada) and searched using Protein Pilot™ v5.0 (SCIEX, Concord, ON, Canada,) via the Uniprot database ‘metazoa’.

2.5.8 Enzymatic Activity Assays

2.5.8.1 Fluorescent Determination of Matrix Metalloprotease and Kallikrein Activity

A working stock solution of freeze dried venom was reconstituted in a buffer containing 50% MilliQ/50% glycerol (>99.9%, Sigma, St Louis, MO, USA) at a 1:1 ratio to preserve enzymatic activity and reduce enzyme degradation. Varying concentrations of crude venom (10 ng/μL and 50 ng/μL) were plated out in triplicates on a 384-well plate (black, Lot#1171125, nunc™ Thermo Scientific, Rochester, NY, USA) and measured by adding 90 μL quenched fluorescent substrate per well (total volume 100 μL/well, 10 μL/ 5mL enzyme buffer, 150 mM NaCl, and 50 mM Tri-HCl (pH 7.3), Fluorogenic Peptide Substrate, R & D systems, Cat#ES001 & ES011, Minneapolis, Minnesota). Fluorescence was monitored by a Fluoroskan Ascent™ (Thermo Scientific, Vantaa, Finland) Microplate Fluorometer (Cat#1506450, Thermo Scientific, Vantaa, Finland) (Cat#ES001 for Matrix Metalloprotease at an excitation of 320 nm, emission at 405 nm; Cat#ES011 for Kallikrein at an excitation of 390 nm, emission at 460 nm) over 400 min or until activity had ceased. Data was collected using Ascent® Software v2.6 (Thermo Scientific, Vantaa, Finland).

2.5.8.2 Fluorescent Determination of PLA_2 Activity

We assessed the continuous Phospholipase A_2 (PLA_2) activity of the venoms using a fluorescence substrate assay (EnzChek® Phospholipase A_2 Assay Kit, Cat#E10217, Thermo Scientific, Rochester, NY, USA), measured on a Fluoroskan Ascent® Microplate Fluorometer (Cat#1506450, Thermo Scientific, Vantaa, Finland). As above, we used a working stock solution of freeze dried venom reconstituted in a buffer containing 50% MilliQ / 50% glycerol (>99.9%, Sigma) at a 1:1 ratio. A concentration of enzyme activity in venom (50 ng/μL) was brought up in 12.5 μL 1× PLA_2 reaction buffer (50 mM Tris-HCL, 100 mM NaCl, 1 mM $CaCl_2$, pH 8.9) and plated out in triplicates on a 384-well plate (black, Lot#1171125, nunc™ Thermo Scientific, Rochester, NY, USA). The triplicates were measured by dispensing 12.5 μL quenched 1 mM EnzChek® (Thermo Scientific, Rochester, NY, USA) Phospholipase A_2 Substrate per well (total volume 25 μL/well) over 100 min or until activity had ceased (at an excitation of 485 nm, emission 538 nm). Purified PLA_2 from bee venom (1 U/mL) was used as a positive control and data was collected using Ascent® Software v2.6 (Thermo Scientific, Vantaa, Finland).

2.5.8.3 Enzymatic Statistical Analysis

For each of the methods performed on the Fluoroskan Ascent™ (Thermo Scientific, Vantaa, Finland) Microplate Fluorometer (Cat#1506450, Thermo Scientific, Vantaa, Finland), data was collected using Ascent® Software v2.6 (Thermo Scientific, Vantaa, Finland). All raw data were firstly blank corrected using the Ascent® software (v2.6, Thermo Scientific, Vantaa, Finland) package and then exported for

further analysis using Windows Excel 2016 and GraphPad PRISM 7.0 (GraphPad Prism Inc., La Jolla, CA, USA).

Graphs: Using Excel, averages of blank corrected data triplicates were calculated. From these averages, maximum absorbance was calculated and absorbance value plotted in a column graph for relative percentages.

Two-way (RM) ANOVA and Tukey's Post-hoc test: the blank corrected data was transformed, setting the top value as 100 and lowest as 0 across sub columns within a data set. A two-way repeated measures (RM) ANOVA was performed, followed by a Tukey's post-hoc multiple comparison test, comparing every mean with every other mean.

2.5.9 Procoagulation Analysis

2.5.9.1 Whole Plasma Clotting

Healthy human plasma (citrate 3.2%, Lot#1690252, approval # 16-04QLD-10) was obtained from the Australian Red Cross (44 Musk Street, Kelvin Grove, Queensland 4059). Coagulopathic toxin effects were measured by a modified procoagulant protocol on a Stago STA-R Max coagulation robot (France) using Stago Analyser software v0.00.04 (Stago, Asniéres sur Seine, France). Plasma clotting baseline parameters were determined by performing the standardised activated Partial Thromboplastin Time (aPTT) test (Stago Cat# T1203 TriniCLOT APTT HS). This was used as a control to determine the health of normal clotting plasma according to the universal standard range of between 27–35 sec. Plasma aliquots of 2 mL, which had been flash frozen in liquid nitrogen and stored in a −80 °C freezer, were defrosted in an Arctic refrigerated circulator SC150-A40 at 37°C. In order to determine clotting times effected by the addition of varying venom concentrations, a modified aPTT test was developed. A starting volume of 50 µL of crude venom (5 µg/50 µL) was diluted with STA Owren Koller Buffer (Stago Cat# 00360). A 14-dilution series of 1 (20 µg/mL), 1/2 (10 µg/mL), 1/3 (6.66 µg/mL), 1/4 (5 µg/mL), 1/6 (3.33 µg/mL), 1/8 (2.5 µg/mL), 1/10 (2 µg/mL),1/15 (1.33 µg/mL), 1/20 (1 µg/mL), 1/30 (0.66 µg/mL), 1/50 (0.4 µg/mL), 1/80 (0.25 µg/mL), 1/160 (0.125 µg/mL), and 1/400 (0.05 µg/mL) was performed in triplicate. $CaCl_2$ (50 µL; 25 mM stock solution Stago Cat# 00367 STA $CaCl_2$ 0.025M) was added with 50 µL phospholipid (solubilized in Owren Koller Buffer adapted from STA C.K Prest standard kit, Stago Cat# 00597). An additional 25 µL of Owren Koller Buffer was added to the cuvette and incubated for 30 sec at 37°C before adding 75 µL of human plasma. Relative clotting was then monitored for 999 sec or until plasma clotted (whichever was sooner). Additional tests were run, both with and without $CaCl_2$ and phospholipid, respectively, to test for $CaCl_2$ or phospholipid dependency. STA Owren Koller Buffer

was used as a substitute, using the same volumes to allow for consistency in the final volumes (250 µL).

2.5.9.2 Antivenom Studies

The monovalent antivenom effects on both *D. typus* and *T. mossambicanus* crude venoms was investigated. Previously established whole plasma clotting times against both venoms were measured and used as a guide for antivenom effects. The South African Institute for Medical Research Boomslang Antivenom (refined equine immunoglobulins, Lot M03852) was purchased from South African Vaccine Producers Pty Ltd (1 Modderfontein Rd Edenvale, Gauteng). One vial of antivenom (10 mL) was centrifuged at 12000 rpm on an Allegra™ X-22R Centrifuge (Lot#982501, Beckman Coulter, Brea, CA, USA) for 10 min at 4 °C, supernatant extracted, filtered (0.45 µm Econofltr PES, Lot#131127028, Agilent Technologies, Beijing, China) and stored at 4 °C. A final stock solution of 10% antivenom and 90% Owren Koller Buffer was produced. Modifying the section 3.4.1 protocol, 25 µL of antivenom stock was used in place of 25 µL of OK buffer, with the venom, Ca^{2+}, phospholipid, and antivenom mixture being incubated for 120 sec at 37°C before adding 75 µL of human plasma and monitoring clotting for 999 sec or until plasma clotted (whichever was sooner). Experiments were conducted in triplicate. Note that antivenom does not clot plasma and that a control was performed to rule out any additional effects antivenom has on the plasma. Antivenom was substituted into the above outlined protocol in replacement of a venom sample.

2.5.10 Statistical Analysis

2.5.10.1 Whole Plasma Clotting EC_{50} Concentration and Asymptotic Time

Venom dilutions in triplicates were mapped over time using GraphPad PRISM 7.0 to produce concentration curves. The statistical program R (Team, 2016) was used to calculate asymptotic clotting times using the Asymptotic Regression Model. This can be written as $y(x) = \phi_1 + (\phi_2 - \phi_1) exp[-exp(\phi_3)x]$, using the nlme package (J. Pinheiro, 2016). This asymptotic regression model was used to model the response of y (time) when approaching a horizontal asymptote, when x (concentration) approaches ∞ (Pinheiro and Bates, 2000). In this example, ϕ_1 is the asymptote as x (concentration) approaches ∞, ϕ_2 is the response at $x = 0$, and $t_{0.5}$ is the half-life. Parameter ϕ_3 is the logarithm of the rate constant that is used to enforce positivity so that an asymptote is reached in the model. The corresponding half-life is written as $t_{0.5} = \log 2/\exp(\phi_3)$. The EC_{50} can be explained as the half-maximal Effective Concentration, or the concentration at which 50% of the maximal effect is observed. To calculate this, the EC_{50} function in GraphPad PRISM 7.0 was used for each data set. Each data set was transformed by the log of the concentration, and the values were normalised by

individual sub data sets. A non-linear regression curve fit was then modelled, and a log-reversed EC_{50} value was produced.

2.5.10.2 Antivenom EC_{50} Concentration

Venom dilutions in triplicates were mapped over time using GraphPad PRISM 7.0 to produce concentration curves. The EC_{50} function in GraphPad PRISM 7.0 was used to calculate the EC_{50} for each data set. Each data set was transformed by the log of the concentration, and the values were normalised by individual sub data sets. A non-linear regression curve fit was then modelled, and a log-reversed EC_{50} value was produced.

Chapter 3: The sweet side of venom: glycosylated prothrombin activating metalloproteases from *Dispholidus typus* (boomslang) and *Thelotornis mossambicanus* (twig snake)

3.1 Abstract

Dispholidus typus and *Thelotornis mossambicanus* are closely related rear-fanged colubrid snakes that both possess strongly procoagulant venoms. However, despite similarities in overall venom biochemistry and resulting clinical manifestations, the underlying venom composition differs significantly between the two species. As a result, the only available antivenom—which is a monovalent antivenom for *D. typus*—has minimal cross reactivity with *T. mossambicanus* and is not a clinically viable option. It was hypothesised that this lack of cross reactivity is due to the additional large metalloprotease protein within *T. mossambicanus* venom, which may also be responsible for faster coagulation times. In this study, we found that *T. mossambicanus* venom is a more powerful activator of prothrombin than that of *D. typus* and that the SVMP transcripts from *T. mossambicanus* form a clade with those from *D. typus*. The sequences from *D. typus* and *T. mossambicanus* were highly similar in length, with the calculated molecular weights of the *T. mossambicanus* transcripts being significantly less than the molecular weights of some isoforms on the 1D SDS-PAGE gels. Analyses utilising degylcosylating enzymes revealed that *T. mossambicanus* SVMPs are glycosylated during post-translational modification, but that this does not lead to the different molecular weight bands observed in 1D SDS-PAGE gels. However, differences in glycosylation patterns may still explain some of the difference between the enzymatic activities and neutralization by antivenom that have been observed in these venoms. The results of this study provide new information regarding the treatment options for patients envenomated by *T. mossambicanus* as well as the evolution of these dangerous snakes.

3.2 Introduction

Procoagulant species of venomous snakes are responsible for devastating effects upon the coagulation systems of envenomed patients. These venoms activate clotting factor zymogens (Factor X or prothrombin) to generate endogenous thrombin, resulting in the production of stable fibrin clots (Lister et al., 2017; Oulion et al., 2018; Rogalski et al., 2017; Sousa et al., 2018; Zdenek et al., 2019). Venoms which activate prothrombin are divided into functional groups (A, B, C, or D) based upon their requirement for the cofactors FVa and calcium (Joseph and Kini, 2002; Kini, 2005a; Kini and Koh, 2016; McCleary and Kini, 2013; Rosing and Tans, 1991; Rosing and Tans, 1992). Group A and B are metalloproteases while C and D are serine proteases. Group A prothrombin activators do not

require the aid of any cofactors and are found in several viper venoms, most notably *Echis carinatus* 'ecarin', while B requires the aid of calcium, such as 'carinactivase-1', also found in *Echis carinatus* (Joseph and Kini, 2002; Kini, 2005a; Kini and Koh, 2016; McCleary and Kini, 2013; Rosing and Tans, 1991; Rosing and Tans, 1992; Yamada et al., 1996, 1997). It must be noted, however, that these convenient functional divisions are artificial distinctions based upon studies of purified toxins. However, the total venom composition is such that the venoms may be quite variable in their cofactor requirements. Thus relative calcium dependence is best viewed a sliding scale, rather than discrete divisions, as has been shown for venoms including vipers such as *Bothrops* and *Echis* and elapids including *Hoplocephalus, Notechis, Oxyuranus, Paroplocephalus, Pseudonaja,* and *Tropidechis* (Lister et al., 2017; Oulion et al., 2018; Rogalski et al., 2017; Sousa et al., 2018; Zdenek et al., 2019). For example, *Echis carinatus* varies from populations activity for which activity is decreased by only 40% in the absence of calcium but with activity decreased over 400% for other populations (Rogalski et al., 2017). Thus the simplistic division into Type A and Type B venoms does not reflect the more complex biological reality. This is a critically important when making conclusions based upon coagulation patterns, for if calcium is not included in the assay conditions there may be a radical shift in the venom patterns and thus evolutionary or clinical interpretations.

In addition to being central to the clinical picture of front-fanged snakes, procoagulation has also been shown to be responsible for the lethal effects of rear-fanged genera such as the closely related rear-fanged colubrid genera *Dispholidus* and *Thelotornis*, with this action being calcium and phospholipid independent in these species (Bradlow et al., 1980; Debono et al., 2017a; Grasset and Schaafsma, 1940; Guillin et al., 1978; Hiestand and Hiestand, 1979; Kamiguti et al., 2000). While *D. typus* has been shown to be a true procoagulant species through prothrombin activation, closely related members of the *Thelotornis* genus have had far less investigation performed, despite their equal medical importance (Atkinson et al., 1980; Chapman, 1968; Debono et al., 2017a; Du Toit, 1980; FitzSimons, 1909a, 1919; FitzSimons, 1962; Weinstein et al., 2011; Weinstein et al., 2013).

In a previous study we investigated the variation in venom composition, activity, and antivenom neutralization between *D. typus* and *T. mossambicanus*. Despite both genera presenting virtually identical clinical symptoms, we found that *T. mossambicanus* venom was far more complex in composition and activity than that of *D. typus*. This was particularly noteworthy among the SVMP toxin family which is largely responsible for the potentially lethal procoagulant action of these venoms. As a result of these differences, *Dispholidus* antivenom had little to no effect on *T. mossambicanus* venom (Debono et al., 2017a). Because of this, replacement therapy is the only treatment available for bite victims (Atkinson et al., 1980; Du Toit, 1980; Grasset and Schaafsma, 1940; Visser and Chapman, 1978; Weinstein et al., 2011). Here we investigated the molecular variation between both *Dispholidus typus* and *Thelotornis mossambicanus* by exploring their venom

gland transcriptomes. We focused on variation within the SVMP toxin family, which could lead to a variation in prothrombin activating capabilities. In addition, we investigated variations in glycosylation within both venoms as this may also contribute to a lack of antivenom neutralisation. This is the first time that factor X or prothrombin activation and transcriptomics have been investigated for *Thelotornis mossambicanus*. This research reinforces the high rates of venom diversification even between closely related snake species and how this can have direct implications for the treatment of envenomed patients.

3.3 Results

3.3.1 Transcriptomics

Transcriptomics recovered a diversity of toxin types including 3FTx, C-type lectin, CRiSP (cysteine rich secretory protein), PLA_2 (phospholipase A_2), PLB (phospholipase B), SVMP (snake venom metalloprotease). PLA_2 toxins were the most diverse toxin family and accounted for the greatest share of Transcripts Per Million (TPM) (72.4%, from 12 transcripts) while SVMPs contributed 11.0% of TPM from 4 transcripts (Figure 3.1Figure 3.1 TPM plots). We recovered 6 unique C-type lectins, yet these were expressed at relatively low levels (4% of total TPM). CRiSP and 3FTx were both responsible for greater shares of TPM despite lower numbers of total transcripts recovered (7.8% from 1 transcript and 4.7% from 2 transcripts, respectively). These results are consistent with our proteomics that showed abundant PLA_2s, but also significant quantities of SVMPs.

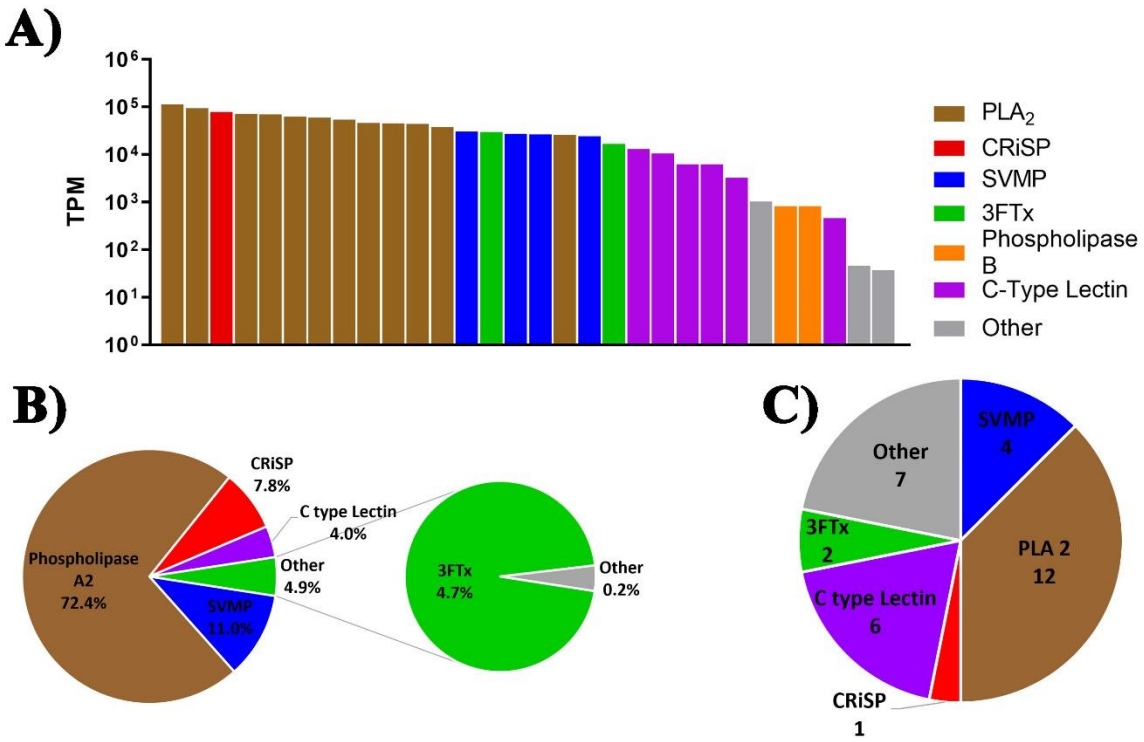

Figure 3.1 TPM plots
A) Transcripts Per Million (Y axis = TPM) for each toxin family from *Thelotornis mossambicanus* venom gland transcriptome, B) Percentage of TPM from toxin families recovered from *T. mossambicanus* transcriptome, C) Total number of transcripts from toxin families recovered from *T. mossambicanus* transcriptome. Other = Kallikrein, Waprin, Kunitz, VEGF, hyaluronidase, SVSPs, PLB.

3.3.2 SVMP phylogeny

Four complete SVMP transcripts were recovered from the *T. mossambicanus* venom gland transcriptome. These transcripts were nested within complete, publicly available *D. typus* SVMPs transcripts (GHOQ01000060, GHOQ01000051, GHOQ01000015), distinct from neighbouring genera *Boiga* and *Ahaetulla* (Figure 3.2). The SVMPs from *D. typus* and *T. mossambicanus* formed a tight, distinct clade within a larger rear-fanged and elapid clade separate from viper SVMPs, thus supporting *D. typus* and *T. mossambicanus* SVMP originating from a common molecular ancestor despite the poor cross-neutralisation of *D. typus* antivenom (Debono et al., 2017a).

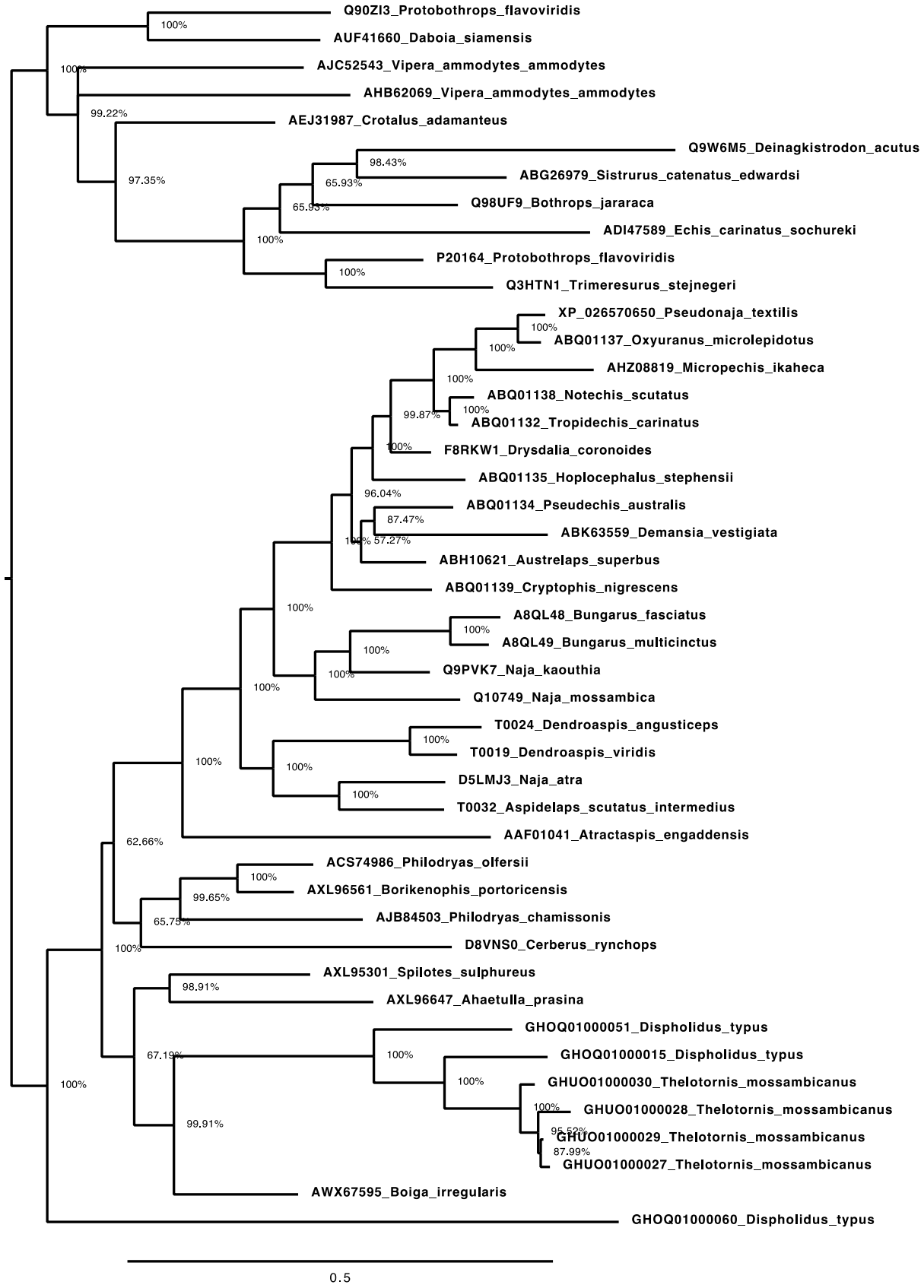

Figure 3.2 SVMP phylogeny

Phylogeny of publicly available SVMPs amino acid sequences, with all recovered *Thelotornis mossambicanus* SVMP venom gland transcriptome sequences. Scale bar represents 0.5 substitutions per site.

3.3.3 Proteomics

As transcriptomes were not available at the time, previous proteomic work focused on protein ID (Debono et al., 2017a) and did not investigate in-depth the structural differences of SVMP between *D. typus* and *T. mossambicanus* that result in the two distinct SVMP bands in *T. mossambicanus* when investigated on 1D SDS-PAGE (bands 5 and 6 in Figure 3.3). Therefore, digestion with a deglycosylation enzyme was undertaken, with both *D. typus* and *T. mossambicanus* SVMP showing evidence of extensive glycosylation, as demonstrated by molecular weight changes between homologous bands in gel lanes with and without the deglycosylation enzyme (Figure 3.4).

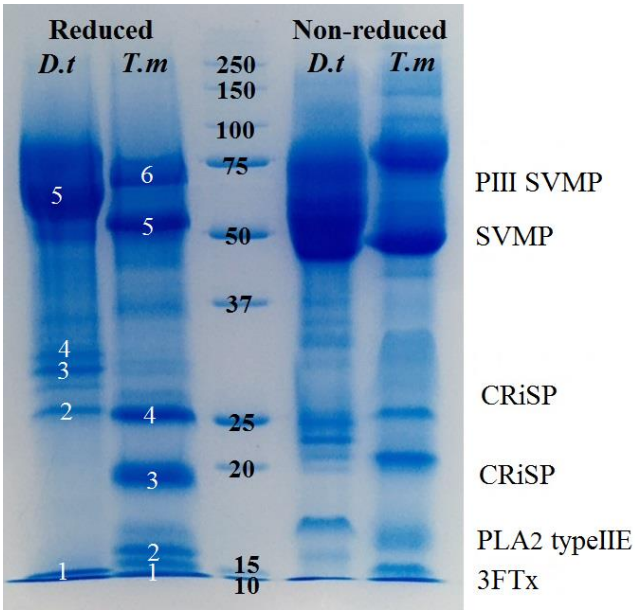

Figure 3.3 1D SDS PAGE
1D SDS page with identified groups of proteins (as previously published by us (Debono et al., 2017a)). D.t = *Dispholidus typus*, T.m = *Thelotornis mossambicanus*. Reduced conditions on the left, Non-reduced conditions on the right. Molecular weight marker indicated by centered numbers (kDa). Annotations (right) refer to bands identified (white numbers) within the reduced column.

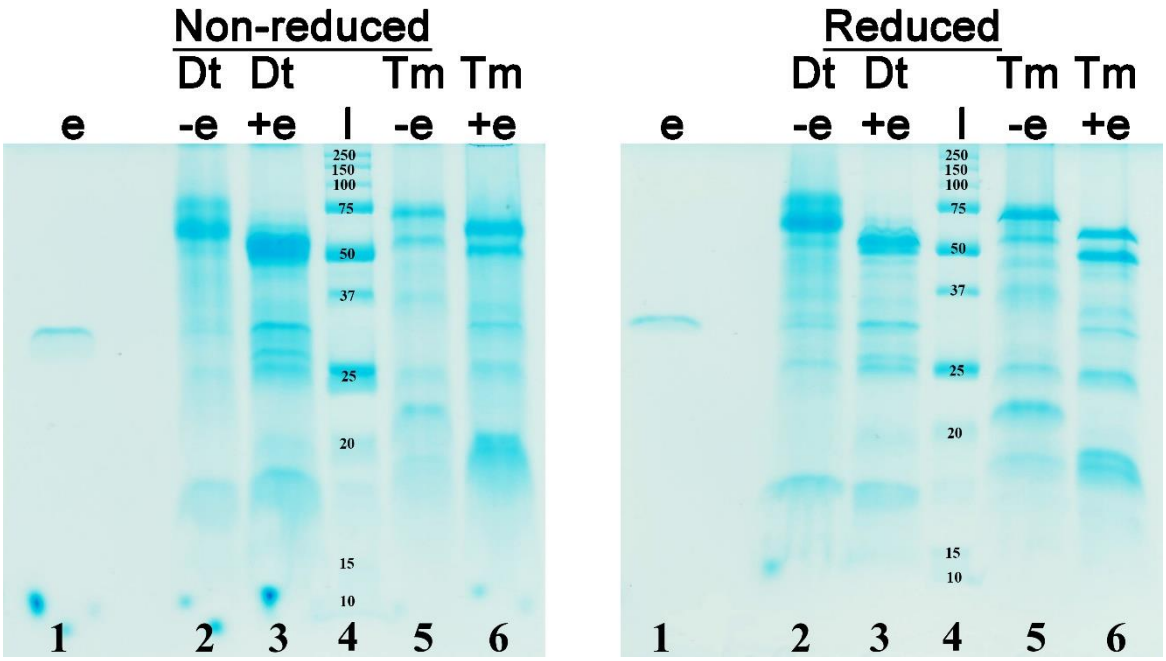

Figure 3.4 De-glycosylation

Differential glycosylation of *Dispholidus typus* and *Thelotornis mossambicanus* venoms. e = ± deglycosylation enzyme, l = ladder. Lane 1 = control enzyme, Lanes 2 and 3 = *D. typus* ± deglycosylation enzyme, Lane 4 = ladder, Lanes 5 and 6 = *T. mossambicanus* ± deglycosylation enzyme.

3.3.4 FX and Prothrombin activation

To evaluate the comparative ability of *D. typus* and *T. mossambicanus* venoms to activate FX and prothrombin, assessment was carried out using a Stago STA R Max coagulation analyser robot following the previously validated colorimetric assay (Debono et al., 2019a). Zymogen testing revealed that neither species was able to activate FX (*data not shown*). While FX activation has also been shown from *Dispholidus typus* (Bradlow et al., 1980), this activity was recovered from ground up venom gland as opposed to venom milking which may have contributed to it being an artefact in activity due to the presence of non-venom proteins or activated blood factors. However, when testing for prothrombin activation, a starting concentration of 20 µg/mL exceeded the maximum reading capacity for both species indicating extremely high activation of prothrombin, so a lower level of venom concentration was tested. At a half dilution concentration of venom (10 µg/mL), *Thelotornis mossambicanus* produced a stronger prothrombin activation effect compared to the positive control of pure thrombin (Liquid Fib, Stago, LOT 253337) which was not diluted (p <0.0001) (Figure 3.5). *Dispholidus typus* also had a strong prothrombin activating response but weaker than that of *T. mossambicanus*, being just slightly less than that of the thrombin control (p <0.0001). This variation was consistent with previously published differential clotting times for both species, indicating their extreme but divergent procoagulant effects (Debono et al., 2017a).

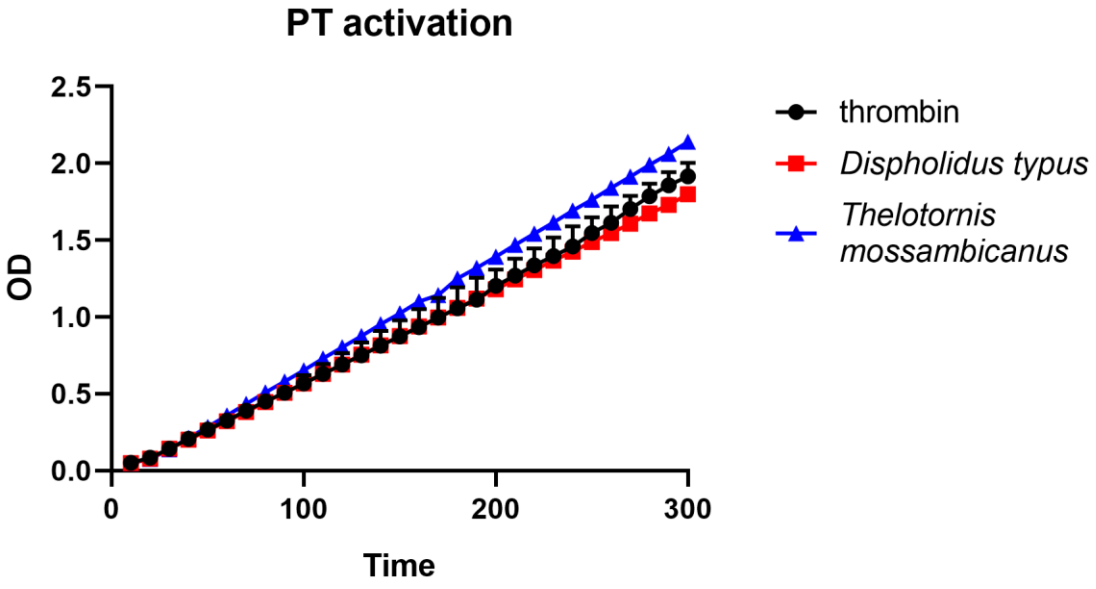

Figure 3.5 Prothrombin activation
Prothrombin activation of *Dispholidus typus* and *Thelotornis mossambicanus* at 10 µg/mL over 300 seconds. Blue line = *T. mossambicanus* activity, Red line = *D. typus* activity, Black line = positive control thrombin. Y axis = OD, optical density. X axis = time (sec). N = 3, data points = average with standard deviation.

3.4 Discussion

Our *Thelotornis mossambicanus* transcriptome revealed major differences in overall venom composition compared to that of *D. typus* (published by (Pla et al., 2017)). While *D. typus* venom is dominated by P-III SVMP (Figure 3.3), *T. mossambicanus* has a higher percentage of smaller toxins such as PLA_2 and CRiSP than *D. typus* (Figure 3.1). The SVMP of both venoms were shown for the first time to be heavily glycosylated (Figure 3.4), as has been previously shown for pit viper venoms such as *Bothrops* species (Andrade-Silva et al., 2016; Oliveira et al., 2010; Zelanis et al., 2012; Zelanis et al., 2010). Despite the fact that *T. mossambicanus* venom contains proportionally less procoagulant SVMPs than *D. typus*, *T. mossambicanus* is much more powerfully procoagulant (Debono et al., 2017a), due to stronger prothrombin activation compared to *Dispholidus typus* (Figure 3.5).

While *D. typus* and *T. mossambicanus* are lethally potent procoagulant colubrids, the currently available antivenom is effective for only one of the species – *D. typus* (Debono et al., 2017a). Therefore, the only currently available treatment for *Thelotornis* bites is replacement therapy, strictly on a case-by-case basis (Weinstein et al., 2013). The potent procoagulant activity of *T. mossambicanus* venom is entirely independent of cofactors, meaning that neither calcium nor phospholipid is required for such fast clotting of plasma (Debono et al., 2017a). This had previously been shown and reported for *D. typus* (Bradlow et al., 1980; Guillin et al., 1978; Hiestand and Hiestand, 1979; Weinstein et al., 2011; Weinstein et al., 2013; Yamada et al., 1997), however not for

T. mossambicanus. SVMPs are the likely source of both species' procoagulant nature as these toxins are known prothrombin activators and both venoms express them at relatively high levels (Joseph and Kini, 2002; Kini, 2005a; Kini and Koh, 2016; Rogalski et al., 2017; Rosing and Tans, 1991; Rosing and Tans, 1992; Rosing and Tans, 2010; Sousa et al., 2018). Furthermore, due to neither species requiring cofactors to cause such potent procoagulation, their potent prothrombin activating SVMPs can be categorised into Group A prothrombin activators (Joseph and Kini, 2002; Kini, 2005a; Kini and Koh, 2016; Rosing and Tans, 1991; Rosing and Tans, 1992; Rosing and Tans, 2010) and are resistant to natural endogenous coagulation inhibitors such as serpins and antithrombin III (Kini, 2005a; Kini and Koh, 2016; Yamada et al., 1996). To date, the best characterised Group A prothrombin activator is ecarin, isolated from *Echis carinatus* (Kini, 2005a; Kini and Koh, 2016; Kornalik and Blombäck, 1975; Rogalski et al., 2017; Rosing and Tans, 1991; Rosing and Tans, 1992). SVMPs from vipers are well documented with many representatives displayed in Figure 3.2. Interestingly, the SVMPs isolated from *T. mossambicanus* and *D. typus* form their own prothrombin activating clade, distinct from other Group A prothrombin activators such as from species within the *Echis* genus of vipers. This is evidence for the first time that the prothrombin activating SVMPs do not cluster with any of the other prothrombin activating SVMPs from other species. This also suggests that prothrombin activation as a neofunctionalisation of SVMP convergently evolved multiple independent occasions, spanning the full advanced snake taxonomical range from rear-fanged colubrids to viperid front-fanged snakes (Figure 3.2).

Despite large similarities in P-III SVMPs from both species, four distinct transcripts were recovered from the venom gland transcriptome of *T. mossambicanus*. The amino acid sequence is identical for 73.9% of the total length of the mature peptide for each of the SVMPs. Because of this, the predicted molecular weights of these transcripts cannot fully explain the different SVMP band pattern between *D. typus* and *T. mossambicanus*. Post-translational modifications such as glycosylation can have significant effects on the weight of mature proteins and variation in glycosylation is a feature that has been shown in pit vipers to be linked to variations in activity and antivenom recognition (Andrade-Silva et al., 2016; Chen et al., 2008; Lin et al., 2010; Oliveira et al., 2010; Zelanis et al., 2012). However, our results revealed similar levels of N-glycosylation in *D. typus* SVMPs as well as both SVMP bands from *T. mossambicanus*. It is possible that each of these possesses different patterns of glycosylation along the length of the actual protein, but determining if that is the case and, if so, what effect that might have on the enzymatic activity of these toxins, is a subject for future studies. The cause of the weight difference between the two bands of *T. mossambicanus* SVMPs remains unclear, but it is likely the result of some other process of post-translational modification.

Irrespective of antivenom efficacy, these two species have been the centre of controversial discussion, with both genera causing infamous deaths to two imminent herpetologists as both species were

deemed non-venomous (Atkinson et al., 1980; Bradlow et al., 1980; Chapman, 1968; Du Toit, 1980; FitzSimons, 1962; Grasset and Schaafsma, 1940). However, decades later, there is plenty of evidence to state otherwise, as both species are extremely procoagulant, with strong prothrombin activation capabilities (Bradlow et al., 1980; Debono et al., 2017a; Du Toit, 1980; FitzSimons, 1909a; Grasset and Schaafsma, 1940; Guillin et al., 1978; Hiestand and Hiestand, 1979; Visser and Chapman, 1978; Weinstein et al., 2011). Differences in venom composition, despite producing identical clinical symptoms, can be best attributed to recent evolutionary pressures from diet and prey escape potential linked to variations in ecology between the two lineages, leading to subtle structural and surfaces changes to key toxin families such as post translational modifications in the form of glycosylation, which should be the focus of future work. Research such as this can lead to improving alternative therapeutic designs and pave the way for further P-III SVMP research and Group A prothrombin activators.

3.5 Materials and Methods

3.5.1 Venom Supplies

Pooled venoms from *Dispholidus typus* (South African origin) and *Thelotornis mossambicanus* (Mozambique) were supplied by Latoxan (Portes-lès-Valence, France).

3.5.2 Venom gland RNA extraction and mRNA purification: reconstruction of SVMP phylogeny

Venom gland tissue (20 mg) was homogenized using a rotor homogenizer and total ribonucleic acid (RNA) extracted using the standard TRIzol Plus methodology (Invitrogen). RNA quality was assessed using a Nanodrop (Nanodrop 2000, Spectrophotometer, Thermo Scientific). mRNA was extracted and isolated using standard Dynabeads mRNA DIRECT Kit (Life Technologies Ambion, 1443431). Dynabeads work by hybridising poly-thymine (polyT) sequences, covalently bound to the Dynabead surface, to the mRNA poly-adenine (polyA) tail. This ensured that mRNA was selected for and not lost in centrifuge and washing stages, while other RNA forms (which do not have a polyA tail) are removed. This therefore facilitates a higher concentration of mRNA yield for sequencing purposes.

3.5.2.1 Sequencing

Venom gland transcriptomics were conducted by the IMB Sequencing Facility (Institute for Molecular Bioscience, The University of Queensland, St Lucia, Qld, Australia). Libraries were prepared with the TruSeq Stranded mRNA kit (Illumina, San Diego, CA, USA), and were sequenced on the Illumina NextSeq (Illumina) 500 using 2 × 150 bp reads and V2 chemistry.

The transcriptome described in this paper was one of several species that were part of a multiplexed run. Throughout our workflow GNU parallel 20170822 was used to run similar tasks in simultaneously, CD-HIT 4.8.1 was used to remove duplicate sequences, and Seqtk 1.2 was used to obtain subsets of sequence files (Fu et al., 2012; Li, 2012; Li and Godzik, 2006; Tange, 2011). Also, as a result of multiplexing, we experienced the common problem of low, but meaningful amounts of cross contamination between our multiplexed samples (Kircher et al., 2011). We attempted to mitigate this issue at several points in our methodology.

3.5.2.2 Assembly

Illumina reads that were likely to be cross contamination between multiplexed samples were removed from our read files by identifying 57 nucleotide k-mers in our focal read set that were present in another read set from the same lane at a 1000-fold or higher level. Reads with 25% or more of their sequence represented by such k-mers were filtered from the data set. This was accomplished using Jellyfish 2.2.6 (Marçais and Kingsford, 2011) and K-mer Analysis Toolkit (KAT) 2.3.4 (Mapleson et al., 2016). We then removed adaptors and low-quality bases from the reads and removed any reads shorter than 75 base pairs using Trim Galore version 0.4.3 (Krueger, 2015). We then used PEAR 0.9.10 (Zhang et al., 2013) to combine pairs of reads whose ends overlapped into one, longer, merged read. We then carried out several independent de novo assemblies of these reads using the programs Extender version 1.04 (Rokyta et al., 2012), Trinity version 2.4.0 (Grabherr et al., 2011), and SOAPdenovo version 2.04 (Xie et al., 2014). SOAPdenovo was run repeatedly with k-mer sizes of 31, 75, 97, and 127.

3.5.2.3 Annotation

The *de novo* assemblies were concatenated and TransDecoder 5.2.0 was used to predict open reading frames within the contigs (Haas et al., 2013). We removed any ORFs that did not include both a start and stop codon. The remaining ORFs were then compared against reference toxin sequences obtained from UniProt using ProteinOrtho 6.01 (Lechner et al., 2011; The UniProt Consortium, 2016). The resulting ORFs with similarity to known toxins were further quality controlled by manual inspection and BLAST searches against the Reptilia subsection of the NCBI Nucleotide database (Altschul et al., 1990; Altschul et al., 1997; Madden et al., 1996). The Burrows–Wheeler Aligner (BWA) 0.7.16a and SAMtools 1.5 were used to align the original reads from each species to the total list of annotated ORFs from every assembly (Li and Durbin, 2009; Li et al., 2009). These results were visualized using Tablet 1.15 to screen for signs of chimerical assembly (Milne et al., 2012). Those that showed sharp discontinuities in coverage maps across all species were removed from further analysis. A combination of read coverage, assembly quality, and BLAST search results were used to confirm the species of origin for each remain ORF. Given the evolutionary distance between the species we

sequenced and the rate at which toxin genes mutate, it is extremely unlikely that any two of these species would express identical toxins. Because of this, we interpret reads from multiple species aligning to a single contig as instances of contamination and tentatively assign the contig to the species with significantly higher expression levels. This assignation can be further reinforced if our BLAST results indicate that the sequence in question is more similar to the high-expression taxon than the lower one. The distribution of reads mapped to the sequence can also be informative if the pattern matches the norm for that toxin family in one species but not the others. For most sequences, all three indicators were unambiguous and in agreement while in a small minority of cases two other indicators could be used to decide between somewhat equivocal results of a third. No sequences that had made it to this point of the quality control process could not be confidently assigned using these methods.

Information regarding the transcriptome, the short reads, and the final toxin sequences that were determined to originate from the transcriptome of *Thelotornis mossambicanus* have been deposited in GenBank under the BioProject accession code PRJNA561062.

3.5.2.4 Phylogenetic reconstruction

Protein sequences for SVMP sequences from representative taxa were downloaded from the UniProt database (The UniProt Consortium, 2016). These were then combined with the translated SVMP sequences from our *T. mossambicanus* transcriptome and all available full-length high quality *Dispholidus typus* SVMP sequences (Pla et al., 2017). The sequences were aligned using the MUltiple Sequence Comparison by Log-Expectation (MUSCLE) algorithm implemented in AliView 1.18 (Edgar, 2004; Larsson, 2014). We reconstructed the phylogeny of these sequences using MrBayes 3.2 for 15,000,000 generations and 1,000,000 generations of burnin with `lset rates=invgamma` (allows rate to vary with some sites invariant and other drawn from a γ distribution) and `prset aamodelpr=mixed` (allows MrBayes to generate an appropriate amino acid substitution model by sampling from 10 predefined models) (Ronquist et al., 2012). The runs were stopped when convergence values reached 0.01.

3.5.3 De-glycosylation of venom proteins:

For protein de-glycosylation under denaturing conditions, 20 µg of crude venom samples from *Dispholidus typus* and *Thelotornis mossambicanus* were subjected to analysis following the manufacturer's instructions from New England Bio Labs 'De-glycosylation' (Lot #10034949, USA). Total reaction volumes of 10 µL were incubated with 1 µL Glycoprotein denaturing buffer (10x) (Bio Labs, Lot #10017111) for 10 min at 100°C. Following denaturing, 2 µL 10x Glycoprotein 2 (Lot #10029303), 2 µL 10% NP-40 (Lot# 10021820) and 1 µL (454 U) PNGase F (Lot #10018057) was

added to the mixture and incubated for 1 hr at 37°C. Post incubation, samples were submitted to 1D SDS PAGE under reducing and non-reducing conditions (by addition of DTT or not) following methods previously described (Debono et al., 2017a).

3.5.4 Factor X activation and prothrombin activation

To determine the relative rate of Factor X activation or prothrombin activation by venom samples, a colorimetric assay was performed previously validated by us (Debono et al., 2019a). A working stock solution (at 1 mg/mL in 50% deionized H_2O+ 50% glycerol) was manually diluted with OK buffer (STA Owren Koller Buffer) (50 µL at 20 µg/mL) to a cuvette. A total of 50 µL of $CaCl_2$ (25 mM), 50 µL phospholipid (cephalin prepared from rabbit cerebral tissue from STA C.K Prest standard kit, solubilized in OK buffer) and 25 µL of OK buffer was added to cuvette and incubated for 120 sec at 37°C before adding 75 µL of a solution containing the colorimetric substrate (Liquid Anti-Xa substrate, Stago Lot #253047) and either 0.01 µg/µL FX (Human Factor X, Lot #HH0315, HTI) or 0.1 µg/µL prothrombin (Human Prothrombin, Lot #GG1026, HTI) (total volume 250 µL/cuvette). A change in the optical density (OD) was measured each second for 300 sec using a STA-R Max® automated analyzer (Stago, Asnières sur Seine, France). All tests were performed in triplicate. The rate of FX activation or prothrombin activation, by the samples, was calculated in comparison to the variation in the optical density – corresponding to the cleavage of the substrate by FXa or thrombin, after the activation of the zymogen by the samples, in relation to direct cleavage of substrate by the samples in the absence of the zymogen. Human FXa (Liquid Anti-Xa FXa Lot #253047) or thrombin (Liquid Fib, Stago, Lot #253337) was used as positive control to ensure quality of the substrate. The samples analyzed, in same conditions, without the presence of the zymogen were used as a negative control to establish and venom-induced baseline substrate cleavage in the absence of the zymogen. A solution containing deionized H_2O/glycerol at a 1:1 ratio was used as a second negative control. Multiple linear regression and ANOVA on the AUC values were used to test for differences between the three treatments and yielded similar results.

Chapter 4: Basal but divergent: Clinical implications of differential coagulotoxicity in a clade of Asian vipers

4.1 Abstract

Envenomations by Asian pit vipers can induce multiple clinical complications resulting from coagulopathic and neuropathic effects. While intense research has been undertaken for some species, functional coagulopathic effects have been neglected. As these species' venoms affect the blood coagulation cascade, we investigated their effects upon the human clotting cascade using venoms of species from the *Azemiops*, *Calloselasma*, *Deinagkistrodon* and *Hypnale* genera. *Calloselasma rhodostoma*, *Deinagkistrodon acutus*, and *Hypnale hypnale* produced net anticoagulant effects through pseudo-procoagulant clotting of fibrinogen, resulting in weak, unstable, transient fibrin clots. *Tropidolaemus wagleri* was only weakly pseudo-procoagulant, clotting fibrinogen with only a negligible net anticoagulant effect. *Azemiops feae* and *Tropidolaemus subannulatus* did not affect clotting. This is the first study to examine in a phylogenetic context the coagulotoxic effects of related genera of basal Asiatic pit-vipers. The results reveal substantial variation between sister genera, providing crucial information about clinical effects and implications for antivenom cross-reactivity.

4.2 Introduction

Snakebite is one of the most neglected tropical diseases worldwide (Fry, 2018; Gutiérrez et al., 2006; Williams et al., 2010; Williams et al., 2011). Human-snake conflicts are increasing due to a myriad of factors including human population expansion and increase in snake activity periods due to climate change (Fry, 2018). Consequently a need for a better understanding into the effects of envenomations in humans is required. Snakebite is considered a current global health crisis, however it has been neglected, ignored, underestimated and misunderstood despite its ever-increasing significance (Fry, 2018). Additionally, there is lack of appropriate medical treatment and assistance to those who are affected by snakebite due to several contributing factors including education, financial aid and proximity to health care facilities. Many people who are envenomated and survive are left with permanent disabilities and crippling medical bills, even if medical treatment is sought out. Although antivenoms do exist for some species, many species of venomous snakes do not have an appropriate antivenom available or it is far too expensive for patients to purchase. Snakebite however is not restricted to the poorer regions of the world and many exotic venomous snake species kept in private collections can inflict potentially fatal envenomations, which is only potentiated by unsupported questionable alternative first aid treatments that are being supplied (Fry, 2018).

Snake venom is made up of a myriad of toxins which can deleteriously affect any part of haemostasis, resulting in an array of variable outcomes. In humans this can range from localised tissue swelling

and damage, to necrosis, respiratory failure, renal failure, kidney failure and haemorrhagic shock (Alirol et al., 2010; Ariaratnam et al., 2008; Dharmaratne and Gunawardena, 1988; Fry, 2018; Oulion et al., 2018; Sutherland, 1983; Tan and Tan, 1989; Tang et al., 2016; White, 2005). Venoms that affect coagulation do so via various coagulotoxic mechanisms ranging from procoagulant through to strong anticoagulant activities, through the disruption of clotting enzymes (Fry et al., 2009a). Procoagulant snake venoms produce endogenous thrombin through the activation of Factor X or prothrombin, resulting in strong, stable fibrin clots while anticoagulant venoms effect upon fibrinogen is either through destructive cleavage of fibrinogen or the pseudo-procoagulant mechanism of cleaving fibrinogen to form abnormal, short-lived fibrin clots (thus having a net anticoagulant effect) (Dambisya et al., 1994; Debono et al., 2019c; Fry et al., 2009a; Isbister, 2009).

The Viperidae snake family mainly affect the blood coagulation system and are responsible for a large proportion of global snake bites. Vipers inhabit Africa, the Americas, Asia, and Europe. Viperidae is split into three sub families; Crotalinae (pit vipers), Viperinae (true vipers) and Azemiopinae (Alencar et al., 2018; Alencar et al., 2016). This split occurred approximately 50 million years ago (MYA) and Crotaline has been under immense diversification and expansion for the past 41 MYA (Alencar et al., 2018; Alencar et al., 2016). Crotalinae occupy a large geographical range, from most of Asia throughout all of the Americas, and includes genera such as, *Bothrops*, *Crotalus*, and *Trimeresurus*. In Asia, a basal clade consists of the morphologically similar terrestrial genera, *Calloselasma*, *Deinagkistrodon* and *Hypnale* along with the highly derived arboreal genus *Tropidolaemus* (Alencar et al., 2018). This clade is a mixture of terrestrial and arboreal species and therefore provides an excellent opportunity to investigate venom adaptive evolution. The highly derived semi-fossorial genus *Azemiops* provides a further point of comparison.

Asian viper venoms are well known for effects on bite victims including haemorrhagic shock, necrosis and thrombocytopenia, spontaneous haemorrhage and acute kidney injury (Ariaratnam et al., 2008; de Silva et al., 1994; Herath et al., 2012; Joseph et al., 2007; Maduwage et al., 2013a; Maduwage et al., 2013b; Tang et al., 2016; Weerakkody et al., 2016; Withana et al., 2014). Haemorrhagic effects are potentiated by fibrinogenolytic enzymes which may act upon fibrinogen to either directly produce anticoagulation, by destructively cleaving fibrinogen, or to indirectly produce anticoagulation by cleaving fibrinogen to form short-lived, weak clots in a pseudo-procoagulant manner (Coimbra et al., 2018; Debono et al., 2019c; Dobson et al., 2018; Esnouf and Tunnah, 1967; Huang et al., 1992; Levy and Del Zoppo, 2006; Nielsen, 2016a; Premawardena et al., 1998; Trookman et al., 2009; Zulys et al., 1989).

There are significant variations in the venoms of this clade which have accumulated during long periods of evolutionary divergence contributing to variable antivenom efficacy (Ali et al., 2013a; Daltry et al., 1996a; Mebs et al., 1994; Tan et al., 2017b; Tang et al., 2016). Previous studies have

shown that some species affect various sites along the cascade such as platelet activity (Kong and Chung, 2001; Navdaev et al., 2011; Shin and Morita, 1998; Wang et al., 1999), FX activation and prothrombin activation (Ainsworth et al., 2018; Leong et al., 2014; Yamada et al., 1997).

The inter-genus venom variation between Asian pit vipers is unknown and some lineages have been left completely unstudied. As a result, there is limited knowledge about their effects on coagulation of the human body. Here we investigate the relationship and mechanisms behind their coagulotoxicity and illustrate the variations within the basal Asian pit vipers genera *Azemiops*, *Calloselasma*, *Deinagkistrodon*, *Hypnale* and *Tropidolaemus*. By contributing to the broader understanding of venom functional variation, improvement in clinical management strategies may be developed, as well as the potential for discovery of novel compounds useful in the advancement of blood clotting disorder therapeutics and diagnostics surrounding thrombosis and haemostasis.

4.3 Results

4.3.1 Enzymatic assays

Significant variation was evident upon artificial substrates which are in general cleaved by metalloproteases (ES001, ES003, ES005, ES010), serine proteases (ES002, ES011), or phospholipase A_2 (Figure 4.1). For all six venoms, none of the substrates displayed a strong taxonomical signal or a pattern regarding ecological niche occupied (arboreal versus terrestrial). None of the venoms cleaved ES005, and therefore this data is not shown.

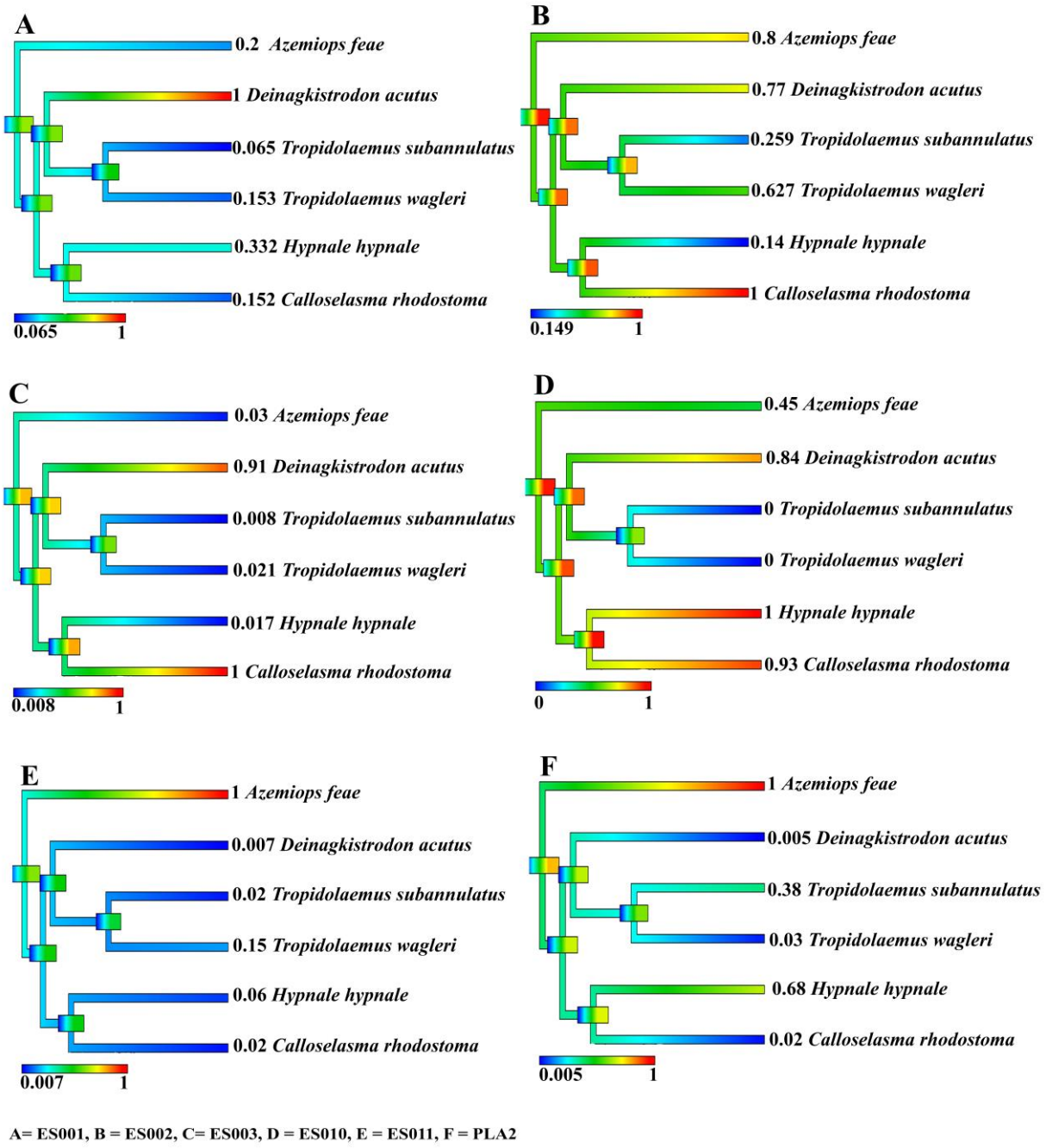

Figure 4.1 Enzymatic substrate activity

Ancestral state reconstruction of enzymatic substrate activity of the Basal clade species based on their ability to cleave the following substrates; A: fluorogenic peptide substrate (Mca-PLGL-Dpa-AR-NH2 Fluorogenic Matrix Metalloprotease Substrate, Cat#ES001), B: fluorogenic peptide substrate (Mca-RPKPVE-Nval-WRK(Dnp)-NH2 Fluorogenic MMP Substrate, Cat#ES002) which detects additional metalloprotease activity and Factor X, C: fluorogenic peptide substrate (Mca-PLAQAV-Dpa-RSSSR-NH2 Fluorogenic Peptide Substrate, Cat#ES003) which detects additional metalloprotease activity, D: fluorogenic peptide substrate (Mca-KPLGL-Dpa-AR-NH2 Fluorogenic Peptide Substrate, Cat#ES010) which detects additional metalloprotease activity, E: fluorogenic peptide substrate (Boc-VPR-AMC Fluorogenic Peptide Substrate, Cat#ES011) which detects serine protease activity, F: Phospholipase A_2 substrate activity, EnzChek® (Cat# E10217). Warmer colours represent more potent substrate cleavage. Bars indicate 95% confidence intervals for the estimate at each node. Phylogeny follows (Alencar et al., 2016).

4.3.2 Coagulation analysis: human plasma and fibrinogen

At the initial 20 µg/mL venom concentration, only *C. rhodostoma* (20.5 ± 2.6 sec), *D. acutus* (41.9 ± 0.5) and *H. hypnale* displayed the ability to clot plasma quicker than the negative control (spontaneous clotting of recalcified plasma) time of 300 ± 50 sec (Figure 4.2). All other species were equal or above the negative control. 8-point dilution series were undertaken with the two most potent venoms (*C. rhodostoma* and *D. acutus*) under three experimental conditions: with both cofactors (calcium and phospholipid), with just calcium, and with just phospholipid. While the phospholipid cofactor was not a significant variable for either venom, for calcium there was an area under the curve shift of 79.3 ± 4 % for *D. acutus* and a shift of 49.1 ± 1 % for *C. rhodostoma* (if there was no shift in the area under the curve, the value would have been zero) (Figure 4.2). An 8-point dilution series were also undertaken for *C. rhodostoma* and *D. acutus* with fibrinogen under three experimental conditions: with both cofactors (calcium and phospholipid), with just calcium, and with just phospholipid (Figure 4.3). While phospholipid was again not a significant variable for either venom, there was a strong dependency evident for calcium, with the area of the curve shifting 123.1 ± 15.2 % for *C. rhodostoma* and 345.1 ± 5.4 % *D. acutus* (if there was no shift in the area under the curve, the value would have been zero) (Figure 4.3).

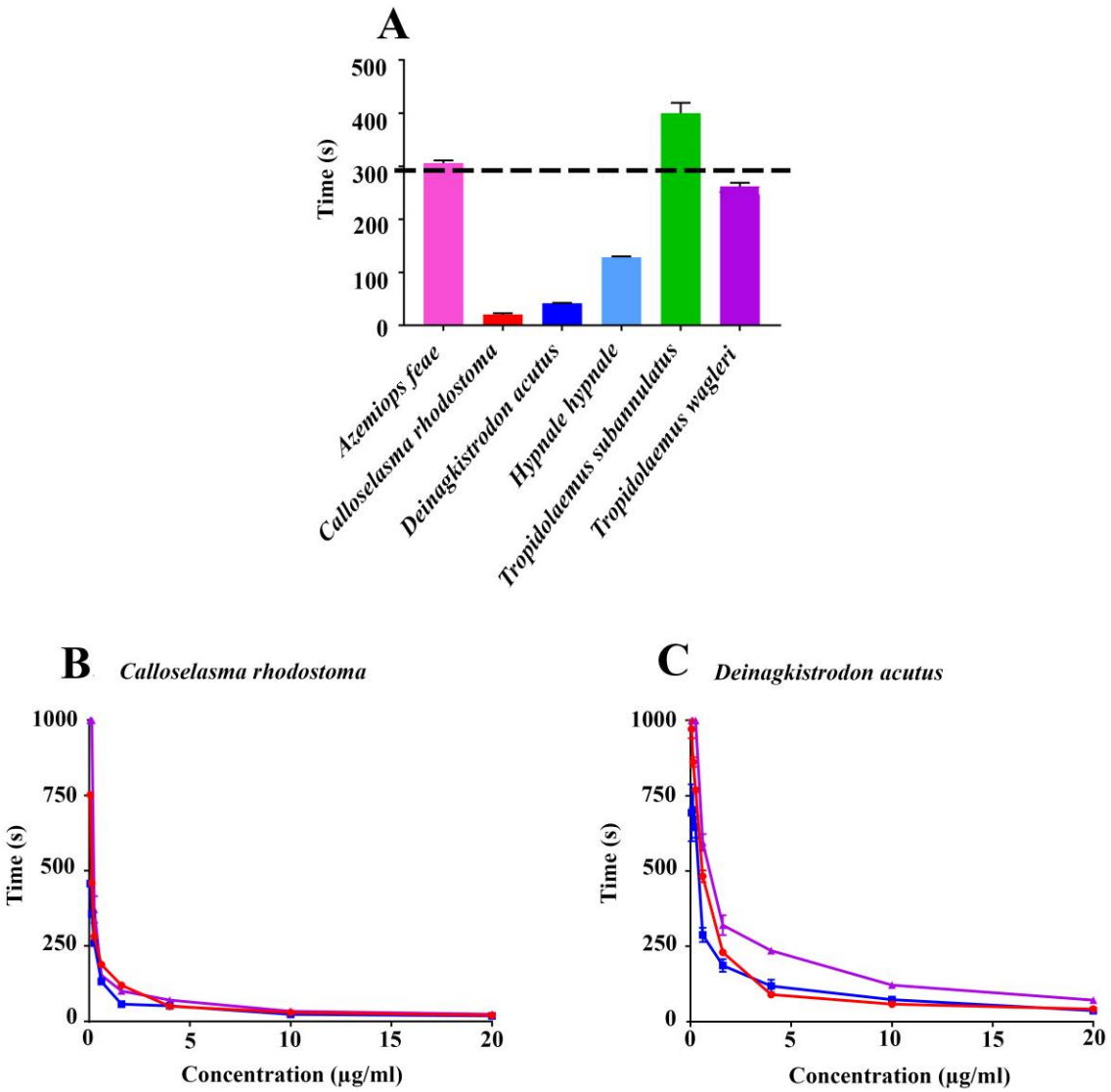

Figure 4.2 Coagulation analysis

A) Effect of 20 µg/mL venom concentration upon plasma clotting relative to the negative control (spontaneous clotting of recalcified plasma, shown with dashed line) time of 300 ± 50 sec. Also shown are 8-point dose-response curves with both calcium and phospholipid (red line), with just calcium (blue line), and with just phospholipid (purple line) for B) *C. rhodostoma* and C) *D. acutus.* Data points are N = 3 with standard deviations. Note that for the line graphs in (B) and (C) the error bars are in some cases smaller than the line icons.

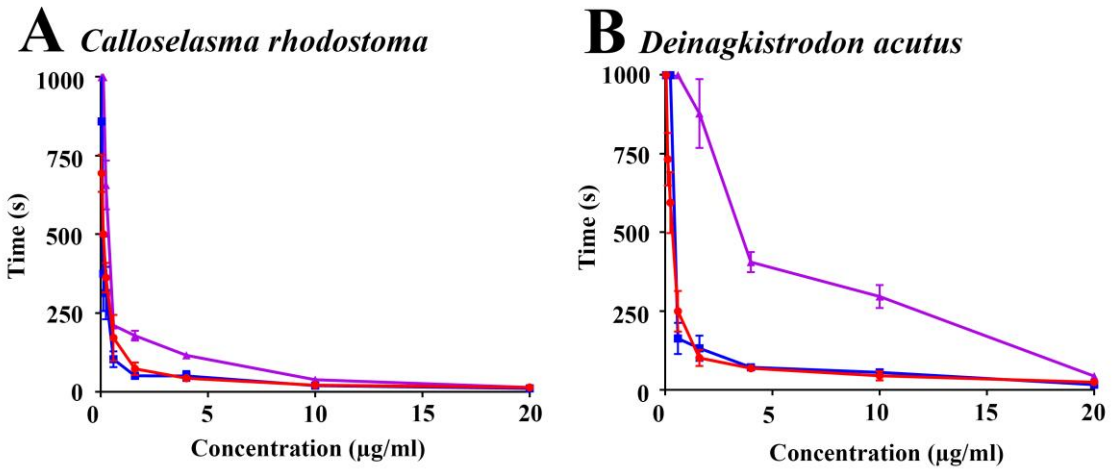

Figure 4.3 Fibrinogen clotting activity
8-point dose-response curves of fibrinogen clotting activity with both calcium and phospholipid (red line), with just calcium (blue line), and with just phospholipid (purple line) for A) *C. rhodostoma* and B) *D. acutus.* Data points are N = 3 with standard deviations.

4.3.3 Thromboelastography: plasma and fibrinogen

Thromboelastography studies on plasma (Figure 4.4) revealed that while *C. rhodostoma* and *D. acutus* both rapidly clotted plasma, consistent with the coagulation analyser results above, only *C. rhodostoma* formed strong, stable clots and therefore was truly procoagulant. Similarly, *H. hypnale* also formed strong stable clots despite being much slower to clot plasma in the above analyses. In contrast, *D. acutus* rapidly formed weak, unstable clots and therefore was pseudo-procoagulant. None of the other venoms differed significantly from the spontaneous clotting negative control. Thromboelastography studies on fibrinogen (Figure 4.5) revealed *C. rhodostoma* to also have the ability directly clot fibrinogen in a pseudo-procoagulant manner, in contrast to the procoagulant manner on endogenous thrombin. Consistent with the plasma results, *D. acutus* displayed the ability to clot fibrinogen in a pseudo-procoagulant manner while *H. hypnale* showed only a weak ability. *T. wagleri* also showed a weak ability to clot fibrinogen in a pseudo-procoagulant manner while its sister species *T. subannulatus* displayed a weak ability to cleave fibrinogen in a non-clotting, destructive manner. *A. feae* neither clotted nor destroyed fibrinogen.

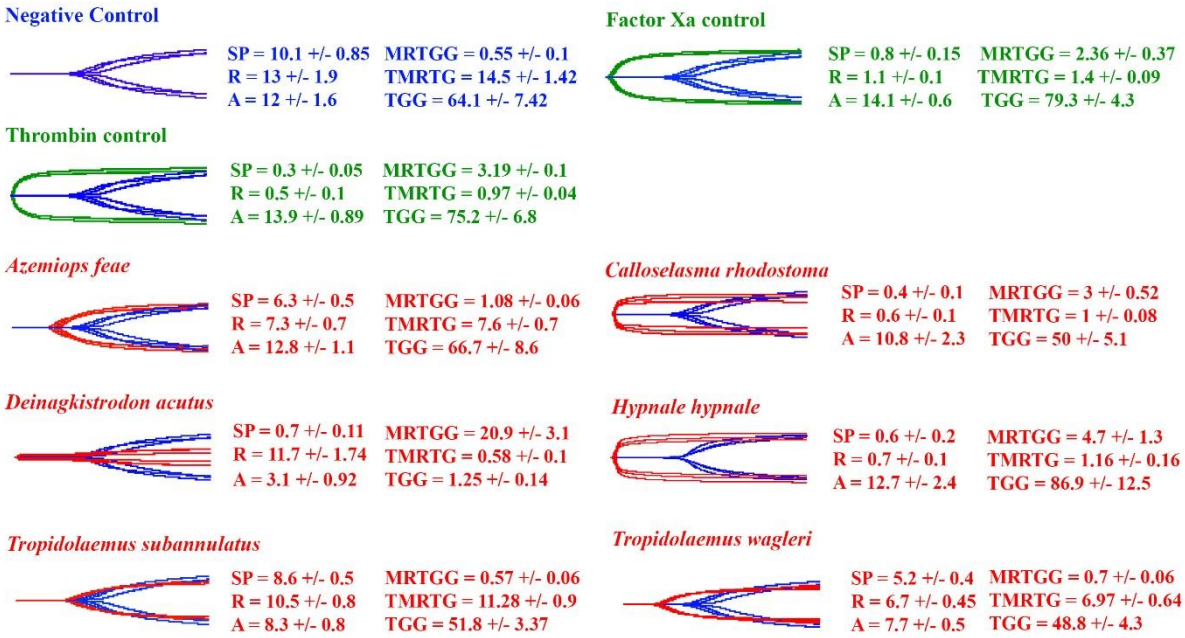

Figure 4.4 Thromboelastography plasma traces

Overlaid thromboelastography traces showing effects of venoms ability to clot plasma relative to spontaneous clot control where species cleave plasma in a clotting manner to form weak clots. Blue traces = spontaneous clot controls, green traces = thrombin induced clot or Factor Xa induced clot, red traces = samples. SP = split point, time taken until clot begins to form (min). R = time to initial clot formation where formation is 2mm+ (min). A = amplitude of detectable clot (mm). MRTGG = maximum rate of thrombus generation (dsc, dynes/cm^2/sec). TMRTG = time to maximum rate of thrombus generation (min). TGG= total thrombus generation (dynes/cm^2). Overlaid traces are N = 3 for each set of control or experimental conditions. Values are N = 3 means and standard deviation.

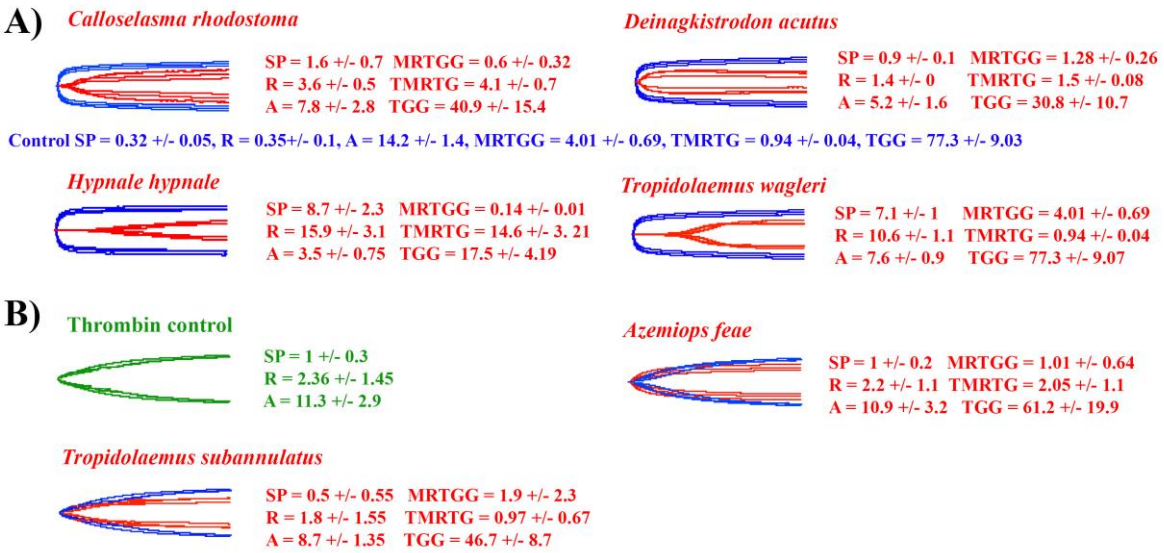

Figure 4.5 Thromboelastography fibrinogen traces

Overlaid thromboelastography traces showing tests for A) ability to clot fibrinogen relative to thrombin control; or B) test for the ability to degrade fibrinogen for species which did not clot in (A) whereby thrombin was added at the end of the 30 min runs to test for intact fibrinogen. Green traces = thrombin controls, red traces = samples. SP = split point, time taken until clot begins to form (min). R = time to initial clot formation where formation is 2mm+ (min). A = amplitude of detectable clot

(mm). MRTGG = maximum rate of thrombus generation (dynes/cm^2/sec). TMRTG = time to maximum rate of thrombus generation (min). TGG= total thrombus generation (dynes/cm^2). Overlaid traces are N = 3 for each set of control or experimental conditions. Values are N = 3 means and standard deviation.

4.3.4 FX activation and prothrombin activation

As *C. rhodostoma*, *H. hypnale* and *D. acutus* displayed clotting ability, they were investigated for their ability activate FX and prothrombin, to establish if they generated endogenous thrombin and therefore were true procoagulant venoms. *C. rhodostoma* activated FX yet only minimal activity was recorded for *H. hypnale* from the sister genus *Hypnale*, and no activity was recorded for *D. acutus* (Figure 4.6). There was no activity recorded for prothrombin activation by any species (*data not shown*).

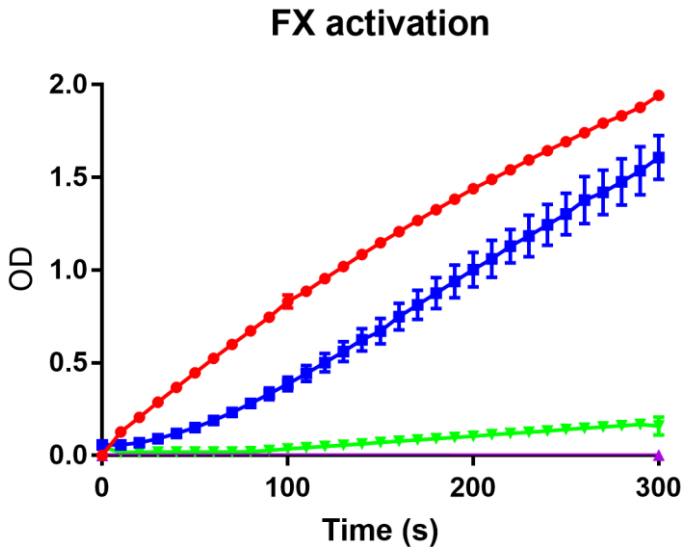

Figure 4.6 Factor X activation
Factor X activation via colourimetric analysis over time performed on a Stage STA R Max. Y axis = OD, optical density, X axis = time (sec). Red line = control FXa, blue line = *Calloselasma rhodostoma*, green line = *Hypnale hypnale*, purple line = *Deinagkistrodon acutus*. Data points are n = 3, means and SD.

4.3.5 Fibrinolysis ± tPA

The ability for species' venoms within the basal clade to actively lyse tissue factor-induced plasma clots was tested at varying venom concentrations. None of the species tested returned a positive result of lysing a clot. However compared to a normal clot lysis time (CLT), this was decreased in the presence of *C. rhodostoma* and *D. acutus* venoms and tPA (Figure 4.7).

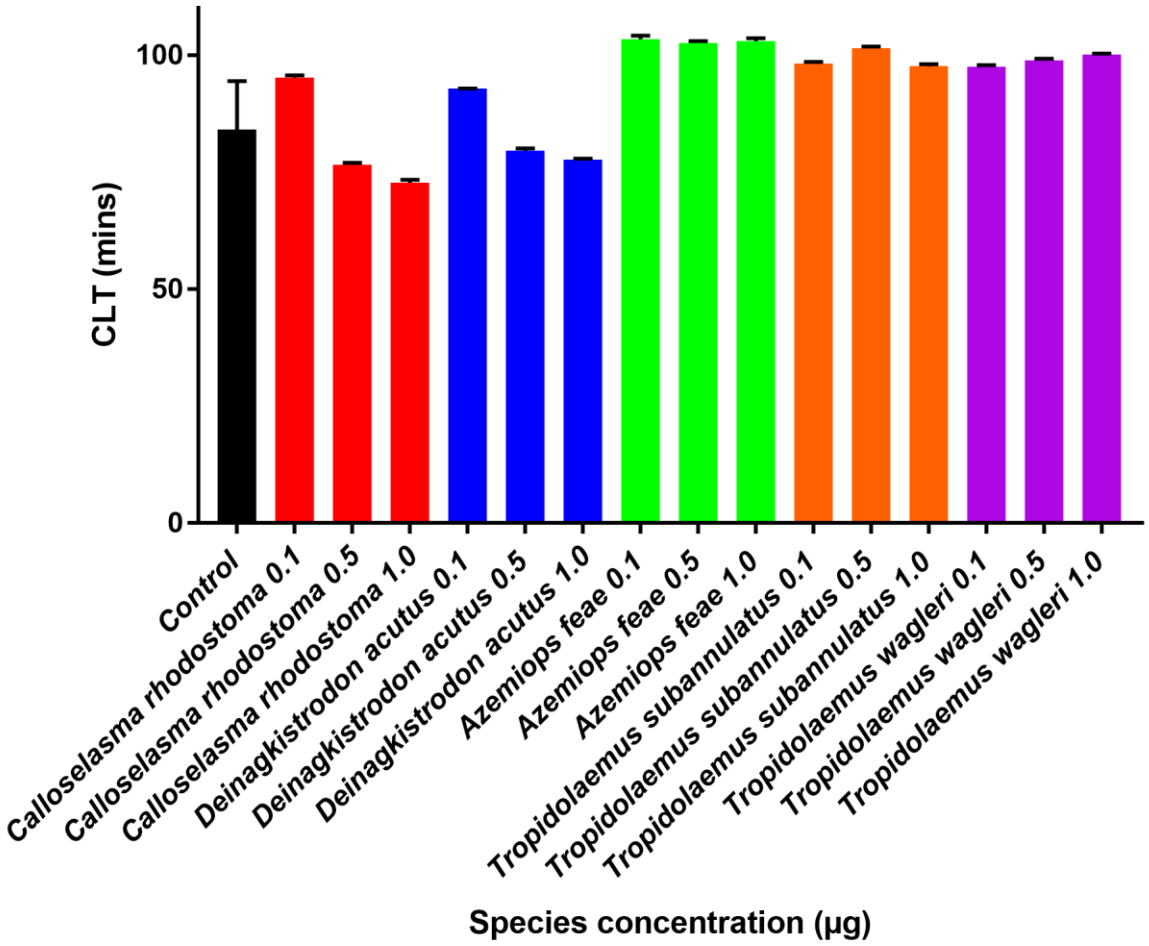

Figure 4.7 Fibrinolysis
Clot Lysis Time (CLT) for each species within the basal clade in the presence of tPA at 0.1 µg, 0.5 µg and 1 µg venom concentrations. Control is indicated in black. Columns are averages of triplicates and error bars given for each. Bars which are lower than the control lysed the plasma clot quicker than under normal tPA conditions.

4.3.6 Fibrinogen gels

Time-dependent cleavage of fibrinogen chains was also investigated using electrophoresis. Venom from *Azemiops feae* failed to cleave any of the fibrinogen, while *Tropidolaemus wagleri* and *Hypnale hypnale* cleaved all 3 chains within 30 minutes (Figure 4.8 and Figure 4.9). Venom from *Calloselasma rhodostoma*, *Tropidolaemus subannulatus* and *Deinagkistrodon acutus* all cleaved the alpha chain rapidly, while slowly cleaving the beta chain but with no effect on the gamma chain (Figure 4.8 and Figure 4.9).

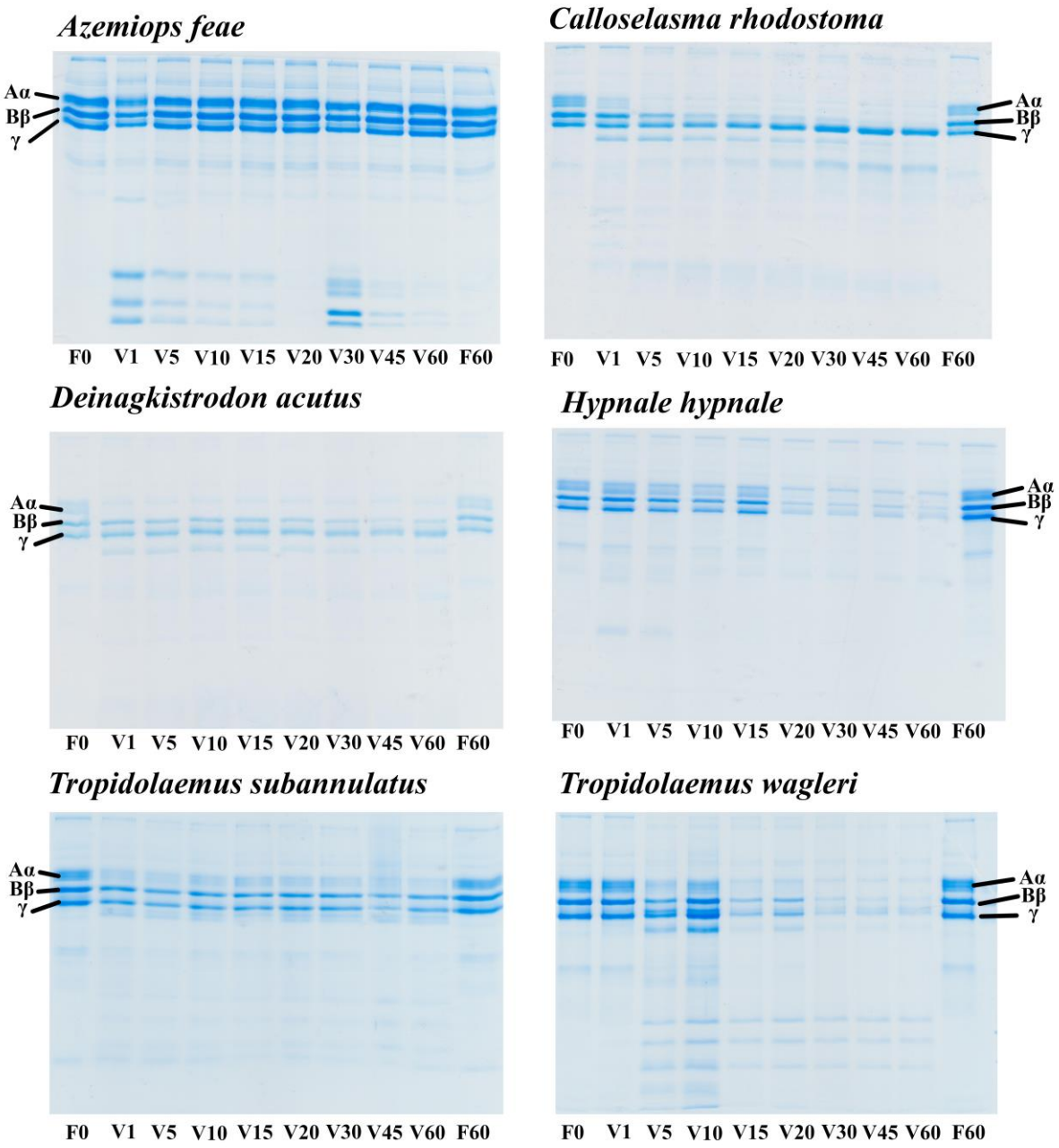

Figure 4.8 Fibrinogen chain cleavage - gel
1D SDS PAGE time dependent fibrinogen chain degradation (α, β or γ) by venom at 0.1 µg/µL concentration at 37ºC over 60 min. F = fibrinogen at 0 min or 60 min incubation controls, V = venom at 1, 5… 60 min incubation.

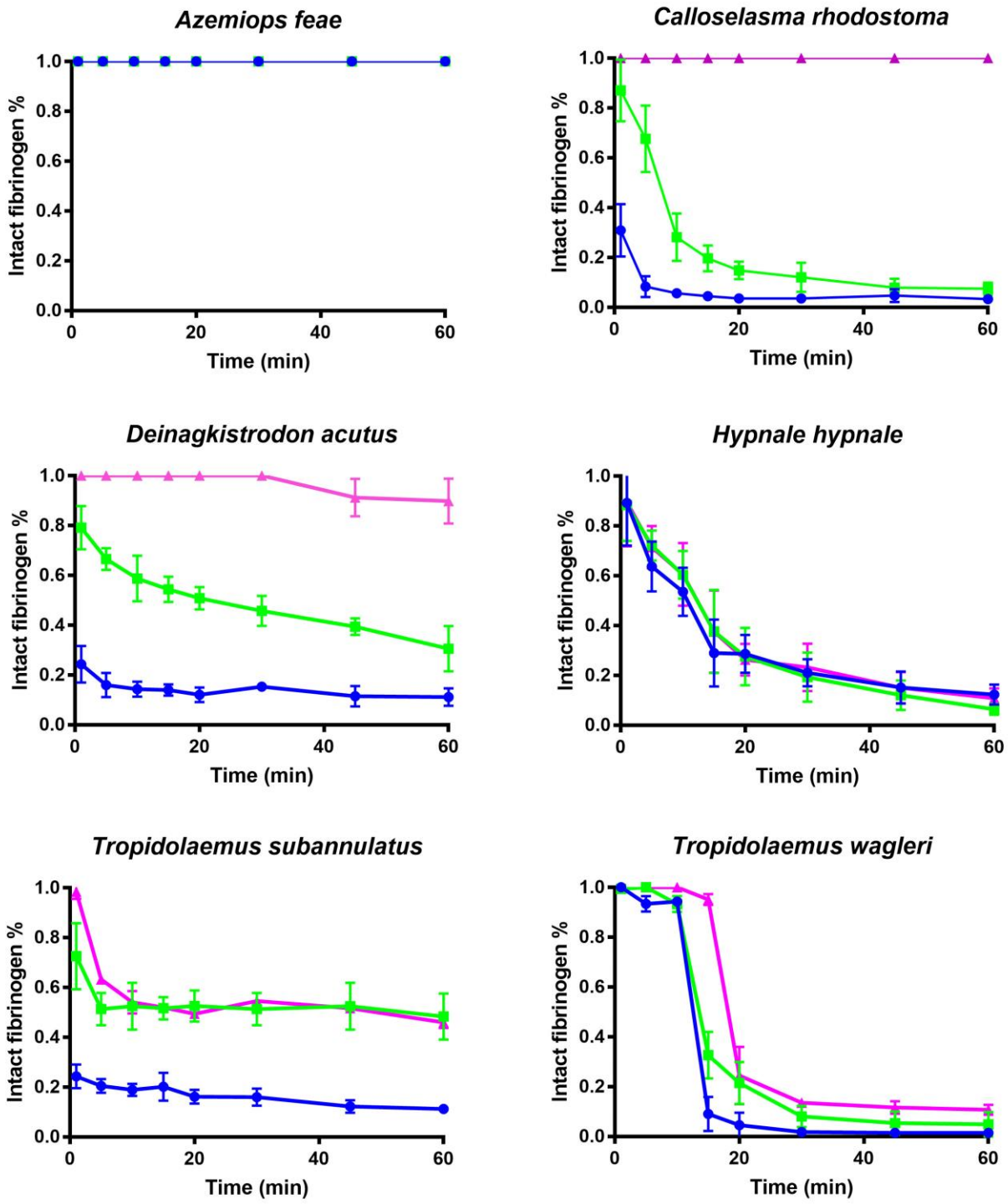

Figure 4.9 Fibrinogen chain cleavage - % intact
Relative cleavage of alpha (blue), beta (green) or gamma (pink) chains of fibrinogen. X-axis is time (min), y-axis is percentage of intact chain remaining. Error bars indicate standard deviation and N = 3 means.

4.4 Discussion

The venoms within the clade studied here, formed by the genera *Azemiops*, *Calloselasma*, *Hypnale*, *Deinagkistrodon* and *Tropidolaemus*, were as functionally diverse as the snakes are themselves in morphology and ecological niche occupied, with the snakes ranging from semi-fossorial species, to ambush feeding, heavily camouflaged terrestrial, to arboreal species. There were no phylogenetic or ecological patterns in their actions upon enzymatic substrates (Figure 4.1) or in the functional tests. The camouflaged, sit and wait ambush specialists (*C. rhodostoma*, *H. hypnale* and *D. acutus*) were similar in that they clotted plasma and fibrinogen (Figure 4.2, Figure 4.3, Figure 4.4 and Figure 4.5), but the underlying mechanics were starkly different.

Consistent with previous reports of this venom (Ainsworth et al., 2018; Nielsen and Bazzell, 2017; Yamada et al., 1997) *C. rhodostoma* was a true procoagulant venom. In this study it was shown to activate Factor X generating endogenous thrombin, forming a strong, stable fibrin clot. In contrast, *H. hypnale* venom produced a strong stable clot upon plasma but did not activate Factor X or Prothrombin and formed a very weak, unstable clot when tested on fibrinogen (Figure 4.4, Figure 4.5 and Figure 4.6). *Deinagkistrodon acutus* venom, however, was shown to be pseudo-procoagulant in that it acted directly upon fibrinogen to produce transient, weak fibrin clots (Figure 4.4 and Figure 4.5).

Calloselasma rhodostoma retained the ability to directly clot fibrinogen in a pseudo-procoagulant manner, however this action was significantly slower than the true-procoagulant action of Factor X activation, resulting in the generation of endogenous thrombin (Figure 4.5). Therefore, prey subjugation would be facilitated through the induction of stroke, as has been seen convergently for other venoms, not only other vipers such as *Echis* (Rogalski et al., 2017) and *Bothrops* (Sousa et al., 2018) but also diverse snakes from other families such as *Dispholidus* and *Thelotornis* with the Colubridae (Debono et al., 2017a), *Hoplocephalus*, *Notechis*, *Paroplocephalus* and *Tropidechis* within the Elapidae (Lister et al., 2017) and *Atractaspis* within the Lamprophiidae (Oulion et al., 2018). However, in human bite victims the larger blood volume would dilute the venom and lessen the likelihood of large blood clots forming. Instead there would be a depletion of fibrinogen and clotting factors, as a consequence of endogenous thrombin generation which would result in a venom induced consumptive coagulopathy (VICC), creating a net anticoagulant state (Isbister, 2010). Therefore, while prey items which rapidly succumb due to venom-inducted stroke, the longer survival of envenomed humans would allow sufficient time for potentiation of the net anticoagulation effects due to the secondary action upon the remaining fibrinogen - the pseudo-procoagulant cleavage to form weak, transient clots with remaining fibrinogen (Ho et al., 1986; Tang et al., 2016; Warrell et al., 1986).

In contrast, the transient, weak fibrin clots shown in this study for *D. acutus* venom, consistent with previous reports (Nielsen and Frank, 2018) would have a short half-life due to their inherent instability. Thus the effects upon both prey and humans envenomated by *D. acutus* venoms would therefore be similar: a rapid decrease in fibrinogen levels leading to an anticoagulant state (Cheng et al., 2017; Ouyang and Teng, 1976, 1978), with death resulting from haemorrhagic shock, like has been shown for the *Protobothrops* genus (Debono et al., 2019c). Both *D. acutus* and *H. hypnale* venoms displayed similar biochemistry for their pseudo-procoagulant action, which required calcium for full action (Nielsen, 2016b; Nielsen and Bazzell, 2017). The activity that *H. hypanle* displays upon plasma still remains a mystery, as the venom does not activate Factor X or Prothrombin (Figure 4.6). Additional investigation into the mechanisms behind this activity would be the focus of future research, such as activation of other clotting factors (ie IX or XI).

Of the other species within this study, in the thromboelastography studies, only *T. wagleri* displayed evidence of action upon fibrinogen, showing only a moderate level of pseudo-procoagulant activity, yet its sister species *T. subannulatus* did not display such activity. *Azemiops feae* also did not display any coagulotoxic action. The low to non-existent coagulotoxic activity is consistent with *Azemiops* and *Tropidolaemus* both known to have contain novel neurotoxic peptides rather than the larger enzymes typical of viperid venoms (Schmidt and Weinstein, 1995; Shelukhina et al., 2018; Tan et al., 2017b). In both cases, it has been shown that the neurotoxic peptides emerged in the venoms from *de novo* evolution of novel bioactive peptides in the propeptide-region of the venom forms of C-type natriuretic peptides (Brust et al., 2013; Debono et al., 2017b). However, as these genera are not sister to each other and occupy very different ecological niches (semi-fossorial for *Azemiopis* and arboreal for *Tropidolaemus*) the selection pressure for the molecular evolution of the peptides was differential.

The functional variation extended to the patterns of fibrinogen chain cleavage as revealed in the SDS PAGE gels (Figure 4.8 and Figure 4.9). *Calloselasma rhodostoma* and *D. acutus* were similar in rapidly cleaving the A-alpha and B-beta chains but not the gamma, which is consistent with both venoms having the ability for pseudo-procoagulant direct action upon fibrinogen (Figure 4.5). *T. wagleri* was the only other venom to display significant action in the fibrinogen thromboelastography studies, having a moderate pseudo-procoagulant activity (Figure 4.5), and this venom cleaved all three fibrinogen chains (Figure 4.8 and Figure 4.9). The sister species *T. subannulatus* displayed a similar, but weaker, activity on the fibrinogen gels (Figure 4.8 and Figure 4.9) despite not having a significant functional activity in the venom concentration tested in the thromboelastography studies (Figure 4.5). Consistent with the functional studies (Figure 4.5), *A. feae* did not have any activity on the fibrinogen gels (Figure 4.8 and Figure 4.9).

Just as the neurotoxicity exhibited by some species in this clade of snakes are unique, so too is the thrombin generating activity of *C. rhodostoma.* In contrast, *D. acutus* was more like the typical Asian

pit-viper, which are broadly known for their haemorrhagic-shock inducing venoms (Cheng et al., 2017; Debono et al., 2019c; Hutton et al., 1990; Joseph et al., 2007; Maduwage et al., 2013a; Rojnuckarin et al., 1998; Warrell et al., 1986; Withana et al., 2014). Haemorrhagic effects are a result of anticoagulation mechanisms, or a net anticoagulant outcome. As previously mentioned, haemorrhagic effects were demonstrated within this group as irregular degradation of fibrinogen chains, which creates weak clots such as was evident for the *D. acutus* venom in the thromboelastography studies (Figure 4.4 and Figure 4.5). Such degradation of fibrinogen has previously been shown with the isolation and purification of a 'thrombin-like enzyme' (TLE) 'Ancrod' from *C. rhodostoma*, a serine protease which is able to cleave α from Aα chain (Markland, 1998; Nolan et al., 1976; Vaiyapuri et al., 2015).

An in-depth investigation into these mechanisms controlling coagulation has somewhat been neglected from the literature, and a thorough analysis into the actions upon the blood system is required. The addition of co-factor analysis and dependency is extremely important when investigating these lineages, and the true representation of either a procoagulant or anticoagulant action can be demonstrated. Applying this knowledge and gaining a more complete understanding of venom diversification and evolution is important for predictions of potential clinical effects and evidence-based management strategies, in addition to biodiscovery research.

4.5 Materials and Methods

4.5.1 Venoms

Six species of Asian Viperidae (Alencar et al., 2016) were investigated for venom composition and coagulation effects via a multidisciplinary approach of venomics, functionality and bioactivity. Pooled, lyophilized venom samples from species *Azemiops feae, Calloselasma rhodostoma, Deinagkistrodon acutus, Hypnale hypnale, Tropidolaemus subannulatus* and *Tropidolaemus wagleri* were procured from captive collections (unknown localities of founding stocks). Venoms were resuspended in deionized H_2O and protein concentrations (mg/mL) determined using a ThermoFisher Scientific Nanodrop™ 2000c Spectrophotometer. Working stocks of 50% deionized water/50% glycerol (> 99%, Sigma-Aldrich) for all venoms were prepared at 1 mg/mL and stored at -20°C to preserve enzymatic activity and reduce enzyme degradation. Venoms included in the following assays were subject to availability at the time of analysis.

4.5.2 Enzyme assays

Various enzymatic assays were performed to investigate activity on specific artificial substrates, as well as PLA_2, plasminogen activation, prothrombin activation and FX activation. Investigation followed that described by (Debono et al., 2019c). Phytools heat mapping followed that of (Lister et al., 2017). Details are as follows.

4.5.2.1 Fluorescent substrate activation

In order to investigate Fluorescent Determination of matrix metalloprotease (ES001, ES003, ES005, ES010), serine protease activity (ES002, ES011) and phospholipase A_2 (PLA_2) enzymatic assays were undertaken as previously described by us (Debono et al., 2017a). For matrix metalloprotease and serine protease assays a working stock solution of freeze dried venom was reconstituted in a buffer containing 50% MilliQ/50% glycerol (>99.9%, Sigma, St Louis, MO, USA) at a 1:1 ratio to preserve enzymatic activity and reduce enzyme degradation. Varying concentrations of crude venom (10 ng/μL and 50 ng/μL) were plated out in triplicates on a 384-well plate (black, Lot#1171125, nunc™ Thermo Scientific, Rochester, NY, USA) and measured by adding 90 μL quenched fluorescent substrate per well (total volume 100 μL/well, 10 μL/ 5mL enzyme buffer, 150 mM NaCl, and 50 mM Tri-HCl (pH 7.3), Fluorogenic Peptide Substrate, R & D systems, Cat#ES001, ES003, ES005, ES010, ES011, Minneapolis, Minnesota). Fluorescence was monitored by a Fluoroskan Ascent™ (Thermo Scientific, Vantaa, Finland) Microplate Fluorometer (Cat#1506450, Thermo Scientific, Vantaa, Finland) (Cat#ES001, ES003, ES005, ES010 for Matrix Metalloprotease at an excitation of 320 nm, emission at 405 nm; Cat#ES011 for Kallikrein at an excitation of 390 nm, emission at 460 nm) over 400 min or until activity had ceased. Data was collected using Ascent® Software v2.6 (Thermo Scientific, Vantaa, Finland).

For PLA_2 analysis we assessed the continuous Phospholipase A_2 (PLA_2) activity of the venoms using a fluorescence substrate assay (EnzChek® Phospholipase A_2 Assay Kit, Cat#E10217, Thermo Scientific, Rochester, NY, USA), measured on a Fluoroskan Ascent® Microplate Fluorometer (Cat#1506450, Thermo Scientific, Vantaa, Finland). As above, we used a working stock solution of freeze dried venom reconstituted in a buffer containing 50% MilliQ / 50% glycerol (>99.9%, Sigma) at a 1:1 ratio. A concentration of enzyme activity in venom (50 ng/μL) was brought up in 12.5 μL 1× PLA_2 reaction buffer (50 mM Tris-HCL, 100 mM NaCl, 1 mM $CaCl_2$, pH 8.9) and plated out in triplicates on a 384-well plate (black, Lot#1171125, nunc™ Thermo Scientific, Rochester, NY, USA). The triplicates were measured by dispensing 12.5 μL quenched 1 mM EnzChek® (Thermo Scientific, Rochester, NY, USA) Phospholipase A_2 Substrate per well (total volume 25 μL/well) over 100 min or until activity had ceased (at an excitation of 485 nm, emission 538 nm). Purified PLA_2 from bee venom (1 U/mL) was used as a positive control and data was collected using Ascent® Software v2.6 (Thermo Scientific, Vantaa, Finland).

4.5.2.2 Plasminogen activation

The same working stock solution of 1 mg/mL (outlined above and in (Debono et al., 2017a) of freeze dried venom was used to make the following dilutions: 10 ng/μL, 50 ng/μL and 100 ng/μL. These varying concentrations of enzyme activity in venom were plated out on a 384-well plate (black,

Lot#1171125, nunc™ Thermo Scientific, Rochester, NY, USA) in triplicates, with and without 10 ng/µL plasminogen per well (Lot#FF0125 HCPG-0130, Haematologic Technologies Inc., Essex Junction, VT, USA). Plasminogen, a serine protease, can be activated by a serine protease specific substrate (Fluorogenic Peptide Substrate, R & D systems, Cat# ES011, Minneapolis, Minnesota). Plasmin was used as a positive control (10 ng/µL per positive control well, Lot#EE1120, HCPM-0140, Haematologic Technologies Inc., Essex Junction, VT, USA). Activation from venoms was measured by adding 90 µL quenched fluorescent substrate per well (total volume 100 µL/well; 20 µL/5mL enzyme buffer - 150 mM NaCl and 50 mM Tri-HCl (pH 7.3), Fluorogenic Peptide Substrate, R & D systems, Cat#ES011, Minneapolis, Minnesota). Fluorescence was monitored by a Fluoroskan Ascent™ Microplate Fluorometer (Cat#1506450, Thermo Scientific, Vantaa, Finland) at excitation 390 nm and emission at 460 nm over 150min or until activity had ceased. Data was collected using Ascent® Software v2.6 (Thermo Scientific, Vantaa, Finland). Experiments were conducted in triplicate.

4.5.2.3 Prothrombin activation

The ability for the above crude venom to directly activate prothrombin was investigated and measured by modifying the above protocol used for plasminogen activation. Plasminogen was replaced with prothrombin (Lot#EE0930, HCP-0010, Haematologic Technologies Inc., Essex Junction, VT, USA) and plasmin was replaced with thrombin (Lot#FF0315, HCT-0020, Haematologic Technologies Inc., Essex Junction, VT, USA) as a positive control (10 ng/µL per positive control well). Data was collected using Ascent® Software v2.6 (Thermo Scientific, Vantaa, Finland). Experiments were conducted in triplicate.

4.5.2.4 Factor X activation

The ability for the above crude venom to directly activate blood coagulation Factor X (FX) was investigated and measured by modifying the above protocol used for plasminogen activation using FX (Lot#FF0407, HCX-0050, Haematologic Technologies Inc., Essex Junction, VT, USA) as the experimental target and FXa (Lot#EE1102, HCXA-0060, Haematologic Technologies Inc., Essex Junction, VT, USA) as the positive control (10 ng/µL per positive control well). Data was collected using Ascent® Software v2.6 (Thermo Scientific, Vantaa, Finland). Experiments were conducted in triplicate.

4.5.3 Phylogenetic comparative analyses

Observed venom activities of the different snake species were investigated in an evolutionary framework by mapping them on a taxon tree using Mestique and analyses were performed via the R package Phytools as per that of (Lister et al., 2017; Rogalski et al., 2017) using phylogenetic

Generalized Least Squares (PGLS). The phylogeny was adapted from (Alencar et al., 2016) Analyses were implemented in R v3.2.5 (Team, 2016) using the APE package for basic data manipulation (Paradis et al., 2004). Ancestral states of each substrate functional trait (ES001, ES002, ES003, ES005, ES010, ES011, PLA_2, coagulation) were estimated via maximum likelihood with the contMap function in phytools (Revell, 2012).

4.5.4 Coagulation assays

4.5.4.1 Action upon plasma and fibrinogen: Clot formation or inhibition assays

Ability to affect clotting of plasma and fibrinogen, including relative co-factor dependency, was investigated using a Stago STA-R Max coagulation analyser using protocols previously described by us (Debono et al., 2019c; Debono et al., 2017a). In order to investigate whole plasma and fibrinogen clotting and co-factor dependency clotting, we prepared healthy human plasma (citrate 3.2%, Lot#1690252, approval #16-04QLD-10), obtained from the Australian Red Cross (44 Musk Street, Kelvin Grove, Queensland 4059) and human fibrinogen (4 mg/mL, Lot#F3879, Sigma Aldrich, St. Louis, Missouri, United States). Coagulopathic toxin effects were measured by a modified procoagulant protocol on a Stago STA-R Max coagulation robot (France) using Stago Analyser software v0.00.04 (Stago, Asniéres sur Seine, France). Plasma clotting baseline parameters were determined by performing the standardised activated Partial Thromboplastin Time (aPTT) test (Stago Cat# T1203 TriniCLOT APTT HS). This was used as a control to determine the health of normal clotting plasma according to the universal standard range of between 27–35 s. Plasma aliquots of 2 mL, which had been flash frozen in liquid nitrogen and stored in a −80 °C freezer, were defrosted in an Arctic refrigerated circulator SC150-A40 at 37°C. In order to determine clotting times effected by the addition of varying venom concentrations, a modified aPTT test was developed. A starting volume of 50 µL of crude venom (5 µg/50 µL) was diluted with STA Owren Koller Buffer (Stago Cat# 00360). An 8-dilution series of 1 (20 µg/mL), 1/2 (10 µg/mL), 1/5 (4 µg/mL), 1/12 (1.6 µg/mL), 1/30 (0.66 µg/mL), 1/80 (0.25 µg/mL), 1/160 (0.125 µg/mL), and 1/400 (0.05 µg/mL) was performed in triplicate. $CaCl_2$ (50 µL; 25 mM stock solution Stago Cat# 00367 STA $CaCl_2$ 0.025M) was added with 50 µL phospholipid (solubilized in Owren Koller Buffer adapted from STA C.K Prest standard kit, Stago Cat# 00597). An additional 25 µL of Owren Koller Buffer was added to the cuvette and incubated for 120 sec at 37°C before adding 75 µL of human plasma. Relative clotting was then monitored for 999 sec or until plasma clotted (whichever was sooner). Additional tests were run, both with and without $CaCl_2$ and phospholipid, respectively, to test for $CaCl_2$ or phospholipid dependency. STA Owren Koller Buffer was used as a substitute, using the same volumes to allow for consistency in the final volumes (250 µL).

4.5.4.2 Thromboelastography

Venoms were investigated for their ability to affect clot strength ability of plasma and fibrinogen using a Thromboelastography® 5000 using protocols previously described by us (Debono et al., 2019c) and (Coimbra et al., 2018; Oulion et al., 2018). Using human fibrinogen (4 mg/mL) and human plasma venoms were investigated using a Thrombelastogram® 5000 Haemostasis analyser (Haemonetics®, Haemonetics Australia Pty Ltd, North Rdye, Sydney 2113, Australia) for their ability in clot strength. Human fibrinogen (4 mg/mL, Lot#F3879, Sigma Aldrich, St. Louis, Missouri, United States) was reconstituted in enzyme buffer (150 mM NaCl and 50 mM Tri-HCl (pH 7.3)). Natural pins and cups (Lot# HMO3163, Haemonetics Australia Pty Ltd, North Rdye, Sydney 2113, Australia) were used with the following solution; 7 µL venom working stock (1 mg/mL outlined in (Debono et al., 2017a)) or 7 µL thrombin as a positive control (stable thrombin from Stago Liquid Fib kit, unknown concentration from supplier (Stago Cat#115081 Liquid Fib)), 72 µL $CaCl_2$ (25mM stock solution Stago Cat# 00367 STA), 72 µL phospholipid (solubilized in Owren Koller Buffer adapted from STA C.K Prest standard kit, Stago Cat# 00597), and 20 µL Owren Koller Buffer (Stago Cat# 00360) was combined with 189 µL fibrinogen or human plasma and run immediately for 30 min to allow for ample time for clotting formation. An additional positive control of 7 µL Factor Xa (unknown concentration from supplier, Liquid Anti-Xa FXa Cat#253047, Stago) was also incorporated for plasma only. When no clot was formed from the effects of anticoagulant venoms, an additional 7 µL thrombin was added to the pin and cup to generate a clot and to determine the effects of fibrinogen degradation.

4.5.4.3 Fibrinogen SDS PAGE electrophoresis and gel image analysis

Venoms from *Azemiops feae*, *Calloselasma rhodostoma*, *Deinagkistrodon acutus*, *Hypnale hypnale*, *Tropidolaemus subannulatus* and *Tropidolaemus wagleri* were investigated for ability to cleave fibrinogen using protocols previously described by us (Debono et al., 2019c; Dobson et al., 2018). Human fibrinogen (Lot#F3879, Sigma Aldrich, St. Louis, Missouri, United States) was reconstituted to a concentration of 1 mg/mL in isotonic saline solution, flash frozen in liquid nitrogen and stored at -80ºC until use. Freeze-dried venom was reconstituted in deionised H_2O and concentrations were measured using a Thermo Fisher Scientific™ NanoDrop 2000 (Waltham, MA, USA). Assay concentrations were a 1:10 ratio of venom:fibrinogen. Human fibrinogen (Lot#F3879, Sigma Aldrich, St. Louis, Missouri, United States) stock of 1 mg/mL was dispensed into ten 120 µL aliquots. Fibrinogen from each aliquot (10 µL) was added to 10 µL buffer dye (5 µL of 4× Laemmli sample buffer (Bio-Rad, Hercules, CA, USA), 5 µL deionised H_2O, 100 mM DTT (Sigma-Aldrich, St. Louis, MO, USA)) as an untreated control lane. An additional fibrinogen aliquot (10 µL) was firstly incubated for 60 min at 37ºC before immediately adding 10 µL buffer dye. Venom stock (1 µL at 1

mg/mL) was added to the remaining 100 µL fibrinogen aliquot and incubated over 60 min at 37ºC, taking out 10 µL at varying time points (1, 5, 10, 15, 20, 30, 45 and 60 min). This 10 µL was immediately added to an additional 10 µL buffer dye. Once all 8-time points including the two controls (untreated, unincubated fibrinogen and untreated, incubated fibrinogen 60min at 37ºC) were added to the buffer dye these were incubated at 100ºC for 4 minutes then immediately loaded into the precast 1D SDS-PAGE gel. Gels were prepared in triplicate under the described conditions per venom and were run in 1× gel running buffer (as described by (Debono et al., 2017a; Koludarov et al., 2017) at room temperature at 120 V (Mini Protean3 power-pack from Bio-Rad, Hercules, CA, USA) until the dye front neared the bottom of the gel. Gels were stained with colloidal coomassie brilliant blue G250 (34% methanol (VWR Chemicals, Tingalpa, QLD, Australia), 3% orthophosphoric acid (Merck, Darmstadt, Germany), 170 g/L ammonium sulfate (Bio-Rad, Hercules, CA, USA), 1 g/L Coomassie blue G250 (Bio-Rad, Hercules, CA, USA), and destained in deionised H_2O.

Fibrinogen gel analysis (ImageJ and PRISM)

Using the publicly available software ImageJ (V1.51r, Java 1.6.0_24, National Institutes of Health, Bethesda, Maryland, USA) (Schneider et al., 2012), gels that had been scanned using a standard printer/scanner were loaded onto the software. Scans were changed to 32 bit to emphasise darken bands of fibrinogen chains so that the image could be manipulated to view individual peaks and troughs representing the alpha, beta and gamma chains. The intensity represents the amount of protein within that particular band and as the chain degrades the intensity decreases. Using the 'wand function' each peak within the graph was selected automatically producing a quantity for the area under the curve. AUC was graphed using GraphPad PRISM 7.0 (GraphPad Prism Inc., La Jolla, CA, USA). This process was repeated for all three triplicates for each venom.

4.5.4.4 Factor X activation and prothrombin activation

To determine the relative rate of Factor X activation or prothrombin activation by venom samples, a working stock solution (at 1 mg/mL in 50% deionized H_2O+ 50% glycerol) was manually diluted with OK buffer (STA Owren Koller Buffer) (50 µL at 20 µg/mL) to a cuvette. A total of 50 µL of $CaCl_2$ (25 mM), 50 µL phospholipid (cephalin prepared from rabbit cerebral tissue from STA C.K Prest standard kit, solubilized in OK buffer) and 25 µL of OK buffer was added to cuvette and incubated for 120 sec at 37°C before adding 75 µL of a solution containing the colorimetric substrate (Liquid Anti-Xa substrate, Stago LOT 253047) and either 0.01 µg/µL FX (Human Factor X, Lot #HH0315, HTI) or 0.1 µg/µL prothrombin (Human Prothrombin, Lot # GG1026, HTI) (total volume 250 µL/cuvette). A change in the optical density (OD) was measured each second for 300 sec using a STA-R Max® automated analyzer (Stago, Asnières sur Seine, France). All tests were performed in triplicate. The rate of FX activation or prothrombin activation, by the samples, was calculated in

comparison to the variation in the optical density – corresponding to the cleavage of the substrate by FXa or thrombin, after the activation of the zymogen by the samples, in relation to direct cleavage of substrate by the samples in the absence of the zymogen. Human FXa (Liquid Anti-Xa FXa LOT 253047) or thrombin (Liquid Fib, Stago, LOT 253337) was used as positive control to ensure quality of the substrate. The samples analyzed, in same conditions, without the presence of the zymogen were used as a negative control to establish and venom-induced baseline substrate cleavage in the absence of the zymogen. A solution containing deionized H_2O/glycerol at a 1:1 ratio was used as a second negative control.

4.5.4.5 Fibrinolysis ± tPA

The ability of venoms from *Azemiops feae*, *Calloselasma rhodostoma*, *Deinagkistrodon acutus*, *Tropidolaemus subannulatus* and *Tropidolaemus wagleri* to activity lyse clots was investigated in the presence or absence of tPA following methods described previously by us (Debono et al., 2019c). To investigate the fibrinolysis ability of the above venoms, varying concentrations of venom (100 ng/μL, 500 ng/μL and 1 μg/μL) were tested under varying conditions with the addition of tissue plasminogen activator (tPA, Sekisui Diagnostics, Lexington, MA, USA). Aliquots (100 μL) of normal pooled human plasma (Leiden University Medical Center (Leiden, NL)) stored at -80°C were defrosted in a water bath at 37°C. A 96-well plate was prepared under the following conditions: 6 pM tissue factor (TF) (Innovin, Siemens, USA) was added to 10 μM phospholipid vesicles (PCPS, 75% phosphatidylcholine and 25% phosphatidylserine, Avanti Polar Lipids, Alabama, USA) in HEPES buffer (25 mM HEPES, 137mM NaCl, 3.5 mM KCl, 0.1% BSA (Bovine Serum Albumin A7030, Sigma Aldrich, St Louis, MD, USA)) and gently incubated at 37ºC for 1 hr in a water bath. 17 mM CaCl and 37.5 U/mL tPA (diluted in dilution buffer (20 mM HEPES, 150 mM NaCl, 0.1% PEG-8000 (Polyethylene glycol 8000,1546605 USP, Sigma Aldrich, St Louis, MD, USA), pH 7.5)) was then added to the solution. A volume of 30 μL of this solution was added to each experimental well, along with 10 μL of venom at varying concentrations and an additional 10 μL of HEPES buffer, prepared on ice (total well volume of 100 μL). Normal pooled plasma (50 μL) was immediately added to each well (heated to 37ºC). Absorbance measuring commenced immediately and was measured every 30 sec over 3 hr at 405 nm on a Spectra Max M2^e (Molecular Devices, Sunnyvale, CA, USA) plate reader, heated to 37ºC. Measurements were captured on Softmax Pro software (V 5.2, Molecular Devices, Sunnyvale, CA, USA) and data points analysed using GraphPad PRISM 7.0 (GraphPad Prism Inc., La Jolla, CA, USA). All experimental conditions were repeated in triplicates and averaged.

Chapter 5: Habu coagulotoxicity: Clinical implications of the functional diversification of *Protobothrops* snake venoms

---

5.1 Abstract

Venom can affect any part of the body reachable via the bloodstream. Toxins which specifically effect the coagulation cascade do so either by anticoagulant or procoagulant mechanisms. Here we investigated the coagulotoxic effects of six species within the medically important viper genus *Protobothrops* (Habu) from the Chinese mainland and Japanese islands, a genus known to produce hemorrhagic shock in envenomed patients. Differential coagulotoxicity was revealed: *P. jerdonii* and *P. mangshanensis* produced an overall net anticoagulant effect through the pseudo-procoagulant clotting of fibrinogen; *P. flavoviridis* and *P. tokarensis* exhibit a strong anticoagulant activity through the destructive cleavage of fibrinogen; and while *P. elegans* and *P. mucrosquamatus* both cleaved the A-alpha and B-beta chains of fibrinogen they did not exhibit strong anticoagulant activity. These variations in coagulant properties were congruent with phylogeny, with the closest relatives exhibiting similar venom. The results indicate that anticoagulation mediated by pseudo-procoagulant cleavage of fibrinogen is the basal state, while anticoagulation produced by destructive cleavage of fibrinogen is the derived state within this genus. This is the first in depth study of its kind highlighting extreme enzymatic variability, functional diversification and clotting diversification within one genus surrounding one target site, governed by variability in co-factor dependency. The documentation that the same net overall function, anticoagulation, is mediated by differential underlying mechanics suggests limited antivenom cross-reactivity, although this must be tested in future work. These results add to the body of knowledge necessary to inform clinical management of the envenomed patient.

5.2 Introduction

Venom is defined as a secretion produced in specialised cells that is delivered to a target animal through a wound, and consequently disrupts normal physiological or biochemical processes (Fry et al., 2009a; Fry et al., 2009b; Jackson and Fry, 2016; Jackson et al., 2017; Nelsen et al., 2014). Venoms are complex mixtures of enzymes, toxins, peptides, organic molecules and salts (Fry et al., 2009a; Fry et al., 2009b) which are used to facilitate feeding, (Fry et al., 2008; Fry et al., 2013; Fry et al., 2009b; Jackson et al., 2013) defence such as that found in spitting cobras (Cascardi et al., 1999; Hayes et al., 2008; Panagides et al., 2017) or competition (Deufel and Cundall, 2003) for the producing organism (Fry and Wüster, 2004; Sunagar et al., 2013). Numerous studies have demonstrated that venom genes evolve at a much faster rate than housekeeping genes, facilitating a drive towards a highly specialised and complex venom composition (Casewell et al., 2013; Jackson et al., 2013; Sunagar et al., 2013; Vonk et al., 2013). This facilitated diversification allows toxins within venom

to evolve rapidly, and at different rates, through a variety of different selective mechanisms. These mechanisms include but are not limited to ecological niche occupation, which is in-turn directly related to prey ecology, and in some cases taxon-specific toxins including the potential for prey escape or prey retaliation (Daltry et al., 1996b; Fry et al., 2013; Jackson et al., 2013; Koludarov et al., 2014; Li et al., 2005; Pawlak et al., 2006; Pawlak et al., 2009; Sunagar et al., 2013; Sunagar et al., 2014; Yang et al., 2016).

Snake venoms are made up of a myriad of mutated protein families, each responsible for varying pathophysiological effects (Fry, 2005). Coagulatoxins target the blood coagulation cascade via one of two mutually exclusive functional mechanisms: anticoagulation or procoagulation (Fry et al., 2009a). Anticoagulation that is mediated via proteolytic cleavage is accomplished through two different mechanisms: cleavage in a non-clotting, destructive manner which results in direct anticoagulation; or cleavage in a pseudo-procoagulant manner, resulting in weak fibrin clots with very short-half lives. While kallikrein-type serine proteases and snake venom metalloproteases (SVMP) both may cleave fibrinogen in a non-clotting, destructive manner (Casewell et al., 2015; Vaiyapuri et al., 2015), only kallikrein toxins are currently known for the pseudo-procoagulant activity.

Fibrinogen is a trinodular protein, present in high concentrations in plasma (Wolberg, 2007), and is made up of three polypeptide chains (Aα, Bβ, γ). Under normal cleavage by thrombin, fibrinopeptides A and B are cleaved from the Aα and Bβ chains, thereby exposing the γ chain and producing strong, well-ordered lattices. These fibrin clots are further strengthened by thrombin-mediated activation of Factor XIII into FXIIIa, with FXIIIa in turn additionally cross linking the fibrin strands (Bagoly et al., 2012; Collet et al., 2000; Koh and Kini, 2012; Longstaff and Kolev, 2015; Ryan et al., 1999; Wolberg, 2007). When fibrinogen is cleaved by snake venom in a non-clotting manner, SVMPs cleave the Aα-chain while kallikreins cleave the Bβ-chain (Kini, 2005b; Kini and Koh, 2016; Sajevic et al., 2011; Swenson and Markland, 2005) with both cleaving at sites distinct from that of thrombin. In contrast, when fibrinogen is cleaved in a pseudo-procoagulant manner by kallikreins, fibrinopeptides A or B (or both) are cleaved from their respective chains but through aberrant cleavage sites, resulting in disordered lattice-works and weak, short-lived clots (Sajevic et al., 2011; Swenson and Markland, 2005).

The wide-ranging Asian pit viper genus *Protobothrops* occupies the islands of Japan, mainland China and islands off China. *Protobothrops* bites are known for potent haemorrhagic shock effects in prey and human bite victims (Chen et al., 2009; Nishimura et al., 2016). Target sites include impeding primary haemostasis by disruption along the cascade from the blockage of platelet aggregation through to inhibiting clot formation due to the unnatural cleavage of fibrinogen (Collet et al., 2000; Kolev and Longstaff, 2016; Longstaff and Kolev, 2015; Mosesson, 2005).

Despite the medical importance of these snakes, a comprehensive examination of intra-genus venom variation has not been undertaken. Such data will provide fundamental information which may aid the prediction of clinical effects and thus guide snake bite case management. This study used a myriad of techniques to investigate the effects of six *Protobothrops* venoms upon the clotting cascade, with a particular focus upon their actions upon fibrinogen.

5.3 Results

5.3.1 Enzymatic assays on the Fluoroskan Ascent

Enzymatic assays were using substrates typically cleaved by metalloproteases (ES001, ES003, and ES010), serine proteases (ES002 and ES011) or PLA_2. While these are artificial substrates and may not necessarily directly correlate with 'real world' bioactivity, they are useful for elucidating differences between the venoms. Indeed, significant variation was observed between the venoms for each substrate class (Figure 5.1). In addition to variation between venoms, there was also significant variation between substrate types, whereby the strongest for one substrate type was not the strongest for another substrate within the same generalised class (whether within the metalloprotease or serine protease class). For ES001 *P. flavoviridis* was twice as active as the next strongest venom (the sister species *P. tokarensis*), and three times as active as *P. mucrosquamatus* with the other species only showing low levels of activity (Figure 5.1A). A broadly similar pattern was observed for ES010, with *P. flavoviridis* being significantly more active than the other venoms, however with some venoms that showed only trace activity upon ES001 showing significant activity upon ES010 (*P. elegans,* and *P. mangshanensis*) (Figure 5.1D). In contrast, for ES003 (also a metalloprotease substrate), *P. mucrosquamatus* was much more active than all other venoms, being four times as active as the next potent species (*P. tokarensis*) (Figure 5.1C). A similar level of variation between the serine protease substrates was also observed, where *P. elegans* was the most potent, but all other venoms displaying at least moderate levels of activity, while for *P. jerdonii* and *P. mangshanensis* were both potent while all other venoms displayed only trace or undetectable levels of activity (Figure 5.1B and 1E). *P. flavoviridis* displayed the highest activity upon the PLA_2 substrate, with the next nearest venom (*P. elegans*) being 66% as potent, followed by *P. tokarensis* (33%), and all others showing only very low levels of activity (Figure 5.1F). These variations are strongly suggestive of differential activity of the venoms under physiological conditions. The extreme variation between species was evident in the ancestral state reconstructions (Figure 5.1), which is consistent with rapid diversification away from the ancestral state.

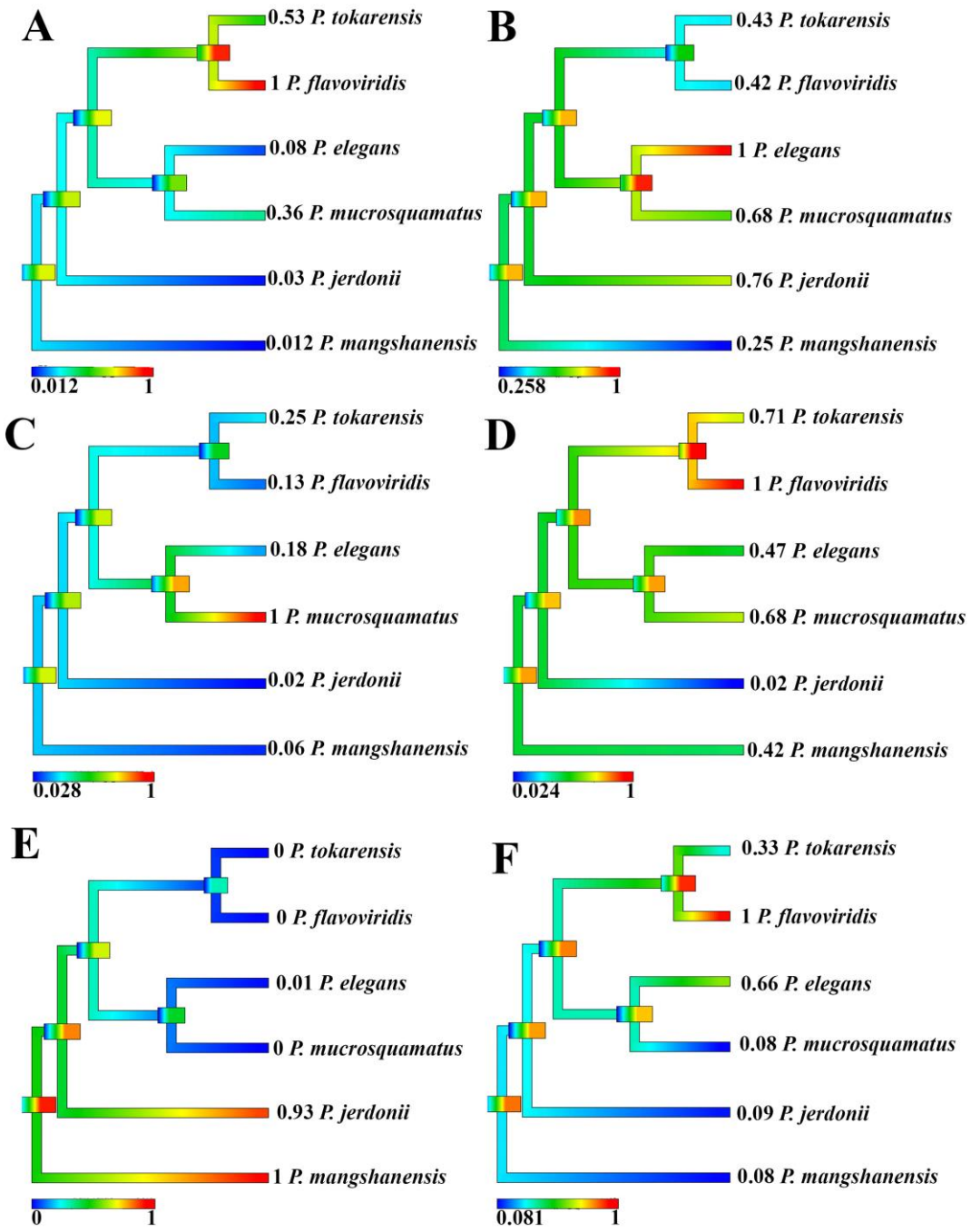

Figure 5.1 Enzyme substrate activity

Ancestral state reconstruction of enzymatic substrate activity of *Protobothrops* species based on their normalised relative ability to cleave the following substrates; A: fluorogenic peptide substrate (Mca-PLGL-Dpa-AR-NH2 Fluorogenic Matrix Metalloprotease Substrate, Cat#ES001), B: fluorogenic peptide substrate (Mca-RPKPVE-Nval-WRK(Dnp)-NH2 Fluorogenic MMP Substrate, Cat#ES002) which detects additional metalloprotease activity and Factor X, C: fluorogenic peptide substrate (Mca-PLAQAV-Dpa-RSSSR-NH2 Fluorogenic Peptide Substrate, Cat#ES003) which detects additional metalloprotease activity, D: fluorogenic peptide substrate (Mca-KPLGL-Dpa-AR-NH2 Fluorogenic Peptide Substrate, Cat#ES010) which detects additional metalloprotease activity, E: fluorogenic peptide substrate (Boc-VPR-AMC Fluorogenic Peptide Substrate, Cat#ES011) which detects serine protease activity, F: Phospholipase A_2 substrate activity, EnzChek® (Cat# E10217). Warmer colours represent more potent substrate cleavage. Bars indicate 95% confidence intervals for the estimate at each node. Phylogeny follows (Alencar et al., 2016).

5.3.2 Coagulation analyses

5.3.2.1 Action upon plasma

Plasma clotting and co-factor dependency of Ca^{2+} and phospholipid

Only *P. elegans, P. mangshanensis*, and *P. jerdonii* and displayed the ability to clot human plasma (Figure 5.2). At a 20µg/mL venom concentration, *P. mangshanensis* was able to clot plasma in 32.0 ± 5.4 sec, compared to *P. jerdonii* (139.0 ± 11.9 sec) and *P. elegans* (98.9 ± 6.66 sec), relative to the spontaneous clotting time of the recalcified plasma of 325.0 ± 25.0 sec. In contrast, the *P. flavoviridis* and *P. tokarensis* venom demonstrated a potently anticoagulant effect, with both species reaching the machine maximum clotting time measurement of 999.99 sec. *P. mucrosquamatus* venom was also anticoagulant at a 20 µg/mL venom concentration but weaker than *P. flavoviridis* and *P. tokarensis* (Figure 5.2). The venoms displayed significant variation in the relative dependency upon calcium or phospholipid, with calcium being a much stronger variable (Figure 5.2).

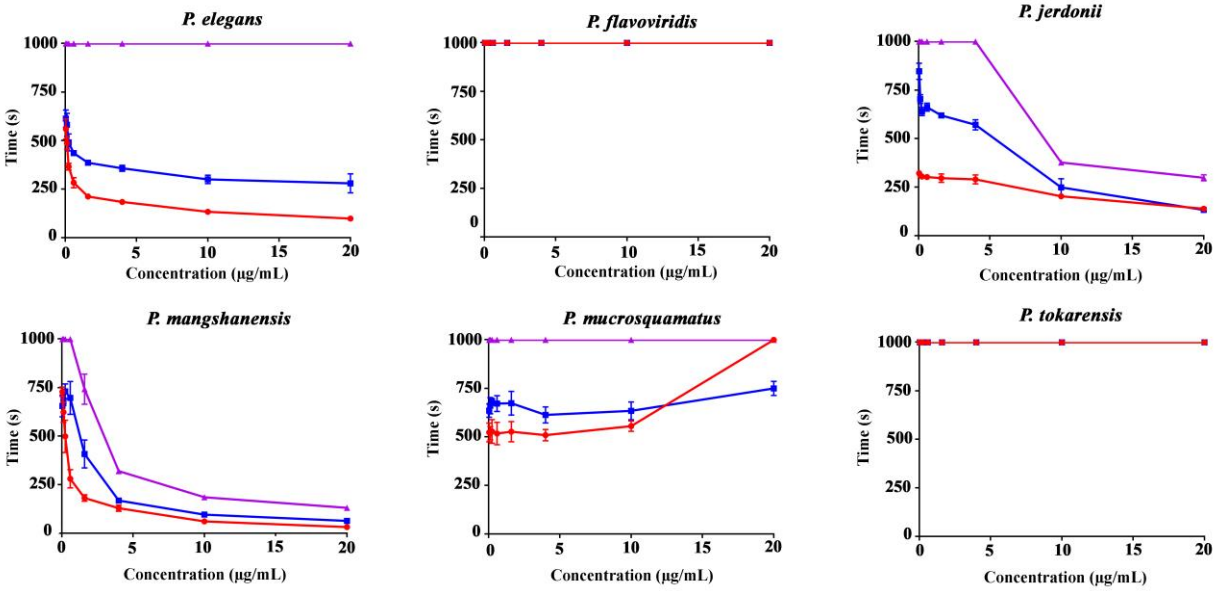

Figure 5.2 Procoagulant co-factor dependency
Comparison of procoagulant co-factor dependency clotting curves of *Protobothrops* at varying venom concentrations on human plasma. *X* axis: final venom concentration (µg/mL), *Y* axis: clotting time in seconds. Data points are N = 3 and error bards indicate standard deviation. Red line = procoagulant dilution series with calcium and phospholipid against human plasma. Blue line = Phospholipid dependency, procoagulant dilution series with calcium added only against human plasma. Purple line = Calcium dependency, procoagulant dilution series with phospholipid added only against human plasma.

As the clotting of plasma could be due to procoagulant functions through the generation of endogenous thrombin (producing strong fibrin clots), or pseudo-procoagulant functions by directly acting upon fibrinogen (producing weak clots), additional tests were conducted to ascertain the ability to activate Factor X or prothrombin, and also to determine the relative strength of fibrin clots in the

plasma tests. None of the venoms, even the ones which produced clots in the above analyses, were able to activate FX or PT. Further, the clots formed by the venoms in plasma were weak, indicated by reduced clot strength relative to the controls (Figure 5.3). As this was strongly suggestive of direct action upon fibrinogen in a pseudo-procoagulant manner (Oulion et al., 2018), additional tests were undertaken to characterise the cleavage and clotting effects upon fibrinogen.

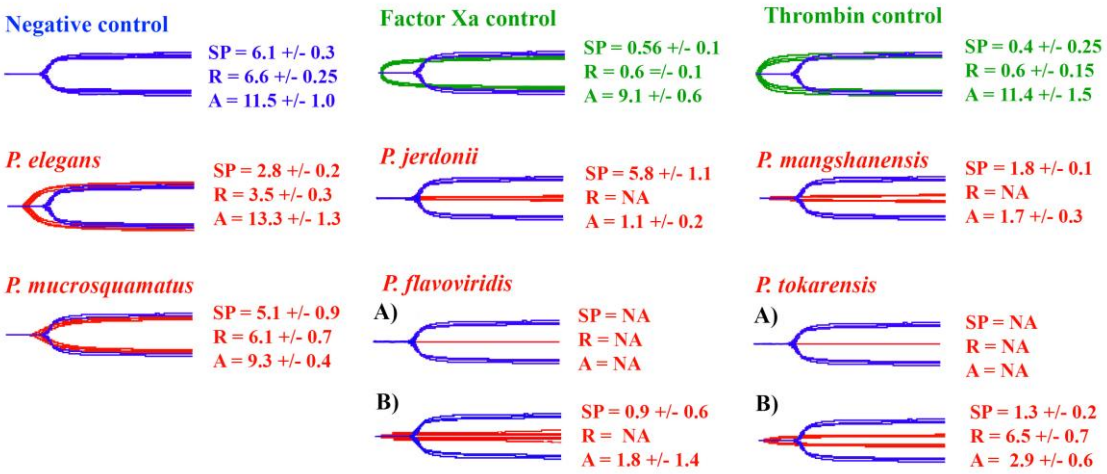

Figure 5.3 Thromboelastography plasma traces
Overlaid thromboelastography traces showing effects of 20 µg/mL venoms ability to clot plasma relative to spontaneous clot control: blue traces = re-calcified plasma spontaneous clotting control; green traces = Factor Xa or thrombin controls; red traces = venom samples. SP = split point, time taken until clot begins to form. R = time to initial clot formation where formation is 2 mm^{+} (min). A (parameter) = detectable clot strength (mm) which may be < 2 mm. As *P. flavoviridis* and *P. tokarensis* did not induce a clot in A), thrombin was added in B) in order to induce a clot and measure fibrinogen degradation. Overlaid traces are N = 3 for each set of control or experimental conditions. Values are N = 3 means and standard deviation.

Plasma anticoagulant inhibition – FXa and thrombin

Additional testing was conducted to investigate the anticoagulant properties of the two most potent anticoagulant species, *P. tokarensis* and *P. flavoviridis* based off their initial inability to clot human plasma (Figure 5.2). Given that both species failed to form any clot (Figure 5.2), their venom components may interfere with specific reactions in the coagulation cascade. FXa inhibition and thrombin inhibition were investigated across a range of concentrations. While both venom species were unable to successfully inhibit thrombin, they were able to inhibit FXa, with *P. flavoviridis* being much more potent than *P. tokarensis* (Figure 5.4).

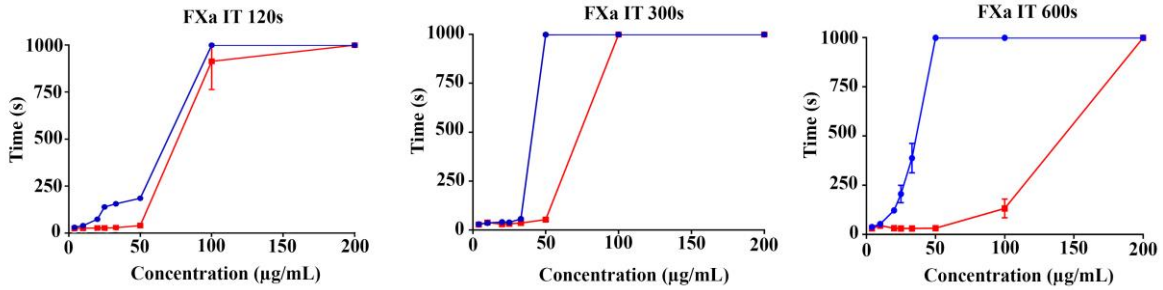

Figure 5.4 Factor Xa inhibition
Factor Xa inhibition tests (FXa IT) for *P. flavoviridis* and *P. tokarensis* measured over 120, 300 and 600 sec incubation times. X axis: final venom concentration (µg/mL), Y axis: clotting time in seconds. Data points are N = 3 and error bars indicate standard deviation. Red line: *P. tokarensis.* Blue line: *P. flavoviridis*.

5.3.2.2 Action upon fibrinogen

As the above tests suggested that the clotting venoms are pseudo-procoagulant in that they are producing weak fibrin clots, additional tests were undertaken to determine the specific effects upon fibrinogen.

Fibrin clot formation

Using the same STA-R Max coagulation analyser protocol as above for plasma, we tested the ability of the venoms to form fibrin clots by replacing plasma with 4 mg/mL human fibrinogen. Consistent with the plasma results, and demonstrative of direct effect upon fibrinogen in a pseudo-procoagulant manner, the *P. mangshanensis* and *P. jerdonii* venoms were the only ones able to effectively trigger the formation of fibrin clots (Figure 5.5). In testing for the relative influence of the physiological co-factors calcium and phospholipid, extensive variation was noted between the cofactors and between the species for a particular cofactor. Removal of calcium slowed the reaction, resulting in a 65.1 ± 0.7% increase in the area under the curve, but the removal of phospholipid had a negligible effect, with the area under the curve increasing by only 6.6 ± 1.8%. In contrast, *P. mangshanensis* showed a 128.9 ± 0.8% increase in the area under the curve when calcium was removed and a 37.2 ± 0.7% increase when phospholipid was removed.

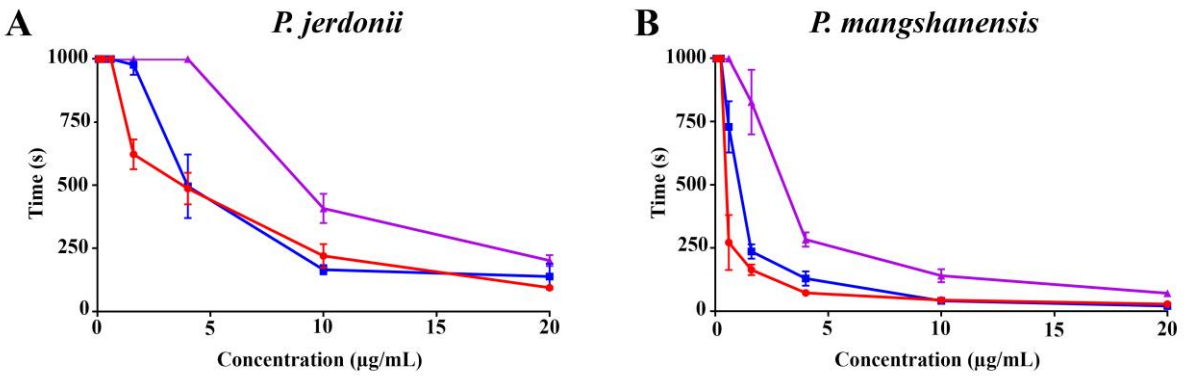

Figure 5.5 Procoagulant co-factor dependency – fibrinogen
Comparison of procoagulant co-factor dependency clotting curves of two *Protobothrops* species at varying venom concentrations on human fibrinogen (4 mg/mL). *X* axis: final venom concentration (µg/mL), *Y* axis: clotting time in seconds. A = *P. jerdonii*, B = *P. mangshanensis.* Red line: procoagulant dilution series with calcium and phospholipid against human fibrinogen, Blue line: procoagulant dilution series with calcium only against human fibrinogen, Purple line: procoagulant dilution series with phospholipid only against human fibrinogen. Data points are N = 3 and error bars indicate standard deviation. Area under the curve: for A = calcium dependency 0.651 ± 0.068, phospholipid dependency 0.066 ± 0.018. For B = calcium dependency 1.289 ± 0.008, phospholipid dependency 0.372 ± 0.007.

Thromboelastography using TEG5000s

In order to determine the strength of the clots formed by fibrinogen cleavage, we investigated the ability for venom to clot fibrinogen in the presence of Ca^{2+} and phospholipid. The thrombin control rapidly (SP = 0.2 ± 0 min, R = 0.23 ± 0.06 min) produced a strong (13.37 ± 1.24 mm). While *P. mangshanensis* was the most potent of the venoms, the clot was formed slower (SP = 1.5 ± 0.4 min, R = 2.07 ± 0.68 min) and weaker (7.33 ± 1.08) than the thrombin control (Figure 5.6). *P. jerdonii* and *P. elegans* also clotted the fibrinogen but slower and weaker than *P. mangshanensis* (Figure 5.6).

As *P. flavoviridis*, *P. mucrosquamatus* and *P. tokarensis* did not display any ability to directly clot fibrinogen, additional tests were undertaken in order to ascertain if the venoms were cleaving the fibrinogen in a destructive manner that impeded the ability of thrombin to clot fibrinogen. Thrombin was added to the wells after the 30 min primary run in which no clot was formed. Consistent with destructive cleavage of fibrinogen by *P. mucrosquamatus* and *P. tokarensis* venoms, the addition of thrombin failed to produce a clot (Figure 5.6). In contrast, *P. flavoviridis* neither clotted the fibrinogen and displayed a weaker level of destructive cleavage. As this venom showed a strong anticoagulation activity upon the plasma (Figure 5.6), the low activity upon fibrinogen indicates that the anticoagulation activity is due to the direct inhibition of a clotting factor, which is consistent with the results showing an ability to inhibit FXa (Figure 5.4).

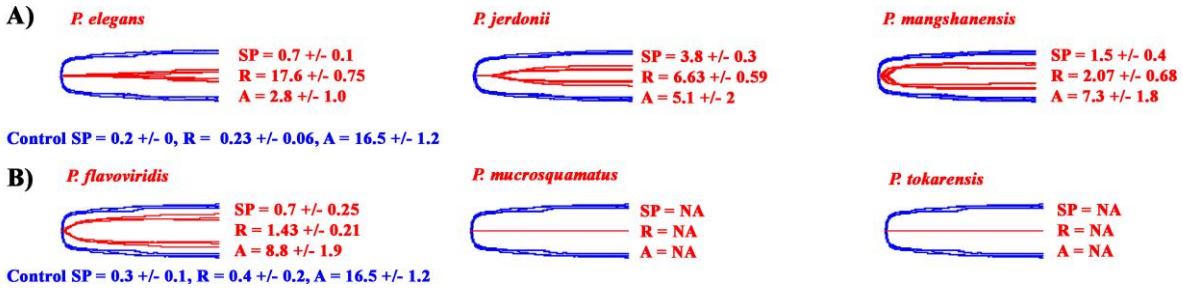

Figure 5.6 Thromboelastography fibrinogen traces
Overlaid thromboelastography traces showing effects of 20 µg/mL venoms: A) ability to clot fibrinogen relative to thrombin control; B) ability to clot whereby thrombin was added to samples which did not clot fibrinogen after 30 min in order to test for venom-induced fibrinogen degradation relative to blank control. Blue traces = thrombin controls, red traces = venom samples. SP = split point, time taken until clot begins to form. R = time to initial clot formation where formation is 2 mm+ (min). A (parameter) = detectable clot strength (mm) which may be <2 mm. Overlaid traces are N = 3 for each set of control or experimental conditions. Values are N = 3 means and standard deviation.

Fibrinogen gels

In order to determine the specific fibrinogen chains cleaved by the venoms, additional assays were undertaken to determine the time-dependent effects upon each chain. A consistent pattern emerged with all venoms displayed the ability to cleave the α chain (with differential potency), while the β chain was cleaved more slowly and only fully cleaved by the most potent α chain acting venoms (Figure 5.7, Figure 5.8 and Figure 5.9). Similarly, the γ chain was cleaved more slowly and only cleaved by the most potent α and β chain cleavers. Full cleavage of α, β and γ fibrinogen chains were only exhibited in *P. mangshanensis* and *P. jerdonii*. *P. mangshanensis* however cleaved all 3 chains much more quickly than *P. jerdonii* (Figure 5.6, Figure 5.7 and Figure 5.8). Cleavage of only the α and β chains were exhibited in *P. elegans* and *P. mucrosquamatus*, while *P. flavoviridis* and *P. tokarensis* only exhibited α chain degradation (Figure 5.7, Figure 5.8 and Figure 5.9). Ancestral state reconstruction suggested that the ability to cleave the α, β and γ fibrinogen chains was the basal condition, with the other cleavage patterns thus being derivations (Figure 5.9).

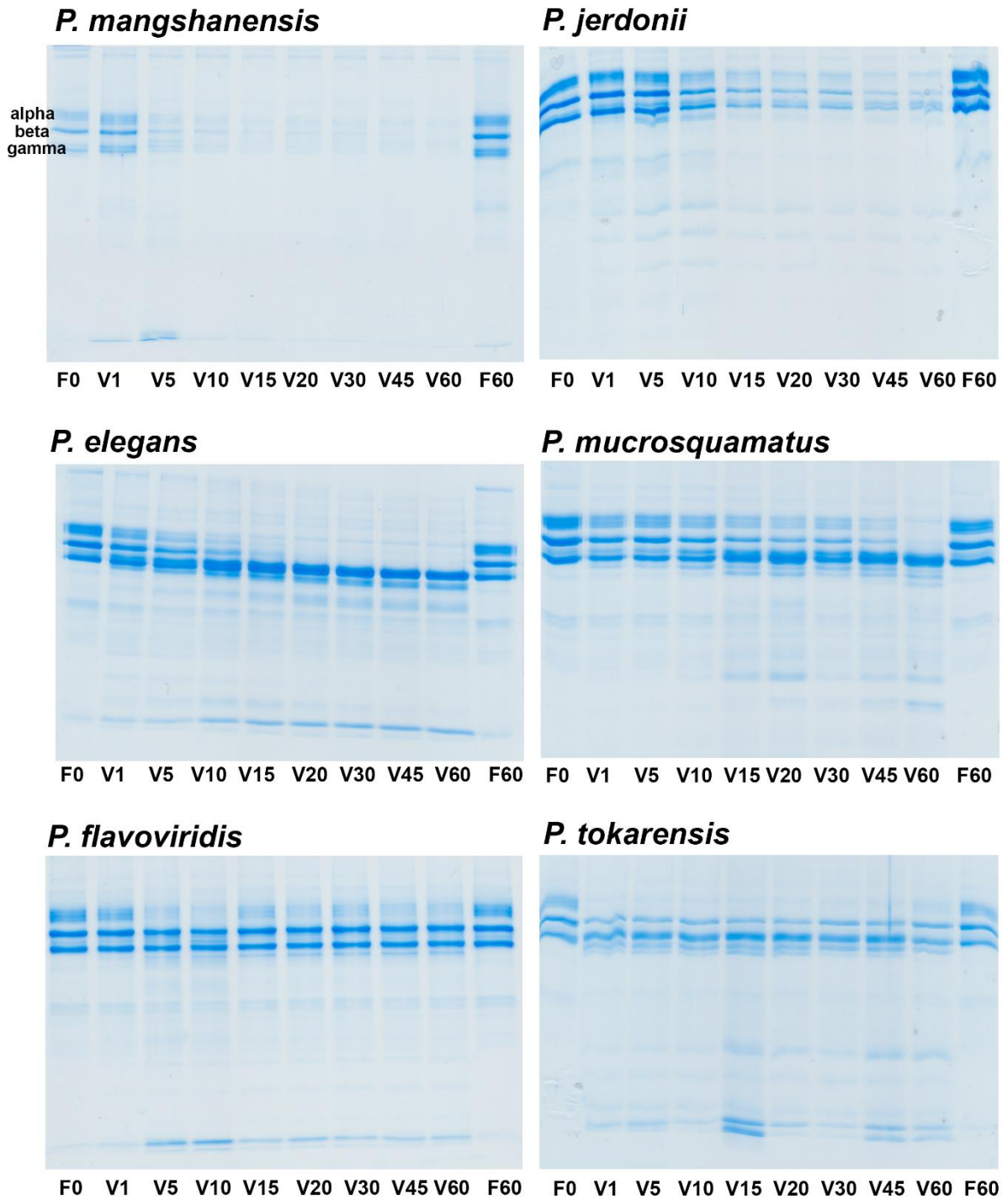

Figure 5.7 Fibrinogen chain cleavage - gel
1D SDS PAGE time dependent fibrinogen chain degradation (α, β or γ) by venom at 0.1 µg/µL concentration, with the fibrinogen at 1 µg/µL, at 37ºC over 60 min. F = fibrinogen at 0 min or 60 min incubation controls, V = venom incubation times (min).

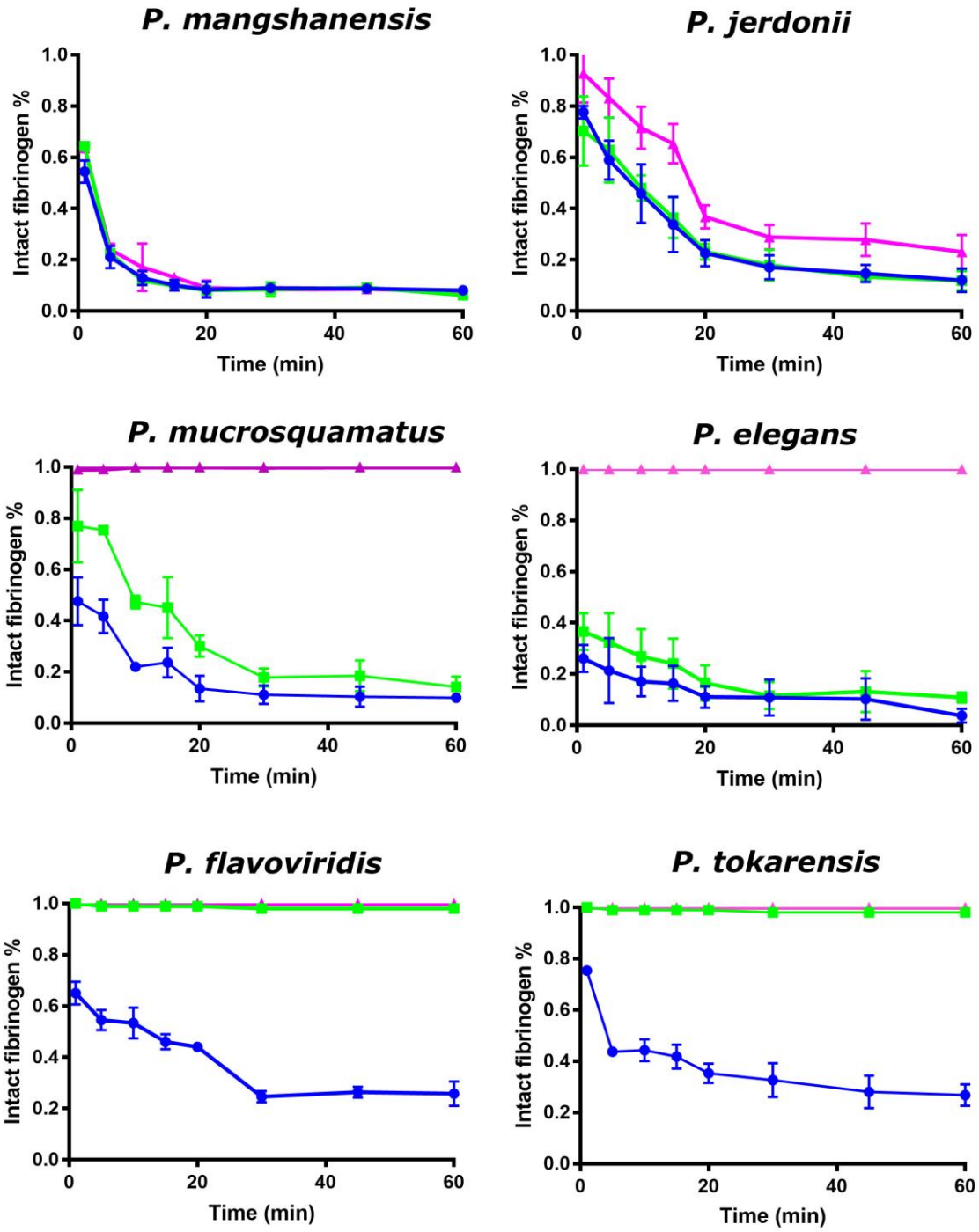

Figure 5.8 Fibrinogen chain cleavage - % intact
Relative cleavage of alpha (blue), beta (green) or gamma (pink) chains of fibrinogen. X-axis is time (min), y-axis is percentage of intact chain remaining. Data points are N = means and error bars indicate standard deviation.

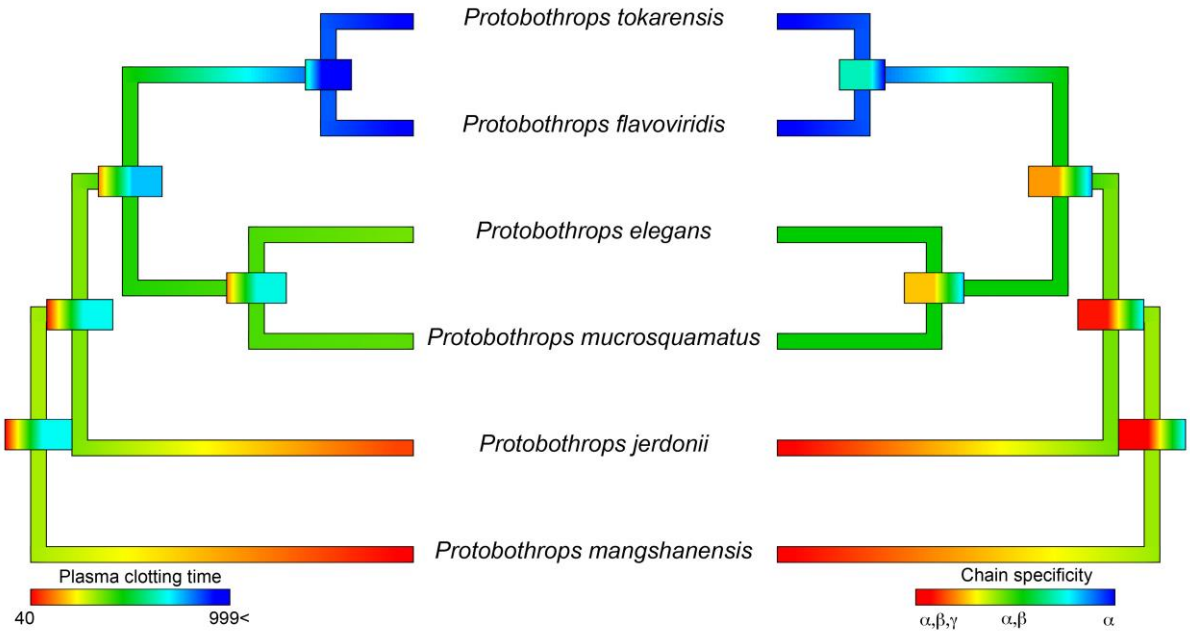

Figure 5.9 Ancestral state reconstruction of coagulation clotting times
Ancestral state reconstruction of coagulation clotting times on human plasma relative to fibrinogen chain cleavage specificity. Warmer colours represent more potent substrate cleavage. Bars indicate 95% confidence intervals for the estimate at each node. Phylogeny follows (Alencar et al., 2016).

Fibrinolysis ± tPA

The ability for *Protobothrops* crude venom to actively lyse a plasma clot was investigated under the presence or absence of tPA (tissue plasminogen activator) at varying concentrations. None of the 6-species tested at any of the concentrations successfully lysed plasma clots without the presence of tPA. However, in the presence of tPA, clot lysis times (CLT) were shortened relative to the control (tPA against plasma) (Figure 5.10). *Protobothrops mangshanensis*, *P. jerdonii*, *P. mucrosquamatus* and *P. elegans* venoms demonstrated a reduced CLT in the presence of tPA as compared to the control. Consistent with its potent anticoagulant effect, plasma in the presence of *P. flavoviridis* venom failed to form a clot due to complete degradation by venom at 1µg concentration.

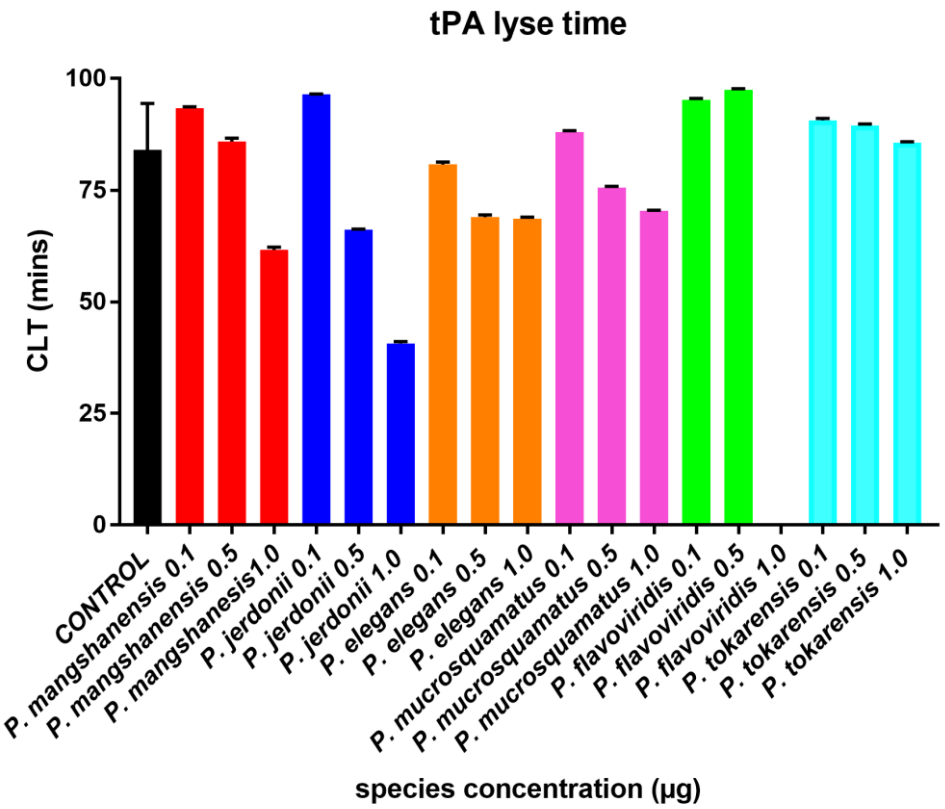

Figure 5.10 Fibrinolysis
Clot lysis Time (CLT) for each *Protobothrops* species in the presence of tPA at 0.1µg, 0.5µg and 1µg venom concentrations. Control is indicated in black. Data points are N = 3 and error bars indicate standard deviation. Bars which are lower than the control lysed the plasma clot quicker than under normal tPA conditions.

5.3.2.3 Platelet agglutination and inhibition

The ability for *Protobothrops* crude venom to agglutinate and inhibit platelets was investigated, with only *P. tokarensis* and *P. flavoviridis* potently inhibiting platelet agglutination (Figure 5.11).

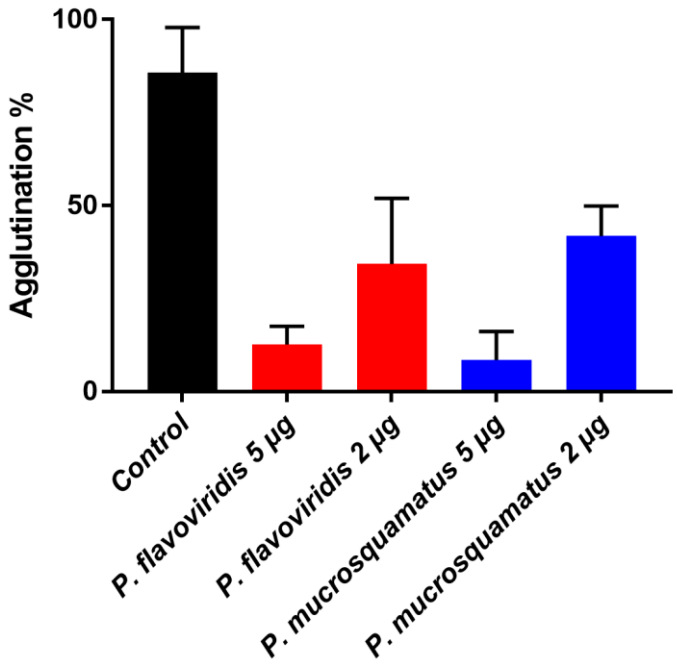

Figure 5.11 Platelet agglutination inhibition
Platelet agglutination inhibition at 5 µg and partial inhibition at 2 µg for *P. flavoviridis* and *P. tokarensis*. Black column indicates control run, red column indicates *Protobothrops flavoviridis*, blue column indicates *Protobothrops mucrosquamatus* run. Y axis: platelet agglutination percentage. Data points are N = 3 and error bars indicate standard deviation.

5.4 Discussion

Extensive functional diversification was evident between the six *Protobothrops* venoms tested, both in artificial environments (enzyme substrate testing) and physiological conditions (plasma and fibrinogen testing). This was evident by the ancestral state reconstructions (Figure 5.1 and Figure 5.9) showing rapid diversification away from the basal condition. Enzyme substrate testing patterns were differential between the substrate types tested, whether metalloprotease or serine protease, with no consistent functional or phylogenetic pattern, consistent with rapid radiation away from the ancestral state. While these substrates do not necessarily correlate with a particular physiological effect, the differential activity indicates that the venoms would have highly variable effects in a physiological system. This was shown to be the case with the venoms displaying a wide variation of coagulotoxic activity, ranging from potently pseudo-procoagulant to potently anticoagulant. A correlation, however, was evident between the nature and potency of the coagulotoxicity, with the strongest pseudo-procoagulant venoms (*P. jerdonii* and *P. mangshanensis*) displaying an ability to aberrantly cleave the alpha, beta and gamma chains of fibrinogen, with this putatively being the ancestral state, while the most potent anticoagulant venoms (*P. flavoviridis* and *P. tokarensis*) cleaving only the alpha chain, with this representing an extreme derivation away from the ancestral state.

Thromboelastography testing confirmed the pseudo-procoagulant function of *P. jerdonii* and *P. mangshanensis* venoms, with both being the most rapid in clotting fibrinogen but producing only weak clots. As these are the two most basal species (Alencar et al., 2018; Alencar et al., 2016), and the two most potent anticoagulant species are sister to each other, this suggests that pseudo-procoagulant activity is the basal condition within this genus, and that anticoagulant venoms represent the derived state.

Consistent with the extreme variation in their venoms, *Protobothrops* species are highly variable in morphology and ecological niche occupied, ranging from heavily built terrestrial species (eg *P. mangshanensis*) to gracile semi-arboreal species (eg *P. flavoviridis*). While the venom variation is suggestive of this feature being a driver in their adaptive radiation, it is also indicative of the potential to produce differential clinical effects, in that while haemorrhagic shock may be produced by all (Chen et al., 2009; Nishimura et al., 2016), the underlying mechanics may be different.

In addition to net anticoagulation produced by direct action upon fibrinogen (whether pseudo-procoagulant or anticoagulant), anticoagulation was also produced by these venoms as a by-product of irregular fibrinogen cleavage. This was evident in the fibrinolysis assays, whereby plasmin was able to lyse clots much quicker when venom from species was present (Figure 5.10). It is hypothesised that this is due to venoms from some species forming a weak clot via incorrect fibrinogen degradation and irregular fibrin strand linking. This has been demonstrated in the literature that fibrin diameter and the architecture of the fibrin strands can influence the clot strength and stability (Collet et al., 2000; Longstaff and Kolev, 2015; Mosesson, 2005; Wolberg, 2007; Wolberg and Campbell, 2008). Albeit both species are able to cleave all three fibrinogen chains, fibrinogen is cleaved in incorrect places, as opposed to where thrombin cleaves fibrinogen. This would result in larger fibrin strands which do not form a well-constructed clot and instead form a turbid, highly permeable clot (Collet et al., 2000; Wolberg, 2007; Wolberg and Campbell, 2008). In addition, FXIII is not activated and covalent cross linking, which would also strengthen clots, does not occur. This overall activity would result in a net anticoagulant outcome, despite neither species being able to activate plasminogen, which would aid in this weak anticoagulant effect.

In addition to their wide-ranging fibrinogen action, co-factor dependency of fibrinogen action also impacts on the physiological degree of fibrinogenolysis that the venom exhibits. The co-factor dependency of the two most potent species, *P. jerdonii* and *P. mangshanensis*, shows that not only does the effect on fibrinogen differ, but also the degree of co-factor dependency for either calcium or phospholipid and between the two species for a particular co-factor. This is the first study to show such an extensive shift in co-factor dependency on fibrinogen action from any snake species, illustrating that not only does the co-factor dependency differ but it also differs between species of a single genus. This reinforces the fundamental importance of including both co-factors in order to

replicate physiological conditions. While some venom studies have done this (Bos et al., 2016; Chester and Crawford, 1982; Debono et al., 2017a; Lister et al., 2017; Oulion et al., 2018; Pirkle et al., 1972; Rogalski et al., 2017), the inclusion of which is necessary to replicate physiological conditions, while others have neglected to include phospholipid (Isbister et al., 2010b; O'Leary and Isbister, 2010; Still et al., 2017; Vargas et al., 2011), or both cofactors (Ainsworth et al., 2018; Nielsen et al., 2018; Resiere et al., 2018; Williams et al., 1994) thereby skewing the results and hampering the interpretation as to the effects upon coagulation and therefore limiting the clinical and evolutionary relevance of the results.

In addition to this variation in net anticoagulation produced, it was shown that the two most potent anticoagulant species of the genus, *P. flavoviridis* and *P. tokarensis* (those that did not form a plasma or fibrinogen clot) also inhibited FXa (Figure 5.4). FX inhibition has been described previously by *P. flavoviridis* due to lectin toxins (Arlinghaus et al., 2015; Atoda et al., 1995) while it has not been described for *P. tokarensis.*

This continued variation in venom activity, enzymatic activity, functional diversification and clotting diversification creates further problems with predictive antivenom production raised against specific species, or species of a specific region. At present there are only two antivenoms that are produced for two of the eight species of *Protobothrops,* registered for *P. mucrosquamatus* and *P. flavoviridis,* with no available antivenom for the remainder of the genus. These include the 'Bivalent Antivenin Pit Viper, National Institute of Preventative Medicine, Taiwan', produced from *P. mucrosquamatus* and *Trimeresurus stejnegeri*, and the 'Habu Antivenom (Kaketsuken), The Chemo-Sero-Therapeutic Research Institute (Kaketsuken), Japan', produced from *P. flavoviridis*. Future works should investigate the ability of these antivenoms to specifically neutralise coagulotoxic effects and to what degree the antivenoms cross-react with non-immunising venoms. This study therefore not only reveals evolutionary trends of interest to biologists, but also documents substantial variation in the nature and potency of coagulotoxic effects that would directly inform upon potential clinical effects and management strategies.

5.5 Materials and Methods

A multidisciplinary approach was used to investigate the venomics and bioactivity of a range of representative species from the Asian pit viper genus *Protobothrops*. Venom samples from six *Protobothrops* species (*P. mangshanensis, P. jerdonii, P. elegans, P. muscrosquamatas, P. tokarensis, P. flavoviridis*) were from captive snakes: *P. elegans* (unknown locality founding stock), *P. flavoviridis* (Okinowa, Japan founding stock), *P. jerdonii* (Chinese founding stock), *P. mangshanensis* (Mt Mang, Hunan, China founding stock), *P. mucrosquamatus* (Sa Pa, Vietnam founding stock) and *P. tokarensis* (Tokara Island, Japan founding stock). Human plasma was obtained from the Australian Red Cross (Research agreement #18-03QLD-09 and University of Queensland

Human Ethics Committee Approval #2016000256). All plasma was prepared as 3.2% citrated stock, aliquoted into 1 mL quantities, which were snap frozen in liquid nitrogen, and stored in a -80°C freezer until needed, at which time an aliquot was defrosted by placing into a 37°C water bath for 10 minutes. All venom and plasma work was undertaken under the University of Queensland Biosafety Approval #IBC134BSBS2015.

5.5.1 Enzyme assays

5.5.1.1 Fluorescent substrate activation

In order to investigate Fluorescent Determination of matrix metalloprotease (ES001, ES003, ES005, ES010), serine protease activity (ES002, ES011) and phospholipase A_2 (PLA_2) enzymatic assays were undertaken as previously described by us (Debono et al., 2017a). For matrix metalloprotease and serine protease assays a working stock solution of freeze dried venom was reconstituted in a buffer containing 50% MilliQ/50% glycerol (>99.9%, Sigma, St Louis, MO, USA) at a 1:1 ratio to preserve enzymatic activity and reduce enzyme degradation. Varying concentrations of crude venom (10 ng/μL and 50 ng/μL) were plated out in triplicates on a 384-well plate (black, Lot#1171125, nunc™ Thermo Scientific, Rochester, NY, USA) and measured by adding 90 μL quenched fluorescent substrate per well (total volume 100 μL/well, 10 μL/ 5mL enzyme buffer, 150 mM NaCl, and 50 mM Tri-HCl (pH 7.3), Fluorogenic Peptide Substrate, R & D systems, Cat#ES001, ES003, ES005, ES010, ES011, Minneapolis, Minnesota). Fluorescence was monitored by a Fluoroskan Ascent™ (Thermo Scientific, Vantaa, Finland) Microplate Fluorometer (Cat#1506450, Thermo Scientific, Vantaa, Finland) (Cat#ES001, ES003, ES005, ES010 for Matrix Metalloprotease at an excitation of 320 nm, emission at 405 nm; Cat#ES011 for Kallikrein at an excitation of 390 nm, emission at 460 nm) over 400 min or until activity had ceased. Data was collected using Ascent® Software v2.6 (Thermo Scientific, Vantaa, Finland).

For PLA_2 analysis we assessed the continuous Phospholipase A_2 (PLA_2) activity of the venoms using a fluorescence substrate assay (EnzChek® Phospholipase A_2 Assay Kit, Cat#E10217, Thermo Scientific, Rochester, NY, USA), measured on a Fluoroskan Ascent® Microplate Fluorometer (Cat#1506450, Thermo Scientific, Vantaa, Finland). As above, we used a working stock solution of freeze dried venom reconstituted in a buffer containing 50% MilliQ / 50% glycerol (>99.9%, Sigma) at a 1:1 ratio. A concentration of enzyme activity in venom (50 ng/μL) was brought up in 12.5 μL 1× PLA_2 reaction buffer (50 mM Tris-HCL, 100 mM NaCl, 1 mM $CaCl_2$, pH 8.9) and plated out in triplicates on a 384-well plate (black, Lot#1171125, nunc™ Thermo Scientific, Rochester, NY, USA). The triplicates were measured by dispensing 12.5 μL quenched 1 mM EnzChek® (Thermo Scientific, Rochester, NY, USA) Phospholipase A_2 Substrate per well (total volume 25 μL/well) over

100 min or until activity had ceased (at an excitation of 485 nm, emission 538 nm). Purified PLA_2 from bee venom (1 U/mL) was used as a positive control and data was collected using Ascent® Software v2.6 (Thermo Scientific, Vantaa, Finland).

5.5.1.2 Plasminogen activation

The same working stock solution of 1 mg/mL (outlined above and in (Debono et al., 2017a) of freeze dried venom was used to make the following dilutions: 10 ng/µL, 50 ng/µL and 100 ng/µL. These varying concentrations of enzyme activity in venom were plated out on a 384-well plate (black, Lot#1171125, nunc™ Thermo Scientific, Rochester, NY, USA) in triplicates, with and without 10 ng/µL plasminogen per well (Lot#FF0125 HCPG-0130, Haematologic Technologies Inc., Essex Junction, VT, USA). Plasminogen, a serine protease, can be activated by a serine protease specific substrate (Fluorogenic Peptide Substrate, R & D systems, Cat# ES011, Minneapolis, Minnesota). Plasmin was used as a positive control (10 ng/µL per positive control well, Lot#EE1120, HCPM-0140, Haematologic Technologies Inc., Essex Junction, VT, USA). Activation from venoms was measured by adding 90 µL quenched fluorescent substrate per well (total volume 100 µL/well; 20 µL/5mL enzyme buffer - 150 mM NaCl and 50 mM Tri-HCl (pH 7.3), Fluorogenic Peptide Substrate, R & D systems, Cat#ES011, Minneapolis, Minnesota). Fluorescence was monitored by a Fluoroskan Ascent™ Microplate Fluorometer (Cat#1506450, Thermo Scientific, Vantaa, Finland) at excitation 390 nm and emission at 460 nm over 150 min or until activity had ceased. Data was collected using Ascent® Software v2.6 (Thermo Scientific, Vantaa, Finland). Experiments were conducted in triplicate.

5.5.1.3 Prothrombin activation

The ability for *Protobothrops* crude venom to directly activate prothrombin was investigated and measured by modifying the above protocol used for plasminogen activation. Plasminogen was replaced with prothrombin (Lot#EE0930, HCP-0010, Haematologic Technologies Inc., Essex Junction, VT, USA) and plasmin was replaced with thrombin (Lot#FF0315, HCT-0020, Haematologic Technologies Inc., Essex Junction, VT, USA) as a positive control (10 ng/µL per positive control well). Data was collected using Ascent® Software v2.6 (Thermo Scientific, Vantaa, Finland). Experiments were conducted in triplicate.

5.5.1.4 Factor X activation

The ability for *Protobothrops* crude venom to directly activate blood coagulation Factor X (FX) was investigated and measured by modifying the above protocol used for plasminogen activation using FX (Lot#FF0407, HCX-0050, Haematologic Technologies Inc., Essex Junction, VT, USA) as the experimental target and FXa (Lot#EE1102, HCXA-0060, Haematologic Technologies Inc., Essex

Junction, VT, USA) as the positive control (10 ng/μL per positive control well). Data was collected using Ascent® Software v2.6 (Thermo Scientific, Vantaa, Finland). Experiments were conducted in triplicate.

5.5.1.5 Protein C activation

The ability for *Protobothrops* crude venom to directly activate Protein C was investigated and measured by modifying the above protocol used for plasminogen activation. Plasminogen was replaced with Protein C (Lot#FF0802, HCPC-0070, Haematologic Technologies Inc., Essex Junction, VT, USA) and plasmin was replaced with activated Protein C (Lot#FF0325, HCAPC-0080, Haematologic Technologies Inc., Essex Junction, VT, USA) as a positive control (10 ng/μL per positive control well). Data was collected using Ascent® Software v2.6 (Thermo Scientific, Vantaa, Finland). Experiments were conducted in triplicate.

5.5.2 Phylogenetic comparative analyses

Observed venom activities of the different snake species were investigated in an evolutionary framework by mapping them on a taxonomical tree (phylogeny was adapted from (Alencar et al., 2016)), generated using the Mestique software package and analyses subsequently performed using the R package Phytools using Phylogenetic Generalized Least Squares (PGLS) (Lister et al., 2017; Rogalski et al., 2017). Analyses were implemented in R v3.2.5 (Team, 2016) using the APE package for basic data manipulation (Paradis et al., 2004). Ancestral states of each substrate functional trait (ES001, ES002, ES003, ES005, ES010, ES011, PLA_2, coagulation) were estimated via maximum likelihood with the contMap function in phytools (Revell, 2012).

5.5.3 Coagulation analysis

5.5.3.1 Action upon plasma

Plasma clotting and co-factor dependency of Ca^{2+} and phospholipid

As per (Debono et al., 2017a), in order to investigate whole plasma clotting and co-factor dependency clotting, we prepared healthy human plasma (citrate 3.2%, Lot#1690252, approval # 16-04QLD-10), obtained from the Australian Red Cross (44 Musk Street, Kelvin Grove, Queensland 4059). Coagulopathic toxin effects were measured by a modified procoagulant protocol on a Stago STA-R Max coagulation robot (France) using Stago Analyser software v0.00.04 (Stago, Asniéres sur Seine, France). Plasma clotting baseline parameters were determined by performing the standardised activated Partial Thromboplastin Time (aPTT) test (Stago Cat# T1203 TriniCLOT APTT HS). This was used as a control to determine the health of normal clotting plasma according to the universal standard range of between 27–35 sec. Plasma aliquots of 2 mL, which had been flash frozen in liquid nitrogen and stored in a -80°C freezer, were defrosted in an Arctic refrigerated circulator SC150-A40

at 37°C. In order to determine clotting times effected by the addition of varying venom concentrations, a modified aPTT test was developed. A starting volume of 50 µL of crude venom (5 µg/50 µL) was diluted with STA Owren Koller Buffer (Stago Cat# 00360). An 8-dilution series of 1 (20 µg/mL), 1/2 (10 µg/mL), 1/5 (4 µg/mL), 1/12 (1.6 µg/mL), 1/30 (0.66 µg/mL), 1/80 (0.25 µg/mL), 1/160 (0.125 µg/mL), and 1/400 (0.05 µg/mL) was performed in triplicate. $CaCl_2$ (50 µL; 25 mM stock solution Stago Cat# 00367 STA $CaCl_2$ 0.025M) was added with 50 µL phospholipid (solubilized in Owren Koller Buffer adapted from STA C.K Prest standard kit, Stago Cat# 00597). An additional 25 µL of Owren Koller Buffer was added to the cuvette and incubated for 120 sec at 37°C before adding 75 µL of human plasma. Relative clotting was then monitored for 999 sec or until plasma clotted (whichever was sooner). Additional tests were run, both with and without $CaCl_2$ and phospholipid, respectively, to test for $CaCl_2$ or phospholipid dependency. STA Owren Koller Buffer was used as a substitute, using the same volumes to allow for consistency in the final volumes (250 µL).

Plasma anticoagulant inhibition – FXa and thrombin

The ability for *Protobothrops* crude venom to directly prevent a fibrin clot from forming was investigated. Species were chosen based off the above described protocol and initial screening of which venoms were unable to clot plasma. FXa inhibition and thrombin inhibition were investigated as alternative targets. Clotting baseline parameters were established by performing FXa-initiated clotting in human plasma utilising liquid FXa from Stago Liquid Anti FXa kit (Stago Cat#250491 Liquid Anti FXa kit). This was used as a control to determine the normal clotting of plasma caused by the activation of prothrombin via FXa under these specific conditions (between 12.5 ± 0.2 sec). A starting volume of 50 µL of crude venom (at 10 mg/mL) was diluted with STA Owren Koller Buffer (Stago Cat# 00360). An 8-dilution series of 1 (200 µg/mL), 1/2 (100 µg/mL), 1/4 (55 µg/mL), 1/6 (30 µg/mL), 1/8 (25 µg/mL), 1/10 (20 µg/mL), 1/20 (10 µg/mL), and 1/50 (4 µg/mL) was performed in triplicate. Following, 50 µL $CaCl_2$ (25mM stock solution Stago Cat# 00367 STA) was added to 50 µL phospholipid (solubilized in Owren Koller Buffer adapted from STA C.K Prest standard kit, Stago Cat# 00597) and 50 µL Factor Xa (unknown concertation from supplier, Liquid Anti-Xa FXa Cat#253047, Stago) or 50 µL TCT thrombin kit (unknown concentration from supplier, Thrombin, Lot#252818, Stago) and incubated for 120 sec. Post incubation 50 µL of either human plasma for the FXa inhibition test (citrate 3.2%, Lot#1690252, approval # 16-04QLD-10, obtained from the Australian Red Cross (44 Musk Street, Kelvin Grove, Queensland 4059) (defrosted in an Arctic refrigerated circulator SC150-A40 at 37°C)) or human fibrinogen for the thrombin inhibition test (at 4 mg/mL, (Lot#F3879, Sigma Aldrich, St. Louis, Missouri, United States, reconstituted in enzyme buffer (150 mM NaCl and 50 mM Tri-HCl (pH 7.3)) was added to the reaction and each test run in triplicate for each concentration. Relative clotting was then monitored for 999 sec or until plasma

clotted (whichever was sooner) on a Stago STA-R Max coagulation robot (France) using Stago Analyser software v0.00.04 (Stago, Asniéres sur Seine, France). Additional tests were run with increased incubation times of 300 sec and 600 sec. Venom dilutions in triplicates were mapped over time using GraphPad PRISM 7.0 (GraphPad Prism Inc., La Jolla, CA, USA) to produce concentration curves.

5.5.3.2 Action upon fibrinogen

Fibrinogen clotting and co-factor dependency of Ca^{2+} and phospholipid

The ability for *Protobothrops* crude venom to directly clot human fibrinogen was investigated and measured by following that described by (Debono et al., 2017a) such that human fibrinogen (4 mg/mL, Lot#F3879, Sigma Aldrich, St. Louis, Missouri, United States), was used in place of human plasma. Relative clotting was then monitored for 999 sec or until fibrinogen clotted (whichever was sooner). Experiments were conducted in triplicate. Venom dilutions in triplicates were mapped over time using GraphPad PRISM 7.0 (GraphPad Prism Inc., La Jolla, CA, USA) to produce concentration curves.

Thromboelastography® 5000

The clotting ability of *Protobothrops* venom using human fibrinogen (4 mg/mL) and human plasma was investigated using a Thrombelastogram® 5000 Haemostasis analyser (Haemonetics®, Haemonetics Australia Pty Ltd, North Rdye, Sydney 2113, Australia). Human fibrinogen (4 mg/mL, Lot#F3879, Sigma Aldrich, St. Louis, Missouri, United States) was reconstituted in enzyme buffer (150 mM NaCl and 50 mM Tri-HCl (pH 7.3)). Natural pins and cups (Lot# HMO3163, Haemonetics Australia Pty Ltd, North Rdye, Sydney 2113, Australia) were used with the following solution; 7 µL venom working stock (1 mg/mL outlined in (Debono et al., 2017a)) or 7 µL thrombin as a positive control (stable thrombin from Stago Liquid Fib kit, unknown concentration from supplier (Stago Cat#115081 Liquid Fib)), 72 µL $CaCl_2$ (25mM stock solution Stago Cat# 00367 STA), 72 µL phospholipid (solubilized in Owren Koller Buffer adapted from STA C.K Prest standard kit, Stago Cat# 00597), and 20 µL Owren Koller Buffer (Stago Cat# 00360) was combined with 189 µL fibrinogen or human plasma and run immediately for 30 min to allow for ample time for clotting formation. An additional positive control of 7 µL Factor Xa (unknown concentration from supplier, Liquid Anti-Xa FXa Cat#253047, Stago) was also incorporated for plasma only. When no clot was formed from the effects of anticoagulant venoms, an additional 7 µL thrombin was added to the pin and cup to generate a clot and to determine the effects of fibrinogen degradation.

Fibrinogen gels

To investigate fibrinogenolysis activity demonstrating α, β and γ chain cleavage, 1D SDS PAGE 12% acrylamide gels were cast, run and stained following the protocol described in (Ali et al., 2013b; Debono et al., 2017a) outlining 1D SDS PAGE preparation and running conditions. Human fibrinogen (Lot#F3879, Sigma Aldrich, St. Louis, Missouri, United States) was reconstituted to a concentration of 1 mg/mL in isotonic saline solution, flash frozen in liquid nitrogen and stored at −80ºC until use. Freeze-dried venom was reconstituted in deionised H_2O and concentrations were measured using a Thermo Fisher Scientific™ NanoDrop 2000 (Waltham, MA, USA). Assay concentrations were a 1:10 ratio of venom:fibrinogen. Human fibrinogen (Lot#F3879, Sigma Aldrich, St. Louis, Missouri, United States) stock of 1 mg/mL was dispensed into ten 120 µL aliquots. Fibrinogen from each aliquot (10 µL) was added to 10 µL buffer dye (5 µL of 4× Laemmli sample buffer (Bio-Rad, Hercules, CA, USA), 5 µL deionised H_2O, 100 mM DTT (Sigma-Aldrich, St. Louis, MO, USA)) as an untreated control lane. An additional fibrinogen aliquot (10 µL) was firstly incubated for 60 min at 37ºC before immediately adding 10 µL buffer dye. Venom stock (1 µL at 1 mg/mL) was added to the remaining 100 µL fibrinogen aliquot and incubated over 60 min at 37ºC, taking out 10 µL at varying time points (1, 5, 10, 15, 20, 30, 45 and 60 min). This 10 µL was immediately added to an additional 10 µL buffer dye. Once all 8-time points including the two controls were added to the buffer dye these were incubated at 100ºC for 4 minutes then immediately loaded into the precast 1D SDS-PAGE gel. The following set up within the gel was as follows: Lane 1: untreated, unincubated fibrinogen, Lane 2: 1-min 37ºC incubation, Lane 3: 5 min 37ºC incubation, Lane 4: 10 min 37ºC incubation, Lane 5: 15 min 37ºC incubation, Lane 6: 20 min 37ºC incubation, Lane 7: 30 min 37ºC incubation, Lane 8: 45 min 37ºC incubation, Lane 9: 60 min 37ºC incubation, Lane 10: untreated fibrinogen that has been incubated for 60 min at 37ºC. Gels were prepared in triplicate under the described conditions per venom and were run in 1× gel running buffer (as described by (Debono et al., 2017a; Koludarov et al., 2017) at room temperature at 120 V (Mini Protean3 power-pack from Bio-Rad, Hercules, CA, USA) until the dye front neared the bottom of the gel. Gels were stained with colloidal coomassie brilliant blue G250 (34% methanol (VWR Chemicals, Tingalpa, QLD, Australia), 3% orthophosphoric acid (Merck, Darmstadt, Germany), 170 g/L ammonium sulfate (Bio-Rad, Hercules, CA, USA), 1 g/L Coomassie blue G250 (Bio-Rad, Hercules, CA, USA), and destained in deionised H_2O.

Fibrinogen gel analysis (ImageJ and PRISM)

Using the publicly available software ImageJ (V1.51r, Java 1.6.0_24, National Institutes of Health, Bethesda, Maryland, USA) (Schneider et al., 2012), gels that had been scanned using a standard printer/scanner were loaded onto the software. Scans were changed to 32 bit to emphasise darken bands of fibrinogen chains so that the image could be manipulated to view individual peaks and

troughs representing the alpha, beta and gamma chains. The intensity represents the amount of protein within that particular band and as the chain degrades the intensity decreases. Using the 'wand function' each peak within the graph was selected automatically producing a quantity for the area under the curve. AUC was graphed using GraphPad PRISM 7.0 (GraphPad Prism Inc., La Jolla, CA, USA). This process was repeated for all three triplicates for each venom.

Fibrinolysis ± tPA

To investigate the fibrinolysis ability of *Protobothrops* venoms, varying concentrations of venom (100 ng/µL, 500 ng/µL and 1 µg/µL) were tested under varying conditions with the addition of tissue plasminogen activator (tPA, Sekisui Diagnostics, Lexington, MA, USA). Aliquots (100 µL) of normal pooled human plasma (Leiden University Medical Center (Leiden, NL)) stored at -80ºC were defrosted in a water bath at 37°C. A 96-well plate was prepared under the following conditions: 6 pM tissue factor (TF) (Innovin, Siemens, USA) was added to 10 µM phospholipid vesicles (PCPS, 75% phosphatidylcholine and 25% phosphatidylserine, Avanti Polar Lipids, Alabama, USA) in HEPES buffer (25 mM HEPES, 137mM NaCl, 3.5 mM KCl, 0.1% BSA (Bovine Serum Albumin A7030, Sigma Aldrich, St Louis, MD, USA)) and gently incubated at 37ºC for 1 hr in a water bath. 17 mM CaCl and 37.5 U/mL tPA (diluted in dilution buffer (20 mM HEPES, 150 mM NaCl, 0.1% PEG-8000 (Polyethylene glycol 8000,1546605 USP, Sigma Aldrich, St Louis, MD, USA), pH 7.5)) was then added to the solution. A volume of 30 µL of this solution was added to each experimental well, along with 10 µL of venom at varying concentrations and an additional 10 µL of HEPES buffer, prepared on ice (total well volume of 100 µL). Normal pooled plasma (50 µL) was immediately added to each well (heated to 37ºC). Absorbance measuring commenced immediately and was measured every 30 sec over 3 hr at 405 nm on a Spectra Max M2^{e} (Molecular Devices, Sunnyvale, CA, USA) plate reader, heated to 37ºC. Measurements were captured on Softmax Pro software (V 5.2, Molecular Devices, Sunnyvale, CA, USA) and data points analysed using GraphPad PRISM 7.0 (GraphPad Prism Inc., La Jolla, CA, USA). All experimental conditions were repeated in triplicates and averaged.

5.5.3.3 Platelet agglutination and inhibition

The ability to aggregate platelets via the GP Ib/IX receptor was tested for both venoms at varying concentrations (1 µg/µL, 2 µg/µL and 5 µg/µL) using the ristocetin cofactor assay (Lot# H081032, Chrono-log™, Havertown, PA, USA) under modified conditions. For a control sample, in a modified glass cuvette with a rubber spacer and electrode stir bar, 200 µL of platelets (Lot# 1087-40) reconstituted in TRIS-buffer saline (Lot# 1091-35) was combined with 25 µL Ristocetin (10 mg/mL, Lot# 1088-33), reconstituted in Ultra-pure water. Prior to aggregation tracking performed on a

Chrono-log 700 multichannel system (Chrono-log, DKSH, Vic, Australia), 0% and 100% baselines were established. Agglutination of platelets was measured for 6 min under the following conditions: slope length 16, gain 0.05, mode optical. For experimental samples, 200 μL of reconstituted platelets was combined with an additional 40 μL TRIS-buffer saline and incubated at 37°C for 2 min. After incubation, 10 μL of crude venom/TRIS-buff saline solution at varying concentrations (100 ng/μL, 200 ng/μL and 5 μg/μL) were injected into the cuvette and run for 6 min under the same conditions. Controls and experimental samples were run in triplicate.

Chapter 6: Clinical implications of coagulotoxic variations in Mamushi (Viperidae: *Gloydius*) snake venoms

6.1 Abstract

Snake bite is currently one of the most neglected tropical diseases affecting much of the developing world. Asian pit vipers are responsible for a considerable amount of envenomations annually and bites can cause a multitude of clinical complications resulting from coagulopathic and neuropathic effects. While intense research has been undertaken for some species of Asian pit viper, functional coagulopathic effects have been neglected for others. We investigated their effects upon the human clotting cascade using venoms of four species of *Gloydius* and *Ovophis okinavensis*, a species closely to *Gloydius*. All species of included within this investigation displayed varying fibrinogenolytic effects, resulting in a net anticoagulant outcome. *Gloydius saxatilis* and *Gloydius ussuriensis* displayed the most variable effects from differing localities, sampled from Russia and Korea. As this *Gloydius* investigation includes some geographical variation, notable results indicate key variations of these species that point to possible limitations in antivenom cross-reactivities, which may have implications for the clinical care of victims envenomed by these snakes.

6.2 Introduction

Snake bite is currently a globally neglected tropical disease with many of the poorer regions of the world mostly effected as they live in extremely close proximity to highly venomous snakes (Fry, 2018; Gutiérrez et al., 2017; Kasturiratne et al., 2008). Snake venoms are complex cocktails of toxins that exert effects on any part of the body reachable by the bloodstream (Casewell et al., 2013). These mixtures of toxins have evolved and diversified over millions of years primarily to facilitate predation (and defence in some cases (Panagides et al., 2017)), and the toxin combinations differ between snake families, genus and species with many varying clinical effects (Fry et al., 2008). Clinical effects range from wide spread neurotoxicity, myotoxicity, necrosis and coagulotoxicity through to debilitating permanent damages if bite victims survive (Casewell et al., 2013; Fry, 2018; Fry et al., 2008; Slagboom et al., 2017).

Coagulotoxic venom components interfere with normal haemostasis and are capable of eliciting an immediate procoagulant or anticoagulant (*i.e.* haemorrhagic) response upon injection into the bloodstream. Procoagulant venoms are known to activate Factor X or prothrombin, resulting in the generation of endogenous thrombin and subsequent stable fibrin clots (Joseph and Kini, 2002; Kini, 2005a, 2006; Kornalik and Blombäck, 1975; Lister et al., 2017; Oulion et al., 2018; Rogalski et al., 2017; Rosing and Tans, 1991; Rosing and Tans, 1992; Rosing and Tans, 2010; Sousa et al., 2018; Tans and Rosing, 2002; Yamada et al., 1996; Zdenek et al., 2019). Anticoagulant effects can be

accomplished through the inhibition of clotting enzymes, such as Factors Xa, XIa, IXa or thrombin, or through fibrinogenolytic effects (Youngman et al., 2018). Fibrinogen cleavage occurs either in a non-clotting, destructive manner, or results in the formation of aberrant fibrin clots that are short lived and rapidly degraded (Coimbra et al., 2018; Debono et al., 2019c). Both types of fibrinogen cleavage have a net anticoagulant effect through a reduction in the amount of normal, intact fibrinogen available for cleavage by endogenous thrombin to form stable fibrin clots.

Asian pit vipers are characterised by haemorrhagic venoms. *Gloydius* is a wide-spread Asian pit viper genus, spanning Japan, China, Mongolia and surrounding borders, Siberian Russia and Korea, occupying many distinct and variable climatic locations (Vogel, 2006). There has been little comparative research performed on species of this genus despite thousands of Mamushi (*G. blomhoffi*) bites (and related species) each year across Japan and surrounding areas (Hifumi et al., 2015; Hifumi et al., 2011). Bite case reports describe classic haemorrhagic pit viper symptoms including wide spread bleeding which can be fatal (Okamoto et al., 2017; Toh Yoon et al., 2017). The mechanisms behind these widespread symptoms has been subjected to minimal investigation, with majority of the results illustrating fibrinogenolytic effects upon coagulation (Cho et al., 2001; Choi and Lee, 2013; Huang et al., 2011; Zhang et al., 2007). Most studies have focussed not on functional aspects but rather concentrated on proteomic isolation and purification from single species (Cho et al., 2001; Choi and Lee, 2013; Fujisawa et al., 2009; Huang et al., 2011; Sun et al., 2006; Yang et al., 2015; Zhang et al., 2007).

It has been established in the literature that venom composition between closely related species, or within different populations of a single species, may vary considerably due to differential pressures regarding prey availability and prey escape potential. This variation has direct implications for the relative clinical usefulness of antivenoms against species not included in the immunising mixture, or varying populations of the species used (Debono et al., 2017a; Dobson et al., 2018; Fry et al., 2003a; Lister et al., 2017; Rogalski et al., 2017; Sousa et al., 2018; Sunagar et al., 2014; Tan et al., 2016; Tan et al., 2017a; Yang et al., 2016; Zdenek et al., 2019). Many current antivenomic strategies are mostly limited to the immunoreactivity of the antivenom towards the venom components, these do not ascertain whether the antivenom is effective in neutralising venom pathological functions (Jones et al., 2019; Williams et al., 2011; Xu et al., 2017). Out of the ten commonly described *Gloydius* species, antivenom exists only for four (*G. blomhoffii*, *G. brevicaudus*, *G. halys* and *G. ussuriensis*) (Supplementary Table 6.1). With antivenom available for only a select few species, this creates potential life-threatening challenges for bite victims of other *Gloydius* species. In addition, localities for these species from which antivenom is made is restricted, resulting in unknown medical challenges if a bite victim is bitten by a species from an alternative geographical location.

In this study we investigated the effects on coagulation of the venoms from multiple species of *Gloydius*, and populations within some species, in addition to *Ovophis okinavensis*, which sits basal to *Gloydius* rather than being closely related to other species within the *Ovophis* genus, and therefore may be considered as part of an expanded *Gloydius* genus (Alencar et al., 2018; Malhotra and Thorpe, 2004). We aimed to highlight coagulotoxic differences between the venoms and how this relates to potential clinical effects of the envenomed patient. This investigation will provide important insight into the key variations of these species which is fundamental for clinical care as well as snake bite management across varying localities within Japan and surrounding countries.

Table 6.1 Species list
Species list of samples from the genus *Gloydius* and *Ovophis*. Pooled samples are of an unknown number of species and unknown specific localities.

Species	Sample composition	Sex	Origin
Gloydius brevicaudus	Individual	Female	Hapcheon-gun, Gyeongsangnam-do, Korea
Gloydius saxatilis	Pooled	NA	Russia
Gloydius saxatilis	Individual	Male	Yangsan-si, Gyeongsangnam-do, Korea
Gloydius saxatilis	Individual	Male	Yangsan-si, Gyeongsangnam-do, Korea
Gloydius tsushimaensis	Pooled	NA	Tsushuma Island, Japan
Gloydius ussuriensis	Pooled	NA	Russia
Gloydius ussuriensis	Individual	Male	Wonju-si, Gangwon-do, Korea
Gloydius ussuriensis	Individual	Female	Wonju-si, Gangwon-do, Korea
Gloydius ussuriensis	Individual	Female	Wonju-si, Gangwon-do, Korea
Ovophis okinavensis	Pooled	NA	Ryukyu Islands, Japan

6.3 Results

6.3.1 Procoagulation and anticoagulation studies

At the initial 20 μg/mL venom concentration, only *G. tsushimaensis* (35 ± 3.7 sec) and *O. okinavensis* (54.6 ± 1 sec) displayed the ability to clot plasma quicker than the negative control (spontaneous clotting of recalcified plasma) time of 350 ± 50 sec (Figure 6.1). All other venom species were equal or above the negative control (data not shown). An 8-point dilution series was undertaken with the two clotting venoms (*G. tsushimaensis* and *O. okinavensis*) under three experimental conditions: with

both cofactors (calcium and phospholipid), in the absence of phospholipids, and in the absence of calcium (Figure 6.1). Phospholipid was not a significant variable for either venom, shifting the clotting curve only 0.06 ± 0.01% for *G. tsushimaensis* and 0.004 ± 0.001 for *O. okinavensis*. However, for the calcium-dependence there was an area under the curve shift of 90 ± 4% for *G. tsushimaensis* (p = 0.0075 and therefore significant) and a shift of 65 ± 1% for *O. okinavensis* (p = 0.0004 and therefore significant) (Figure 6.1). An 8-point dilution series was also undertaken for *G. tsushimaensis* and *O. okinavensis* with fibrinogen under the same three experimental conditions (Figure 6.2). *Gloydius tsushimaensis* had an area under the curve shift of 52 ± 3% for phospholipid dependence (p = 0.07, and therefore only marginally insignificant), while *O. okinavensis* displayed a lower phospholipid dependence with a curve shift of 20 ± 5% (p = 0.25 and therefore insignificant). There was a significant dependency evident for calcium for *G. tsushimaensis*, with the area of the curve shifting 152 ± 5% (p = 0.007), while *O. okinavensis* displayed only lower calcium dependency with an area under the curve shift of 21 ± 2% (p = 0.25 and therefore insignificant) (Figure 6.2). As the clotting of plasma could be due to procoagulant functions through the generation of endogenous thrombin (producing strong fibrin clots), or pseudo-procoagulant functions by directly acting upon fibrinogen (producing weak clots), additional tests were conducted to ascertain the ability to activate Factor X or prothrombin, and also to determine the relative strength of fibrin clots in the plasma tests. None of the venoms, even the ones which produced clots in the above analyses, were able to activate FX or prothrombin, thus indicating pseudo-procoagulant actions directly upon fibrinogen.

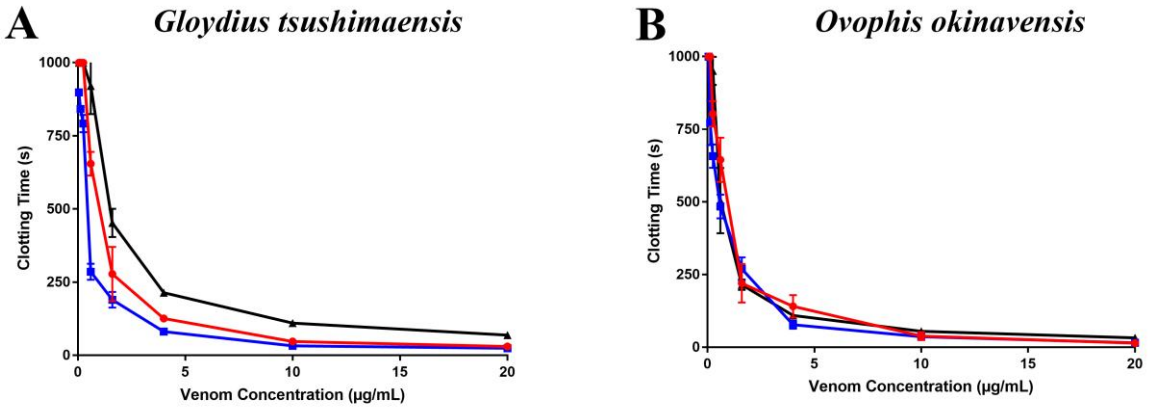

Figure 6.1 Cofactor dependency – plasma
Concentration-response curves the ability of the venoms to clot human plasma in the presence of both calcium and phospholipid (red line), in the absence of phospholipids (blue line), or in the absence of calcium (black line) for A) *G. tsushimaensis* and B) *O. okinavensis.* Data points are N = 3 with standard deviations.

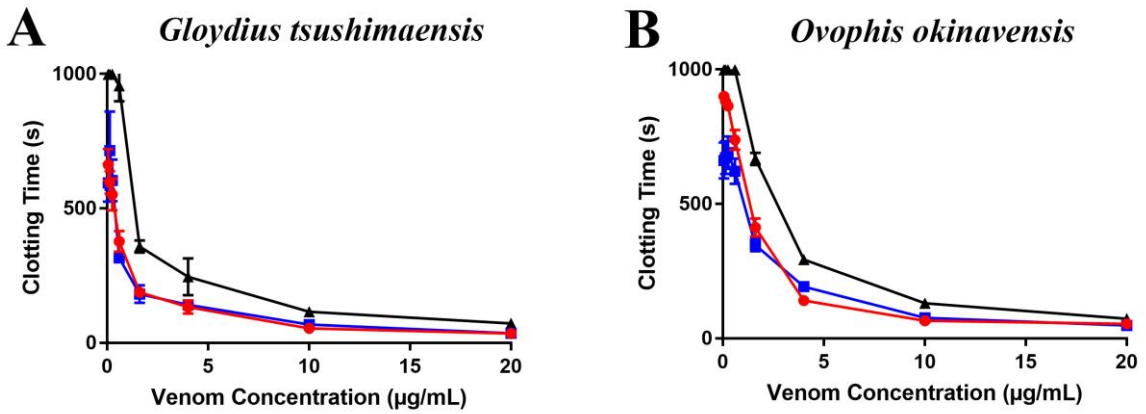

Figure 6.2 Cofactor dependency – fibrinogen
Concentration-response curves the ability of the venoms to clot human fibrinogen in the presence of both calcium and phospholipid (red line), in the absence of phospholipids (blue line), or in the absence of calcium (black line) for A) *G. tsushimaensis* and B) *O. okinavensis.* Data points are N = 3 with standard deviations.

Our study aimed to characterise the function and underlying haemorrhagic mechanisms of the *Gloydius* genus. Addition of the remaining venoms to recalcified human plasma extended the clotting time which exceeded the machine maximum reading time of 999 sec. Investigations to determine the site of action proceeded in a stepwise manner in order to ascertain specific sites of action (Table 6.2): i) incubation with FXa followed by addition of plasma to determine the ability to directly inhibit FXa; ii) incubation with plasma followed by addition of FXa to determine effects on prothrombinase complex formation (with the site of action determined by comparison with iii and iv, whereby if a strong effect was noted here but corresponding strong effects were not noted in iii or iv, then this indicated inhibition of the formation of the prothrombinase complex, as previously validated by us (Youngman et al., 2018); iii) incubation with thrombin followed by addition of fibrinogen to determine direct inhibition of thrombin; and iv) incubation with fibrinogen followed by addition of thrombin to determine the ability to degrade fibrinogen. Results were as follows (Figure 6.3): i) intra-specific and inter-specific variation in FXa inhibition was notable, with the Russian *G. saxatilis* population being potent in this regard, but the Korean *G. saxatilis* were low in activity, with the other species showing activities levels approximately half of that of the Russian *G. saxatilis* (*G. brevicaudus, G. tsushimaensis,* and *G. ussuriensis*) or inactive in this assay (*O. okinavensis*) (Figure 6.3A); ii) incubation with plasma followed by addition of FXa did not produce a relative strong effect for any of the venoms (Figure 6.3B); iii) incubation with thrombin also revealed negligible effects in this inhibitory function (Figure 6.3C); iv) incubation with fibrinogen revealed a very strong non-clotting, destructive fibrinogenolytic effect for *G. brevicaudus,* a lower but still strong effect for on *G. ussuriensis* male venom sample, but only moderate to low for all other samples (Figure 6.3D).

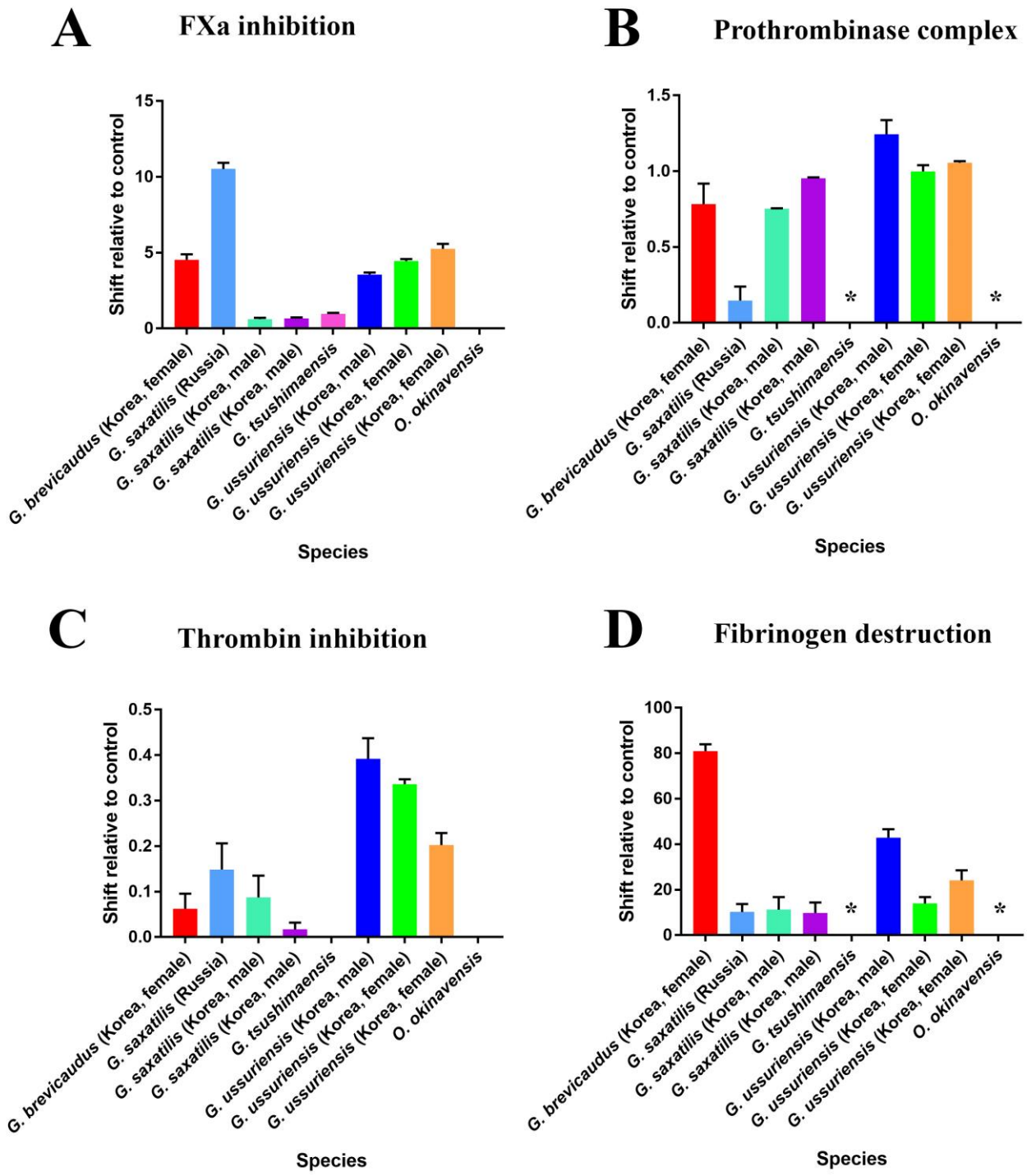

Figure 6.3 Clotting factor inhibition

Clotting factor inhibition showing the relative inhibitory effects of *Gloydius* and *Ovophis* venom on preventing the activation of: A) FXa, B) Prothrombin to thrombin (Prothombinase complex), C) Thrombin inhibition and D) destruction of fibrinogen. For A) and C) venom was incubated with FXa or thrombin for 2 min before adding plasma or fibrinogen, with clot time then immediately measured. For B) and D) venom was incubated with human plasma or fibrinogen for 2 min before adding Factor Xa or thrombin with clot time then immediately measured. Data points are N = 3 displayed as a shift away from the control with standard deviations (no shift from control values would be a zero value). Star icons represent values that could not be recorded due to premature clotting of plasma or fibringoen prior to addition of thrombin or FXa, thus no inhibition.

6.3.2 Fibrinolytic activity

In order to determine the specific fibrinogen chains cleaved by the venoms, additional assays were undertaken to determine the time-dependent effects upon fibrinogen each chain (Figure 6.4 and Figure 6.5). A wide variation in pattern emerged, with many of the venoms displaying the ability to cleave the alpha chain (with the exception of *G. saxatilis* [Korea, male]). In most other samples, the alpha chain was initially quite rapidly degraded, quickly followed by the beta chain, and in some cases the gamma chain (*O. okinavensis*) displaying full cleavage of all three chains, with partial degradation of the gamma chain noted for *G. ussuriensis* and *G. tsushimaensis*. *Ovophis okinavensis* degraded all three chains the quickest, congruent with its ability to clot plasma. There was a geographical variation pattern emerging between Russian localities and Korean localities, with diversity in chain degradation shown among *G. ussuriensis* samples and *G. saxatilis* samples, with *G. saxatilis* being the most notable. For species with multiple samples (*G. saxatilis* Korea males and *G. ussuriensis* Korea male/females), representatives were chosen to be displayed as there was no differences between fibrinolytic actions and chain degradation within this assay (*data not shown*).

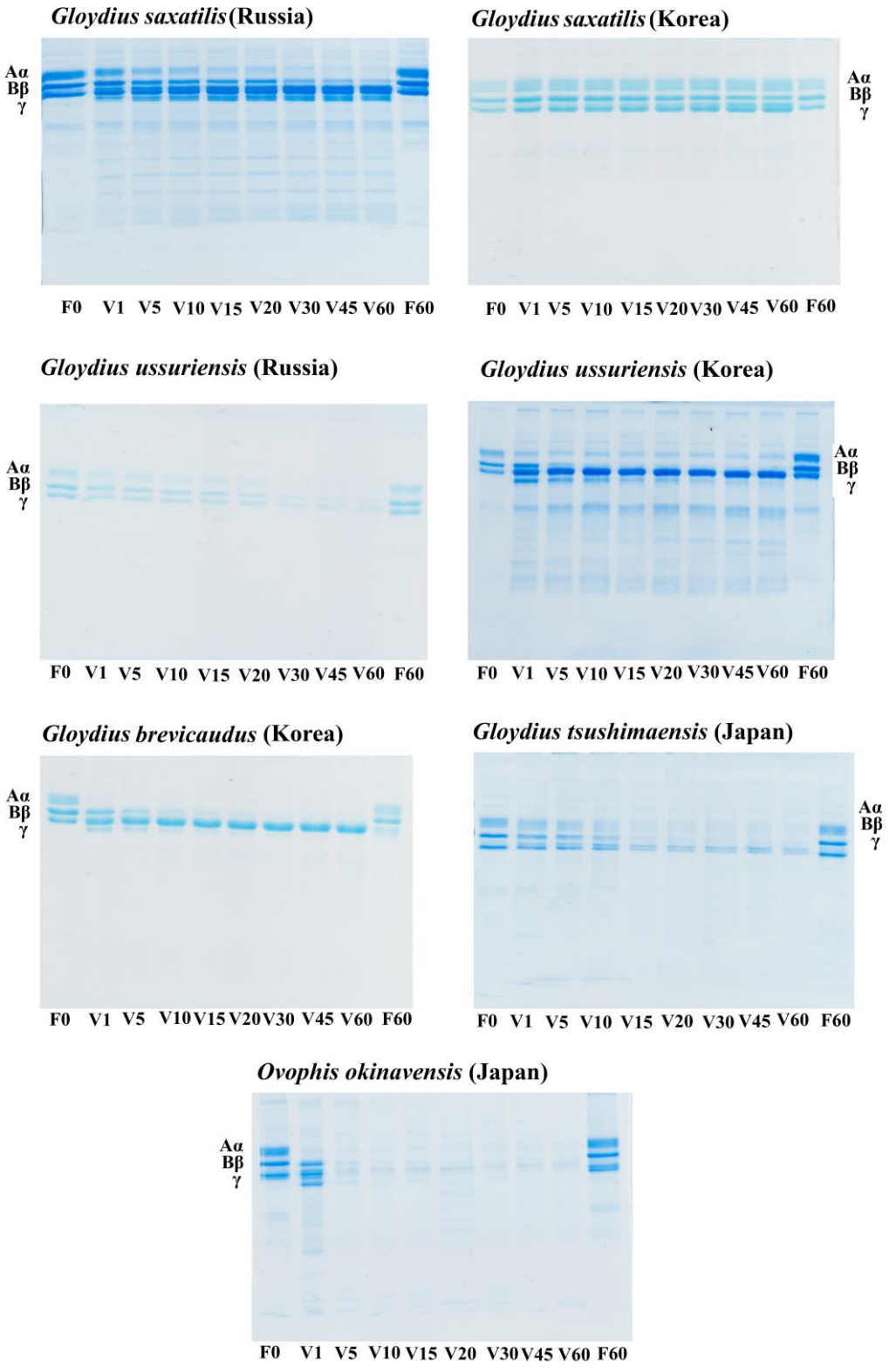

Figure 6.4 Fibrinogen chain cleavage - gel

1D SDS PAGE time dependent fibrinogen chain degradation (α, β or γ) by venom at 0.1µg/µL concentration at 37ºC over 60 min. F = fibrinogen at 0 min or 60 min incubation controls, V = venom at 1, 5… 60 min incubation.

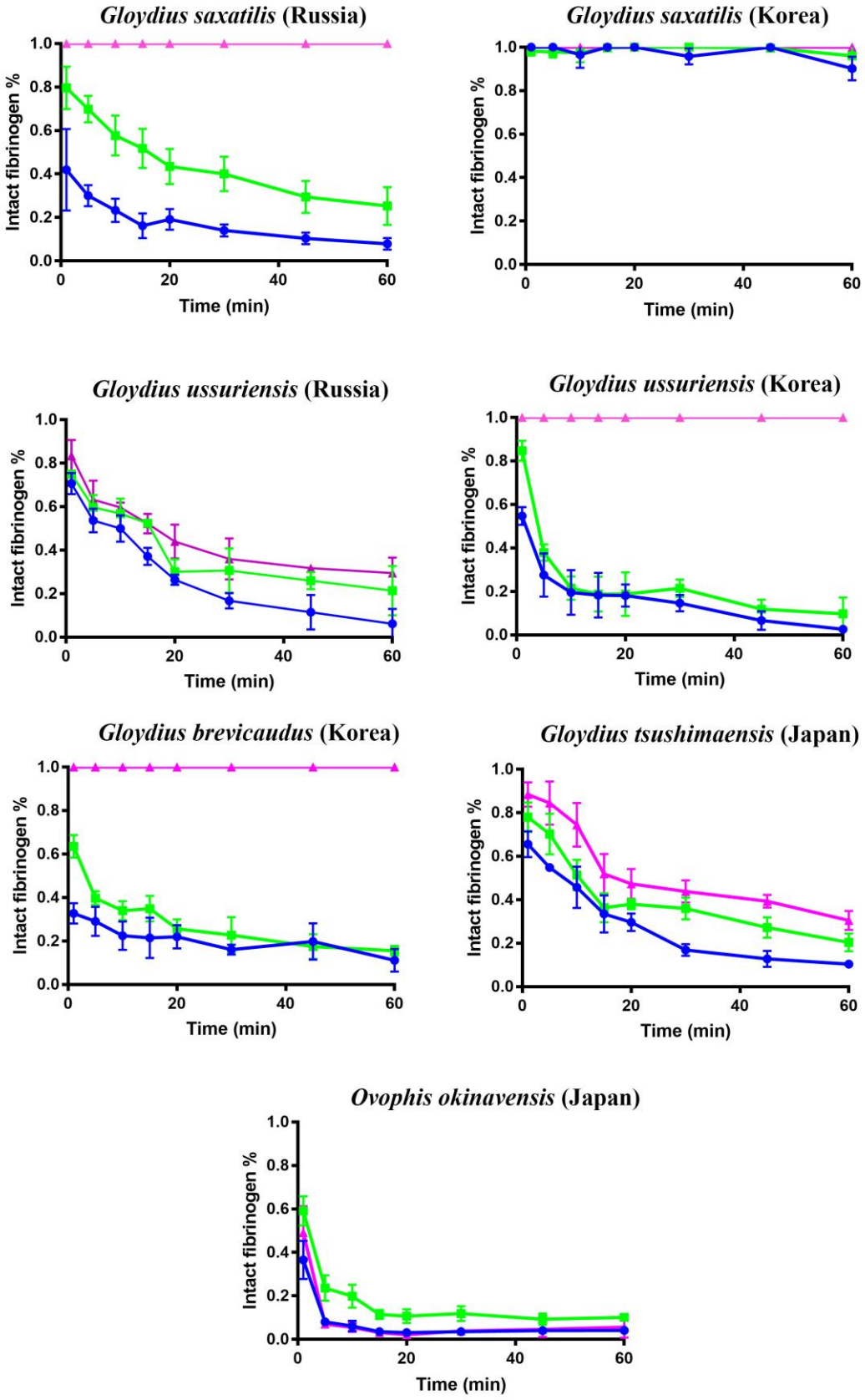

Figure 6.5 Fibrinogen chain cleavage - % intact
Relative cleavage of alpha (blue), beta (green) or gamma (pink) chains of fibrinogen. X-axis is time (min), Y-axis is percentage of intact chain remaining. Error bars indicate standard deviation and N = 3 means.

6.3.3 Thromboelastography

Clot strength on plasma was investigated in the presence of Ca^{2+} and phospholipid using thromboelastography (Figure 6.6). There was a wide variation in ability to clot plasma, however these results coincided with additional above analysis on plasma. Plasma clotted faster than that of the negative control (SP = 8.5 ± 0.8, R = 9.9 ± 0.7, A = 15.4 ± 0.7, MRTGG 1.35 ± 0.09, TMRTG 11.8 ± 0.9 and TGG 90.7 ± 5.4), for *G. ussuriensis* (Russia) which formed a very small, weak clots (SP = 2.5 ± 0.3, R = 18.5 ± 2.1, A = 2.9 ± 0.8, MRTGG = 0.17 ± 0.01, TMRTG = 2.86 ± 0.34 and TGG = 14.2 ± 4.2); *G. tsushimaensis* which formed a very small, weak clot (SP = 1.9 ± 0.1, R = NA, A = 1.4 ± 0.05, MRTGG 0.27 ± 0.02, TMRTG 2.4 ± 0.2 and TGG 6.8 ± 0.3); *O. okinavensis* produced a more robust clot, albeit this being smaller than that of the controls (SP = 2.1 ± 0.1, R = 9.4 ± 2.5, A = 10.4 ± 0.5, MRTGG = 0.4 ± 0.08, TMRTG = 10.7 ± 4.5 and TGG = 57.3 ± 3.1). In contrast, *G. saxatilis* (Russia) delayed the formation of the clot, consistent with the FXa inhibition noted in Figure 6.3A, and decreased the clot strength consistent with destructive, non-clotting cleavage of fibrinogen. *Gloydius brevicaudus, G. saxatilis* (Korea, male), and *G. ussuriensis* all prevented plasma spontaneous clotting, indicative of destructive, non-clotting cleavage of fibrinogen.

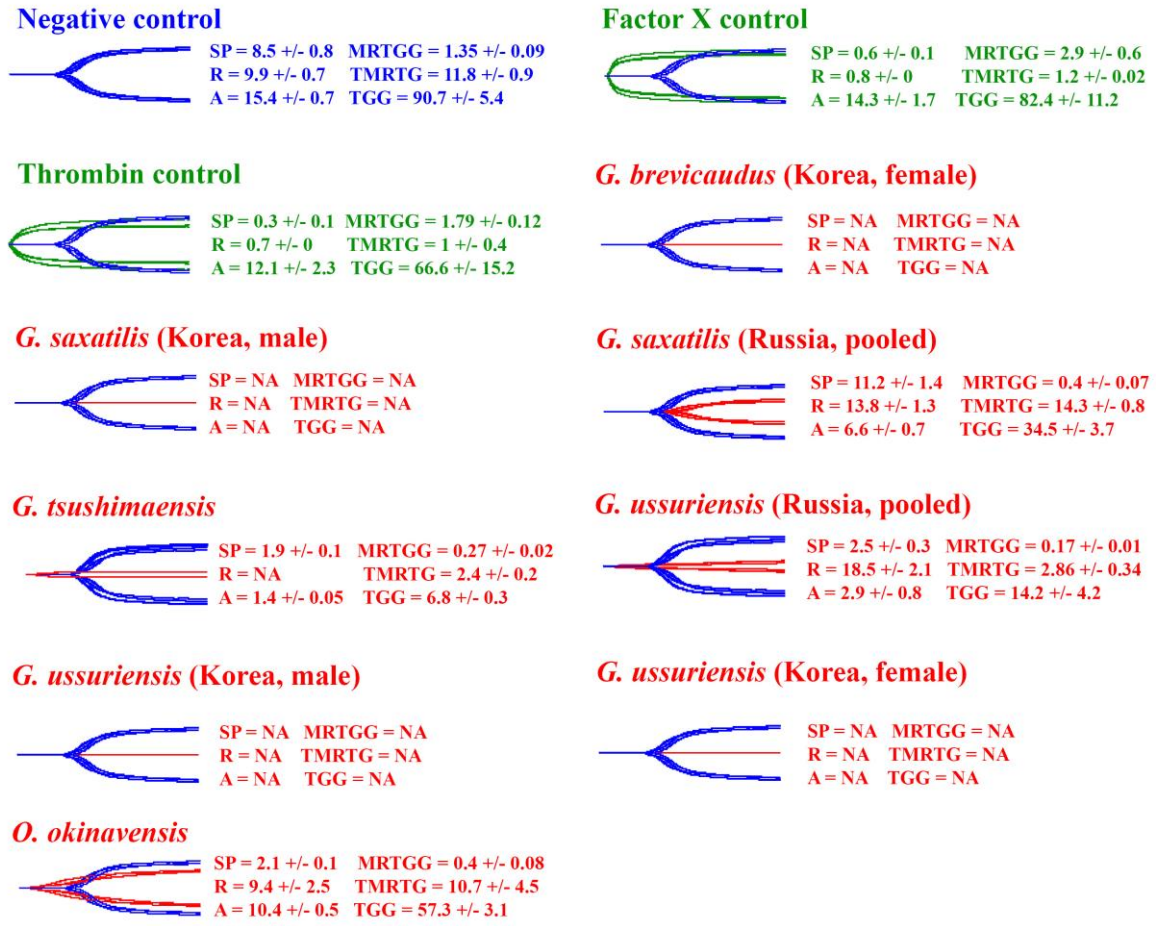

Figure 6.6 Thromboelastography plasma traces
Overlaid thromboelastography traces showing effects of venoms ability to clot plasma relative to spontaneous clot control where species cleave plasma in a clotting manner to form weak clots. Blue traces = spontaneous clot controls, green traces = thrombin induced clot or Factor Xa induced clot, red traces = samples. SP = split point, time taken until clot begins to form (min). R = time to initial clot formation where formation is 2 mm+ (min). A = amplitude of detectable clot (mm). MRTGG = maximum rate of thrombus generation (dsc, dynes/cm^2/sec). TMRTG = time to maximum rate of thrombus generation (min). TGG = total thrombus generation (dynes/cm^2). Overlaid traces are N = 3 for each set of control or experimental conditions. Values are N = 3 means and standard deviation.

As the actions of *G. ussuriensis* (Russia), *G. tsushimaensis*, and *O. okinavensis* indicated pseudo-procoagulant effects whereby fibrinogen was directly cleaved by the venom, to produce weak fibrin clots, additional thromboelastography studies were undertaken. In addition, these additional studies would determine if *G. brevicaudus*, *G. saxatilis* (Korea, male), and *G. ussuriensis* prevented plasma spontaneous clotting through the destructive, non-clotting cleavage of fibrinogen. In order to determine the strength of the clots formed by venom-dependent fibrinogen cleavage, we investigated the ability for the venoms to clot fibrinogen in the presence of Ca^{2+} and phospholipid using thromboelastography (Figure 6.7). Results revealed wide variation between the venoms. Consistent with the effects noted upon plasma, *G. tsushimaensis*, *G. ussuriensis* (Russian pooled sample) and *O. okinavensis* all clotted fibrinogen within the initial 30 min analysis in a pseudo-procoagulant manner

with a reduction in clot strength relative to the thrombin control. As the remainder of the samples did not display any ability to directly clot fibrinogen within the allocated 30 min, thrombin was added after 30 minutes to attempt to generate a clot and to determine if the venoms were destroying fibrinogen directly to impede a clot being formed (Figure 6.7). All fibrinogen samples which were not clotted by the venoms directly, displayed high level of destructive cleavage of fibrinogen after the addition of thrombin, whereby thrombin produced only weak clots for some venoms (*G. brevicaudus*, and *G. ussuriensis* female), consistent with substantial degradation of the fibrinogen by the venoms, yet was unable to produce clots at all for other venoms (*G. ussuriensis* male, and *G. saxatilis*) consistent with complete destruction of fibrinogen by the venoms. Diversification in fibrinogenolytic activity was shown between *G. ussuriensis* samples from Korea versus Russia. For species with multiple samples (*G. saxatilis* Korea males and *G. ussuriensis* Korea females), representatives were chosen to be displayed as there was no differences in clot time, clot strength or clot output among them within these assays (*data not shown*).

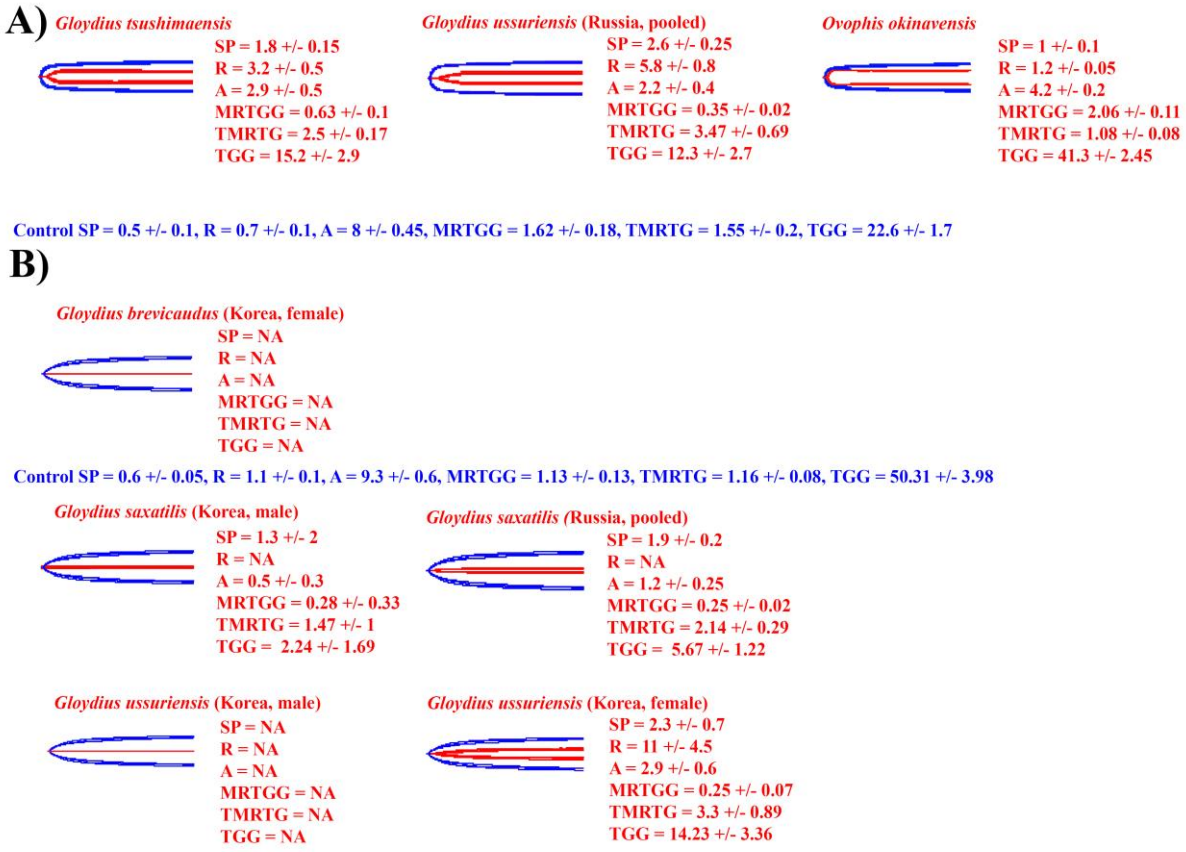

Figure 6.7 Thromboelastography fibrinogen traces
Overlaid thromboelastography traces showing tests for A) ability to clot fibrinogen relative to thrombin control; or B) test for the ability to degrade fibrinogen for species which did not clot in (A) whereby thrombin was added at the end of the 30 min runs to test for intact fibrinogen. Blue traces = thrombin controls, red traces = samples. SP = split point, time taken until clot begins to form (min).

R = time to initial clot formation where formation is 2 mm+ (min). A = amplitude of detectable clot (mm). MRTGG = maximum rate of thrombus generation (dynes/cm^2/sec). TMRTG = time to maximum rate of thrombus generation (min). TGG = total thrombus generation (dynes/cm^2). Overlaid traces are N = 3 for each set of control or experimental conditions. Values are N = 3 means and standard deviation.

6.3.4 Fibrinolysis assessment

The ability for the venoms to actively lyse plasma clots was investigated with the presence and absence of tPA (tissue plasminogen activator) (Figure 6.8). Although plasma clots were unable to be lysed by any of the venoms, some species increased the ability for tPA to lyse clots. In the presence of tPA, some species (*G. brevicaudus*, *G. tsushimaensis* pooled) were able to decrease clot lyses time (CLT) as compared to the control (Figure 6.8). This could be due to fibrinogen structure of the clot in the presence of venom whereby tPA is better able to lyse a particular structure. Albeit, coupled with thromboelastography clot strength outputs, the ability for these specific venoms to reduce clot strength was demonstrated by all. Due to venom availability at the time of assay completion, certain venoms were unable to be included in this assay.

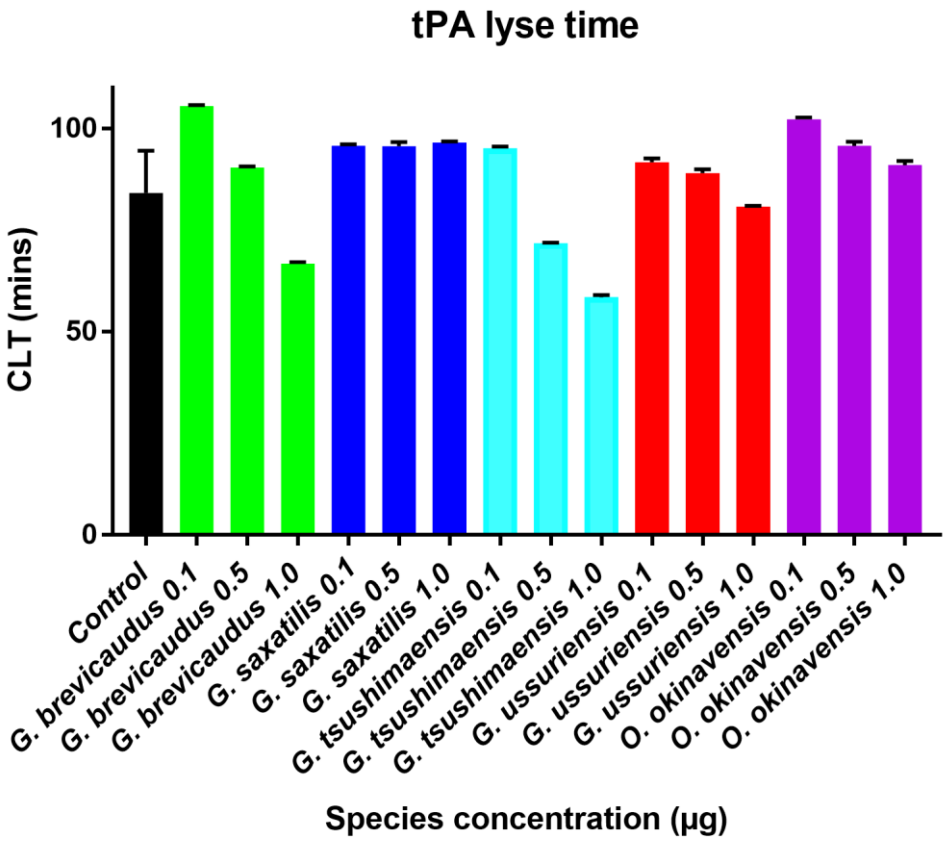

Figure 6.8 Fibrinolysis
Clot Lysis Time (CLT) for each species within the basal clade in the presence of tPA at 0.1 µg, 0.5 µg and 1 µg venom concentrations. The CLT of normal human plasma in the absence of venom is indicated in black. Columns are averages of triplicates and error bars given for each.

6.3.5 Snake venom serine protease contribution

As *Gloydius tsushimaensis* and *Ovophis okinavensis* both displayed clotting ability in the above analysis, both species were subjected to additional inhibition studies. Fibrinogen clotting by *Ovophis okinavensis* venom was completely inhibited by 2 mM AEBSF (venom without inhibitor = 23.5 ± 1.3, while venom + inhibitor = 999.99 ± 0 sec), while that of the *G. tsushimaensis* venom was only partially inhibited (venom without inhibitor = 59.0 ± 1.6, while venom + inhibitor 207.8 ± 27.6 sec) under these conditions (Figure 6.9), as clotting times for fibrinogen did not reach the maximum output of 999.99 sec for *G. tsushimaensis*. This indicates that the venom of *O. okinavensis* is heavily dominated by SVSP proteins actively responsible for fibrinogen-specific coagulation effects, as opposed to *G. tsushimaensis*, which may have a wider composition of coagulatoxic proteins including contribution by metalloproteases.

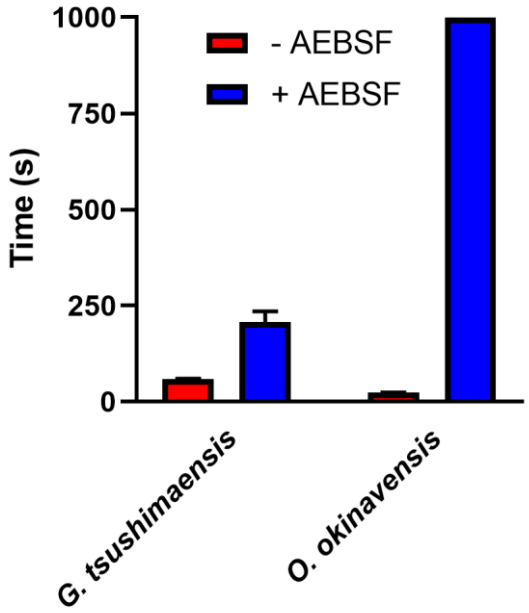

Figure 6.9 SVSP inhibition
Snake venom serine protease inhibition. Venom-induced fibrin clot formation of fibrinogen was analysed for *G. tsushimaensis* or *O. okinavensis* venom in the presence or absence of the serine protease inhibitor AEBSF (2 mM). The values represent the average ± S.D. of three identical experiments.

6.4 Discussion

Our study aimed to investigate the differential coagulotoxic mechanisms within *Gloydius* venoms across majority of the genus, with the addition of *O. okinavensis. Ovophis okinavensis* was added as an additional species as it sits basal to *Gloydius* and is phylogenetically distinct from all other species currently placed in the *Ovophis* genus (Alencar et al., 2018; Malhotra and Thorpe, 2004) and therefore may be included in an expanded consideration of the *Gloydius* genus along with '*Trimeresurus*' *gracilis.* Extensive functional and coagulotoxic variation was evident among all samples tested across

a myriad of assays, depicting variances across the genus and within a single species of differing geographical locations, with venoms falling into two broad anticoagulant functional categories in regards to their actions upon fibrinogen: directly anticoagulant through the destructive cleavage of fibrinogen (*G. brevicaudus, G. saxatilis, G. ussuriensis* [Korea population]); and pseudo-procoagulant whereby fibrinogen levels are depleted by cleavage to form weak, unstable, short-lived fibrin clots (*G. tsushimaensis, G. ussuriensis* [Russia population], and *O. okinavensis*). Inhibition of clotting enzymes was not shown to be a major feature, with the exception of the potent FXa inhibition effect noted for the Russian population of *G. saxatilis*, and more moderate yet still considerable FXa inhibition by *G. brevicaudus* and *G. ussuriensis*. Inhibition of FXa would have a synergistic anticoagulant activity with the depletion of fibrinogen levels. Coagulotoxic effects from *O. okinavensis* can be directly attributed to its venom composition being dominated by SVSPs (Figure 6.9) (Aird et al., 2013). Comparatively, *G. tsushimaensis* pseudo-procoagulant effects are due to a more complex venom composition, as fibrinogen clotting was only partially inhibited by the known serine protease inhibitor AEBSF (Kuniyoshi et al., 2017; Torres-Bonilla et al., 2018; Xin et al., 2009; Yamashita et al., 2014). This variation between two pseudo-procoagulant venoms with seemingly similar venom actions *in vitro* can have vast implications clinically as the variation in underlying venom biochemistry is indicative of differential toxins exerting the pathophysiological actions, which may therefore result in variations in antivenom efficacy. Future work is needed however to elucidate such variations in antivenom efficacy in order to fully ascertain such clinical implications.

Variation in action upon fibrinogen was shared among the other species included within this study. Ecological niche partitioning and a shift in diet would contribute to venom evolution of the species across varying localities and habitats, with consequential impacts upon relative clinical effects (Casewell et al., 2013; Fry et al., 2008). Such wide variation depicted within a single genus has also been shown within many other groups of closely related snakes, each inhabiting slightly varied ecological niches (Debono et al., 2019a; Debono et al., 2019c; Debono et al., 2017a; Dobson et al., 2018; Rogalski et al., 2017) as well as variation between localities of the same species (Sousa et al., 2018). While some ontogenetic shift has been shown within one species of *Gloydius* (Gao et al., 2013), due to lack of sample availability the impact upon relative coagulotoxicity was not investigated in the present study and should be the subject of future work.

Variation in venom, dependent on its geographical location, can create many new challenges when seeking medical attention post envenomation. With antivenoms being reared among one or two species of a single locality, envenomation from another locality is not always effectively neutralised, as shown, for example, for the *Bothrops* genus of pit vipers of South America (Sousa et al., 2018), *Crotalus* (Dobson et al., 2018), and *Echis* genus of true vipers in Africa (Rogalski et al., 2017). Such complications must be taken into consideration by clinicians when treating an envenomated patient,

while differences in venom composition lead to differences in relative venom efficacy. Future work should investigate the variations in antivenom efficacy for the available antivenoms against these species (and others within this genus) in order to map out problematic species or localities.

The variations exhibited by these species in this study highlight the importance of a combined evolutionary and clinical approach to snake venom research. While clinical biology can demonstrate physiological effects, evolutionary biology can communicate variations among a genus and infer possible explanations as seen with *G. tsushimaensis* and *O. okinavensis*, two species with similar *in vitro* effects occupying two extremely isolated habitats. Although this study included only a select few species and of geographical locations, the results are indicative of a large clinical and biodiscovery potential for future medical implications and bite case management. The substantial differences in fundamental venom biochemistry of these species indicate potential limitations in intra-specific and inter-specific cross-reactivity for antivenoms which include *Gloydius* venoms in the immunizing mixtures. Future research should investigate such limitations in these life-saving medications.

6.5 Material and methods

6.5.1 Venoms

Lyophilized venom from a total of nine venom samples from four adult *Gloydius* species (pooled or sourced from single specimen) and one sample from an adult *O. okinavensis* species were investigated for effects upon coagulation (Table 6.1) (Alencar et al., 2016; Malhotra and Thorpe, 2004). Venoms were resuspended in deionized H_20 and protein concentrations (mg/mL) determined using a ThermoFisher Scientific Nanodrop™ 2000c Spectrophotometer. Working stocks of 50% deionized water/50% glycerol (> 99%, Sigma-Alrich) for all venoms were prepared at 1 mg/mL and stored at --20°C to preserve enzymatic activity and reduce enzyme degradation. Where possible, both pooled and individual samples were tested for maximum variation. Where results were the same, representatives were used to minimise redundancy. All venom work was undertaken under University of Queensland Biosafety Approval #IBC134BSBS2015.

6.5.2 Coagulation analysis

Venoms were ascertained for their ability to clot or inhibit the clotting of recalcified plasma, or to form fibrin clots in fibrinogen solutions using methods previously validated by us (Debono et al., 2019a; Debono et al., 2019c; Debono et al., 2017a). Healthy human plasma (citrate 3.2%, Lot#1690252, approval #16-04QLD-10) was obtained from the Australian Red Cross (44 Musk Street, Kelvin Grove, Queensland 4059). Human fibrinogen (Lot#F3879, Sigma Aldrich, St. Louis, Missouri, United States) was reconstituted to a concentration of 1 mg/mL in isotonic saline solution, flash frozen in liquid nitrogen and stored at −80ºC until use. Coagulopathic toxin effects were

measured by a modified procoagulant protocol on a Stago STA-R Max coagulation robot using Stago Analyser software v0.00.04 (Stago, Asniéres sur Seine, France). Plasma clotting baseline parameters were determined by performing the standardised activated Partial Thromboplastin Time (aPTT) test (Stago Cat# T1203 TriniCLOT APTT HS). In order to determine clotting times effected by the addition of varying venom concentrations, a modified aPTT test was developed, in which 50 µL of venom (20 – 0.05 µg/mL) dilutions in STA Owren Koller Buffer (Stago Cat# 00360), 50 µL$CaCl_2$ (5 mM final, Stago Cat# 00367 STA $CaCl_2$ 0.025M), and 50 µL phospholipid (solubilized in Owren Koller Buffer adapted from STA C.K Prest standard kit, Stago Cat# 00597) in a final volume of 175 µL in Owren Koller Buffer was incubated for 120 sec at 37°C before adding 75 µL of human plasma. Relative clotting was then monitored for 999 sec or until plasma clotted (whichever was sooner). Calcium or phospholipid dependency was assessed by replacing calcium or phospholipid for Owren Koller Buffer, respectively.

Inhibition of venom serine protease activity was determined using 4-benzenesulfonyl fluoride hydrochloride (AEBSF), a known serine protease inhibitor (Kuniyoshi et al., 2017; Torres-Bonilla et al., 2018; Xin et al., 2009; Yamashita et al., 2014) in the modified aPTT assay. For this purpose, 25 µL of (diluted) venom, 50 µL$CaCl_2$ (5 mM final), 50 µL phospholipid, and 50 µL AEBSF (2 mM final) were incubated for 2 min at 37°C before adding 75 µL of human fibrinogen (1.2 mg/mL final). Additional procoagulation (Factor X and prothrombin activation) or anticoagulation (inhibition of FXa, prothrombinase complex formation, thrombin, or fibrinogen cleavage, Table 6.2) assays were also conducted, using methods previously validated by us (Debono et al., 2019a; Debono et al., 2019c; Youngman et al., 2018). To identify the possible target in the clotting cascade which the venom was acting upon, inhibition assays were performed in which either plasma or individual clotting factors were incubated with the sample venom, as shown in (Youngman et al., 2018). Data was analysed using GraphPad PRISM 8.0 (GraphPad Prism Inc., La Jolla, CA, USA).

Table 6.2 Anticoagulation assay details

FXa inhibition assay	Step 1. 50 µL 0.1 µg/mL venom (1 mg/mL 50% glycerol stock diluted with OK buffer) + 50 µL 0.025 M calcium (Stago catalog # 00367 + 50 µL phospholipid (Stago catalog #00597) + 25 µL FXa (Stago catalog # 00311). Step 2. 120 second incubation. Step 3. Addition of 75 µL plasma.
Prothombinase complex inhibition assay	Step 1. 50 µL 0.1 µg/mL venom (1 mg/mL 50% glycerol stock diluted with OK buffer) + 50 µL 0.025 M calcium + 50 µL phospholipid + 75 µL plasma Step 2. 120 second incubation. Step 3. Addition of 25 µL Factor Xa
Fibrinogen destruction assay	Step 1. 50 µL 0.1 µg/mL venom (1 mg/mL 50% glycerol stock diluted with OK buffer) + 50 µL 0.025 M calcium + 50 µL phospholipid + 75 µL 4 mg/mL fibrinogen. Step 2. 60 minute incubation. Step 3. Addition of 25 µL thrombin (Stago catalog #00673)
Thrombin inhibition assay	Step 1. 50 µL 0.1 µg/mL venom (1 mg/mL 50% glycerol stock diluted with OK buffer) + 50 µL 0.025 M calcium + 50 µL phospholipid + 25 µL thrombin (Stago catalog # 00611). Step 2. 120 second incubation. Step 3. Addition of 75 µL 4 mg/mL fibrinogen.

6.5.3 Fibrinolytic activity

Fibrinogenolytic activity was assessed as previously described (Debono et al., 2019a; Debono et al., 2019c). In brief, fibrinogen (1 mg/mL final) was incubated with venom (10 µg/mL final) for 60 min at 37°C, and fibrinogen cleavage was assessed at several time points (1, 5, 10, 15, 20, 30, 45 and 60 min) using SDS-PAGE analysis under reducing conditions followed by staining with Coomassie Brilliant Blue R-250. The visualized protein fragments were quantified using ImageJ software (V1.51r, Java 1.6.0_24, National Institutes of Health, Bethesda, Maryland, USA) and analysed using GraphPad PRISM 7.0 (GraphPad Prism Inc., La Jolla, CA, USA).

6.5.4 Thromboelastography (fibrinogen and plasma)

Venoms were investigated for clot strength ability on fibrinogen and plasma employing thromboelastography using a Thrombelastogram® 5000 Haemostasis analyser (Haemonetics®, Haemonetics Australia Pty Ltd, North Rdye, Sydney 2113, Australia) as described (Debono et al., 2019a; Debono et al., 2019c). Human fibrinogen was reconstituted in enzyme buffer (150 mM NaCl and 50 mM Tri-HCl (pH 7.3)). Briefly, 7 µL venom working stock (1 mg/mL outlined in (Debono et al., 2017a)) or 7 µL thrombin as a positive control (stable thrombin from Stago Liquid Fib kit, Stago Cat#115081 Liquid Fib), 72 µL $CaCl_2$ (25mM stock solution Stago Cat# 00367 STA), 72 µL

phospholipid (solubilized in Owren Koller Buffer adapted from STA C.K Prest standard kit, Stago Cat# 00597), and 20 µL Owren Koller Buffer (Stago Cat# 00360) were combined with 189 µL fibrinogen or human plasma and run immediately for 30 min to allow for ample time for clotting formation. An additional positive control of 7 µL Factor Xa (Liquid Anti-Xa FXa Cat#253047, Stago) was also incorporated for plasma only. When no clot was formed from the effects of anticoagulant venoms, an additional 7 µL thrombin was added to the pin and cup to generate a clot and to determine the effects of fibrinogen degradation.

6.5.5 Fibrinolysis

The ability for venoms of the *Gloydius* and *Ovophis* genus to actively lyse fibrin clots was investigated following methods described previously (Debono et al., 2019a; Debono et al., 2019c). Varying concentrations of crude venom (1 – 0.1 µg/µL) were tested either with or without the addition of tissue plasminogen activator (tPA, Sekisui Diagnostics, Lexington, MA, USA). Briefly, tissue factor (TF) (Innovin, Siemens, USA) and phospholipid vesicles (PCPS, 75% phosphatidylcholine and 25% phosphatidylserine, Avanti Polar Lipids, Alabama, USA) were incubated at 37°C for 1 hour in HEPES buffer (25 mM HEPES, 137mM NaCl, 3.5 mM KCl, 0.1% BSA (Bovine Serum Albumin A7030, Sigma Aldrich, St Louis, MD, USA), pH 7.4). To the TF/PCPS mixture (1.8 pM/3 µM final), CaCl2 (17 mM final), tPA (37.5 U/mL final, diluted in 20 mM HEPES, 150 mM NaCl, 0.1% PEG-8000, pH 7.5), venom (50% v/v), and plasma (50% v/v, prewarmed at 37°C) were added. The fibrin clot formation and the subsequent lysis was monitored by measuring the absorbance at 405 nm for every 30 sec during 3 hr at 37°C in a SpectraMax M2e microplate reader. The onset of clot formation was defined as the time point at which the turbidity increased (delta absorbance > 0.04); the clotting time was the time from the start of the assay to the onset of clot formation. The clot lysis time was the interval between the clear to turbid transition (defined as the midpoint between the onset of clot formation and the maximum turbidity) and the turbid to clear transition; the latter was determined by a sigmoidal fit of the turbidity plots using GraphPad Prism 8.0.

Chapter 7: Clinical implications of differential antivenom efficacy in neutralising coagulotoxicity produced by venoms from species within the arboreal viperid snake genus *Trimeresurus*

7.1 Abstract

Snake envenomation globally is attributed to an ever-increasing human population encroaching into snake territories. Responsible for many bites in Asia is the widespread genus *Trimeresurus*. While bites lead to haemorrhage, only a few species have had their venoms examined in detail. We found that *Trimeresurus* venom causes haemorrhaging by cleaving fibrinogen in a pseudo-procoagulation manner to produce weak, unstable, short-lived fibrin clots ultimately resulting in an overall anticoagulant effect due to fibrinogen depletion. The monovalent antivenom 'Thai Red Cross Green Pit Viper antivenin', varied in efficacy ranging from excellent neutralisation of *T. albolabris* venom through to *T. gumprechti* and *T. mcgregori* being poorly neutralised and *T. hageni* being unrecognised by the antivenom. While the results showing excellent neutralisation of some non-*T. albolabris* venoms (such as *T. flavomaculaturs*, *T. fucatus*, and *T. macrops*) needs to be confirmed with *in vivo* tests, conversely the antivenom failure *T. hageni*, and the very poor results against *T. gumprechti* and *T. mcgregori*, despite being conducted in the ideal scenario of preincubation of antivenom:venom, indicates that the likelihood of clinically relevant cross-reactivity for these species is low (*T. gumprechti* and *T. mcgregori*) to non-existent (*T. hageni*). These same latter three species were also not inhibited by the serine protease inhibitor AEBSF, suggesting that the toxins leading to a coagulotoxic effect in these species are non-serine proteases while in contrast *T. albolabris* coagulotoxicity was completely impeded by AEBSF, and thus driven by kallikrein-type serine proteases. There was a conspicuous lack of phylogenetic pattern in venom variation, with the most potent venoms (*T. albolabris* and *T. hageni*) being distant to each other on the organismal tree, and with the three most divergent and poorly neutralised venoms (*T. gumprechti*, *T. hageni* and *T. mcgregori*) were also not each other's closest relatives. This reinforces the paradigm that the fundamental dynamic evolution of venom results in organismal phylogeny being a poor predictor of venom potency or antivenom efficacy. This study provides a robust investigation on the differential venom effects from a wide range of *Trimeresurus* species on coagulation, highlighting differential fibrinogenolytic effects, while also investigating the relative antivenom neutralisation capabilities of the widely available Thai Red Cross Green Pit Viper antivenom. These results therefore have immediate, real-world implications for patients envenomed by *Trimeresurus* species.

7.2 Introduction

Effective treatment for snake envenomation is becoming increasingly important, with a rise in reported snake bites worldwide (Fry, 2018; Gutiérrez et al., 2017; Gutiérrez et al., 2006; Kasturiratne et al., 2008). Human-snake conflicts are increasing due to a myriad of factors including human population expansion and urban development encroaching into snake territories, and an increase in snake activity periods due to climate change (Fry, 2018). In addition, the increase in exotic pets outside of zoological facilities also increases the risk of bites from exotic species of snake, which means that the issue of snakebite is no longer restricted to the developing world (Fry, 2018; Gutiérrez et al., 2017; Kasturiratne et al., 2008). Across Asia there are many species of highly venomous snakes, and populations of humans existing in close contact with these species is ever increasing. Pit vipers are responsible for a major proportion of envenomation due to large population densities of people that bring increased agriculture to regions overlapping with the pit viper habitat, coupled with poor snakebite management and education (Alirol et al., 2010; Chippaux, 1998).

Trimeresurus is a genus of pit viper that is widespread across much of Asia. *Trimeresurus albolabris* is a particularly commonly encountered species, and envenomations are considered medically significant with effects ranging from local blistering and necrosis, shock, to spontaneous systemic bleeding, defibrinogenation, thrombocytopenia and leucocytosis (Hutton et al., 1990). As a result, *T. albolabris* envenomation and venom composition has been the centre of much research focus (Chotenimitkhun and Rojnuckarin, 2008; Greene et al., 2017; Hutton et al., 1990; Lin et al., 2009; Muanpasitporn and Rojnuckarin, 2007; Peng et al., 1992; Pradniwat and Rojnuckarin, 2015; Rojnuckarin et al., 1999; Tan et al., 2017a; Tan et al., 2012) and is the main *Trimeresurus* species targeted by available antivenoms, such as the monovalent Green Pit Viper Antivenin produced by the Thai Red Cross. However, in many of the regions where *Trimeresurus* species exist, a specific antivenom is lacking (Tan et al., 2017a). Moreover, the venom composition and function of most other species within the genus have been comparably neglected, with a few exceptions such as *T. flavomaculatus*, *T. insularis*, *T. macrops*, *T. purpureomaculatus*, and *T. stejnegeri* (Clark and Davidson, 1997; Jones et al., 2019; Mitrakul, 1973; Rojnuckarin et al., 1999; Tai et al., 2004; Tan et al., 2017a; Tan, 2010; Tan et al., 1994; Visudhiphan et al., 1989; Witharana et al., 2019; Wongtongkam et al., 2005).

Correct treatment for envenomation is crucial for patient care, to reduce both morbidity and mortality rates (Fry, 2018). Having a better understanding of the effects of such species' venom on the coagulation cascade can aid in this knowledge and improve current treatments available. Coagulotoxicity from *Trimeresurus* envenomations results in anticoagulant effects which clinically manifests into haemorrhaging, most commonly attributed to fibrinogenolytic activity, as seen for many pit-vipers (Bell, 1997; Debono et al., 2019a; Debono et al., 2019b; Debono et al., 2019c; Kolev

and Longstaff, 2016; Longstaff and Kolev, 2015; Mosesson, 2005; Visudhiphan et al., 1989; Wolberg, 2007; Wolberg and Campbell, 2008). Fibrinogenolytic enzymes may act upon fibrinogen either directly induce an anticoagulant effect by destructive cleavage of fibrinogen, or indirectly by aberrant cleavage of fibrinogen, resulting in short-lived, weak clots in a pseudo-procoagulant manner, with both actions leading to a net anticoagulant state due to depletion of the levels of intact fibrinogen (Coimbra et al., 2018; Debono et al., 2019a; Debono et al., 2019b; Debono et al., 2019c; Dobson et al., 2018; Esnouf and Tunnah, 1967; Huang et al., 1992; Levy and Del Zoppo, 2006; Nielsen, 2016a; Premawardena et al., 1998; Trookman et al., 2009; Zulys et al., 1989). This effect has been demonstrated in many other species of Asian pit viper (Dambisya et al., 1994; Debono et al., 2019a; Debono et al., 2019b; Debono et al., 2019c; Levy and Del Zoppo, 2006; Liu et al., 2011; Nielsen, 2016a; Nolan et al., 1976; Zulys et al., 1989).

Understanding exactly how these anticoagulant effects arise and persist can drastically improve patient care and thus positive outcomes. Here we investigated the differential coagulotoxic effects of a total of 13 of the 37 known and described *Trimeresurus* species (Alencar et al., 2018; Alencar et al., 2016) and ascertained the relative effectiveness of available monovalent Green Pit Viper antivenom in neutralising fibrinogenolytic actions for each species. Note: we follow Alencar et al., 2016 in considering *Trimeresurus* as the genus name for all species and do not subscribe to proposed division into several genera as proposed by Malhotra and Thorpe, 2004, as the more inclusive definition of *Trimeresurus* renders these snakes as a well-defined monophyletic clade sharing ecological, evolutionary, and morphological features distinctive of these speices relative to all other Asian pit vipers. These venoms are evolving under unique selection pressures due to the species being unique amongst Asian pit vipers in being arboreal specialists and thus there is a high chance of prey escape. These venoms may also be diversification hot spots due to limited gene flow as a consequence of arboreality. Thus there may be real world implications of such venom variation for the envenomed patient as a consequence of differential efficacy by available antivenoms.

7.3 Results

7.3.1 Coagulation analyses on plasma

The ability of the *Trimeresurus* venoms to affect clot formation of human plasma was investigated. Using a final concentration of 20 µg/mL venom, five of the venoms displayed the ability to clot plasma quicker than the negative control (spontaneous clotting of recalcified plasma: 584 ± 35 sec): *T. albolabris* (62 ± 9 sec), *T. borneensis* (82 ± 8 sec), *T. gumprechti* (90 ± 1 sec), *T. hageni* (71 ± 2 sec), and *T. mcgregori* (78 ± 1 sec) (Figure 7.1A). For these five procoagulant venoms (*T. albolabris, T. borneensis, T. gumprechti, T. hageni* and *T. mcgregori*), their cofactor-dependent clotting activity was assessed in further detail, with the cofactors being calcium and/or phospholipid. The absence of

phospholipid did not significantly affect the shift in AUC (AUC shift of 4 ± 2% for *T. albolabris*, 22 ± 1% for *T. borneensis*, 4 ± 2% for *T. gumprechti*, 5 ± 0% for *T. hageni*, and a shift of 6 ± 5 % for *T. mcgregori*; Figure 7.1B-F). In contrast, a pronounced shift in the AUC was observed for the clotting activity obtained in the absence of calcium (AUC shift of 172 ± 0% for *T. albolabris*, 75 ± 11% for *T. borneensis*, 102 ± 1% for *T. gumprechti*, 75 ± 0% for *T. hageni*, and 85 ± 1% for *T. mcgregori*).

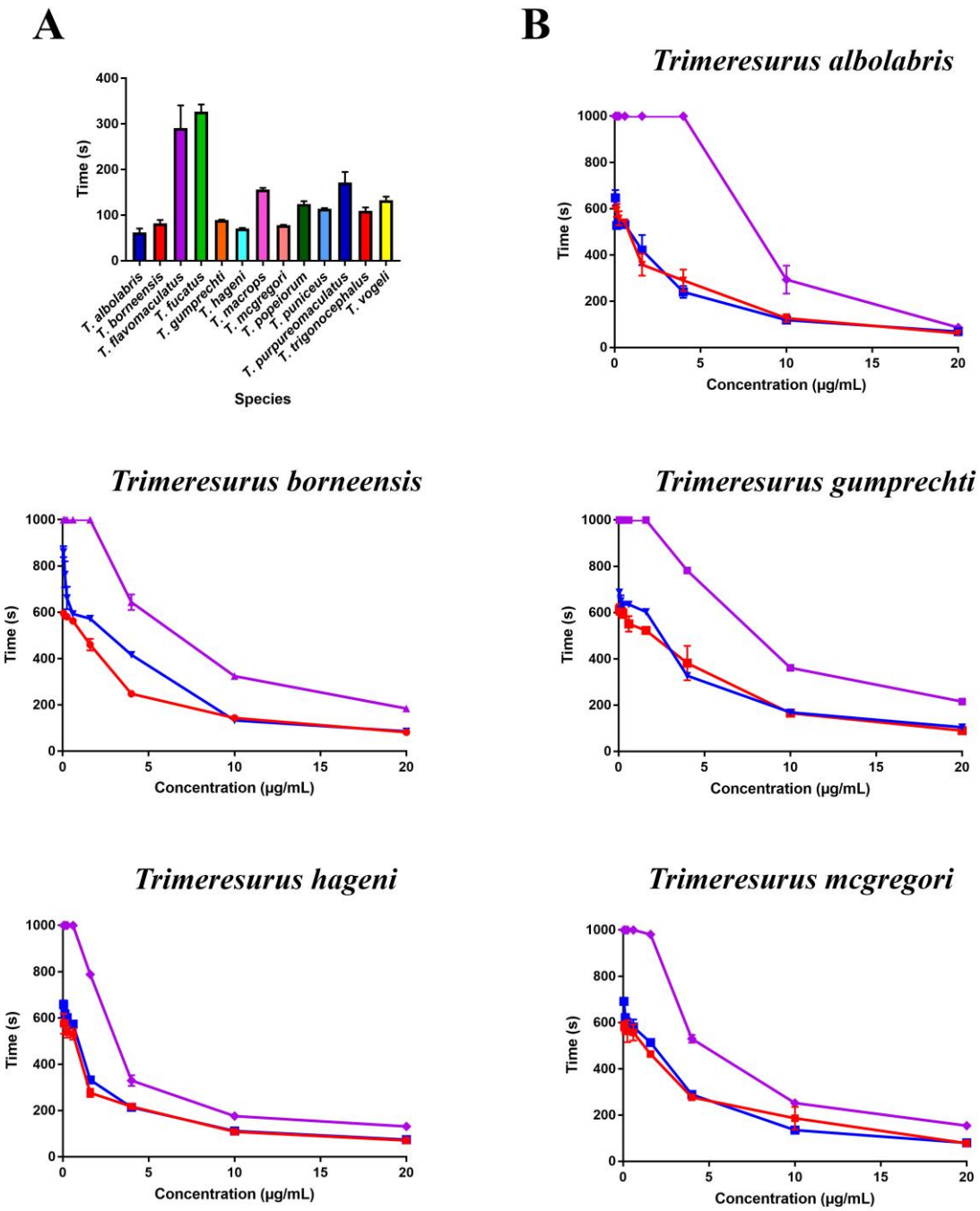

Figure 7.1 Cofactor dependency – plasma
A) Initial 20 µg/mL venom concentration clotting times on human plasma for all species included in study. B) 8-point dose-response curves of human plasma clotting activity with both calcium and phospholipid (red line), with just calcium (blue line), and with just phospholipid (purple line) for *T.*

albolabris, T. borneensis, T. gumprechti, T. hageni and *T. mcgregori*. Y-axis = Clotting time (sec). Data points are N = 3 with standard deviations.

7.3.2 Coagulation analyses on fibrinogen

To gain further insight into the mechanism by which the five *Trimeresurus* venoms (*T. albolabris, T. borneensis, T. gumprechti, T. hageni* and *T. mcgregori*) induce fibrin clot formation in plasma, their clotting activity using purified fibrinogen as substrate was assessed. At a final concentration of 20 µg/mL venom, *T. albolabris* (49 ± 13 sec), *T. borneensis* (63 ± 11 sec), *T. gumprechti* (77 ± 0 sec), *T. hageni* (42 ± 2 sec) and *T. mcgregori* (59 ± 6 sec) displayed the ability to directly clot fibrinogen (Figure 7.2A). Assessment of the cofactor-dependent fibrinogen clotting activity indicated that phospholipid was not a major contributing cofactor (AUC shift of 12 ± 7% for *T. albolabris*, 35 ± 2% for *T. borneensis*, 26 ± 1% for *T. gumprechti*, 38 ± 1% for *T. hageni*, and a shift of 30 ± 0% for *T. mcgregori*; Figure 7.2B-F), corroborating our findings obtained for plasma clotting (Figure 7.1B-F). While the venom-induced clotting of fibrinogen appeared to dependent on calcium as a cofactor, the shift in the AUC was lower than that observed for venom-induced plasma clotting in the absence of calcium (AUC shift of 32 ± 0% for *T. albolabris*, 104 ± 4% for *T. borneensis*, 89 ± 0% for *T. gumprechti*, 77 ± 0% for *T. hageni* and 92 ± 0% for *T. mcgregori*).

Monovalent antivenom from *T. albolabris* (Thai Red Cross Green Pit viper antivenin) was tested against all 13 *Trimeresurus* species included in this study for its neutralising capabilities on fibrinogen clotting. Most species were eventually neutralised by the antivenom, except for *T. gumprechti, T. hageni* and *T. mcgregori* where the antivenom had negligible effects (Figure 7.3). In contrast, *Trimeresurus albolabris* was completely neutralised even at the highest venom concentrations, as too were *T. flavomaculatus, T. fucatus, T. macrops* and *T. popeiorum*. The remainder of the tested venom species reached complete neutralisation at lower concentrations of venom (Figure 7.3), indicating an intermediate effectiveness of the antivenom. There was no phylogenetic signal of antivenom efficacy, with the closest relative of *T. albolabris* only moderately neutralised while in other cases, such as *T. flavomaculatus* and *T. mcgregori*, two species who are each other's closest relatives, were diametrically opposed in their relative neutralisation (Figure 7.4).

To ascertain the relative contribution of snake venom serine proteases (SVSPs) to fibrinogen clotting, the effect of AEBSF (a well-characterised serine protease inhibitor (Torres-Bonilla et al., 2018; Xin et al., 2009; Yamashita et al., 2014)) was investigated. The fibrinogen clotting activity of both *T. albolabris* and *T. borneensis* venom was completely inhibited by incubation with 2 mM AEBSF, indicated by an undetectable fibrinogen clotting time in the presence of the inhibitor (>999 sec; Figure 7.5). These observations suggest that SVSPs are responsible for the coagulotoxic effects upon fibrinogen for *T. albolabris* and *T. borneensis* venoms, On the other hand, the fibrinogen clotting activity of the *T. gumprechti, T. hageni,* and *T. mcgregori* venoms was only partially inhibited upon

AEBSF incubation (Figure 7.5). These observations suggest that SVSPs are only partially contributing to the coagulotoxic effects upon fibrinogen by the *T. gumprechti*, *T. hageni*, and *T. mcgregori* venoms and that metalloproteases are responsible for the majority of the fibrinogen clotting effects of these venoms.

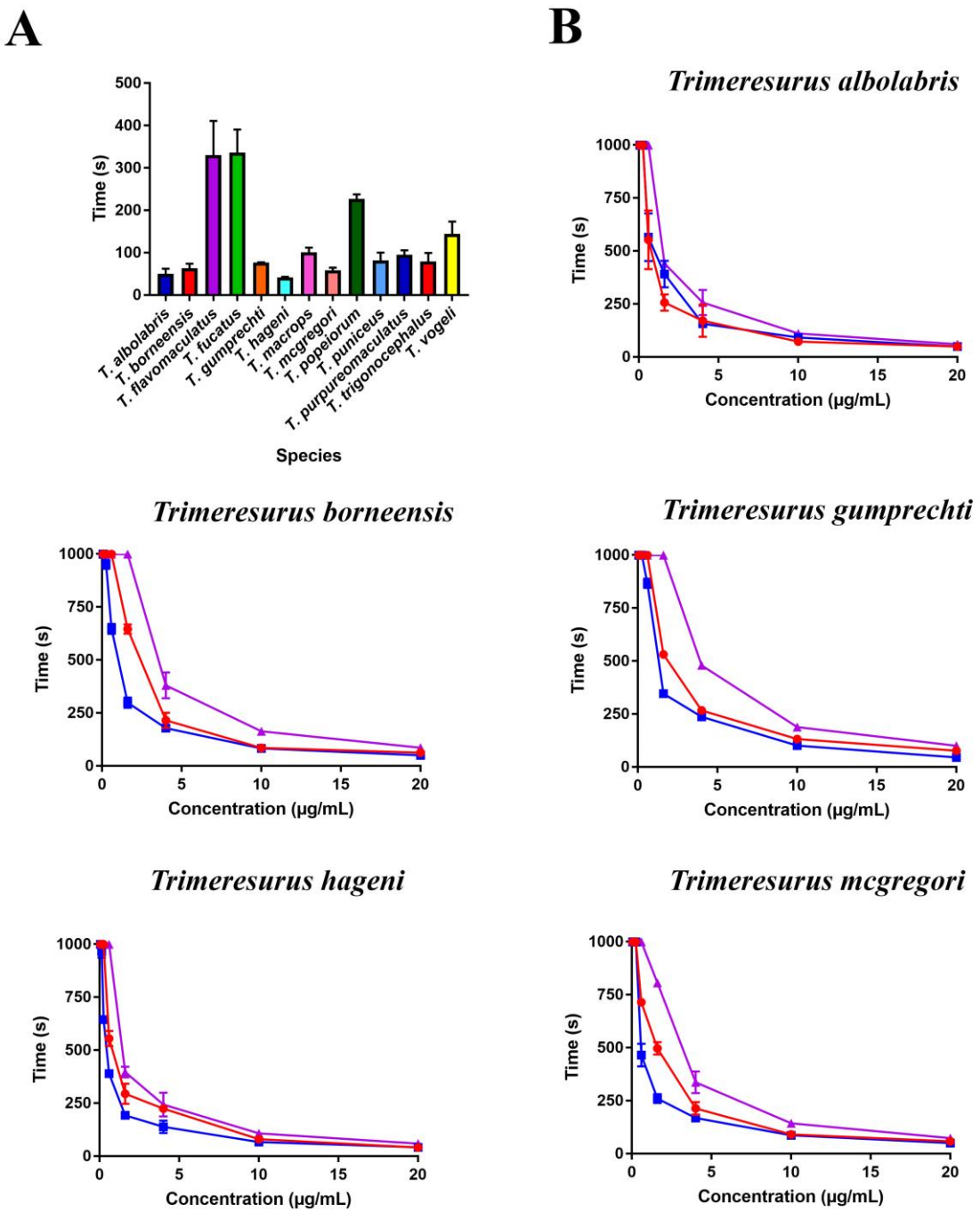

Figure 7.2 Cofactor dependency – fibrinogen
A) Initial 20 µg/mL venom concentration clotting times on human fibrinogen for all species included in study. B) 8-point dose-response curves of human fibrinogen clotting activity with both calcium and phospholipid (red line), with just calcium (blue line), and with just phospholipid (purple line) for *T. albolabris, T. borneensis, T. gumprechti, T. hageni* and *T. mcgregori.* Y-axis = Clotting time (sec). Data points are N = 3 with standard deviations.

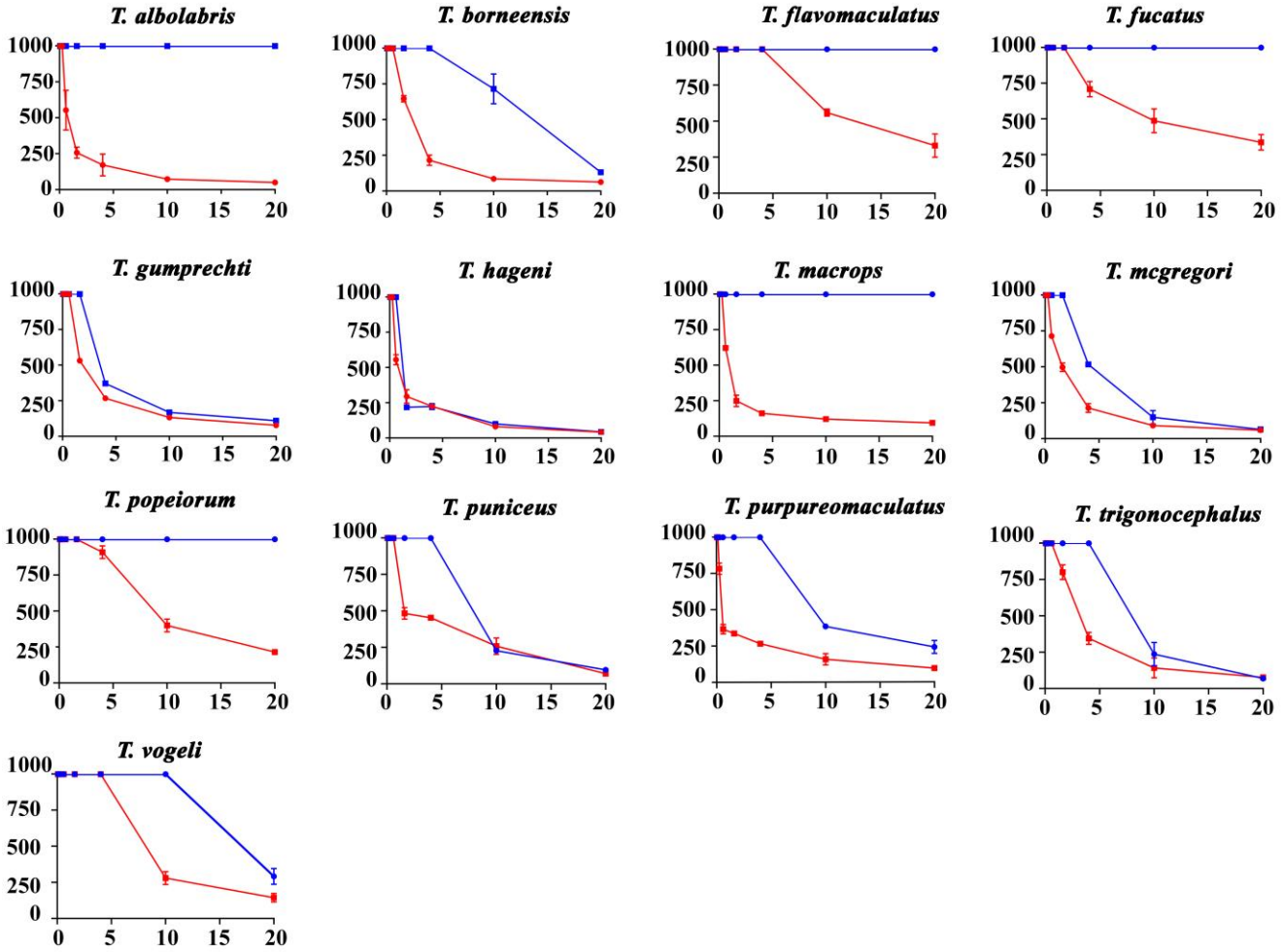

Figure 7.3 Antivenom neutralization

Comparison of relative Thai Red Cross Green Pit Viper antivenom cross neutralisation across various species of *Trimeresurus* on fibrinogen (1.2 mg/mL final concentration). Fibrinogen+venom clotting curve = red line, venom+antivenom clotting curve = blue line. X axis: final venom concentration (µg/mL), Y axis: clotting time in seconds. Values are averages of triplicates (single dilution measured three times) and standard deviation error bars are shown for each, although for most the error range is smaller than the line icon.

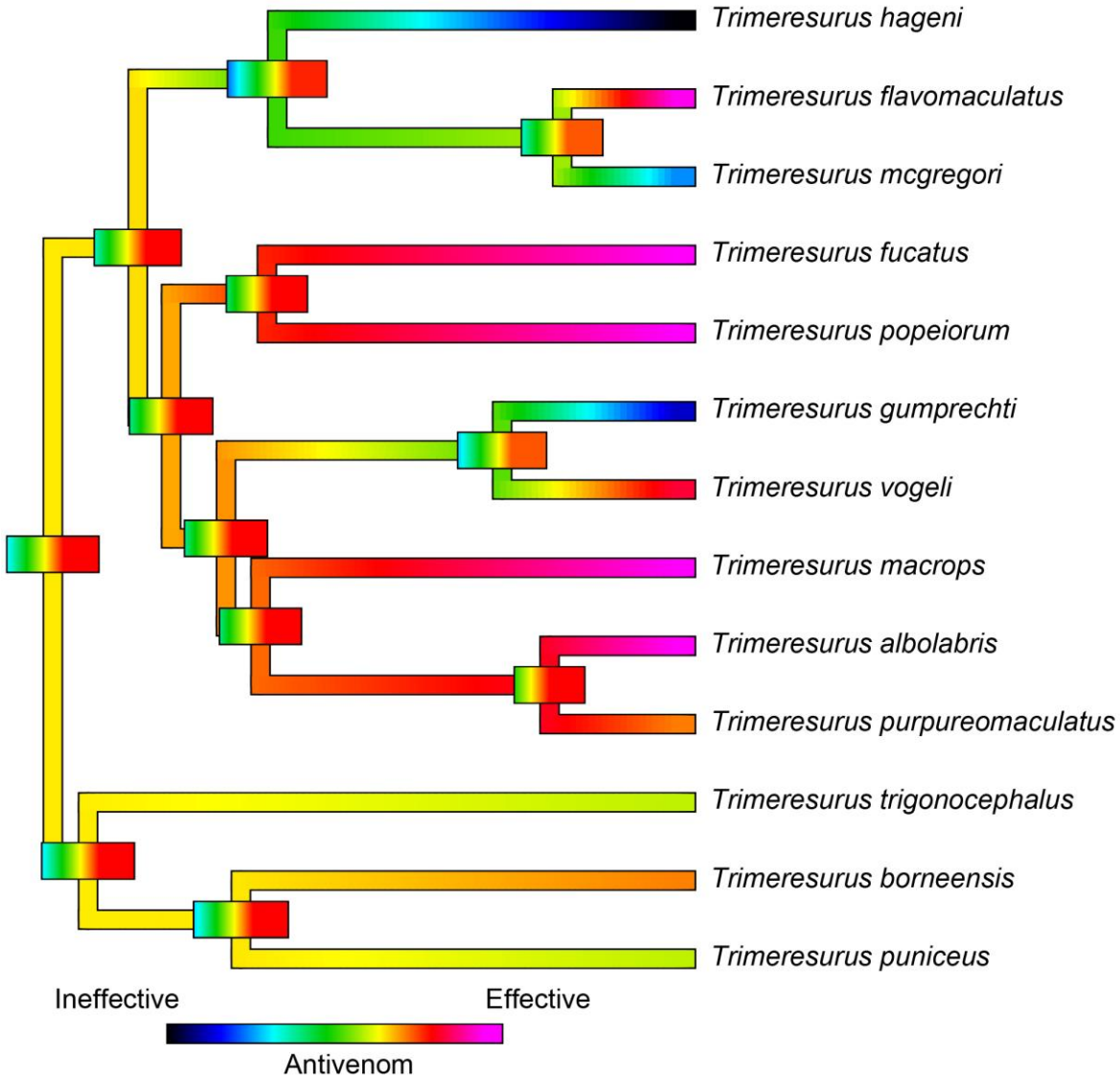

Figure 7.4 Antivenom neutralization efficacy heat map
Heat map of Green Pit Viper antivenom neutralisation efficacy against *Trimeresurus* venoms. Organismal phylogeny was based on Alencar et al. (2016) and Alencar et al. (2018).

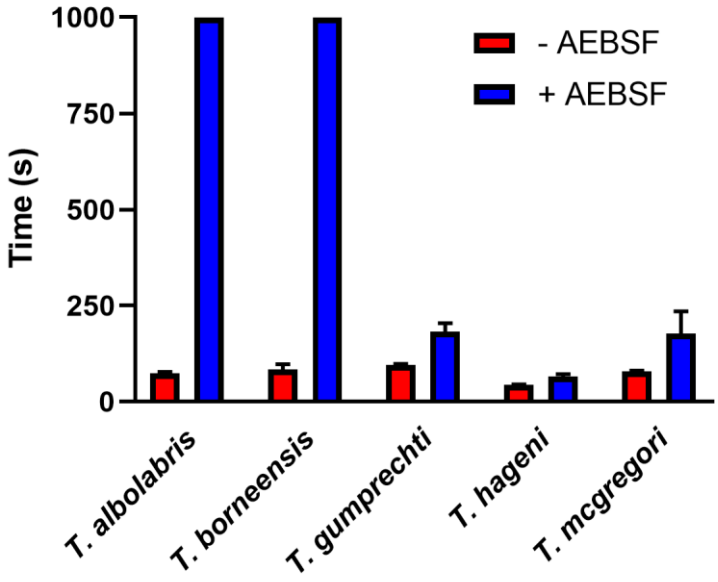

Figure 7.5 SVSP Inhibition
Inhibition of SVSPs by AEBSF (2 mM) against 20 µg venom from pseudo-procoagulant species performed on a Stago STA R Max. Clotting time was measured against 4 mg human fibrinogen with the addition of cofactors calcium and phospholipid. Red columns = venom without 2mM (end concentration) inhibitor, blue columns = venom with 2 mM (end concentration) inhibitor incubated together for 20 min at 37ºC. clot time was measured for a max reading time of 999.99 sec or until fibrinogen had clotted. Y axis = clot time (s), X axis = venom species. N = 3.

7.3.3 Thromboelastography (plasma)

The clot strength of venom-induced clotted plasma was investigated in the presence of calcium and phospholipid using thromboelastography (Figure 7.6). While the clotting activity of the tested *Trimeresurus* venoms on the plasma varied widely, as demonstrated by the variation in speed of action and in strength of fibrin clot formed, all clots produced were extremely small and weak relative to the control plasma clots, and therefore the action is pseudo-procoagulant, not a true procoagulant activity. However, *T. popoeirum* venom was the only species that did not clot the plasma directly, producing a trace very similar to that of the spontaneous control clot.

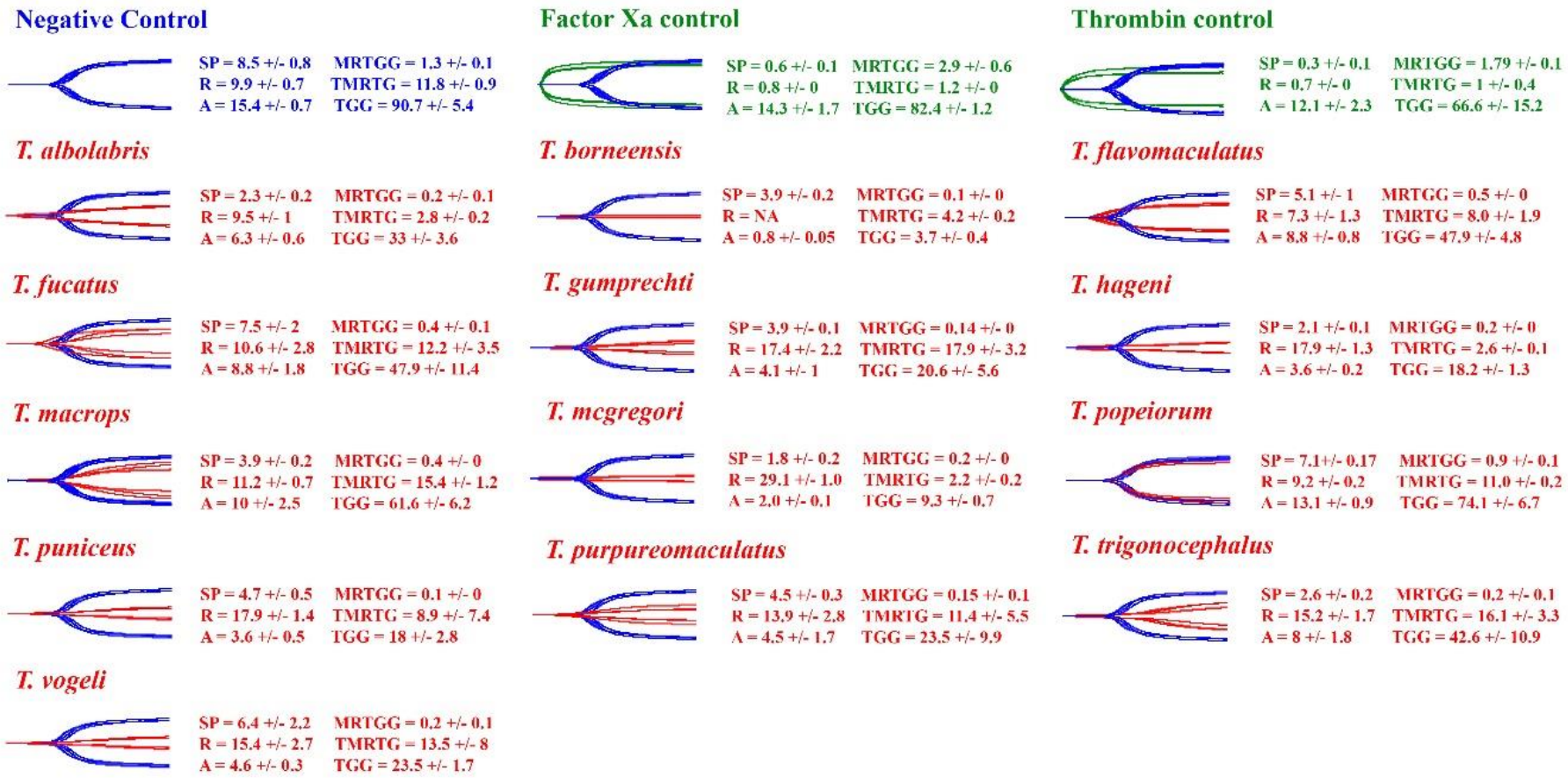

Figure 7.6 Thromboelastography Plasma traces

Overlaid thromboelastography traces showing effects of venoms ability to clot plasma relative to spontaneous clot control where species cleave plasma in a clotting manner to form weak clots. Blue traces = spontaneous clot controls, green traces = thrombin induced clot or Factor Xa induced clot, red traces = samples. SP = split point, time taken until clot begins to form (min). R = time to initial clot formation where formation is 2mm+ (min). A = amplitude of detectable clot (mm). MRTGG = maximum rate of thrombus generation (dsc, dynes/cm^2/sec). TMRTG = time to maximum rate of thrombus generation (min). TGG = total thrombus generation (dynes/cm^2). Overlaid traces are N = 3 for each set of control or experimental conditions. Values are N = 3 means and standard deviation.

7.3.4 Thromboelastography (fibrinogen)

Next, the direct clotting effects of the *Trimeresurus* venoms upon fibrinogen were assessed, again using thromboelastography in the presence of calcium and phospholipid (Figure 7.7). As with the plasma tests, the results revealed wide variation between the venom-induced clots in both speed of action and the relative clot strength. Consistent with the previous observations on plasma clot strength, all clots formed were weak relative to the thrombin-induced control. All *Trimeresurus* species tested (with the exception of *T. flavomaculatus*) clotted fibrinogen within the initial 30 min in a pseudo-procoagulant manner indicated by a reduction in clot strength relative to the thrombin control. *Trimeresurus popoeirum* was very slow in the action upon fibrinogen, which is consistent with its inability to clot plasma before spontaneous clotting occurred (see section above). In the case of *T. flavomaculatus,* which did not display any ability to directly clot fibrinogen within the initial 30 min, thrombin was subsequently added with the aim of generating a clot to test for destructive cleavage of fibrinogen by the venom. Indeed, the thrombin-induced clot displayed a greatly reduced clot strength in comparison to the thrombin control in the absence of venom, which is consistent with destructive (non-clotting) cleavage of fibrinogen by *T. flavomaculatus* venom (Figure 7.7).

Consistent with the extreme variance in speed of action and clot strength, Phylogenetic Generalized Least Squares PGLS analysis confirmed that there is no statistical correlation between the speed of reaction and the strength of the fibrin clot produced ($t = 0.9240$, $p = 0.3753$, $df = 1$) (Figure 7.8). This indicates that the strength of the clot (A) is independent of the time to maximum thrombus generation (TMRTG). Interestingly, *T. mcgregori*, which produced the strongest clot (A = 8 ± 1.8, TGG = 43.2 ± 10.4) registers at mid-range in terms of speed of clot formation (SP = 2.9 ± 0.2, MRTGG = 0.4 ± 0.02), while one of the fastest to produce a clot, *T. trigonocephalus*, (SP = 2.6 ± 0.4, MRTGG = 0.2 ± 0.02) produces one of the weakest clots (A = 1.8 ± 0.05, TGG = 8.8 ± 0.03).

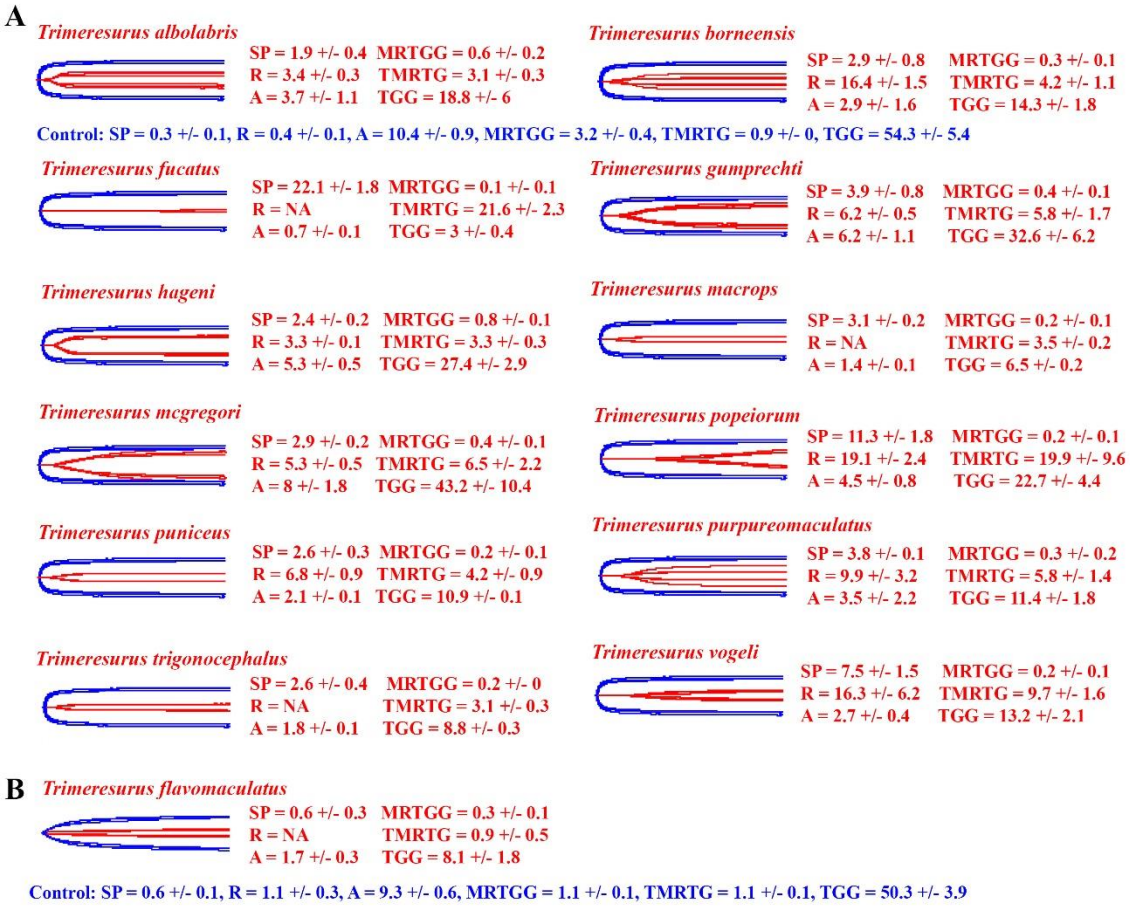

Figure 7.7 Thromboelastography fibrinogen traces

Overlaid thromboelastography traces showing effects of venoms A) ability to clot fibrinogen relative to thrombin control; or B) test for the ability to degrade fibrinogen for species which did not clot in (A) whereby thrombin was added at the end of the 30 min runs to test for intact fibrinogen. Blue traces = thrombin clot controls, red traces = samples. SP = split point, time taken until clot begins to form (min). R = time to initial clot formation where formation is 2 mm+ (min). A = amplitude of detectable clot (mm). MRTGG = maximum rate of thrombus generation (dsc, dynes/cm^2/sec). TMRTG = time to maximum rate of thrombus generation (min). TGG = total thrombus generation (dynes/cm^2). Overlaid traces are N = 3 for each set of control or experimental conditions. Values are N = 3 means and standard deviation.

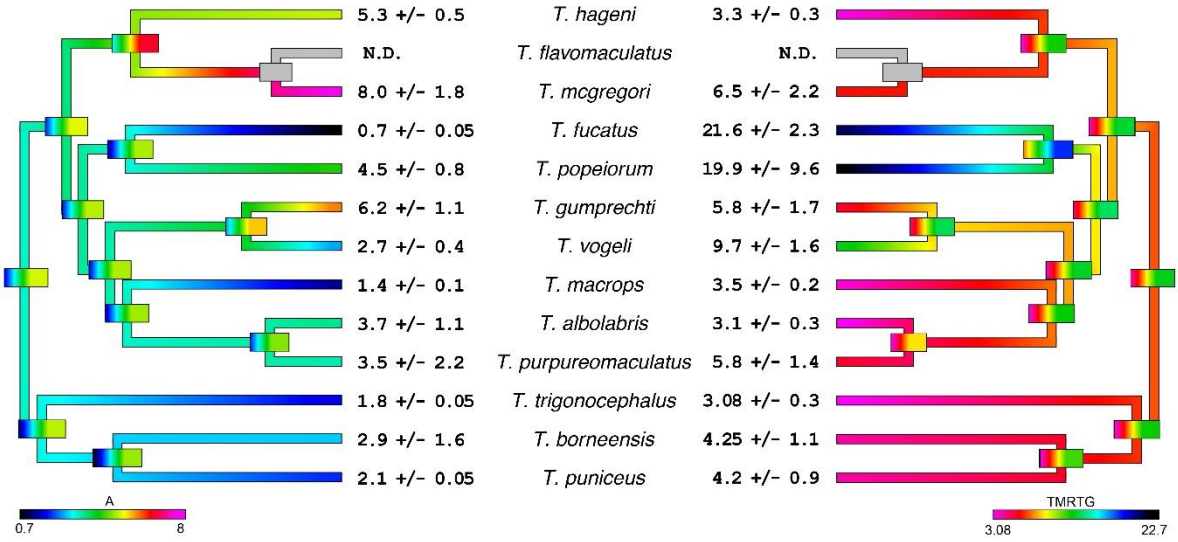

Figure 7.8 Heat map overlay phylogeny fibrinogen thromboelastography
Heat map overlay phylogeny of sampled *Trimeresurus* species tested for their ability to clot fibrinogen using a Thromboelastography (Figure 7). Heat map illustrates the relationship between amplitude (A) of generated clot vs Time to Maximum Rate of Thrombus Generation (min) (TMRTG). Cooler colours are smaller amplitudes and longer time taken to generate thrombus, while warmer colours are larger amplitudes with a shorter time taken to generate thrombus. PGLS analysis showed no statistical correlation between speed of reaction and clot size formed on fibrinogen for any species (t = 0.9240, p = 0.3753, df = 1). Values are N = 3 means and standard deviation. Organismal phylogeny was based on (Alencar et al., 2016; Malhotra and Thorpe, 2004). *T. flavomaculatus* is in gray as it does not clot fibrinogen within the assay time period.

7.3.5 Fibrinogen chain degradation

In order to determine the specific fibrinogen chain cleavage by the various *Trimeresurus* venoms, time-dependent assays were conducted to illustrate effects upon each chain (Figure 7.9 and Figure 7.10). A wide variation in pattern emerged, with many of the venoms displaying the ability to cleave the alpha chain (with the exception of *T. gumprechti* and *T. popeiorum*). In most venom samples, the alpha chain was initially quite rapidly degraded within the first 5 minutes, followed by the beta chain. *Trimeresurus albolabris*, *T. borneensis*, *T. flavomaculatus*, *T. hageni*, *T. mcgregori*, *T. purpureomaculatus*, *T. trigonocephalus* and *T. vogeli* also cleaved the gamma chain, thereby displaying the ability to cleave all three chains, with partial degradation of the gamma chain noted for *T. puniceus*. Some species (*T. flavomaculatus* and *T. purpureomaculatus*) degraded all three chains the quickest, however this ability was not congruent with their ability to clot plasma (Figure 7.1 and Figure 7.6) or fibrinogen (Figure 7.2 and Figure 7.7), indicative of at least some cleavage being destructive rather than clot forming. Other species, however, which did display an ability to clot plasma in a timely manner did not necessarily cleave all three chains rapidly (*T. albolabris*), nor did they cleave both alpha and beta (*T. gumprechti*). This suggests notable variation in destructive chain degradation leading to versus systematic degradation of chains leading to clot formation (albeit

with weak and unstable fibrin structures), but both effects leading to a net depletion of fibrinogen levels.

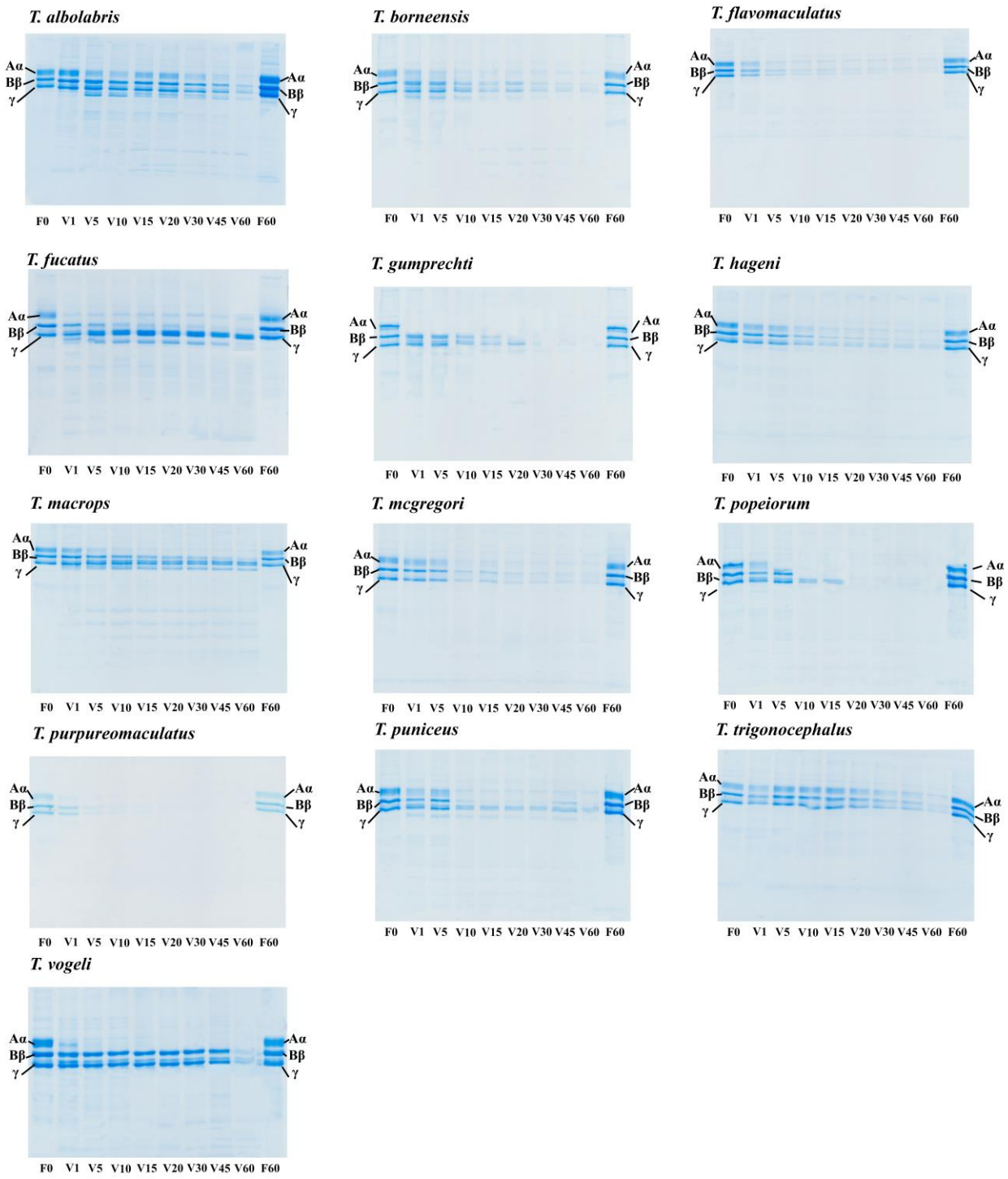

Figure 7.9 Fibrinogen chain cleavage - gel
1D SDS PAGE time dependent fibrinogen chain degradation (α, β or γ) by venom at 0.1µg/µL concentration at 37ºC over 60 min. F = fibrinogen at 0 min or 60 min incubation controls, V = venom at 1, 5… 60 min incubation.

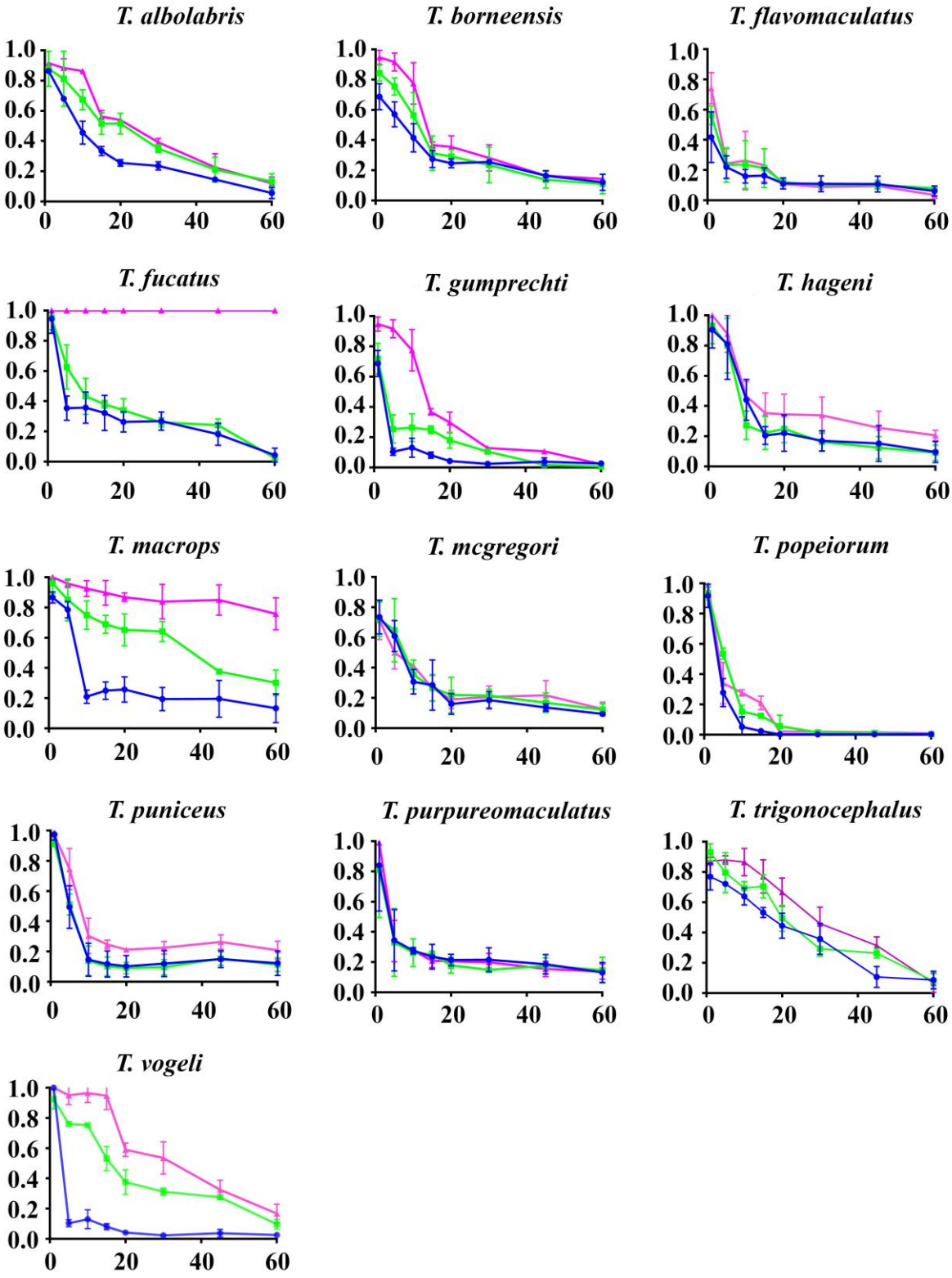

Figure 7.10 Fibrinogen chain cleavage - % intact
Relative cleavage of alpha (blue), beta (green) or gamma (pink) chains of fibrinogen. X-axis is time (min), y-axis is percentage of intact chain remaining. Error bars indicate standard deviation and N = 3 means.

7.3.6 Fibrinolysis

The ability of the venoms to actively lyse plasma clots was investigated in the presence and absence of tPA (tissue plasminogen activator) (Figure 7.11). Although plasma clots were unable to be directly lysed by any of the venoms, some species increased the ability of tPA to induce fibrinolysis. These species (*T. albolabris*, *T. borneensis*, *T. gumprechti*, *T. hageni*, *T. macrops*, *T. popeiorum*, *T. puniceus*, *T. purpureomaculatus*, *T. trigonocephalus* and *T. vogeli*) were able to shorten the clot lysis time (CLT) as compared incubations in the absence of venom.

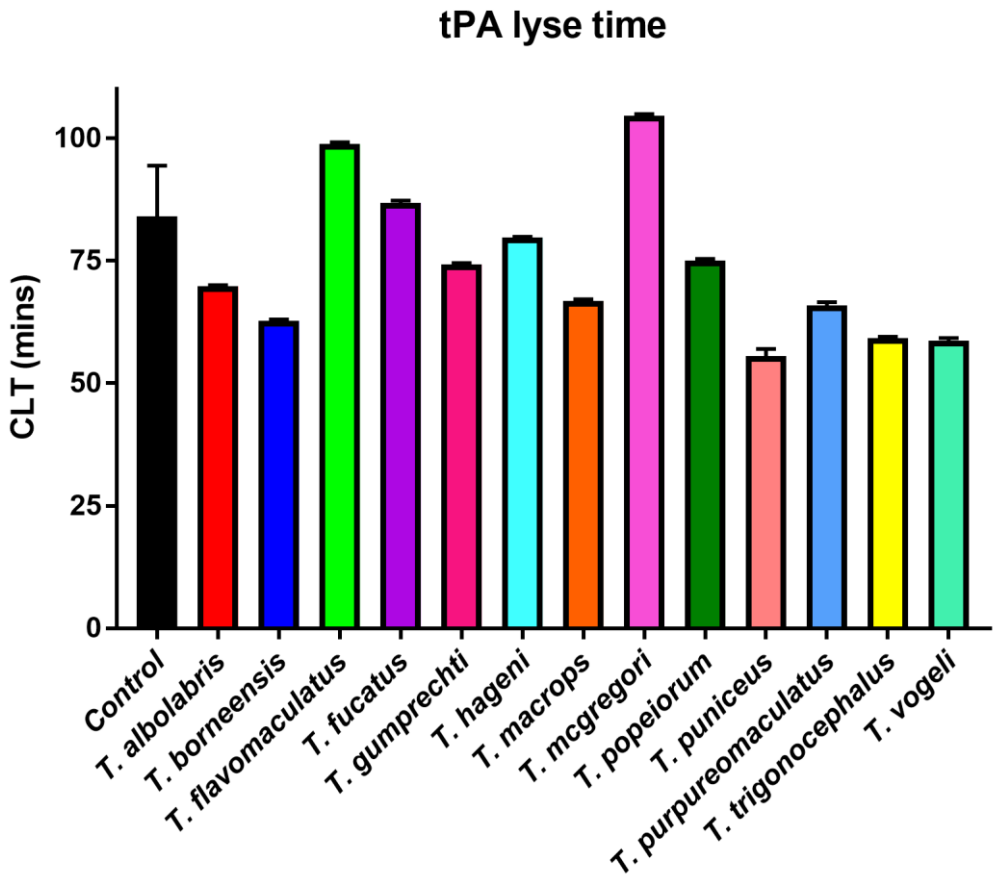

Figure 7.11 Fibrinolysis
Clot Lysis Time (CLT) for each species in the presence of tPA at 500 ng/μL venom concentrations (other concentrations not shown). Control is indicated in black. Columns are averages of triplicates and error bars given for each. Bars which are lower than the control lysed the plasma clot quicker than under normal tPA clot lyse conditions.

7.3.7 FXa, thrombin and FIXa enzyme inhibition studies

Investigations to determine the sites of potential venom-dependent enzyme inhibition proceeded in a stepwise manner in order to ascertain specific sites of action: i) incubation of venom with FIXa followed by the addition of plasma to determine the venom's ability to directly inhibit FIXa; ii) incubation of venom with FXa followed by the addition of plasma to determine the ability of the venom to directly inhibit FXa; iii) incubation of venom with plasma followed by the addition of FXa

to determine the effects of the venom on prothrombinase complex formation; iv) incubation of venom with thrombin followed by the addition of fibrinogen to determine direct inhibition of thrombin.

The results were as follows (Figure 7.12): i) incubation with FIXa revealed a wide variation in the level of inhibitory activity of the venoms with some species displaying stronger inhibitory effects than others (*T. borneensis* and *T. mcgregori*) (Figure 7.12A); ii) a wide variation in FXa inhibition was notable across the genus. (Figure 7.12B); iii) incubation of the venom with plasma followed by the addition of FXa did not result in a prolonged clotting time and thus potential inhibition of prothrombinase, with the exception of *T. puniceus* venom which also showed inhibition towards FXa (Figure 7.12C); iv) no substantial inhibition of thrombin-dependent fibrinogen cleavage was observed following incubation with *Trimeresurus* venom (Figure 7.12D). However, as these enzymes work as a cascade, the cumulative effect of the inhibition may strongly contribute to the anticoagulant actions of these venoms.

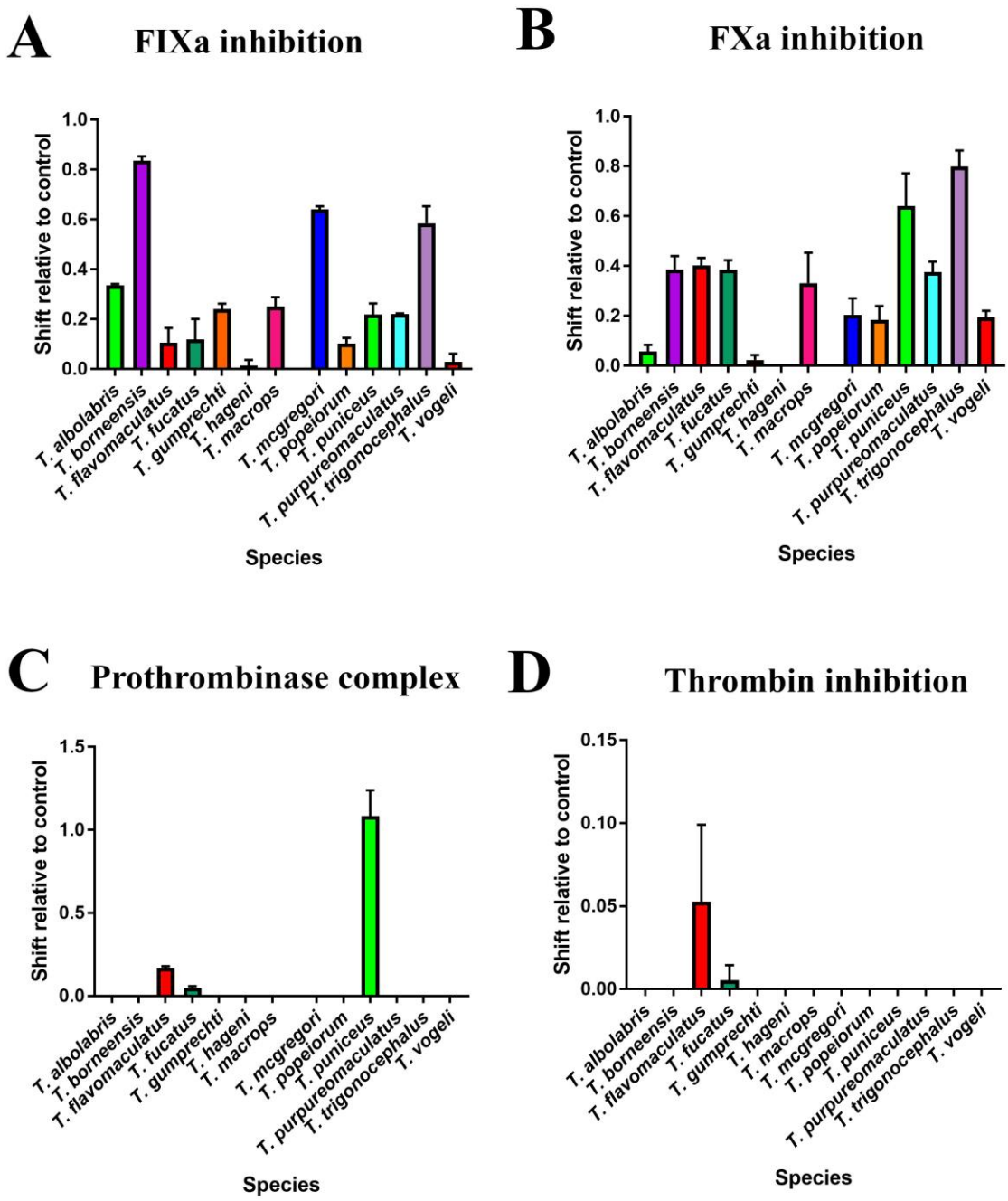

Figure 7.12 Clotting factor inhibition

Clotting factor inhibition panel showing the relative inhibitory effects of *Trimeresurus* venom on preventing the activation of: A) FIXa, B) FXa, C) Prothrombin to thrombin (Prothombinase complex) and D) Thrombin inhibition. For A) venom was incubated with FIXa for 2 min before adding plasma, with clot time then immediately measured. For B) venom was incubated with human plasma for 2 min before adding Factor Xa with clot time then immediately measured. For C) and D) venom was incubated with FXa or thrombin for 2 min before adding plasma or fibrinogen, with clot time then immediately measured. Data points are N = 3 displayed as a shift away from the control with standard deviations (no shift from control values would be a zero value).

7.4 Discussion

Species of *Trimeresurus* are wide spread throughout the Asian continent. As arboreal specialists, they are under extreme selection pressure due to high prey escape potential combined with prey variation. Arboreality also restricts gene flow, which in turn creates a diversification hot spot for many species to flourish and for venom to diverge. Such venom diversification within a genus can have real world implications for the treatment of envenomed patients due to differential coagulopathy and therefore a variable response to antivenom.

Despite species *Trimeresurus* species being very similar ecologically and morphologically, this study has revealed that their venoms are extremely functionally diverse and therefore capable of producing divergent clinical effects that are variably neutralised by antivenom. We observed coagulotoxic effects of the venom on plasma and fibrinogen of pseudo-procoagulant cleavage of fibrinogen to produce weak, unstable, short-lived fibrin clots. Such venom-mediated proteolysis of fibrinogen results in a depletion of fibrinogen levels, thus leading to a net anticoagulant state. The anticoagulation was potentiated by inhibition of clotting enzymes.

These laboratory findings are consistent with the haemorrhagic clinical manifestations of envenomation by *Trimeresurus* species (Chan et al., 1993; Chotenimitkhun and Rojnuckarin, 2008; Cockram et al., 1990; Greene et al., 2017; Hutton et al., 1990; Rojnuckarin et al., 2007; Rojnuckarin et al., 1999; Tan et al., 2017a; Visudhiphan et al., 1989; Witharana et al., 2019; Wongtongkam et al., 2005). In particular, the venoms have been shown clinically to produce rapid and pronounced decrease in fibrinogen levels leading to a net anticoagulant state (Collet et al., 2000; Longstaff and Kolev, 2015; Ryan et al., 1999), which is consistent with the results presented here. These effects are similar to that produced by other Asian pit vipers (Debono et al., 2019a; Debono et al., 2019b; Debono et al., 2019c).

Previous analysis of fibrinogen degradation on a very limited range of *Trimeresurus* species only provided qualitative, descriptive data and did not quantify the rates of fibrinogen chain cleavage (Jones et al., 2019). Further, this prior study did not attempt to determine the effect fibrinogen cleavage had upon clotting or the ability of antivenom to neutralise these pathological effects. In addition, prior studies also only measured antivenom binding through the use ELISA or Western Blot, which would reveal only simple antivenom binding to venom proteins, with no kinetic information, and, crucially prior studies did not ascertain whether the antivenom was effective in neutralising the venom's pathological functions(Jones et al., 2019; Tan et al., 2017a). In contrast, in this study we not only quantified the effects upon fibrinogen but also investigated the ability of the Thai Red Cross Green Pit Viper Antivenin to neutralise the coagulotoxic effects of the 13 species of *Trimeresurus* investigated here. As expected, since the antivenom is made using *T. albolabris* venom, this species was completely neutralised even at the highest venom concentration. *Trimeresurus borneensis*, *T.*

flavomaculatus, *T. macrops* and *T. popeiorum* were also extremely well neutralised. Other venoms were differentially neutralised by the antivenom, with notably poor effects upon *T. gumprechti*, and *T. mcgregori* and no detectable effect upon *T. hageni*. There was not, however, a phylogenetic pattern in regards to which species were well neutralised or poorly neutralised, which is consistent with the rapid molecular evolution characteristic of predatory venoms (Casewell et al., 2013).

In addition to investigating the effects upon fibrinogen by the venoms, this study also ascertained inhibition of clotting enzymes by the venoms. *Trimeresurus trigonocephalus* displayed the most pronounced inhibition of FXa, while *T. borneensis* displayed the largest inhibitory effect on FIXa. The inhibition of clotting enzymes would have a synergistic relationship with the depletion of fibrinogen levels, thereby potentiating the net anticoagulant effect. Indeed, anticoagulation is a major clinical feature in patients envenomated by *Trimeresurus* species (Chotenimitkhun and Rojnuckarin, 2008; Cockram et al., 1990; Greene et al., 2017; Hutton et al., 1990; Rojnuckarin et al., 2007; Rojnuckarin et al., 1999; Rojnuckarin et al., 1998). Fibrinogenolytic effects have frequently been reported leading to swelling, excessive bleeding and defibrination. Antivenom has been reported as being effective for *T. albolabris* and *T. macrops* envenomations (Chan et al., 1993; Hutton et al., 1990; Rojnuckarin et al., 2007; Yang et al., 2007), which is consistent with the results we obtained for both species in this study. Haemorrhagic shock would be further potentiated by the anticoagulant mechanisms we have identified in this study working synergistically with metalloprotease enzymes that damage the vascular wall (Escalante et al., 2011; Gutiérrez et al., 2011).

Consistent the poor neutralisation from the tested antivenom on *T. gumprechti,* and *T. mcgregori* venoms, and the lack of effect upon *T. hageni*, these same three species were also not inhibited by the known serine protease inhibitor AEBSF, which was effective in neutralising the effects of the other species. Thus, while the actions upon fibrinogen for species such as *T. albolabris* and *T. borneensis* are due to serine proteases, the coagulotoxic effects from *T. gumprechti*, *T. hageni* and *T. mcgregori* are due to the other fibrinogenolytic enzyme class present in the venoms: metalloproteases. Interestingly, these three species are not closely related to each other and therefore this unique activity has been derived on three independent occasions. As antivenom is made using the venom of *T. albolabris* venom, which contains fibrinogenolytic serine proteases, this explains the poor performance against the venoms which are rich in fibrinogenolytic metalloproteases. As these three species were phylogenetically distinct from each other, and therefore convergently derived their venoms away from the plesiotypic serine protease driven actions upon fibrinogen with the consequent impact upon antivenom cross-neutralisation, this underscores the unreliability of organismal phylogeny as a predictor of antivenom efficacy. Similarly, organismal was a poor predictor of venom potency, with the two most potent venoms (*T. albolabris* and *T. hageni*) being distant to each other on the organismal tree.

These findings therefore have real world implications for the treatment of patients envenomed by *Trimeresurus* species using the widely available Thai Red Cross Green Pit Viper antivenom. An important caveat is that the positive cross-reactivity with *T. flavomaculatus* and *T. fucatus* requires *in vivo* confirmation before clinical recommendations can be made regarding treatment protocols. However, as *T. macrops* was also well neutralised, consistent with clinical reports, the congruent positive effects upon *T. flavomaculatus* and *T. fucatus* in the tests conducted in this study are strongly suggestive of clinical usefulness of the antivenom against these species. In contrast, the poor performance of the antivenom against *T. gumprechti* and *T. mcgregori*, and failure against *T. hageni*, is cause for significant concern, despite the ideal scenario of preincubation of antivenom:venom, is cause for significant concern and the likelihood of clinical usefulness for these species is low (*T. gumprechti* and *T. mcgregori*) to non-existent (*T. hageni*). Another important note to be made is that the antivenom efficacy in this paper is purely from the perspective fibrinogenolysis. Studies into other clinically relevant pathophysiological functions, such as myotoxicity, may produce differential antivenom efficacy patterns and should be the subject of future research.

7.5 Materials and Methods

7.5.1 Venoms

A total of 13 venoms from the Asian pit viper genus *Trimeresurus* were investigated for their coagulotoxic effects (*T. albolabris, T. borneensis, T. flavomaculatus, T. fucatus, T. gumprechti, T. hageni, T. macrops, T. mcgregori, T. popeiorum, T. puniceus, T. purpureomaculatus, T. trigonocephalus, T. vogeli*), which were obtained from the long-term cryogenic collection of the Venom Evolution Lab. Pooled (N = 3 adult males for each), lyophilized venom samples were resuspended in deionized H_2O and protein concentrations (mg/mL) were determined using a ThermoFisher Scientific Nanodrop™ 2000c Spectrophotometer. Working stocks of 50% deionized water/50% glycerol (>99%, Sigma-Alrich) for all venoms were prepared at 1 mg/mL and stored at -20°C to preserve enzymatic activity and reduce enzyme degradation. All venom and plasma work was undertaken under the University of Queensland Biosafety Approval #IBC134BSBS2015.

7.5.2 Coagulation analyses on plasma and fibrinogen

The ability of the *Trimeresurus* venoms to affect clotting of plasma and/or fibrinogen was investigated using a Stago STA-R Max coagulation analyser as previously described (Debono et al., 2019a; Debono et al., 2019b; Debono et al., 2019c; Debono et al., 2017a). Human plasma (3.2% citrate) was supplied by the Red Cross Blood Service (under Research Supply Agreement 18-03QLD-09), and all work was undertaken under University of Queensland Biosafety Approval #IBC134BSBS2015 (1/1/2015) and Human Ethics Approval # 2016000256 (1/6/2016). Human fibrinogen (4 mg/mL, Lot#F3879, Sigma Aldrich) was reconstituted to a concentration of 1 mg/mL

in 150 mM $NaCl_2$, 50 mm Tris, pH 7.3, flash frozen in liquid nitrogen and stored at −80 ºC until further use. Coagulopathic toxin effects were measured by a modified procoagulant protocol on a Stago STA-R Max coagulation robot (France) using Stago Analyser software v0.00.04 (Stago, Asniéres sur Seine, France). Plasma clotting baseline parameters were determined by performing the standardised activated Partial Thromboplastin Time (aPTT) assay (TriniCLOT APTT HS, Stago). In order to determine clotting times effected by the addition of varying venom concentrations, a modified clotting test was developed, in which 50 µL of venom (20 – 0.05 µg/mL) dilutions in STA Owren Koller Buffer (Stago Cat# 00360), 50 µL$CaCl_2$ (25mM stock solution Stago Cat# 00367 STA), and 50 µL phospholipid (solubilized in Owren Koller Buffer adapted from STA C.K Prest standard kit, Stago Cat# 00597) in a final volume of 175 µL in Owren Koller Buffer was incubated for 120 sec at 37°C before adding 75 µL of human plasma or human fibrinogen (1.2 mg/mL final). Relative clotting was then monitored for 999 sec or until plasma clotted (whichever was sooner). The calcium or phospholipid dependence was assessed by replacing calcium or phospholipid for Owren Koller Buffer, respectively. Inhibition of venom serine protease activity was determined using 4-benzenesulfonyl fluoride hydrochloride (AEBSF), a known serine protease inhibitor (Kuniyoshi et al., 2017; Torres-Bonilla et al., 2018; Xin et al., 2009; Yamashita et al., 2014) in the modified clotting assay. For this purpose, 25 µL of (diluted) venom, 50 µL $CaCl_2$ (5 mM final), 50 µL phospholipid, and 50 µL AEBSF (2 mM final) were incubated for 2 min at 37°C before adding 75 µL of human fibrinogen (1.2 mg/mL final). As a control, fibrinogen clotting was measured using thrombin (stable thrombin from Stago Liquid Fib kit, unknown concentration from supplier (Stago Cat#115081 Liquid Fib)). Change in Area Under the Curve (AUC) was used as a statistical representation to relative influence of cofactors (calcium or phospholipid) or the impact of antivenom. An increase in the AUC represents longer clotting times compared to the optimum conditions (control). AUC values were calculated using the program GraphPad PRISM 8.0 (GraphPad Prism Inc., La Jolla, CA, USA) using the following formula: $\Delta X*(Y1+Y2)/2$. Each experimental condition AUC was divided by control AUC for each venom, and then 1 subtracted so that if there was no change, then this would have been a value of zero. The results were then multiplied by 100 in order to present them as % change.

7.5.3 Inhibition of FIXa, FX or thrombin

Additional studies in which the inhibition of serine proteases FXa, prothrombinase complex formation, thrombin, or FIXa (working stock of 0.17 mg/mL so that 5 µg/mL of FIXa is in end concentration, Haematological technologies Cat# HCIXA-0050, Essex Junction VT USA), Table 7.1) by *Trimeresurus* venoms were performed using previously validated methods (Debono et al., 2019a; Debono et al., 2019b; Debono et al., 2019c; Youngman et al., 2018). All species were subjected to these assays. To identify the possible target in the clotting cascade which the venom was acting upon

to result in the anticoagulant activity, either plasma or individual factors of the clotting cascade were incubated with the sample venom as the incubation step allows venom to bind and inhibit its target. Data was analysed calculating a shift away from the control for each assay using GraphPad PRISM 8.0 (GraphPad Prism Inc., La Jolla, CA, USA) as described above.

Table 7.1 Anticoagulation assay details

FXa inhibition assay	Step 1. 50 µL 0.1 µg/mL venom (1 mg/mL 50% glycerol stock diluted with OK buffer) + 50 µL 0.025 M calcium (Stago catalog # 00367) + 50 µL phospholipid (Stago catalog #00597) + 25 µL FXa (Stago catalog # 00311). Step 2. 120 second incubation. Step 3. Addition of 75 µL plasma.
Prothombinase complex inhibition assay	Step 1. 50 µL 0.1 µg/mL venom (1 mg/mL 50% glycerol stock diluted with OK buffer) + 50 µL 0.025 M calcium + 50 µL phospholipid + 75 µL plasma Step 2. 120 second incubation. Step 3. Addition of 25 µL Factor Xa
FIXa inhibition assay	Step 1. 25 µL 0.1 µg/mL venom (2 mg/mL 50% glycerol stock diluted with OK buffer) + 75 µL 0.025 M calcium (2:1 ratio of $CaCl_2$ + OK buffer) + 50 µL phospholipid + 25 µL FIXa (Haematological technologies Cat# HCIXA-0050) Step 2. 120 second incubation. Step 3. Addition of 75 µL plasma
Thrombin inhibition assay	Step 1. 50 µL 0.1 µg/mL venom (1 mg/mL 50% glycerol stock diluted with OK buffer) + 50 µL 0.025 M calcium + 50 µL phospholipid + 25 µL thrombin (Stago catalog # 00611). Step 2. 120 second incubation. Step 3. Addition of 75 µL 4 mg/mL fibrinogen.

7.5.4 Thromboelastography analyses on plasma and fibrinogen

Venoms were investigated for their ability to clot or impede clotting of plasma and fibrinogen using a Thrombelastogram® 5000 Haemostasis analyser (Haemonetics®, Haemonetics Australia Pty Ltd, North Rdye, Sydney 2113, Australia) as previously described (Coimbra et al., 2018; Debono et al., 2019a; Debono et al., 2019b; Debono et al., 2019c; Oulion et al., 2018). Human fibrinogen (4 mg/mL,) was reconstituted in enzyme buffer (150 mM NaCl and 50 mM Tri-HCl (pH 7.3)). Briefly, 7 µL venom working stock (1 mg/mL) or 7 µL thrombin as a positive control (stable thrombin from the Stago Liquid Fib kit, unknown concentration from supplier, (Stago Cat#115081 Liquid Fib)), 72 µL $CaCl_2$ (25mM stock solution, Stago Cat# 00367 STA), 72 µL phospholipid (solubilized in Owren Koller Buffer adapted from STA C.K Prest standard kit, Stago Cat# 00597), and 20 µL Owren Koller Buffer (Stago Cat# 00360) was combined with 189 µL fibrinogen or human plasma and run immediately for 30 min to allow for ample time for clot formation. An additional positive control of

7 µL Factor Xa (unknown concentration from supplier, Liquid Anti-Xa FXa Cat#253047, Stago) was also incorporated for plasma only. If no clot was formed for a venom in the fibrinogen assay by 30 minutes, 7 µL thrombin (stable thrombin from Stago Liquid Fib kit, unknown concentration from supplier (Stago Cat#115081 Liquid Fib)) was added to ascertain if destructive cleavage of fibrinogen had occurred due to the venom.

Parameters obtained from thromboelastography analysis were: SP = split point, time taken until clot begins to form (min); R = time to initial clot formation where formation is 2 mm+ (min); A = amplitude of detectable clot (mm); MRTGG = maximum rate of thrombus generation (dsc, dynes/cm^2/sec); TMRTG = time to maximum rate of thrombus generation (min); and TGG = total thrombus generation (dynes/cm^2). Statistical analysis of speed of reaction and the clot size formed was conducted using Phylogenetic Generalized Least Squares (PGLS), including the parameters *p* = p value, probability, *df* = degrees of freedom and *t* = t value, calculated difference of standard error.

7.5.5 Fibrinogenolysis analysis

Fibrinogenolytic activity was assessed as previously described (Debono et al., 2019a; Debono et al., 2019b; Debono et al., 2019c). In brief, fibrinogen (1 mg/mL reaction concentration, 150 mM NaCl / 50 mM Tri-HCl (pH 7.3), Lot#F3879, Sigma Aldrich, St. Louis, Missouri, United States) was incubated with venom (10 µg/mL reaction concentration) for 60 min at 37ºC, and fibrinogen cleavage was assessed at several time points (1, 5, 10, 15, 20, 30, 45 and 60 min) using SDS-PAGE analysis under reducing conditions followed by staining with Coomassie Brilliant Blue R-250. The visualized protein fragments were quantified using ImageJ software (V1.51r, Java 1.6.0_24, National Institutes of Health, Bethesda, Maryland, USA) and analysed using GraphPad PRISM 7.0 (GraphPad Prism Inc., La Jolla, CA, USA).

7.5.6 Fibrinolysis

The ability of venoms to actively lyse clots was investigated following methods described previously (Debono et al., 2019a; Debono et al., 2019b; Debono et al., 2019c). Varying concentrations of venom (1 – 0.1 µg/µL) were tested either with or without the addition of tissue plasminogen activator (tPA, Sekisui Diagnostics, Lexington, MA, USA). Briefly, tissue factor (TF, Innovin, Siemens, USA) and phospholipid vesicles (PCPS, 75% phosphatidylcholine and 25% phosphatidylserine, Avanti Polar Lipids, Alabama, USA) were incubated at 37°C for 1 hour in HEPES buffer (25 mM HEPES, 137mM NaCl, 3.5 mM KCl, 0.1% BSA (Bovine Serum Albumin). To the TF/PCPS mixture (1.8 pM/3 µM final), CaCl2 (17 mM final), tPA (37.5 units/mL reaction concentration, diluted in 20 mM HEPES, 150 mM NaCl, 0.1% PEG-8000, pH 7.5), venom (50% v/v), and plasma (50% v/v, prewarmed at 37°C) were added. The fibrin clot formation and the subsequent lysis was monitored by measuring

the absorbance at 405 nm for every 30 sec during 3 hr at 37°C in a SpectraMax M2e microplate reader. The onset of clot formation was defined as the time point at which the turbidity increased (delta absorbance > 0.04); the clotting time was the time from the start of the assay to the onset of clot formation. The clot lysis time was the interval between the clear to turbid transition (defined as the midpoint between the onset of clot formation and the maximum turbidity) and the turbid to clear transition; the latter was determined by a sigmoidal fit of the turbidity plots using GraphPad PRISM 8.0 (GraphPad Prism Inc., La Jolla, CA, USA).

7.5.7 Antivenom efficacy assessment

The monovalent antivenom effects on all 13 *Trimeresurus* crude venoms was investigated using fibrinogen clotting assays as described above. The monovalent Green Pit Viper Antivenin (*Trimeresurus albolabris*) (Lot #TA00119, Expiry date: 15th Jan 2024) was purchased from Queen Saovabha Memorial Institute, The Thai Red Cross Society, Bangkok, Thailand. One vial of dry antivenom was reconstituted in 10 mL provided saline solution (using manufacturers guide) and centrifuged at 12000 rpm on an Allegra™ X-22R Centrifuge (Lot#982501, Beckman Coulter, Brea, CA, USA) for 10 min at 4°C, upon which the supernatant was removed, filtered (0.45 µm Econofltr PES, Agilent Technologies, Beijing, China), aliquoted, and stored at 4°C. For each experiment, a working stock of 5% antivenom and 95% Owren Koller Buffer was prepared, and the final antivenom concentration for each reaction was 0.5%. Briefly, 25 µL of antivenom diluted in STA Owren Koller Buffer, 50 µL of venom (20 – 0.05 µg/mL) dilutions in STA Owren Koller Buffer, 50 µL $CaCl_2$ (5 mM final), and 50 µL phospholipid in a final volume of 175 µL in Owren Koller Buffer was incubated for 120 sec at 37°C before adding 75 µL of human fibrinogen (1.2 mg/mL final). Relative clotting was then monitored for 999 sec or until plasma clotted (whichever was sooner). Note that antivenom does not clot fibrinogen and that a control was performed to rule out any additional effects antivenom has on fibrinogen, in which antivenom was substituted into the above outlined protocol in replacement of a venom sample.

7.5.8 Phylogenetic comparative analyses

The phylogenetic tree used was based upon a previously published species tree (Alencar et al., 2016; Malhotra and Thorpe, 2004). and manually recreated using Mesquite software (version 3.2) and then imported to Rstudio using the APE package (Paradis et al., 2004). Ancestral states were estimated for all traits using maximum likelihood as implemented in the contMap function of the R package phytools (Revell, 2012). As in previous studies with these methods (Lister et al., 2017; Rogalski et al., 2017), we used the phytools script shown in Supplementary Figure 1.

Chapter 8: Viper venom botox: the molecular origin and evolution of the waglerin peptides used in anti-wrinkle skin cream

8.1 Abstract

The molecular origin of waglerin peptides has remained enigmatic despite their industrial application in skin cream products to paralyse facial muscles and thus reduce the incidence of wrinkles. Here we show that these neurotoxic peptides are the result of *de novo* evolution within the prepro region of the C-type natriuretic peptide gene, at a site distinct from the domain encoding for the natriuretic peptide. The precursor region for the molecular evolution is a biodiversity hotspot that has yielded other novel bioactive peptides with novel activities. We detail the diversity of components in this region in order to explore what characteristics enable it to be such a biodiscovery treasure trove.

8.2 Introduction

Tropidolaeumus (temple vipers) venoms are unusually neurotoxic for vipers, selectively blocking the post-synaptic nicotinic acetylcholine receptors (epsilon subunit) to produce rapid collapse, spasms, ocular proctosis and tachypnea in prey, with death resulting from respiratory failure (Fry et al., 2015b; Lin et al., 1995; McArdle et al., 1999; Schmidt and Weinstein, 1995; Schmidt et al., 1992). These effects are produced by short (21 amino acid) peptides which do not display any homology to any other known peptide type and thus the gene precursor identity is unknown (Fry, 2005; Fry et al., 2015a).

A skin-cream with the trade name Syn®-Ake has been developed using the tripeptide synthetic compound dipeptide diaminobutyroyl benzylamide diacetate (molecular formula of $C_{23}H_{37}N_5O_7$ and a molecular weight of 495.57 g/m) to mimic the action of the full length peptide (Balaev et al., 2014; Trookman et al., 2009). Similar to botox, it blocks signal transmission and relaxes the muscles at the area of application, in order to reduce the formation and appearance of wrinkles.

Despite the industrial usefulness of these peptides, their molecular origin and evolution has remained unelucidated. It has previously been hypothesised that based on the proline-rich nature, that they share evolutionary relationships with the neurotoxic peptides from *Azemiops feae* (Brust et al., 2013; Fry, 2005; Fry et al., 2003b). However, in the absence of a gene sequence, this link has remained speculative.

8.3 Results and Discussion

Sequence blasting revealed cDNA library ORFs containing regions with homology to waglerin peptides (Figure 8.1 and Figure 8.2). Like waglerins 2 and 4 from *T. wagleri*, the version from *T. subannulatus* contained a -CYPPC- motif instead of CHPPC as seen in waglerins 1/3 from *T. wagleri*, a change that slightly decreases activity (Schmidt et al., 1992). As toxins evolve under selection

pressure towards a more potent form, this indicates that the -CYPPC- motif is the plesiotypic form, with the change from Y to H as a structural derivation that impacts upon functionality.

Blasting of the full length gene sequence identified the precursor as that which encodes for C-type natriuretic peptides. Sequence alignment (Figure 8.1) revealed that the wagerlin peptides evolved within the same proline-rich region of the prepro domain as did the Azemiopsin peptides from *Azemiops feae* (Brust et al., 2013) but in a region distinct from that encoding for the also *de novo* evolved bradykinin potentiating peptides such as Captopril (Fry et al., 2015a). Phylogenetic analysis showed the affinity of the waglerin peptides with the Azemiopsis peptides, confirming that the two types of post-synaptic nicotinic acetylcholine receptor binding peptides share a common molecular evolutionary history, with the cysteines of waglerin peptides representing a derived state.

De novo evolution of novel proline-rich bioactive peptides within the propeptide region of natriuretic peptides has not only occurred in the snake venoms (Fry et al., 2015a), but also independently in the natriuretic peptide form (B-type) convergently evolved within lizard venoms (Fry et al., 2015d). This reinforces the dynamic nature of this region, which is distinct from that encoding the plesiotypic natriuretic peptide. Genes coding for the normal body form do not have such proline rich regions (Figure 8.1). Another example of *de novo* evolution of bioactive peptides within a propeptide region has occurred in *Psammophis mossambicus* which has a myriad of bioactive peptides (Brust et al., 2013; Fry et al., 2008). These include novel neurotoxins which have explosively evolved within the propeptide region of the snake venom metallaprotease gene, accompanied by stop-codons, preventing expression of the metalloprotease enzyme that was the original function of this gene

These variants underscore the dynamic nature of venom evolution, which not only accelerates the molecular evolution of the plesiotypic proteins, but may result in neofunctionalisation in gene regions not normally associated with a secreted product. This study also reinforces the value of studying evolutionarily diverse lineages as sources of novel lead compounds for drug design and development.

8.4 Methods

Sequencing and phylogenetic analysis of Bicol, Philippines *Tropidolaemus subannulatus* cDNA library sequences were undertaken using methods previously described by us (Fry et al., 2008).

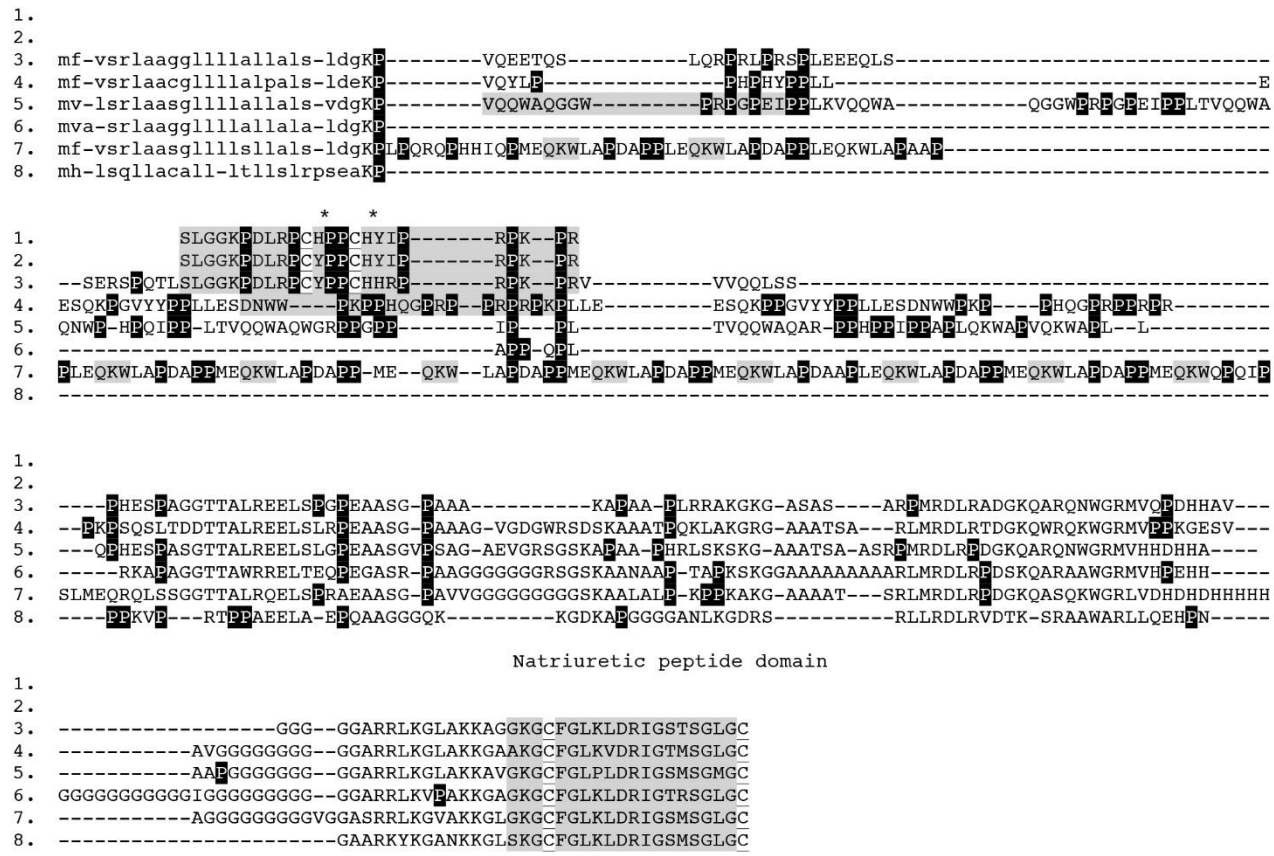

Figure 8.1 Waglerin's natriuretic peptide

1. P24335 (waglerin-1/3) *Tropidolaeumus wagleri*, 2. P58930 (waglerin-2/4) *Tropidolaeumus wagleri* 3. S9L004TR1742 *Tropidolaeumus subannulatus*, 4. K4IT20 *Azemiops feae*, 5. Q9PW56 *Bothrops jararaca*, 6. A0A0B4SX88 *Philodryas chamisso*, 7. A8YPR6 *Echis ocellatus*, 8. P23582 *Homo sapiens*. Post-translationally cleaved peptides are highlighted in gray, including the ancestral natriuretic gene, cysteines are underlined.

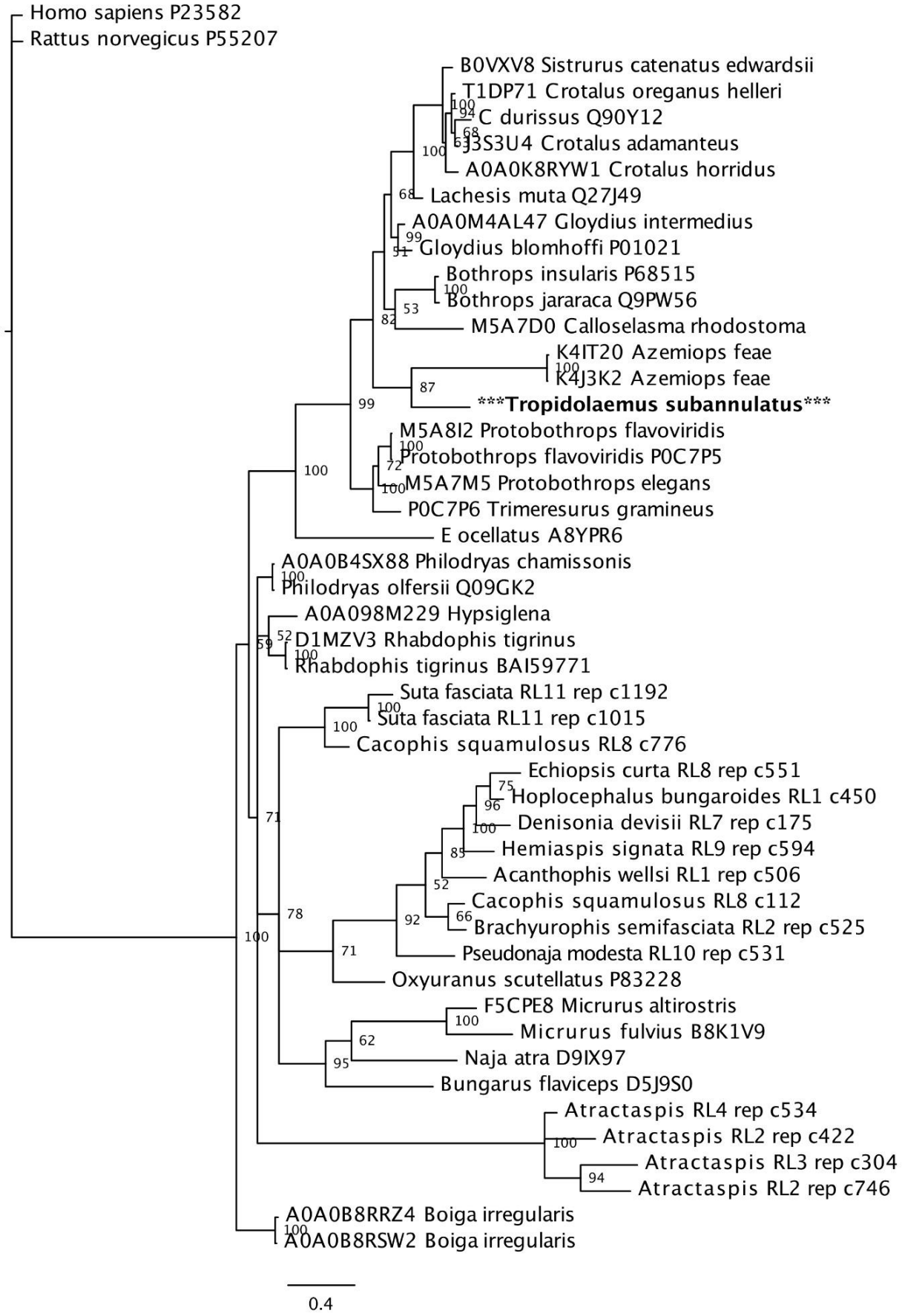

Figure 8.2 Bayesian reconstruction of C-type NP
Bayesian reconstruction of venom CNP molecular evolution.

Chapter 9: Conclusions and future directions

9.1 Research overview

The venomous snake species chosen for this thesis are a representation of a wide array of coagulotoxic venoms targeting multiple aspects of the clotting cascade from a broad spectrum of genera and geographical locations. All species included within this thesis are medically important or significant, effect the coagulation cascade, have limited research and understanding of their venom or have been completely neglected from the literature. Both procoagulant and anticoagulant species were included in order to ascertain differential selection pressures acting upon either mechanisms. Each chapter is a piece of the puzzle into increasing our understanding of snake venom coagulotoxins and novel drug design. Chapters 2 and 3 explored the procoagulant venoms of the infamous colubrid species the boomslang and the twig snake of Africa, while chapters 4-8 explored the extreme diversification that is Asian pit viper venom which was broken up into genus or smaller clades for easier digestion of results. In doing so, the following key findings could be achieved over the course of this research.

9.2 Key findings

9.2.1 Procoagulation

As mentioned previously, procoagulation in venom is the more derived mechanism for subjugation of prey, with anticoagulation being an ancestral characteristic of snake venoms. Procoagulation is the result of toxins activating either Factor X or prothrombin to generate endogenous thrombin, which in turn cleaves fibrinogen to form strong, stable fibrin clots The boomslang (*D. typus*) and the twig snake (*T. mossambicanus*) are two procoagulant species which produce hemorrhagic symptoms in human bite victims. This is due to the mass production of microscopic clot formations, which combined with unregulated clotting from check points such as tPA, antithrombin or activated protein C, causes mass hemorrhaging post-envenomation. Both species have evolved their venom to activate prothrombin producing endogenous thrombin in large amounts, ultimately leading to a stroke (in prey items) or hemorrhaging (in larger victims) *via* PIII-SVMPs. Interestingly, unlike well know procoagulant species such as *Pseudonaja textilis, Oxyuranus scutellatus* or *Notechis scutatus*, which all require (to varying degrees) calcium and phospholipid as co-factors, *D. typus* and *T. mossambicanus* do not require the additional co factors calcium or phospholipid to produce such striking procoagulation effects. This has only ever been previously described from *Echis carinatus* 'Ecarin', which is routinely used in diagnostic tools. Furthermore, as these two species produce such extremely similar clinical symptoms and occupy the same habitat, it is interesting that antivenom exists and is only effective against one species, *D. typus*. As SVMPs are the driving force behind the prothrombin activation exhibited by both species, we hypothesized that the additional SVMP

identified and isolated from *T. mossambicanus* was why the *D. typus* antivenom was almost completely ineffective at cross neutralization due to differences in the surface geometry (antigenicity) driving down the effectiveness of the *D. typus* antivenom against *T. mossambicanus*.

Procoagulation was also evident among the Asian pit vipers, with results indicating *Calloselasma rhodostoma* as a true procoagulant species in contrast to the anticoagulation displayed by other Asian pit vipers. Although this has been mentioned previously within the literature eg (Tang et al., 2016; Yamada et al., 1997), our investigation was able to distinguish that *C. rhodostoma* activates Factor X to produce endogenous thrombin, resulting in strong, stable clots. *Deinagkistrodon actus* and *Hypnale hypnale* also displayed the ability to clot plasma; however, *H. hypnale* only activated FX mildly, while *D. actus* did not activate FX. All three species were able to cleave fibrinogen as an alternative site of action; however, fibrinogen cleavage alone did not form strong, stable clots and therefore it was not concluded that *H. hypnale* or *D. actus* were also true procoagulant species but were pseudo-procoagulant in that they produced weak, transient fibrin clots resulting in the depletion of fibrinogen levels. Additional activation sites using *H. hypanle* venom were also investigated however only negative results were obtained and so it remains a mystery as to the coagulation mechanism of *H. hypnale* venom.

9.2.2 Anticoagulation

As shown throughout this thesis, there are multiple ways to cause an anticoagulant effect. The main site of action for species investigated was fibrinogen. By disrupting fibrinogen either via destructive cleavage of fibrinogen so that no fibrin clot is formed, or via irregular cleavage of fibrinogen so that weak, transient clots are formed resulting in a pseudo-procoagulant effect (due to their inherent instability), depletion of available fibrinogen can be achieved resulting in an overall net anticoagulant effect. Effects on fibrinogen as a mode of action is evident across the entire Asian pit viper clade, and supports clinical manifestations and presentations of hemorrhaging. Surprisingly, a pseudo-procoagulant mode of action was more common than direct anticoagulant effects, as exhibited by species *Gloydius brevicaudus*, *G. saxatilis*, *G. ussuriensis*, *Protobothrops flavoviridis*, *P. mucrosquamatus* and *P. tokarensis*. All of these species acted directly as anticoagulant venoms by effecting FXa inhibition in some capacity, whether potently or moderately, however destructive cleavage of fibrinogen was the main site of action. On the other hand, pseudo procoagulation dominated the remainder of the species within the Asian pit viper clade with varying effects on time-to-clot and strength of clot. Some species exhibited procoagulant tendencies such as *Gloydius tsushimaensis*, *Ovophis okinavensis*, *Protobothrops jerdonii*, *P. mangshanensis*, *Trimeresurus albolabris* and *T. borneensis*, which all exhibited quick clotting times on plasma and fibrinogen (with varying degrees of co factor dependency). However, with further investigation into clot strength via

thromboelastography, the true nature of clots produced by these venoms could be determined as pseudo-procoagulant. In addition to these species (as well as others), the toxins which contribute to this effect differ and belong to either a venom dominated by metalloproteases or serine proteases. This in itself, along with mode of action, depicts the extreme diversification that is Asian pit viper venom, and the rapid radiation that has occurred since their divergence.

9.2.3 Other toxins

Not all species investigated within this thesis exhibited coagulotoxic affects. Members of the basal clade (Chapter 4), including *Azemiops feae*, *Tropidolaemus subannulatus* and *T. wagleri*, either had no effect on coagulation or only limited response to coagulation investigations. Thromboelastography studies illustrated that only *T. wagleri* displayed action upon fibrinogen, albeit only a moderate level resulting in a pseudo-procoagulant activity, while *T. subannulatus* (sister species) did not display such activity. *Azemiops feae* also did not display any coagulotoxic action. Both *Azemiops* and *Tropidolaemus* are known to have venom which contains novel neurotoxic peptides rather than the larger enzymes typical of viperid venoms (Schmidt and Weinstein, 1995; Shelukhina et al., 2018; Tan et al., 2017b), which is consistent with these findings. As shown in Chapter 8, the neurotoxic peptides emerged in the venoms from *de novo* evolution of novel bioactive peptides in the propeptide-region of the venom forms of C-type natriuretic peptides (Brust et al., 2013; Debono et al., 2017b). However, as these genera are not sister and occupy very different ecological niches (semi-fossorial for *Azemiopis* and arboreal for *Tropidolaemus*), selection pressures for the molecular evolution of the peptides differ. These findings again point to the extreme diversification within Asian pit viper venom, and the need for thorough investigation into these amazing venoms.

9.2.4 Therapeutic applications

While our knowledge of venom evolution and venom composition increases, so does the avenues for novel therapeutic applications from these aforementioned venoms. The diversification within one genus, let alone a whole clade of venoms, highlights the importance of such research to improve current treatments available, improve antivenom cross neutralization and open doors for novel drug design for blood clotting disorders. Harnessing such naturally diverse modes of action upon the coagulation cascade can facilitate much improved drug design and application. For example, designing diagnostic applications utilizing the Group A Prothrombin activating PIII-SVMPs of *T. mossambicanus*, or preventative stroke medications based off the selective fibrinogen chain degradation of a multitude of species similar to that of *Calloselasma rhodostoma* (namely ‘Arvin’), or the FX procoagulant effects of *Calloselasma rhodostoma* for use in surgery are all potential therapeutic avenues. ‘Venoms to drugs’ is not a newly coined term, and has been the subject of much

investigation for the past 50+ years. However, as our understanding of the human body and the diseases that come with it increases, our need for more naturally derived products to combat such disorders rises. And so, venom and its use in therapeutic applications is now more important than ever, and the treasure trove that is venom is endless.

9.3 Future directions

The chapters in this thesis provide a comparative insight into a range of coagulotoxic venoms and modes of actions behind such a diverse group of snakes. However, it also introduces a large number of unanswered questions and ideas for future studies. Research into these venoms and their coagulotoxicity reveals areas of further investigation, especially into antivenom cross-neutralization and production. Many venoms within this thesis lack available antivenom, and in many cases the only available antivenom poorly neutralizes the venom in question (for example *Thelotornis mossambicanus* by the Boomslang antivenom, or *Trimeresurus hageni* by the Green pit viper antivenom). Ideally, every venom would have its own antivenom, however this is not feasible due to production issues and costs associated with production. In addition, access to proper medical facilitates is not always easy once envenomated, as well as access to proper education around what to do if bitten. Many of the species investigated within this thesis occupy habitats close to or within human populations, and in the some of the world's poorest communities. If bitten, victims are burdened with the decisions to either 'A', travel to the hospital and possibly receive some sort of antivenom which then will cost the family their annual salary, or 'B', succumb to less than acceptable unproven and not clinically validated 'medical' practices. If the victim survives, they are usually almost always left with permanent, debilitating disabilities, a huge debt and loss of lively hood due to their inability to work. Future directions into either more affordable antivenom, better neutralizing antivenom or snake bite education surrounding these venomous species could lead to some surprising results.

In addition to this, future directions could also be aimed at supplementary anticoagulant investigation into species such as *Hypnale Hypnale*, exploring both FIX and FXI as possible sites of action. Furthermore, directions should also be aimed at specific toxin investigations behind the modes of action and coagulotoxic mechanisms, which would open up therapeutic application specificities. And finally, investigating additional species of *Trimeresurus* and *Gloydius*, as well as their geographical range, for a more robust conclusion surrounding venom shift within a species.

9.4 Conclusion

Coagulation and coagulotoxins are extremely diverse in both type and mode of action. Coagulotoxins can affect any part of the coagulation cascade, and these sites of action can differ widely depending on the type of toxin, be it serine protease or metalloprotease, and the synergistic effects associated

with it. This thesis provides a broad outlook at coagulation effects from two distinct families of venomous snake, Colubridae and Viperidae, each with limited research having been conducted prior to this investigation. This thesis also provides the first in depth investigation into *Thelotornis mossambicanus* and the mechanisms behind its procoagulant venom, as well as the first in depth investigation into the entire clade of Asian pit vipers and their diverse modes of action. This thesis highlights the rapid and extreme venom evolution that has taken place within both families and the results of such selection pressures on their venom. These results also highlight the diversification of venom and substantial variation that exists between sister genera, which can provide valuable information about clinical effects as well as antivenom neutralization. The findings of this thesis provide an important stepping stone in increasing our knowledge of the pathological relationship between venom and the human coagulation cascade, as well as the diversity of components and characteristics which enable venom research to be such a biodiscovery treasure trove in the boundless diversity that exists, providing a firm foundation on which future research can be established.

References

Ainsworth, S., Slagboom, J., Alomran, N., Pla, D., Alhamdi, Y., King, S.I., Bolton, F.M., Gutiérrez, J.M., Vonk, F.J., Toh, C.-H., Calvete, J.J., Kool, J., Robert, H.A., Casewell, N.R., 2018. The paraspecific neutralisation of snake venom induced coagulopathy by antivenoms. Communications Biology 1, 34.

Aird, S.D., Watanabe, Y., Villar-Briones, A., Roy, M.C., Terada, K., Mikheyev, A.S., 2013. Quantitative high-throughput profiling of snake venom gland transcriptomes and proteomes (*Ovophis okinavensis* and *Protobothrops flavoviridis*). BMC Genomics 14, 790.

Al-Horani, R.A., Karuturi, R., Lee, M., Afosah, D.K., Desai, U.R., 2016. Allosteric inhibition of factor XIIIa. Non-saccharide glycosaminoglycan mimetics, but not glycosaminoglycans, exhibit promising inhibition profile. PLoS ONE 11, e0160189.

Alencar, L.R., Martins, M., Greene, H.W., 2018. Evolutionary history of vipers. eLS, 1-10.

Alencar, L.R., Quental, T.B., Grazziotin, F.G., Alfaro, M.L., Martins, M., Venzon, M., Zaher, H., 2016. Diversification in vipers: Phylogenetic relationships, time of divergence and shifts in speciation rates. Mol Phylogenet Evol 105, 50-62.

Ali, S.A., Baumann, K., Jackson, T.N., Wood, K., Mason, S., Undheim, E.A., Nouwens, A., Koludarov, I., Hendrikx, I., Jones, A., Fry, B., 2013a. Proteomic comparison of *Hypnale hypnale* (hump-nosed pit-viper) and *Calloselasma rhodostoma* (Malayan pit-viper) venoms. J. Proteomics 91, 338-343.

Ali, S.A., Yang, D.C., Jackson, T.N., Undheim, E.A., Koludarov, I., Wood, K., Jones, A., Hodgson, W.C., McCarthy, S., Ruder, T., Fry, B.G., 2013b. Venom proteomic characterization and relative antivenom neutralization of two medically important Pakistani elapid snakes (*Bungarus sindanus* and *Naja naja*). J. Proteomics 89, 15-23.

Alirol, E., Sharma, S.K., Bawaskar, H.S., Kuch, U., Chappuis, F., 2010. Snake bite in South Asia: a review. PLoS Negl. Trop. Dis. 4, e603.

Altschul, S.F., Gish, W., Miller, W., Myers, E.W., Lipman, D.J., 1990. Basic local alignment search tool. J Mol Biol 215, 403-410.

Altschul, S.F., Madden, T.L., Schäffer, A.A., Zhang, J., Zhang, Z., Miller, W., Lipman, D.J., 1997. Gapped BLAST and PSI-BLAST: A new generation of protein database search programs. Nucleic Acids Res 25, 3389-3402.

Aman, J.W., Imperial, J.S., Ueberheide, B., Zhang, M.-M., Aguilar, M., Taylor, D., Watkins, M., Yoshikami, D., Showers-Corneli, P., Safavi-Hemami, H., 2015. Insights into the origins of fish hunting in venomous cone snails from studies of *Conus tessulatus*. Proceedings of the National Academy of Sciences 112, 5087-5092.

Andrade-Silva, D., Zelanis, A., Kitano, E.S., Junqueira-de-Azevedo, I.c., Reis, M.S., Lopes, A.S., Serrano, S.M., 2016. Proteomic and glycoproteomic profilings reveal that post-translational modifications of toxins contribute to venom phenotype in snakes. J. Proteome Res. 15, 2658-2675.

Andrews, R.K., Gardiner, E.E., Asazuma, N., Berlanga, O., Tulasne, D., Nieswandt, B., Smith, A.I., Berndt, M.C., Watson, S.P., 2001. A novel viper venom metalloproteinase, alborhagin, is an agonist at the platelet collagen receptor GPVI. J Biol Chem 276, 28092-28097.

Ariaratnam, C., Thuraisingam, V., Kularatne, S., Sheriff, M., Theakston, R.D.G., De Silva, A., Warrell, D., 2008. Frequent and potentially fatal envenoming by hump-nosed pit vipers (*Hypnale hypnale* and *H. nepa*) in Sri Lanka: Lack of effective antivenom. Trans R Soc Trop Med Hyg 102, 1120-1126.

Arlinghaus, F.T., Fry, B.G., Sunagar, K., Jackson, T.N.W., Eble, J.A., Reeks, T., Clemetson, K.J., 2015. Lectin proteins, In: Fry, B.G. (Ed.), Venomous reptiles and their toxins: evolution, pathophysiology and biodiscovery. Oxford University Press, New York, pp. 299-311.

Assafim, M., Frattani, F.S., Ferreira, M.S., Silva, D.M., Monteiro, R.Q., Zingali, R.B., 2016. Exploiting the antithrombotic effect of the (pro) thrombin inhibitor bothrojaracin. Toxicon 119, 46-51.

Atkinson, P., Bradlow, B., White, J., Greig, H., Gaillard, M., 1980. Clinical features of twig snake (*Thelotornis capensis*) envenomation. S Afr Med J 58, 1007-1011.

Atoda, H., Ishikawa, M., Yoshihara, E., Sekiya, F., Morita, T., 1995. Blood coagulation factor IX-binding protein from the venom of *Trimeresurus flavoviridis*: Purification and characterization. The Journal of Biochemistry 118, 965-973.

Bagoly, Z., Koncz, Z., Hársfalvi, J., Muszbek, L., 2012. Factor XIII, clot structure, thrombosis. Thromb. Res. 129, 382-387.

Bakker, H.M., Tans, G., Yukelson, L.Y., Janssen-Claessen, T.W., Bertina, R.M., Hemker, H.C., Rosing, J., 1993. Protein C activation by an activator purified from the venom of *Agkistrodon halys halys*. Blood Coagul. Fibrinolysis 4, 605-614.

Balaev, A., Okhmanovich, K., Osipov, V., 2014. A shortened, protecting group free, synthesis of the anti-wrinkle venom analogue Syn-Ake® exploiting an optimized Hofmann-type rearrangement. Tetrahedron Lett 55, 5745-5747.

Bell, W.R., 1997. Defibrinogenating enzymes. Drugs 54, 18-31.

Bernardoni, J.L., Sousa, L.F., Wermelinger, L.S., Lopes, A.S., Prezoto, B.C., Serrano, S.M., Zingali, R.B., Moura-da-Silva, A.M., 2014. Functional variability of snake venom metalloproteinases: adaptive advantages in targeting different prey and implications for human envenomation. PLoS ONE 9, e109651.

Bos, M.H., Camire, R.M., 2010. Procoagulant adaptation of a blood coagulation prothrombinase-like enzyme complex in Australian elapid venom. Toxins 2, 1554-1567.

Bos, M.H., van't Veer, C., Reitsma, P.H., 2016. Molecular biology and biochemistry of the coagulation factors and pathways of hemostasis, Williams Hematology, 9 ed. McGraw-Hill, New York.

Bradlow, B., Atkinson, P., Gomperts, E., Gaillard, M., 1980. Studies on the coagulant effects of boomslang (*Dispholidus typus*) venom. Clin. Lab. Haematol. 2, 317-331.

Brust, A., Sunagar, K., Undheim, E.A., Vetter, I., Yang, D.C., Casewell, N.R., Jackson, T.N., Koludarov, I., Alewood, P.F., Hodgson, W.C., 2013. Differential evolution and neofunctionalization of snake venom metalloprotease domains. Mol. Cell. Proteomics 12, 651-663.

Calvete, J.J., Schaefer, W., Soszka, T., Lu, W., Cook, J., Jameson, B.A., Niewiarowski, S., 1991. Identification of the disulfide bond pattern in albolabrin, an RGD-containing peptide from the venon of *Trimeresurus albolabris*: Significance for the express of platelet aggregation inhibitory activity. Biochemistry 30, 5225-5229.

Cascardi, J., Young, B.A., Husic, H.D., Sherma, J., 1999. Protein variation in the venom spat by the red spitting cobra, *Naja pallida* (Reptilia: Serpentes). Toxicon 37, 1271-1279.

Casewell, N.R., Sunagar, K., Takacs, Z., Calvete, J.J., Jackson, T.N.W., Fry, B.G., 2015. Snake Venom Metalloprotease Enzymes, Venomous Reptiles and their toxins. Oxford University Press, New York.

Casewell, N.R., Wüster, W., Vonk, F.J., Harrison, R.A., Fry, B.G., 2013. Complex cocktails: the evolutionary novelty of venoms. Trends Ecol Evol 28, 219-229.

Cesarman-Maus, G., Hajjar, K.A., 2005. Molecular mechanisms of fibrinolysis. Br J Haematol 129, 307-321.

Chan, T., Chan, J., Tomlinson, B., Critchley, J., 1993. Clinical features and hospital management of bites by the white-lipped green pit viper (*Trimeresurus albolabris*). The Southeast Asian Journal of Tropical Medicine and Public Health 24, 772-775.

Chapman, D.S., 1968. Treatment of bites of snakes of Africa, In: Bucherl, W., Buckley, E.E., Deulofeu, V. (Eds.), Venomous Animals and Their Venoms: Venomous Vertebrates. Academic Press Inc., New York, pp. 463-527.

Chen, H.S., Chen, J.M., Lin, C.W., Khoo, K.H., Tsai, I.H., 2008. New insights into the functions and N-glycan structures of factor X activator from Russell's viper venom. The FEBS Journal 275, 3944-3958.

Chen, Y.W., Chen, M.H., Chen, Y.C., Hung, D.Z., Chen, C.K., Yen, D.H.T., Huang, C.I., Lee, C.H., Wang, L.M., Yang, C.C., 2009. Differences in clinical profiles of patients with *Protobothrops mucrosquamatus* and *Viridovipera stejnegeri* envenoming in Taiwan. The American journal of Tropical Medicine and Hygiene 80, 28-32.

Cheng, A.-c., Tsai, I.-h., 2014. Functional characterization of a slow and tight-binding inhibitor of plasmin isolated from Russell's viper venom. Biochimica et Biophysica Acta (BBA)-General Subjects 1840, 153-159.

Cheng, C.-l., Mao, Y.-c., Liu, P.-y., Chiang, L.-c., Liao, S.-c., Yang, C.-c., 2017. *Deinagkistrodon acutus* envenomation: A report of three cases. Journal of Venomous Animals and Toxins Tncluding Tropical Diseases 23, 20.

Chester, A., Crawford, G., 1982. In vitro coagulant properties of venoms from Australian snakes. Toxicon 20, 501-504.

Chippaux, J.P., 1998. Snake-bites: appraisal of the global situation. Bull W H O 76, 515.

Cho, S.Y., Hahn, B.-S., Yang, K.Y., Kim, Y.S., 2001. Purification and characterization of calobin II, a second type of thrombin-like enzyme from *Agkistrodon caliginosus* (Korean viper). Toxicon 39, 499-506.

Choi, S.-h., Lee, S.-b., 2013. Isolation from *Gloydius blomhoffii siniticus* venom of a fibrin (ogen) olytic enzyme consisting of two heterogenous polypeptides. Journal of Pharmacopuncture 16, 46.

Chotenimitkhun, R., Rojnuckarin, P., 2008. Systemic antivenom and skin necrosis after Green Pit Viper bites. Clin. Toxicol. 46, 122-125.

Clark, R.F., Davidson, T.M., 1997. Intraarticular envenomation by *Trimeresurus flavomaculatus mcgregori* resulting in joint destruction. Toxicon 35, 837-842.

Cockram, C., Chan, J., Chow, K., 1990. Bites by the white-lipped pit viper (*Trimeresurus albolabris*) and other species in Hong Kong. A survey of 4 years' experience at the Prince of Wales Hospital. The Journal of Tropical Medicine and Hygiene 93, 79-86.

Coimbra, F.C., Dobson, J., Zdenek, C.N., Op den Brouw, B., Hamilton, B., Debono, J., Masci, P., Frank, N., Ge, L., Kwok, H.F., Fry, B.G., 2018. Does size matter? Venom proteomic and functional comparison between night adder species (Viperidae: *Causus*) with short and long venom glands. Comparative Biochemistry and Physiology Part C: Toxicology & Pharmacology 211, 7-14.

Collet, J., Park, D., Lesty, C., Soria, J., Soria, C., Montalescot, G., Weisel, J., 2000. Influence of fibrin network conformation and fibrin fiber diameter on fibrinolysis speed. Atertio. Thromb. Vasc. Biol. 20, 1354-1361.

Daltry, J.C., Ponnudurai, G., Shin, C.K., Tan, N.-h., Thorpe, R.S., Wolfgang, W., 1996a. Electrophoretic profiles and biological activities: intraspecific variation in the venom of the Malayan pit viper (*Calloselasma rhodostoma*). Toxicon 34, 67-79.

Daltry, J.C., Wuster, W., Thorpe, R.S., 1996b. Diet and snake venom evolution. Nature 379, 537.

Dambisya, Y.M., Lee, T.-L., Gopalakrishnakone, P., 1994. Action of *Calloselasma rhodostoma* (Malayan pit viper) venom on human blood coagulation and fibrinolysis using computerized thromboelastography (CTEG). Toxicon 32, 1619-1626.

de Silva, A., Wijekoon, A., Jayasena, L., Abeysekera, C., Bao, C.-X., Button, R., Warrell, D., 1994. Haemostatic dysfunction and acute renal failure following envenoming by Merrem's hump-nosed viper (*Hypnale hypnale*) in Sri Lanka: first authenticated case. Trans R Soc Trop Med Hyg 88, 209-212.

Debono, J., Bos, M.H., Coimbra, F., Ge, L., Frank, N., Kwok, H.F., Fry, B., 2019a. Basal but divergent: Clinical implications of differential coagulotoxicity in a clade of Asian vipers. Toxicol In Vitro 58, 195-206.

Debono, J., Bos, M.H., Do, M.S., Fry, B., 2019b. Clinical implications of coagulotoxic variations in Mamushi (Viperidae: *Gloydius*) snake venoms. Comparative Biochemistry and Physiology Part C: Toxicology & Pharmacology 225, 108567.

Debono, J., Bos, M.H., Nouwens, A., Ge, L., Frank, N., Kwok, H.F., Fry, B.G., 2019c. Habu coagulotoxicity: Clinical implications of the functional diversification of *Protobothrops* snake venoms upon blood clotting factors. Toxicol In Vitro 55, 62-74.

Debono, J., Cochran, C., Kuruppu, S., Nouwens, A., Rajapakse, N.W., Kawasaki, M., Wood, K., Dobson, J., Baumann, K., Jouiaei, M., Jackson, T.N., Koludarov, I., Low, D., Ali, S.A., Smith, A.I., Barnes, A., Fry, B.G., 2016. Canopy venom: proteomic comparison among new world arboreal pit-viper venoms. Toxins 8, 210.

Debono, J., Dobson, J., Casewell, N.R., Romilio, A., Li, B., Kurniawan, N., Mardon, K., Weisbecker, V., Nouwens, A., Kwok, H.F., Fry, B.G., 2017a. Coagulating Colubrids: Evolutionary, pathophysiological and biodiscovery implications of venom variations between Boomslang (*Dispholidus typus*) and Twig Snake (*Thelotornis mossambicanus*). Toxins 9, 171.

Debono, J., Xie, B., Violette, A., Fourmy, R., Jaeger, M., Fry, B.G., 2017b. Viper venom botox: The molecular origin and evolution of the waglerin peptides used in anti-wrinkle skin cream. J Mol Evol 84, 8-11.

Deufel, A., Cundall, D., 2003. Feeding in *Atractaspis* (Serpentes: Atractaspididae): a study in conflicting functional constraints. Zoology 106, 43-61.

Dharmaratne, L., Gunawardena, U., 1988. Generalised bleeding tendency and acute renal ailure following Merrem's hump-nosed viper bite. J. Ceylon. Coll. Physns. 21, 37-42.

Dobson, J., Yang, D.C., Op den Brouw, B., Cochran, C., Huynh, T., Kurrupu, S., Sánchez, E.E., Massey, D.J., Baumann, K., Jackson, T.N., Nouwens, A., Josh, P., Neri-Castro, E., Alagón, A., Hodgson, W.C., Fry, B.G., 2018. Rattling the border wall: Pathophysiological implications of functional and proteomic venom variation between Mexican and US subspecies of the desert rattlesnake *Crotalus scutulatus*. Comparative Biochemistry and Physiology Part C: Toxicology & Pharmacology 205, 62-69.

Dowell, N.L., Giorgianni, M.W., Kassner, V.A., Selegue, J.E., Sanchez, E.E., Carroll, S.B., 2016. The deep origin and recent loss of venom toxin genes in rattlesnakes. Curr Biol 26, 2434-2445.

Du Toit, D., 1980. Boomslang (*Dispholidus typus*) bite. A case report and a review of diagnosis and management. SAMJ 57, 507-510.

Dutertre, S., Jin, A.-H., Vetter, I., Hamilton, B., Sunagar, K., Lavergne, V., Dutertre, V., Fry, B.G., Antunes, A., Venter, D.J., 2014. Evolution of separate predation-and defence-evoked venoms in carnivorous cone snails. Nature Comms 5.

Edgar, R.C., 2004. MUSCLE: multiple sequence alignment with high accuracy and high throughput. Nucleic Acids Res 32, 1792-1797.

Eng, W.S., Fry, B.G., Sunagar, K., Takacs, Z., Jackson, T.N.W., Guddat, L.W., 2015. Kunitz Peptides, In: Fry, B.G. (Ed.), In Venomous Reptiles and Their Toxins: Evolution, Pathophysiology and Biodiscovery. Oxford University Press, New York, NY, USA, pp. 281–290.

Esmon, C.T., Vigano-D'Angelo, S., D'Angelo, A., 1987. Anticoagulation proteins C and S, The New Dimensions of Warfarin Prophylaxis. Springer, pp. 47-54.

Esnouf, M., Tunnah, G., 1967. The isolation and properties of the thrombin-like activity from *Agkistrodon rhodostoma* venom. Br J Haematol 13, 581-590.

FitzSimons, F.W., 1909a. On the toxic action of the bite of the Boomslang or South-African tree-snake (*Dispholidus typus*). J Nat Hist 3, 271-278.

FitzSimons, F.W., 1909b. XXXIV.—On the toxic action of the bite of the Boomslang or South-African tree-snake (*Dispholidus typus*). J Nat Hist 3, 271-278.

FitzSimons, F.W., 1919. The Snakes of South Africa: Their Venom and the Treatment of Snake Bite. TM Miller, Cape Town, South Africa.

FitzSimons, V.F.M., 1962. Snakes of Southern Africa. Purnell, Cape Town.

Fry, B.G., 2005. From genome to "venome": Molecular origin and evolution of the snake venom proteome inferred from phylogenetic analysis of toxin sequences and related body proteins. Genome Res. 15, 403-420.

Fry, B.G., 2015. Venomous reptiles and their toxins: evolution, pathophysiology and biodiscovery. Oxford University Press, New York, NY, USA.

Fry, B.G., 2018. Snakebite: when the human touch becomes a bad touch. Toxins 10, 170.

Fry, B.G., Jackson, T.N.W., Takacs, Z., Reeks, T., Sunagar, K., 2015a. C-Type Natriuretic Peptides, In: Fry, B.G. (Ed.), Venomous Reptiles and Their Toxins: Evolution, Pathophysiology and Biodiscovery. Oxford University Press, New York, NY, USA, pp. 318–326.

Fry, B.G., Richards, R., Earl, S., Cousin, X., Jackson, T.N., Weise, C., Sunagar, K., 2015b. Lesser-known or putative reptile toxins, In: Fry, B.G. (Ed.), Venomous Reptiles & Their Toxins: Evolution, Pathophysiology and Biodiscovery. Oxford University Press, New York, NY, USA, pp. 364-407.

Fry, B.G., Roelants, K., Champagne, D.E., Scheib, H., Tyndall, J.D., King, G.F., Nevalainen, T.J., Norman, J.A., Lewis, R.J., Norton, R.S., 2009a. The toxicogenomic multiverse: Convergent recruitment of proteins into animal venoms. Annual Review of Genomics and Human Genetics 10, 483-511.

Fry, B.G., Scheib, H., de Azevedo, I.d.L.J., Silva, D.A., Casewell, N.R., 2012. Novel transcripts in the maxillary venom glands of advanced snakes. Toxicon 59, 696-708.

Fry, B.G., Scheib, H., van der Weerd, L., Young, B., McNaughtan, J., Ramjan, S.F., Vidal, N., Poelmann, R.E., Norman, J.A., 2008. Evolution of an arsenal: structural and functional diversification of the venom system in the advanced snakes (Caenophidia). Mol. Cell. Proteomics 7, 215-246.

Fry, B.G., Sunagar, K., Casewell, N.R., Kochva, E., Roelants, K., Scheib, H., Wüster, W., Vidal, N., Young, B., Burbrink, F., 2015c. The origin and evolution of the Toxicofera reptile venom system, In: Fry, B.G. (Ed.), Venomous Reptiles and Their Toxins: Evolution, Pathophysiology and Biodiscovery. Oxford Univeristy Press, New York, NY, USA, pp. 1-32.

Fry, B.G., Sunagar, K., Jackson, T.N.W., Reeks, T., Kwok, H.F., 2015d. B-type natriuretic peptides, In: BG, F. (Ed.), Venomous reptiles and their toxins: evolution, pathophysiology and biodiscovery. Oxford University Press, New York.

Fry, B.G., Undheim, E.A., Ali, S.A., Jackson, T.N., Debono, J., Scheib, H., Ruder, T., Morgenstern, D., Cadwallader, L., Whitehead, D., Nabuurs, R., van der Weerd, L., Vidal, N., Roelants, K., Hendrikx, I., Pineda Gonzalez, S., Koludarov, I., Jones, A., King, G.F., Antunes, A., Sunagar, K., 2013. Squeezers and leaf-cutters: Differential diversification and degeneration of the venom system in toxicoferan reptiles. Mol. Cell. Proteomics 12, 1881-1899.

Fry, B.G., Vidal, N., Van der Weerd, L., Kochva, E., Renjifo, C., 2009b. Evolution and diversification of the Toxicofera reptile venom system. J. Proteomics 72, 127-136.

Fry, B.G., Wickramaratana, J.C., Lemme, S., Beuve, A., Garbers, D., Hodgson, W.C., Alewood, P., 2005. Novel natriuretic peptides from the venom of the inland taipan (*Oxyuranus microlepidotus*): Isolation, chemical and biological characterisation. Biochem Biophys Res Commun 327, 1011-1015.

Fry, B.G., Winkel, K.D., Wickramaratna, J.C., Hodgson, W.C., Wüster, W., 2003a. Effectiveness of snake antivenom: Species and regional venom variation and its clinical impact. J. Toxicol.: Toxin Rev. 22, 23-34.

Fry, B.G., Wüster, W., 2004. Assembling an arsenal: Origin and evolution of the snake venom proteome inferred from phylogenetic analysis of toxin sequences. Mol Biol Evol 21, 870-883.

Fry, B.G., Wüster, W., Ramjan, R., Fadil, S., Jackson, T., Martelli, P., Kini, R.M., 2003b. Analysis of Colubroidea snake venoms by liquid chromatography with mass spectrometry: Evolutionary and toxinological implications. Rapid Commun. Mass Spectrom. 17, 2047-2062.

Fu, L., Niu, B., Zhu, Z., Wu, S., Li, W., 2012. CD-HIT: Accelerated for clustering the next-generation sequencing data. Bioinformatics 28, 3150-3152.

Fujisawa, D., Yamazaki, Y., Morita, T., 2009. Re-evaluation of M-LAO, l-amino acid oxidase, from the venom of *Gloydius blomhoffi* as an anticoagulant protein. J. Biochem. 146, 43-49.

Gan, Z., Gould, R., Jacobs, J., Friedman, P., Polokoff, M., 1988. Echistatin. A potent platelet aggregation inhibitor from the venom of the viper, *Echis carinatus*. J Biol Chem 263, 19827-19832.

Gao, J.-F., Qu, Y.-F., Zhang, X.-Q., He, Y., Ji, X., 2013. Neonate-to-adult transition of snake venomics in the short-tailed pit viper, *Gloydius brevicaudus*. J. Proteomics 84, 148-157.

Gould, R.J., Polokoff, M.A., Friedman, P.A., Huang, T.-F., Holt, J.C., Cook, J.J., Niewiarowski, S., 1990. Disintegrins: A family of integrin inhibitory proteins from viper venoms. Exp. Biol. Med. 195, 168-171.

Grabherr, M.G., Haas, B.J., Yassour, M., Levin, J.Z., Thompson, D.A., Amit, I., Adiconis, X., Fan, L., Raychowdhury, R., Zeng, Q., 2011. Full-length transcriptome assembly from RNA-Seq data without a reference genome. Nat. Biotechnol. 29, 644.

Gracheva, E.O., Ingolia, N.T., Kelly, Y.M., Cordero-Morales, J.F., Hollopeter, G., Chesler, A.T., Sánchez, E.E., Perez, J.C., Weissman, J.S., Julius, D., 2010. Molecular basis of infrared detection by snakes. Nature 464, 1006-1011.

Grasset, E., Schaafsma, A., 1940. Studies on the Venom of the "Boom-slang" (*Dispholidus typus*). S Afr Med J 14, 236-241.

Greene, S., Galdamez, L.A., Tomasheski, R., 2017. White-lipped tree viper (*Cryptelytrops albolabris*) envenomation in an American viper keeper. The Journal of Emergency Medicine 53, e115-e118.

Guillin, M.-C., Bezeaud, A., Menache, D., 1978. The mechanism of activation of human prothrombin by an activator isolated from *Dispholidus typus* venom. Biochimica et Biophysica Acta (BBA)-Protein Structure and Moelcular Enzymology 537, 160-168.

Gutiérrez, J.M., Calvete, J.J., Habib, A.G., Harrison, R.A., Williams, D.J., Warrell, D.A., 2017. Snakebite envenoming. Nature Reviews Disease Primers 3, 17063.

Gutiérrez, J.M., Theakston, R.D.G., Warrell, D.A., 2006. Confronting the neglected problem of snake bite envenoming: the need for a global partnership. PLoS Med. 3, e150.

Haas, B.J., Papanicolaou, A., Yassour, M., Grabherr, M., Blood, P.D., Bowden, J., Couger, M.B., Eccles, D., Li, B., Lieber, M., 2013. *De novo* transcript sequence reconstruction from RNA-seq using the Trinity platform for reference generation and analysis. Nat. Protoc. 8, 1494.

Harvey, A., Anderson, A., 1985. Dendrotoxins: snake toxins that block potassium channels and facilitate neurotransmitter release. Pharmacol. Ther. 31, 33-55.

Harvey, A., Karlsson, E., 1980. Dendrotoxin from the venom of the green mamba, *Dendroaspis angusticeps*. Naunyn-Schmiedeberg's Archives of Pharmacology 312, 1-6.

Hayes, W.K., Herbert, S.S., Harrison, J.R., Wiley, K.L., 2008. Spitting versus biting: Differential venom gland contraction regulates venom expenditure in the black-necked spitting cobra, *Naja nigricollis nigricollis*. J Herpetol 42, 453-460.

Heil, A., Weber, J., Büchold, C., Pasternack, R., Hils, M., 2013. Differences in the inhibition of coagulation factor XIII-A from animal species revealed by Michael Acceptor–and thioimidazol based blockers. Thromb. Res. 131, e214-e222.

Herath, N., Wazil, A., Kularatne, S., Ratnatunga, N., Weerakoon, K., Badurdeen, S., Rajakrishna, P., Nanayakkara, N., Dharmagunawardane, D., 2012. Thrombotic microangiopathy and acute kidney injury in hump-nosed viper (*Hypnale* species) envenoming: A descriptive study in Sri Lanka. Toxicon 60, 61-65.

Herrera, M., Fernández, J., Vargas, M., Villalta, M., Segura, Á., León, G., Angulo, Y., Paiva, O., Matainaho, T., Jensen, S.D., 2012. Comparative proteomic analysis of the venom of the taipan snake, *Oxyuranus scutellatus*, from Papua New Guinea and Australia: Role of neurotoxic and procoagulant effects in venom toxicity. J. Proteomics 75, 2128-2140.

Hiestand, P.C., Hiestand, R.R., 1979. *Dispholidus typus* (boomslang) snake venom: Purification and properties of the coagulant principle. Toxicon 17, 489-498.

Hifumi, T., Sakai, A., Kondo, Y., Yamamoto, A., Morine, N., Ato, M., Shibayama, K., Umezawa, K., Kiriu, N., Kato, H., 2015. Venomous snake bites: Clinical diagnosis and treatment. Journal of Intensive Care 3, 16.

Hifumi, T., Yamamoto, A., Morokuma, K., Ogasawara, T., Kiriu, N., Hasegawa, E., Inoue, J., Kato, H., Koido, Y., Takahashi, M., 2011. Surveillance of the clinical use of mamushi (*Gloydius blomhoffii*) antivenom in tertiary care centers in Japan. Japan J Infect Dis 64, 373-376.

Ho, M., Warrell, D.A., Looareesuwan, S., Phillips, R.E., Chanthavanich, P., Karbwang, J., Supanaranond, W., Viravan, C., Hutton, R.A., Vejcho, S., 1986. Clinical significance of venom antigen levels in patients envenomed by the Malayan pit viper (*Calloselasma rhodostoma*). The American Journal of Tropical Medicine and Hygiene 35, 579-587.

Huang, K., Zhao, W., Gao, Y., Wei, W., Teng, M., Niu, L., 2011. Structure of saxthrombin, a thrombin-like enzyme from *Gloydius saxatilis*. Acta Crystallographica Section F: Structural Biology and Crystallization Communications 67, 862-865.

Huang, T.-F., Chang, M.-C., Peng, H.-C., Teng, C.-M., 1992. A novel α-type fibrinogenase from *Agkistrodon rhodostoma* snake venom. Biochimica et Biophysica Acta (BBA)-Protein Structure and Molecular Enzymology 1160, 262-268.

Hutton, R., Looareesuwan, S., Ho, M., Silamut, K., Chanthavanich, P., Karbwang, J., Supanaranond, W., Vejcho, S., Viravan, C., Phillips, R., Warrell, D., 1990. Arboreal green pit vipers (genus *Trimeresurus*) of South-East Asia: Bites by *T. albolabris* and *T. macrops* in Thailand and a review of the literature. Trans R Soc Trop Med Hyg 84, 866-874.

Isbister, G.K., 2009. Procoagulant snake toxins: Laboratory studies, diagnosis, and understanding snakebite coagulopathy, Semin. Thromb. Hemost. Thieme Medical Publishers, pp. 093-103.

Isbister, G.K., 2010. Snakebite doesn't cause disseminated intravascular coagulation: coagulopathy and thrombotic microangiopathy in snake envenoming. Semin. Thromb. Hemost. 36, 444-451.

Isbister, G.K., Scorgie, F., O'LEARY, M., Seldon, M., Brown, S.G., Lincz, L., 2010a. Factor deficiencies in venom-induced consumption coagulopathy resulting from Australian elapid envenomation: Australian Snakebite Project (ASP-10). J. Thromb. Haemost. 8, 2504-2513.

Isbister, G.K., Woods, D., Alley, S., O'Leary, M.A., Seldon, M., Lincz, L.F., 2010b. Endogenous thrombin potential as a novel method for the characterization of procoagulant snake venoms and the efficacy of antivenom. Toxicon 56, 75-85.

J. Pinheiro, D.B., S. DebRoy, D. Sarkar, R Core Team, 2016. nlme: Linear and Nonlinear Mixed Effects Models, 3.1-128 ed. R Core Team, Vienna, Austria

Jackson, T.N., Fry, B.G., 2016. A tricky trait: Applying the fruits of the "function debate" in the philosophy of biology to the "venom debate" in the science of toxinology. Toxins 8, 263.

Jackson, T.N., Koludarov, I., Ali, S.A., Dobson, J., Zdenek, C.N., Dashevsky, D., Masci, P.P., Nouwens, A., Josh, P., Goldenberg, J., 2016. Rapid radiations and the race to redundancy: An investigation of the evolution of Australian elapid snake venoms. Toxins 8, 309.

Jackson, T.N., Sunagar, K., Undheim, E.A., Koludarov, I., Chan, A.H., Sanders, K., Ali, S.A., Hendrikx, I., Dunstan, N., Fry, B.G., 2013. Venom down under: Dynamic evolution of Australian elapid snake toxins. Toxins 5, 2621-2655.

Jackson, T.N., Young, B., Underwood, G., McCarthy, C.J., Kochva, E., Vidal, N., van der Weerd, L., Nabuurs, R., Dobson, J., Whitehead, D., Vonk, F.J., Hendrikx, I., Hay, C., Fry, B.G., 2017. Endless forms most beautiful: The evolution of ophidian oral glands, including the venom system, and the use of appropriate terminology for homologous structures. Zoomorphology 136, 107-130.

Jin, A.-H., Israel, M.R., Inserra, M.C., Smith, J.J., Lewis, R.J., Alewood, P.F., Vetter, I., Dutertre, S., 2015. δ-conotoxin SuVIA suggests an evolutionary link between ancestral predator defence and the origin of fish-hunting behaviour in carnivorous cone snails, Proceedings of the Royal Society, Series Biological Sciences. The Royal Society, p. 20150817.

Jin, N.Z., Gopinath, S.C., 2016. Potential blood clotting factors and anticoagulants. Biomed. Pharmacother. 84, 356-365.

Jones, B.K., Saviola, A., Reilly, S.B., Stubbs, A.L., Arida, E., Iskandar, D.T., McGuire, J.A., Yates, J.R., Mackessy, S.P., 2019. Venom composition in a phenotypically variable pit viper

(*Trimeresurus insularis*) across the Lesser Sunda Archipelago. J. Proteome Res. 18, 2206-2220.
Joseph, J., Simpson, I., Menon, N., Jose, M., Kulkarni, K., Raghavendra, G., Warrell, D., 2007. First authenticated cases of life-threatening envenoming by the hump-nosed pit viper (*Hypnale hypnale*) in India. Trans R Soc Trop Med Hyg 101, 85-90.
Joseph, J.S., Kini, R.M., 2002. Snake venom prothrombin activators homologous to blood coagulation factor Xa. Pathophysiol. Haemost. Thromb. 31, 234-240.
Kamiguti, A., Slupsky, J., Zuzel, M., Hay, C., 1994. Properties of fibrinogen cleaved by Jararhagin, a metalloproteinase from the venom of *Bothrops jararaca*. Thromb. Haemost. 72, 244-249.
Kamiguti, A.S., Hay, C.R., Theakston, R.D.G., Zuzel, M., 1996. Insights into the mechanism of haemorrhage caused by snake venom metalloproteinases. Toxicon 34, 627-642.
Kamiguti, A.S., Theakston, R.D.G., Sherman, N., Fox, J.W., 2000. Mass spectrophotometric evidence for P-III/P-IV metalloproteinases in the venom of the Boomslang (*Dispholidus typus*). Toxicon 38, 1613-1620.
Karlsson, E., Mbugua, P., Rodriguez-Ithurralde, D., 1983. Fasciculins, anticholinesterase toxins from the venom of the green mamba *Dendroaspis angusticeps*. J. Physiol. (Paris) 79, 232-240.
Kasturiratne, A., Wickremasinghe, A.R., de Silva, N., Gunawardena, N.K., Pathmeswaran, A., Premaratna, R., Savioli, L., Lalloo, D.G., de Silva, H.J., 2008. The global burden of snakebite: A literature analysis and modelling based on regional estimates of envenoming and deaths. PLoS Med. 5, e218.
Kini, R.M., 2005a. The intriguing world of prothrombin activators from snake venom. Toxicon 45, 1133-1145.
Kini, R.M., 2005b. Serine proteases affecting blood coagulation and fibrinolysis from snake venoms. Pathophysiol. Haemost. Thromb. 34, 200-204.
Kini, R.M., 2006. Anticoagulant proteins from snake venoms: Structure, function and mechanism. Biochem J 397, 377-387.
Kini, R.M., Koh, C.Y., 2016. Metalloproteases affecting blood coagulation, fibrinolysis and platelet aggregation from snake venoms: Definition and nomenclature of interaction sites. Toxins 8, 284.
Kircher, M., Sawyer, S., Meyer, M., 2011. Double indexing overcomes inaccuracies in multiplex sequencing on the Illumina platform. Nucleic Acids Res 40, e3.
Kisiel, W., Kondo, S., Smith, K.J., McMullen, B.A., Smith, L.F., 1987. Characterization of a protein C activator from *Agkistrodon contortrix contortrix* venom. J Biol Chem 262, 12607-12613.
Kogan, A.E., Bashkov, G.V., Bobruskin, I.D., Romanova, E.P., Makarov, V.A., Strukova, S.M., 1993. Protein C activator from the venom of *Agkistrodon blomhoffi ussuriensis* retards thrombus formation in the arterio-venous shunt in rats. Thromb. Res. 70, 385-393.
Koh, C.Y., Kini, R.M., 2012. From snake venom toxins to therapeutics–cardiovascular examples. Toxicon 59, 497-506.
Kolev, K., Longstaff, C., 2016. Bleeding related to disturbed fibrinolysis. Br J Haematol 175, 12-23.
Koludarov, I., Jackson, T.N., Dobson, J., Dashevsky, D., Arbuckle, K., Clemente, C.J., Stockdale, E.J., Cochran, C., Debono, J., Stephens, C., Panagides, N., Li, B., Manchadi, M.-L.R., Violette, A., Fourmy, R., Hendrikx, I., Nouwens, A., Clements, J., Martelli, P., Kwok, H.F., Fry, B.G., 2017. Enter the dragon: The dynamic and multifunctional evolution of Anguimorpha lizard venoms. Toxins 9, 242.
Koludarov, I., Jackson, T.N., Sunagar, K., Nouwens, A., Hendrikx, I., Fry, B.G., 2014. Fossilized venom: The unusually conserved venom profiles of *Heloderma* species (beaded lizards and gila monsters). Toxins 6, 3582-3595.
Kong, C., Chung, M.C., 2001. Purification and characterization of a variant of rhodocetin from *Calloselasma rhodostoma* (Malayan pit viper) venom. J Protein Chem 20, 383-390.
Kornalik, F., Blombäck, B., 1975. Prothrombin activation induced by Ecarin-a prothrombin converting enzyme from *Echis carinatus* venom. Thromb. Res. 6, 53-63.

Krueger, F., 2015. Trim galore!: A wrapper tool around Cutadapt and FastQC to consistently apply quality and adapter trimming to FastQ files, In: Krueger, F. (Ed.). Babraham Bioinformatics, UK.

Kuniyoshi, A.K., Kodama, R.T., Moraes, L.H.F., Duzzi, B., Iwai, L.K., Lima, I.F., Cajado-Carvalho, D., Portaro, F.V., 2017. *In vitro* cleavage of bioactive peptides by peptidases from *Bothrops jararaca* venom and its neutralization by bothropic antivenom produced by Butantan Institute: Major contribution of serine peptidases. Toxicon 137, 114-119.

Larsson, A., 2014. AliView: a fast and lightweight alignment viewer and editor for large datasets. Bioinformatics 30, 3276-3278.

Lechner, M., Findeiß, S., Steiner, L., Marz, M., Stadler, P.F., Prohaska, S.J., 2011. Proteinortho: detection of (co-) orthologs in large-scale analysis. BMC Bioinformatics 12, 124.

Leong, P.K., Tan, C.H., Sim, S.M., Fung, S.Y., Sumana, K., Sitprija, V., Tan, N.H., 2014. Cross neutralization of common Southeast Asian viperid venoms by a Thai polyvalent snake antivenom (Hemato Polyvalent Snake Antivenom). Acta Trop 132, 7-14.

Levy, D.E., Del Zoppo, G.J., 2006. Ancrod: A potential treatment for acute, ischemic stroke from snake venom. Toxin Rev 25, 323-333.

Li, H., 2012. Toolkit for Processing Sequences in FASTA/Q Formats: Lh3/Seqtk. C.

Li, H., Durbin, R., 2009. Fast and accurate short read alignment with Burrows–Wheeler transform. Bioinformatics 25, 1754-1760.

Li, H., Handsaker, B., Wysoker, A., Fennell, T., Ruan, J., Homer, N., Marth, G., Abecasis, G., Durbin, R., 2009. The sequence alignment/map format and SAMtools. Bioinformatics 25, 2078-2079.

Li, M., Fry, B.G., Kini, R.M., 2005. Eggs-only diet: its implications for the toxin profile changes and ecology of the marbled sea snake (*Aipysurus eydouxii*). J Mol Evol 60, 81-89.

Li, W., Godzik, A., 2006. Cd-hit: a fast program for clustering and comparing large sets of protein or nucleotide sequences. Bioinformatics 22, 1658-1659.

Lin, C.-w., Chen, J.-m., Wang, Y.-m., Wu, S.-w., Tsai, I.-h., Khoo, K.-h., 2010. Terminal disialylated multiantennary complex-type N-glycans carried on acutobin define the glycosylation characteristics of the *Deinagkistrodon acutus* venom. Glycobiology 21, 530-542.

Lin, W., Smith, L., Lee, C., 1995. A study on the cause of death due to waglerin-I, a toxin from *Trimeresurus wagleri*. Toxicon 33, 111-114.

Lin, Y., Yu, X., He, Q., Li, H., Li, D., Song, X., Wang, Y., Wen, H., Deng, H., Deng, J., 2009. Expression and functional characterization of chitribrisin, a thrombin-like enzyme, in the venom of the Chinese green pit viper (*Trimeresurus albolabris*). Protein Expression Purif 67, 48-52.

Lister, C., Arbuckle, K., Jackson, T.N., Debono, J., Zdenek, C.N., Dashevsky, D., Dunstan, N., Allen, L., Hay, C., Bush, B., Gillett, A., Fry, B.G., 2017. Catch a tiger snake by its tail: Differential toxicity, co-factor dependence and antivenom efficacy in a procoagulant clade of Australian venomous snakes. Comparative Biochemistry and Physiology Part C: Toxicology & Pharmacology 202, 39-54.

Liu, S., Marder, V.J., Levy, D.E., Wang, S.-J., Yang, F., Paganini-Hill, A., Fisher, M.J., 2011. Ancrod and fibrin formation: Perspectives on mechanisms of action. Stroke 42, 3277-3280.

Longstaff, C., Kolev, K., 2015. Basic mechanisms and regulation of fibrinolysis. J. Thromb. Haemost. 13, 98-105.

Mackman, N., 2009. The role of tissue factor and factor VIIa in hemostasis. Anesth. Analg. 108, 1447.

Madden, T.L., Tatusov, R.L., Zhang, J., 1996. Applications of network BLAST server. Methods Enzymol 266, 131-141.

Maduwage, K., Isbister, G.K., Silva, A., Bowatta, S., Mendis, S., Gawarammana, I., 2013a. Epidemiology and clinical effects of hump-nosed pit viper (Genus: *Hypnale*) envenoming in Sri Lanka. Toxicon 61, 11-15.

Maduwage, K., Scorgie, F., Silva, A., Shahmy, S., Mohamed, F., Abeysinghe, C., Karunathilake, H., Lincz, L., Gnanathasan, C.A., Isbister, G., 2013b. Hump-nosed pit viper (*Hypnale hypnale*)

envenoming causes mild coagulopathy with incomplete clotting factor consumption. Clin. Toxicol. 51, 527-531.
Malhotra, A., Thorpe, R.S., 2004. A phylogeny of four mitochondrial gene regions suggests a revised taxonomy for Asian pitvipers (*Trimeresurus* and *Ovophis*). Mol Phylogenet Evol 32, 83-100.
Mapleson, D., Garcia Accinelli, G., Kettleborough, G., Wright, J., Clavijo, B.J., 2016. KAT: a K-mer analysis toolkit to quality control NGS datasets and genome assemblies. Bioinformatics 33, 574-576.
Marçais, G., Kingsford, C., 2011. A fast, lock-free approach for efficient parallel counting of occurrences of k-mers. Bioinformatics 27, 764-770.
Markland, F.S., 1998. Snake venoms and the hemostatic system. Toxicon 36, 1749-1800.
Marshall, L., Herrmann, R., 1983. Coagulant and anticoagulant actions of Australian snake venoms. Thromb. Haemost. 50, 707-711.
Martin, C., 1893. On some effects upon the blood produced by the injection of the venom of the Australian black snake (*Pseudechis porphyriacus*). J. Physiol. 15, 380.
Masci, P., Whitaker, A., Sparrow, L., De Jersey, J., Winzor, D., Watters, D., Lavin, M., Gaffney, P., 2000. Textilinins from *Pseudonaja textilis textilis*. Characterization of two plasmin inhibitors that reduce bleeding in an animal model. Blood. Coagul. Fibrin. 11, 385-393.
McArdle, J.J., Lentz, T.L., Witzemann, V., Schwarz, H., Weinstein, S.A., Schmidt, J.J., 1999. Waglerin-1 selectively blocks the epsilon form of the muscle nicotinic acetylcholine receptor. J. Pharmacol. Exp. Ther. 289, 543-550.
McCleary, R.J., Kini, R.M., 2013. Snake bites and hemostasis/thrombosis. Thromb. Res. 132, 642-646.
Mebs, D., Kuch, U., Meier, J., 1994. Studies on venom and venom apparatus of Fea's viper, *Azemiops feae*. Toxicon 32, 1275-1278.
Milne, I., Stephen, G., Bayer, M., Cock, P.J., Pritchard, L., Cardle, L., Shaw, P.D., Marshall, D., 2012. Using Tablet for visual exploration of second-generation sequencing data. Brief. Bioinform. 14, 193-202.
Mitrakul, C., 1973. Effects of green pit viper (*Trimeresurus erythrurus* and *Trimeresurus popeorum*) venoms on blood coagulation, platelets and the fibrinolytic enzyme systems: studies *in vivo* and *in vitro*. Am. J. Clin. Pathol. 60, 654-662.
Mosesson, M., 2005. Fibrinogen and fibrin structure and functions. J. Thromb. Haemost. 3, 1894-1904.
Muanpasitporn, C., Rojnuckarin, P., 2007. Expression and characterization of a recombinant fibrinogenolytic serine protease from green pit viper (*Trimeresurus albolabris*) venom. Toxicon 49, 1083-1089.
Mukherjee, A.K., 2008. Characterization of a novel pro-coagulant metalloprotease (RVBCMP) possessing α-fibrinogenase and tissue haemorrhagic activity from venom of *Daboia russelli russelli* (Russell's viper): Evidence of distinct coagulant and haemorrhagic sites in RVBCMP. Toxicon 51, 923-933.
Mukherjee, A.K., 2014. The pro-coagulant fibrinogenolytic serine protease isoenzymes purified from *Daboia russelii russelii* venom coagulate the blood through factor V activation: Role of glycosylation on enzymatic activity. PLoS ONE 9, e86823.
Nakagaki, T., Kazim, A.L., Kisiel, W., 1990. Isolation and characterization of a protein C activator from tropical moccasin venom. Thromb. Res. 58, 593-602.
Navdaev, A., Lochnit, G., Eble, J.A., 2011. The rhodocetin αβ subunit targets GPIb and inhibits von Willebrand factor induced platelet activation. Toxicon 57, 1041-1048.
Nelsen, D.R., Nisani, Z., Cooper, A.M., Fox, G.A., Gren, E.C., Corbit, A.G., Hayes, W.K., 2014. Poisons, toxungens, and venoms: Redefining and classifying toxic biological secretions and the organisms that employ them. Biol. Rev. 89, 450-465.
Nielsen, V.G., 2016a. Ancrod revisited: Viscoelastic analyses of the effects of *Calloselasma rhodostoma* venom on plasma coagulation and fibrinolysis. J. Thromb. Thrombolys. 42, 288-293.

Nielsen, V.G., 2016b. Iron and carbon monoxide prevent degradation of plasmatic coagulation by thrombin-like activity in rattlesnake venom. HET 35, 1116-1122.
Nielsen, V.G., Bazzell, C.M., 2017. Carbon monoxide releasing molecule-2 inhibition of snake venom thrombin-like activity: Novel biochemical "brake"? J. Thromb. Thrombolys. 43, 203-208.
Nielsen, V.G., Frank, N., 2018. Differential heme-mediated modulation of *Deinagkistrodon*, *Dispholidus*, *Protobothrops* and *Pseudonaja* hemotoxic venom activity in human plasma. Biometals, 1-9.
Nielsen, V.G., Frank, N., Matika, R.W., 2018. Carbon monoxide inhibits hemotoxic activity of Elapidae venoms: Potential role of heme. Biometals 31, 51-59.
Nishida, S., Fujita, T., Kohno, N., Atoda, H., Morita, T., Takeya, H., Kido, J.I., 1995. cDNA cloning and deduced amino acid, sequence of prothrombin activator (Ecarin) from Kenyan *Echis carinatus* venom. Biochemistry 34, 1771-1778.
Nishimura, H., Enokida, H., Kawahira, S., Kagara, I., Hayami, H., Nakagawa, M., 2016. Acute kidney injury and rhabdomyolysis after *Protobothrops flavoviridis* bite: a retrospective survey of 86 patients in a tertiary care center. Am. J. Trop. Med. Hyg. 94, 474-479.
Nolan, C., Hall, L., Barlow, G., 1976. Ancrod, the coagulating enzyme from Malayan pit viper (*Agkistrodon rhodostoma*) venom. Method. Enzymol. 45, 205-213.
O'Leary, M.A., Isbister, G.K., 2010. A turbidimetric assay for the measurement of clotting times of procoagulant venoms in plasma. J. Pharmacol. Toxicol. Methods 61, 27-31.
Okamoto, O., Nakashima, R., Yamamoto, S., Hashimoto, T., Takasaki, T., Tokuda, H., Sato, S., Gamachi, A., Hashimoto, H., Inagaki, N., 2017. A lethal case of mamushi (*Gloydius blomhoffii*) bite: severe bowel symptoms as a lethal sign. AMS 4, 135-139.
Oliveira, A.K., Leme, A.F.P., Asega, A.F., Camargo, A.C., Fox, J.W., Serrano, S.M., 2010. New insights into the structural elements involved in the skin haemorrhage induced by snake venom metalloproteinases. Thromb. Haemost. 104, 485-497.
Osman, O., Ismail, M., El-Asmar, M., 1973. Pharmacological studies of snake (*Dendroaspis angusticeps*) venom. Toxicon 11, 185-192.
Oulion, B., Dobson, J.S., Zdenek, C.N., Arbuckle, K., Lister, C., Coimbra, F.C., Op den Brouw, B., Debono, J., Rogalski, A., Violette, A., Fourmy, R., Frank, N., Fry, B.G., 2018. Factor X activating *Atractaspis* snake venoms and the relative coagulotoxicity neutralising efficacy of African antivenoms. Toxicol. Lett. 288, 119-128.
Ouyang, C., Teng, C.-M., 1976. The effects of the purified thrombin-like and anticoagulant principles of *Agkistrodon acutus* venom on blood coagulation *in vivo*. Toxicon 14, 49-54.
Ouyang, C., Teng, C.-M., 1978. In vivo effects of the purified thrombin-like and anticoagulant principles of *Agkistrodon acutus* (Hundred pace snake) venom. Toxicon 16, 583-593.
Paine, M., Desmond, H., Theakston, R., Crampton, J., 1992. Purification, cloning, and molecular characterization of a high molecular weight hemorrhagic metalloprotease, jararhagin, from *Bothrops jararaca* venom. Insights into the disintegrin gene family. J Biol Chem 267, 22869-22876.
Panagides, N., Jackson, T.N., Ikonomopoulou, M.P., Arbuckle, K., Pretzler, R., Yang, D.C., Ali, S.A., Koludarov, I., Dobson, J., Sanker, B., Asselin, A., Santana, R.C., Hendrikx, I., van der Ploeg, H., Tai-A-Pin, J., van den Bergh, R., Kerkkamp, H.M.I., Vonk, F.J., Naude, A., Strydom, M.A., Jacobsz, L., Dunstan, N., Jaeger, M., Hodgson, W.C., Miles, J., Fry, B.G., 2017. How the cobra got its flesh-eating venom: Cytotoxicity as a defensive innovation and its co-evolution with hooding, aposematic marking, and spitting. Toxins 9, 103.
Panzano, V.C., Kang, K., Garrity, P.A., 2010. Infrared snake eyes: TRPA1 and the thermal sensitivity of the snake pit organ. Sci. Signal. 3, 22.
Paradis, E., Claude, J., Strimmer, K., 2004. APE: analyses of phylogenetics and evolution in R language. Bioinformatics 20, 289-290.
Pawlak, J., Mackessy, S.P., Fry, B.G., Bhatia, M., Mourier, G., Fruchart-Gaillard, C., Servent, D., Ménez, R., Stura, E., Ménez, A., 2006. Denmotoxin, a three-finger toxin from the colubrid

snake *Boiga dendrophila* (Mangrove Catsnake) with bird-specific activity. J Biol Chem 281, 29030-29041.

Pawlak, J., Mackessy, S.P., Sixberry, N.M., Stura, E.A., Le Du, M.H., Ménez, R., Foo, C.S., Ménez, A., Nirthanan, S., Kini, R.M., 2009. Irditoxin, a novel covalently linked heterodimeric three-finger toxin with high taxon-specific neurotoxicity. The FASEB Journal 23, 534-545.

Peng, M., Lu, W., Kirby, E.P., 1991. Alboaggregin-B: A new platelet agonist that binds to platelet membrane glycoprotein Ib. Biochemistry 30, 11529-11536.

Peng, M., Lu, W., Kirby, E.P., 1992. Characterization of three alboaggregins purified from *Trimeresurus albolabris* venom. Thromb. Haemost. 68, 702-707.

Pinheiro, J., Bates, D., 2000. Mixed-effects models in S and S-PLUS. Springer Science & Business Media, Verlag, New York.

Pirkle, H., McIntosh, M., Theodor, I., Vernon, S., 1972. Activation of prothrombin with Taipan snake venom. Thromb. Res. 1, 559-567.

Pla, D., Sanz, L., Whiteley, G., Wagstaff, S.C., Harrison, R.A., Casewell, N.R., Calvete, J.J., 2017. What killed Karl Patterson Schmidt? Combined venom gland transcriptomic, venomic and antivenomic analysis of the South African green tree snake (the boomslang), *Dispholidus typus*. Biochim Biophys Acta 1861, 814-823.

Pope, C.H., 1958. Fatal bite of captive African rear-fanged snake (*Dispholidus*). Copeia 1958, 280-282.

Pradniwat, P., Rojnuckarin, P., 2015. The structure–function relationship of thrombin-like enzymes from the green pit viper (*Trimeresurus albolabris*). Toxicon 100, 53-59.

Premawardena, A., Seneviratne, S., Gunatilake, S., De Silva, H., 1998. Excessive fibrinolysis: the coagulopathy following Merrem's hump-nosed viper (*Hypnale hypnale*) bites. The American Journal of Tropical Medicine and Hygiene 58, 821-823.

Resiere, D., Arias, A.S., Villalta, M., Rucavado, A., Brouste, Y., Cabié, A., Névière, R., Césaire, R., Kallel, H., Mégarbane, B., Mehdaoui, H., Gutiérrez, J.M., 2018. Preclinical evaluation of the neutralizing ability of a monospecific antivenom for the treatment of envenomings by *Bothrops lanceolatus* in Martinique. Toxicon 148, 50-55.

Revell, L.J., 2012. phytools: an R package for phylogenetic comparative biology (and other things). Methods Ecol. Evol. 3, 217-223.

Rijken, D., Lijnen, H., 2009. New insights into the molecular mechanisms of the fibrinolytic system. J. Thromb. Haemost. 7, 4-13.

Rogalski, A., Soerensen, C., Op den Brouw, B., Lister, C., Dashevsky, D., Arbuckle, K., Gloria, A., Zdenek, C.N., Casewell, N.R., Gutiérrez, J.M., 2017. Differential procoagulant effects of saw-scaled viper (Serpentes: Viperidae: *Echis*) snake venoms on human plasma and the narrow taxonomic ranges of antivenom efficacies. Toxicol. Lett. 280, 159-170.

Rojnuckarin, P., Banjongkit, S., Chantawibun, W., Akkawat, B., Juntiang, J., Noiphrom, J., Pakmanee, N., Intragumtornchai, T., 2007. Green pit viper (*Trimeresurus albolabris* and *T. macrops*) venom antigenaemia and kinetics in humans. Trop. Doct. 37, 207-210.

Rojnuckarin, P., Intragumtornchai, T., Sattapiboon, R., Muanpasitporn, C., Pakmanee, N., Khow, O., Swasdikul, D., 1999. The effects of green pit viper (*Trimeresurus albolabris* and *Trimeresurus macrops*) venom on the fibrinolytic system in human. Toxicon 37, 743-755.

Rojnuckarin, P., Mahasandana, S., Intragumthornchai, T., Sutcharitchan, P., Swasdikul, D., 1998. Prognostic factors of green pit viper bites. Am. J. Trop. Med. Hyg. 58, 22-25.

Rokyta, D.R., Lemmon, A.R., Margres, M.J., Aronow, K., 2012. The venom-gland transcriptome of the eastern diamondback rattlesnake (*Crotalus adamanteus*). BMC Genomics 13, 312.

Ronquist, F., Teslenko, M., Van Der Mark, P., Ayres, D.L., Darling, A., Höhna, S., Larget, B., Liu, L., Suchard, M.A., Huelsenbeck, J.P., 2012. MrBayes 3.2: efficient Bayesian phylogenetic inference and model choice across a large model space. Syst Biol 61, 539-542.

Rosing, J., Govers-Riemslag, J.W., Yukelson, L., Tans, G., 2001. Factor V activation and inactivation by venom proteases. Pathophysiol. Haemost. Thromb. 31, 241-246.

Rosing, J., Tans, G., 1991. Inventory of exogenous prothrombin activators. Thromb. Haemost. 66, 627-630.
Rosing, J., Tans, G., 1992. Structural and functional properties of snake venom prothrombin activators. Toxicon 30, 1515-1527.
Rosing, J., Tans, G., 2010. Snake Venom Prothrombin Activators – The History, In: Kini, R.M., Clemetson, K.J., Markland, F.S., McLane, M.A., Morita, T. (Eds.), Toxins and Hemostasis: From Bench to Bedside. Springer Netherlands, Dordrecht, pp. 485-499.
Ryan, E.A., Mockros, L.F., Weisel, J.W., Lorand, L., 1999. Structural origins of fibrin clot rheology. Biophys J 77, 2813-2826.
Sajevic, T., Leonardi, A., Križaj, I., 2011. Haemostatically active proteins in snake venoms. Toxicon 57, 627-645.
Samel, M., Vija, H., Rönnholm, G., Siigur, J., Kalkkinen, N., Siigur, E., 2006. Isolation and characterization of an apoptotic and platelet aggregation inhibiting L-amino acid oxidase from *Vipera berus berus* (common viper) venom. Biochimica et Biophysica Acta (BBA)-Proteins and Proteomics 1764, 707-714.
Samsa, G.P., Matchar, D.B., Williams, G.R., Levy, D.E., 2002. Cost-effectiveness of ancrod treatment of acute ischaemic stroke: Results from the Stroke Treatment with Ancrod Trial (STAT). J. Eval. Clin. Pract. 8, 61-70.
Schmidt, J.J., Weinstein, S.A., 1995. Structure-function studies of waglerin I, a lethal peptide from the venom of Wagler's pit viper, *Trimeresurus wagleri*. Toxicon 33, 1043-1049.
Schmidt, J.J., Weinstein, S.A., Smith, L.A., 1992. Molecular properties and structure-function relationships of lethal peptides from venom of Wagler's pit viper, *Trimeresurus wagleri*. Toxicon 30, 1027-1036.
Schneider, C.A., Rasband, W.S., Eliceiri, K.W., 2012. NIH Image to ImageJ: 25 years of image analysis. Nat. Methods 9, 671.
Shelukhina, I.V., Zhmak, M.N., Lobanov, A.V., Ivanov, I.A., Garifulina, A.I., Kravchenko, I.N., Rasskazova, E.A., Salmova, M.A., Tukhovskaya, E.A., Rykov, V.A., 2018. Azemiopsin, a selective peptide antagonist of muscle nicotinic acetylcholine receptor: Preclinical evaluation as a local muscle relaxant. Toxins 10, 34.
Shi, D.-Y., Wang, S.-J., 2017. Advances of Coagulation Factor XIII. Chin. Med. J. 130, 219.
Shin, Y., Morita, T., 1998. Rhodocytin, a functional novel platelet agonist belonging to the heterodimeric C-type lectin family, induces platelet aggregation independently of glycoprotein Ib. Biochem Biophys Res Commun 245, 741-745.
Shine, R., Harlow, P.S., Branch, W.R., Webb, J.K., 1996. Life on the lowest branch: sexual dimorphism, diet, and reproductive biology of an African twig snake, *Thelotornis capensis* (Serpentes, Colubridae). Copeia, 290-299.
Slagboom, J., Kool, J., Harrison, R.A., Casewell, N.R., 2017. Haemotoxic snake venoms: their functional activity, impact on snakebite victims and pharmaceutical promise. Br J Haematol 177, 947-959.
Smith, H.M., FitzSimons, D.C., 1958. Another rear-fanged South African snake lethal to humans. Herpetologica 14, 198-202.
Sousa, L., Zdenek, C., Dobson, J., Coimbra, F., Gillett, A., Del-Rei, T., Chalkidis, H., Sant'Anna, S., Teixeira-da-Rocha, M., Grego, K., Travaglia Cardoso, S.R., Moura da Silva, A.M., Fry, B.G., 2018. Coagulotoxicity of *Bothrops* (Lancehead Pit-Vipers) venoms from Brazil: Differential biochemistry and antivenom efficacy resulting from prey-driven venom variation. Toxins 10, 411.
Still, K., Nandlal, R.S., Slagboom, J., Somsen, G.W., Casewell, N.R., Kool, J., 2017. Multipurpose HTS Coagulation Analysis: Assay Development and Assessment of Coagulopathic Snake Venoms. Toxins 9, 382.
Sun, M.-Z., Liu, S., Greenaway, F.T., 2006. Characterization of a fibrinolytic enzyme (ussurenase) from *Agkistrodon blomhoffii ussurensis* snake venom: Insights into the effects of Ca2+ on

function and structure. Biochimica et Biophysica Acta (BBA)-Proteins and Proteomics 1764, 1340-1348.
Sunagar, K., Jackson, T.N., Undheim, E.A., Ali, S.A., Antunes, A., Fry, B.G., 2013. Three-fingered RAVERs: Rapid Accumulation of Variations in Exposed Residues of snake venom toxins. Toxins 5, 2172-2208.
Sunagar, K., Undheim, E.A., Scheib, H., Gren, E.C., Cochran, C., Person, C.E., Koludarov, I., Kelln, W., Hayes, W.K., King, G.F., Antunes, A., Fry, B.G., 2014. Intraspecific venom variation in the medically significant Southern Pacific Rattlesnake (*Crotalus oreganus helleri*): Biodiscovery, clinical and evolutionary implications. J. Proteomics 99, 68-83.
Sutherland, S.K., 1983. Australian animal toxins: The creatures, their toxins and care of the poisoned patient. Oxford Univeristy Press, Melbourne, Australia. .
Swenson, S., Markland, F., 2005. Snake venom fibrin (ogen) olytic enzymes. Toxicon 45, 1021-1039.
Tai, H., Wei, Q., Jin, Y., Su, M., Song, J.-X., Zhou, X.-D., Ouyang, H.-M., Wang, W.-Y., Xiong, Y.-L., Zhang, Y., 2004. TMVA, a snake C-type lectin-like protein from *Trimeresurus mucrosquamatus* venom, activates platelet via GPIb. Toxicon 44, 649-656.
Tan, C.H., Liew, J.L., Tan, K.Y., Tan, N.H., 2016. Genus *Calliophis* of Asiatic coral snakes: A deficiency of venom cross-reactivity and neutralization against seven regional elapid antivenoms. Toxicon 121, 130-133.
Tan, C.H., Liew, J.L., Tan, N.H., Ismail, A.K., Maharani, T., Khomvilai, S., Sitprija, V., 2017a. Cross reactivity and lethality neutralization of venoms of Indonesian *Trimeresurus* complex species by Thai Green Pit Viper Antivenom. Toxicon 140, 32-37.
Tan, C.H., Tan, K.Y., Yap, M.K.K., Tan, N.H., 2017b. Venomics of *Tropidolaemus wagleri*, the sexually dimorphic temple pit viper: Unveiling a deeply conserved atypical toxin arsenal. Sci. Rep. 7, 43237.
Tan, N.-h., 2010. Isolation and characterization of the thrombin-like enzyme from *Cryptelytrops purpureomaculatus* venom. Comparative Biochemistry and Physiology Part C: Toxicology & Pharmacology 151, 131-136.
Tan, N.-h., Choy, S.-k., Chin, K.-m., Ponnudurai, G., 1994. Cross-reactivity of monovalent and polyvalent *Trimeresurus* antivenoms with venoms from various species of *Trimeresurus* (lance-headed pit viper) snake. Toxicon 32, 849-853.
Tan, N.-h., Fung, S.-y., Yap, Y.-h.y., 2012. Isolation and characterization of the thrombin-like enzyme from *Cryptelytrops albolabris* (white-lipped tree viper) venom. Comparative Biochemistry and Physiology Part B: Biochemistry and Molecular Biology 161, 79-85.
Tan, N.-h., Tan, C.-s., 1989. The enzymatic activities and lethal toxins of *Trimeresurus wagleri* (speckled pit viper) venom. Toxicon 27, 349-357.
Tang, E.L.H., Tan, C.H., Fung, S.-y., Tan, N.-h., 2016. Venomics of *Calloselasma rhodostoma*, the Malayan pit viper: A complex toxin arsenal unraveled. J. Proteomics 148, 44-56.
Tange, O., 2011. Gnu parallel-the command-line power tool, The USENIX Magazine. usenix.org, pp. 42-47.
Tans, G., Rosing, J., 2002. Snake venom activators of factor X: An overview. Pathophysiol. Haemost. Thromb. 31, 225-233.
Team, R.C., 2016. R: A language and environment for statistical computing, 3.3.1 ed. R Foundation for Statistical Computing, Vienna, Austria.
The UniProt Consortium, 2016. UniProt: The universal protein knowledgebase. Nucleic Acids Res 45, D158-D169.
Toh Yoon, E.W., Otani, Y., Kabuto, S., 2017. Severe Japanese Mamushi (*Gloydius blomhoffii*) bite. Clinical case reports 5, 1548-1549.
Torres-Bonilla, K.A., Andrade-Silva, D., Serrano, S.M., Hyslop, S., 2018. Biochemical characterization of venom from *Pseudoboa neuwiedii* (Neuwied's false boa; *Xenodontinae*; *Pseudoboini*). Comparative Biochemistry and Physiology Part C: Toxicology & Pharmacology 213, 27-38.

Trookman, N.S., Rizer, R.L., Ford, R., Ho, E., Gotz, V., 2009. Immediate and long-term clinical benefits of a topical treatment for facial lines and wrinkles. J Clin Aesthet Dermatol. 2, 38.

Utkin, Y., Sunagar, K., Jackson, T.N.W., Reeks, T., Fry, B.G., 2015. Three-Finger Toxins (3FTxs), In: Fry, B.G. (Ed.), Venomous Reptiles and Their Toxins: Evolution, Pathophysiology and Biodiscovery. Oxford University Press, New York, NY, USA, pp. 215–227.

Vaiyapuri, S., Sunagar, K., Gibbins, J.M., Jackson, T.N.W., Reeks, T., Fry, B.G., 2015. Kallikrein enzymes, In: Fry, B.G. (Ed.), Venomous Reptiles and Their Toxins. Oxford University Press, New York, pp. 267-280.

Vargas, M., Segura, A., Herrera, M., Villalta, M., Estrada, R., Cerdas, M., Paiva, O., Matainaho, T., Jensen, S.D., Winkel, K.D., 2011. Preclinical evaluation of caprylic acid-fractionated IgG antivenom for the treatment of Taipan (*Oxyuranus scutellatus*) envenoming in Papua New Guinea. PLoS Negl. Trop. Dis. 5, e1144.

Visser, J., Chapman, D., 1978. Snakes and snakebite: Venomous snakes and management of snakebite in Southern Africa. Purnell and Sons, Cape Town.

Visudhiphan, S., Tonmukayakul, A., Tumliang, S., Dumavibhat, B., Piankijagum, A., 1989. Dark green pit viper (*Trimeresurus popeorum*) bite: Clinical and serial coagulation profiles in 51 cases. Am. J. Trop. Med. Hyg. 41, 570-575.

Vogel, G., 2006. Venomous snakes of Asia, Edition Chimaira ed. Aquaristik - Consulting & Service GmbH.

Vogler, E.A., Siedlecki, C.A., 2009. Contact activation of blood-plasma coagulation. Biomaterials 30, 1857-1869.

Vonk, F.J., Casewell, N.R., Henkel, C.V., Heimberg, A.M., Jansen, H.J., McCleary, R.J., Kerkkamp, H.M., Vos, R.A., Guerreiro, I., Calvete, J.J., 2013. The king cobra genome reveals dynamic gene evolution and adaptation in the snake venom system. Proceedings of the National Academy of Sciences 110, 20651-20656.

Wang, R., Kini, R.M., Chung, M.C., 1999. Rhodocetin, a novel platelet aggregation inhibitor from the venom of *Calloselasma rhodostoma* (Malayan pit viper): synergistic and noncovalent interaction between its subunits. Biochemistry 38, 7584-7593.

Warrell, D.A., Looareesuwan, S., Theakston, R.D.G., Phillips, R.E., Chanthavanich, P., Viravan, C., Supanaranond, W., Karbwang, J., Ho, M., Hutton, R.A., 1986. Randomized comparative trial of three monospecific antivenoms for bites by the Malayan pit viper (*Calloselasma rhodostoma*) in southern Thailand: Clinical and laboratory correlations. Am. J. Trop. Med. Hyg. 35, 1235-1247.

Weerakkody, R.M., Lokuliyana, P.N., Lanerolle, R.D., 2016. Transient distal renal tubular acidosis following hump nosed viper bite: Two cases from Sri Lanka. Saudi J. Kidney Dis. Transpl. 27, 1018.

Weinstein, S.A., Warrell, D.A., White, J., Keyler, D.E., 2011. Medically Significant Bites by 'Colubrid' Snakes, 'Venomous' Bites from Non-Venomous Snakes: A Critical Analysis of Risk and Management of Colubrid Snake Bites, 1 ed. Elsevier London, UK.

Weinstein, S.A., White, J., Keyler, D.E., Warrell, D.A., 2013. Non-front-fanged colubroid snakes: a current evidence-based analysis of medical significance. Toxicon 69, 103-113.

White, J., 2005. Snake venoms and coagulopathy. Toxicon 45, 951-967.

WHO, 2010. Blood products and related biologicals. World Health Organisation Geneva.

Williams, D., Gutiérrez, J.M., Harrison, R., Warrell, D.A., White, J., Winkel, K.D., Gopalakrishnakone, P., 2010. The Global Snake Bite Initiative: an antidote for snake bite. The lancet 375, 89-91.

Williams, D.J., Gutiérrez, J.-M., Calvete, J.J., Wüster, W., Ratanabanangkoon, K., Paiva, O., Brown, N.I., Casewell, N.R., Harrison, R.A., Rowley, P.D., 2011. Ending the drought: new strategies for improving the flow of affordable, effective antivenoms in Asia and Africa. J. Proteomics 74, 1735-1767.

Williams, V., White, J., Mirtschin, P., 1994. Comparative study on the procoagulant from the venom of Australian brown snakes (Elapidae; *Pseudonaja* spp.). Toxicon 32, 453-459.

Withana, M., Rodrigo, C., Gnanathasan, A., Gooneratne, L., 2014. Presumptive thrombotic thrombocytopenic purpura following a hump-nosed viper (*Hypnale hypnale*) bite: a case report. J Venom Anim Toxins Incl Trop Dis 20, 26.

Witharana, E., Gnanathasan, A., Dissanayake, A., Wijesinghe, S., Kadahetti, S., Rajapaksha, R., 2019. Sri Lankan green pit viper (*Trimeresurus trigonocephalus*) bites in Deniyaya: A clinico-epidemiological study. Toxicon 169, 34-37.

Wolberg, A.S., 2007. Thrombin generation and fibrin clot structure. Blood Rev. 21, 131-142.

Wolberg, A.S., Campbell, R.A., 2008. Thrombin generation, fibrin clot formation and hemostasis. Transfusion Apheresis Sci. 38, 15-23.

Wongtongkam, N., Wilde, H., Sitthi-Amorn, C., Ratanabanangkoon, K., 2005. A study of 225 Malayan pit viper bites in Thailand. Mil. Med. 170, 342-348.

Wu, Y., 2015. Contact pathway of coagulation and inflammation. Thromb. J. 13, 17.

Xie, Y., Wu, G., Tang, J., Luo, R., Patterson, J., Liu, S., Huang, W., He, G., Gu, S., Li, S., 2014. SOAPdenovo-Trans: de novo transcriptome assembly with short RNA-Seq reads. Bioinformatics 30, 1660-1666.

Xin, Y., Dong, D., Chen, D., Li, R., 2009. Structural and biological characterization of a novel acutobin-like enzyme isolated from the venom of the sharp-nosed pit viper (*Deinagkistrodon acutus*). Biotechnol. Appl. Biochem. 53, 123-131.

Xu, N., Zhao, H.-Y., Yin, Y., Shen, S.-S., Shan, L.-L., Chen, C.-X., Zhang, Y.-X., Gao, J.-F., Ji, X., 2017. Combined venomics, antivenomics and venom gland transcriptome analysis of the monocoled cobra (*Naja kaouthia*) from China. J. Proteomics 159, 19-31.

Yamada, D., Sekiya, F., Morita, T., 1996. Isolation and characterization of carinactivase, a novel prothrombin activator in *Echis carinatus* venom with a unique catalytic mechanism. J Biol Chem 271, 5200-5207.

Yamada, D., Sekiya, F., Morita, T., 1997. Prothrombin and factor X activator activities in the venoms of Viperidae snakes. Toxicon 35, 1581-1589.

Yamashita, K.M., Alves, A.F., Barbaro, K.C., Santoro, M.L., 2014. *Bothrops jararaca* venom metalloproteinases are essential for coagulopathy and increase plasma tissue factor levels during envenomation. PLoS Negl. Trop. Dis. 8, e2814.

Yang, D.C., Deuis, J.R., Dashevsky, D., Dobson, J., Jackson, T.N., Brust, A., Xie, B., Koludarov, I., Debono, J., Hendrikx, I., Hodgson, W.C., Josh, P., Nouwens, A., Baillie, G.J., Bruxner, T.J.C., Alewood, P.F., Lim, K.K.P., Frank, N., Vetter, I., Fry, B.G., 2016. The Snake with the Scorpion's sting: novel three-finger toxin sodium channel activators from the venom of the long-glanded blue coral snake (*Calliophis bivirgatus*). Toxins 8, 303.

Yang, J.Y., Hui, H., Lee, A.C., 2007. Severe coagulopathy associated with white-lipped green pit viper bite. HKMJ 13, 392.

Yang, Z.-M., Yang, Y.-E., Chen, Y., Cao, J., Zhang, C., Liu, L.-L., Wang, Z.-Z., Wang, X.-M., Wang, Y.-M., Tsai, I.-H., 2015. Transcriptome and proteome of the highly neurotoxic venom of *Gloydius intermedius*. Toxicon 107, 175-186.

Youngman, N.J., Zdenek, C.N., Dobson, J.S., Bittenbinder, M.A., Gillett, A., Hamilton, B., Dunstan, N., Allen, L., Veary, A., Veary, E., 2018. Mud in the blood: Novel potent anticoagulant coagulotoxicity in the venoms of the Australian elapid snake genus *Denisonia* (mud adders) and relative antivenom efficacy. Toxicol. Lett. 302, 1-6.

Yushkevich, P.A., Piven, J., Hazlett, H.C., Smith, R.G., Ho, S., Gee, J.C., Gerig, G., 2006. User-guided 3D active contour segmentation of anatomical structures: Significantly improved efficiency and reliability. NeuroImage 31, 1116-1128.

Zdenek, C.N., Hay, C., Arbuckle, K., Jackson, T.N., Bos, M.H., op den Brouw, B., Debono, J., Allen, L., Dunstan, N., Morley, T., Herrera, M., Gutiérrez, J.M., Williams, D.J., Fry, B.G., 2019. Coagulotoxic effects by brown snake (*Pseudonaja*) and taipan (*Oxyuranus*) venoms, and the efficacy of a new antivenom. Toxicol In Vitro 58, 97-109.

Zelanis, A., Serrano, S.M., Reinhold, V.N., 2012. N-glycome profiling of *Bothrops jararaca* newborn and adult venoms. J. Proteomics 75, 774-782.

Zelanis, A., Tashima, A.K., Rocha, M.M., Furtado, M.F., Camargo, A.C., Ho, P.L., Serrano, S.M., 2010. Analysis of the ontogenetic variation in the venom proteome/peptidome of *Bothrops jararaca* reveals different strategies to deal with prey. J. Proteome Res. 9, 2278-2291.

Zhang, J., Kobert, K., Flouri, T., Stamatakis, A., 2013. PEAR: a fast and accurate Illumina Paired-End reAd mergeR. Bioinformatics 30, 614-620.

Zhang, Q., Wang, J., Han, Y., Xie, Q., An, L., Bao, Y., 2007. Identification of a novel thrombin-like phospholipase A2 from *Gloydius ussuriensis* snake venom. Blood Coagul. Fibrinolysis 18, 723-729.

Zulys, V.J., Teasdale, S.J., Michel, E.R., Skala, R.A., Keating, S.E., Viger, J.R., Glynn, M., 1989. Ancrod (Arvin) as an alternative to heparin anticoagulation for cardiopulmonary bypass. Anesthesiology 71, 870-877.

Appendix

Supplementary Table 6.1 *Gloydius* antivenom
Current antivenom manufactured for *Gloydius* species.

http://www.who.int/bloodproducts/snakeantivenoms/database (WHO, 2010).

Antivenom name	Manufacturer	Country	*Gloydius* species included in immunising mixture	Additional species
Freeze-dried Mamushi Antivenom, Equine "Takeda" (SAsTCI01)	Takeda Chemical Industries Ltd.	Japan	*G. blomhoffii* *G. brevicaudus*	None
Freeze-dried Mamushi Antivenom "Kaketsuken" (SAsKKJ01)	The Chemo-Sero-Therapeutic Research Institute (Kaketsuken)	Japan	*G. blomhoffii* *G. brevicaudus*	None
Polyvalent Snake Antivenin (SAsRII02)	Razi Serum and Vaccine Research Institute	I.R. Iran	*Gloydius halys*	*Echis carinatus,* *Macrovipera lebetina,* *Naja oxiana,* *Pseudocerastes persicus,* *Vipera albicornuta,* *Vipera raddei*
Purified *Agkistrodon halys* Antivenom (SAsSIC01)	Shanghai Institute of Biological Products	Peoples Republic of China	*G. halys*	None
Agkistrodon (Salmusa) Antivenom	Korea Vaccine Co. Ltd.	Seoul - Republic of Korea	*G. brevicaudus* *G. intermedius* *G. ussuriensis*	

```
Phytools script
>library(ape)
>library(maps)
>library(phytools)
>#  senci.contMap is a slight modification of errorbar.contMap that trims 95% CIs
of ancestral state reconstructions to a sensible range, e.g., for traits bound
between 0 and 1
     # Example of code for implementing it would be as follows (lines separated
     by semicolons): pasr<-contMap(tree,mapdat,plot=F,lims=c(0,1)) ;
     plot(setMap(pasr,invert=T));
     senci.contMap(setMap(pasr,invert=T),mini=0,maxi=1)
     senci.contMap<-function(obj,...){
     if (hasArg(x))
     x <- list(...)$x
     else x <- setNames(sapply(1:Ntip(obj$tree), function(x, obj) {
     ii <- which(obj$tree$edge[, 2] == x)
     ss <- names(obj$tree$maps[[ii]][length(obj$tree$maps[[ii]])])
     obj$lims[1 ] + as.numeric(ss)/(length(obj$cols) - 1) *
     diff(obj$lims)
     }, obj = obj), obj$tree$tip.label)
     if (hasArg(scale.by.ci))
     scale.by.ci <- list(...)$scale.by.ci
     else scale.by.ci <- TRUE
     if (hasArg(lwd))
     lwd <- list(...)$lwd
     else lwd <- 14
     tree <- obj$tree
     aa <- fastAnc(tree, x, CI = TRUE)
     if (hasArg(min))#added lines here
     for (i in 1:length(aa$CI95[,1])){ #added lines here
     aa$CI95[i,1]<-ifelse(aa$CI95[i,1]<list(...)$min,list(...)$min,aa$CI95[i,1])
     #added lines here
     } #added lines here
     else aa$CI95[,1]<-aa$CI95[,1] #added lines here
     if (hasArg(max)) #added lines here
     for (i in 1:length(aa$CI95[,2])){ #added lines here
     aa$CI95[i,2]<-ifelse(aa$CI95[i,2]>list(...)$max,list(...)$max,aa$CI95[i,2])
     # added lines here
     } #added lines here
     else aa$CI95[,2]<-aa$CI95[,2] #added lines here
     xlim <- range(aa$CI95)
     if (xlim[2] > obj$lims[2] || xlim[1] < obj$lims[1]) {
     cat(paste(" -----\n The range of the contMap object, presently (",
     round(obj$lims[1], 4), ",", round(obj$lims[2], 4),
     "), should be equal to\n or greater than the range of the CIs on ancestral
     states: (",
     round(xlim[1], 4), ",", round(xlim[2], 4), ").\n",
     sep = ""))
     cat(paste(" To ensure that your error bars are correctly plotted, please
     recompute your\n",
     " contMap object and increase lims.\n -----\n",
     sep = ""))
     }
     d <- diff(obj$lims)
     if (scale.by.ci) {
     v <- aa$CI95[, 2] - aa$CI95[, 1]
     v <- v/max(v)
     }
     else v <- rep(0.5, tree$Nnode)
     n <- length(obj$cols) - 1
     lastPP <- get("last_plot.phylo", envir = .PlotPhyloEnv)
     h <- max(nodeHeights(tree))
     for (i in 1:tree$Nnode) {
     ii <- round((aa$CI95[i, 1] - obj$lims[1])/d * n)
```

```
    jj <- round((aa$CI95[i, 2] - obj$lims[1])/d * (n + 1))
    cols <- obj$cols[ii:jj]
    add.color.bar(leg = 0.1 * h * v[i], cols = cols, prompt = FALSE,
    x = lastPP$xx[i + Ntip(tree)] - 0.05 * h * v[i],
    y = lastPP$yy[i + Ntip(tree)], title = "", subtitle = "",
    lims = NULL, lwd = lwd)
    }
    }
>data<-read.csv(file.choose())
>dat<-data
>mapvar<-dat$var
>names(mapvar)<-dat$species
>tree<-read.tree(file.choose())
>tree<-chronos(tree)
>asr<-contMap(tree,mapvar,plot=F)

To have the red (warmer) zone for the higher numbers (eg antivenom) we then used
the below.
>plot(setMap(asr,col=c(1,4,5,3,7,2,6)),lwd=10)
>senci.contMap(setMap(asr,col=c(1,4,5,3,7,2,6)),lwd=20,min=[minimum value from
the dataset],max=[minimum value from the dataset])

To have the red (warmer) zone for smaller numbers (eg clotting time) we then
used the below
>plot(setMap(asr,col=c(6,2,7,3,5,4,1)),lwd=10)
>senci.contMap(setMap(asr,col=c(6,2,7,3,5,4,1)),lwd=20,min=[minimum value from
the dataset],max=[minimum value from the dataset])
```

Supplementary Figure 1: R Phytools script
R script phytools used for phylogenetic comparative analysis throughout thesis.